Research Progress and Accomplishments

2001-2003

A Selection of Papers Chronicling Technical Achievements of the Multidisciplinary Center for Earthquake Engineering Research

The Multidisciplinary Center for Earthquake Engineering Research

The Multidisciplinary Center for Earthquake Engineering Research (MCEER) is a national center of excellence in advanced technology applications that is dedicated to the reduction of earthquake losses nationwide. Headquartered at the University at Buffalo, State University of New York, the Center was originally established by the National Science Foundation (NSF) in 1986, as the National Center for Earthquake Engineering Research (NCEER).

Comprising a consortium of researchers from numerous disciplines and institutions throughout the United States, the Center's mission is to reduce earthquake losses through research and the application of advanced technologies that improve engineering, pre-earthquake planning and post-earthquake recovery strategies. Toward this end, the Center coordinates a nationwide program of multidisciplinary team research, education and outreach activities.

Funded principally by NSF, the State of New York and the Federal Highway Administration (FHWA), the Center derives additional support from the Federal Emergency Management Agency (FEMA), other state governments, academic institutions, foreign governments and private industry.

Research Progress and Accomplishments

2001 - 2003

Multidisciplinary Center for Earthquake Engineering Research
University at Buffalo, State University of New York

May 2003

MCEER-03-SP01
Red Jacket Quadrangle, Buffalo, New York 14261
Tel: (716) 645-3391; Fax: (716) 645-3399; Email: *mceer@mceermail.buffalo.edu*
World Wide Web: *http://mceer.buffalo.edu*

Foreword

by George C. Lee, Director,
Multidisciplinary Center for Earthquake Engineering Research

The ultimate vision of the Multidisciplinary Center for Earthquake Engineering Research (MCEER) is to help establish earthquake resilient communities. The overall goal is to enhance the seismic resiliency of communities through improved engineering and management tools for critical infrastructure systems and emergency management functions. These tools will, in turn, help concerned organizations and communities to mitigate hazards, contain the effects of disasters when they occur, and carry out recovery activities in ways that minimize disruption and mitigate the destructive effects of future earthquakes.

To accomplish its mission, MCEER focuses on improving the resilience of facilities and organizations whose functions are essential for community well-being in the aftermath of earthquake disasters. The flowchart below schematically shows how the Center's research interests contribute collectively to achieve its vision.

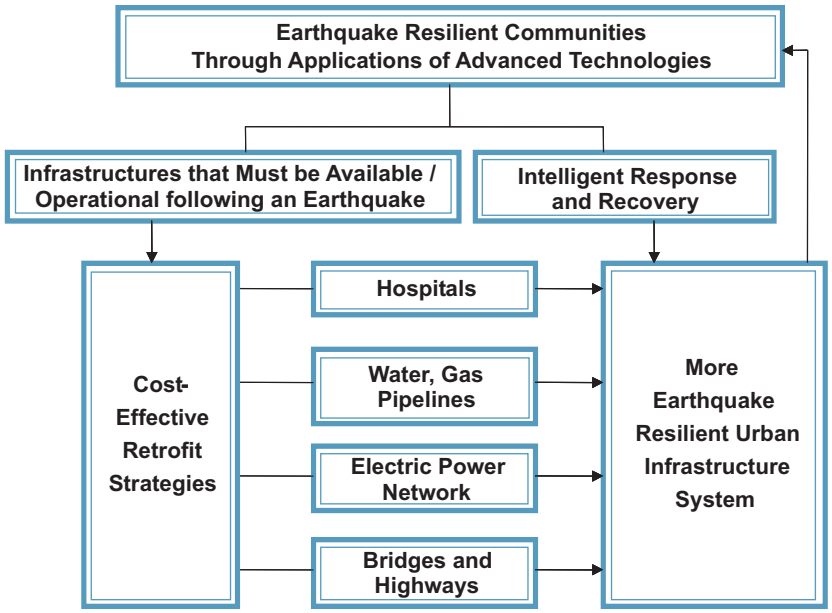

Research on electrical power and water systems, together with transportation systems, focuses on problems germane to the infrastructural backbone of all communities. Research on hospitals addresses issues related to highly complex facilities (structure plus critical non-structural systems) that must remain functional to support essential medical services following earthquakes. Furthermore, in spite of efforts to strengthen existing structures and provide better designs for new structures, the

built environment of many population centers will remain seismically vulnerable and unretrofitted. This condition may result in potential heavy losses and extensive social dislocation when the next major earthquake strikes. Therefore, MCEER's research also concentrates on bringing about improvements to a community's ability to respond to and recover from a disaster.

Each paper in this volume describes an aspect of MCEER's coordinated program to achieve its vision. They represent work in many stages, from just beginning, to those that are introducing new tools and techniques. Some are continuations of progress reported in previous volumes (with the Internet address to the electronic version of the earlier paper(s)), and others report on new efforts. Each paper identifies its sponsor, which is primarily either the National Science Foundation's Earthquake Engineering Research Centers program or the Federal Highway Administration. Next, the Research Team is identified, including the principal investigators, their students, and other integral members of the research team. Since many tasks rely on other tasks for information, these related team members are listed under the MCEER Team heading. Those listed under Collaborative Partners have similarly contributed to the research, but are not directly part of MCEER's research program. Finally, the Internet addresses of sites that contain information related to the research task are provided. These links have been made live in the electronic version of this report (available from the Publications section of MCEER's web site at *http://mceer.buffalo.edu*).

If you would like more information on any of the studies presented herein, or on other MCEER research or educational activities, you are encouraged to contact us by telephone at (716) 645-3391, facsimile (716) 645-3399, or email at *mceer@mceermail.buffalo.edu*.

Contents

Advances in Seismic Performance Evaluation of Power Systems 1
Masanobu Shinozuka, Maria Feng, Xuejiang Dong, Stephanie Chang, Tsen-Chung Cheng, Xianhe Jin and M. Ala Saadeghvaziri

REDARS 1: Demonstration Software for Seismic Risk Analysis of Highway Systems 17
Stuart D. Werner, Jean-Paul Lavoie, Chip Eitzel, Sungbin Cho, Charles Huyck, Shubharoop Ghosh, Ronald T. Eguchi, Craig Taylor and James E. Moore II

Effect of Seismic Retrofit of Bridges on Transportation Networks 35
Masanobu Shinozuka, Yuko Murachi, Xuejiang Dong, Youwei Zhou and Michal J. Orlikowski

Performance Estimates in Seismically Isolated Bridges 51
Gordon P. Warn and Andrew S. Whittaker

Developing Fragility Curves for Concrete Bridges Retrofitted with Steel Jacketing 63
Masanobu Shinozuka and Sang-Hoon Kim

Advanced Technologies for Response Modification of Hospital Buildings 77
Michel Bruneau (Coordinating Author), Andrei M. Reinhorn, Amjad Aref, Sarah L. Billington, Michael C. Constantinou, George C. Lee and Andrew S. Whittaker

Decision Models: Approaches for Achieving Seismic Resilience 97
Daniel J. Alesch (Coordinating Author), Gary F. Dargush, Mircea Grigoriu, William J. Petak and Detlof vonWinterfeldt

Developing an Integrated System for Seismic Risk Analysis of Critical Hospital Facilities 115
George C. Lee, Masanobu Shinozuka and Mai Tong

Resilient Disaster Response: Using Remote Sensing Technologies for Post-Earthquake Damage Detection 125
Ronald T. Eguchi

Resilient Community Recovery: Improving Recovery Through Comprehensive Modeling 139
Stephanie E. Chang and Scott B. Miles

Understanding Sources of Economic Resiliency to Hazards: Modeling the Behavior of Lifeline Service Customers 149
Adam Rose and Shu-Yi Liao

The MCEER Interface Between Research and Education **161**
Andrea S. Dargush (Coordinating Author), Makola M. Abdullah, Anil K. Agrawal, Rupa Purasinghe and Billie F. Spencer, Jr.

Contributors

Makola M. Abdullah, Assistant Professor, Department of Civil Engineering, Florida A&M University

Beverley J. Adams, Project Scientist, ImageCat, Inc.

Anil K. Agrawal, Assistant Professor, Department of Civil Engineering, The City College of the City University of New York

Daniel J. Alesch, Professor Emeritus, Department of Public and Environmental Affairs, University of Wisconsin-Green Bay

Amjad Aref, Assistant Professor, Department of Civil, Structural and Environmental Engineering, University at Buffalo

Michael Astrella, M.S. Student, Department of Civil, Structural and Environmental Engineering, University at Buffalo

Hiram Badillo, M.S. Student, Department of Civil, Structural and Environmental Engineering, University at Buffalo

Jeffrey Berman, Ph.D. Candidate, Department of Civil, Structural and Environmental Engineering, University at Buffalo

Sarah Billington, Assistant Professor, Department of Civil and Environmental Engineering, Cornell University; now at Stanford University

Michel Bruneau, Deputy Director, Multidisciplinary Center for Earthquake Engineering Research and Professor, Department of Civil, Structural and Environmental Engineering, University at Buffalo

Marion Calderon, M.S. Student, Department of Civil Engineering, California State University at Los Angeles

Stephanie E. Chang, Research Assistant Professor, Department of Geography, University of Washington

Robert Chen, Ph.D. Candidate, School of Policy, Planning and Development, University of Southern California

Tsen-Chung Cheng, Lloyd F. Hunt Professor of Electrical Engineering and Director, Electric Power Program, Department of Electrical Engineering, University of Southern California

Art Chianello, M.S. Student, Department of Civil Engineering, California State University at Los Angeles

Sungbin Cho, Senior Transportation Planner, ImageCat, Inc.

Michael C. Constantinou, Professor and Chair, Department of Civil, Structural and Environmental Engineering, University at Buffalo

Andrea S. Dargush, Assistant Director for Education and Research Administration, Multidisciplinary Center for Earthquake Engineering Research

Gary F. Dargush, Professor, Department of Civil, Structural and Environmental Engineering, University at Buffalo

Xuejiang Dong, Post Doctoral Researcher, Department of Civil and Environmental Engineering, University of California, Irvine

Ronald T. Eguchi, President, ImageCat, Inc.

Chip Eitzel, Partner, Geodesy

Maria Q. Feng, Professor, Department of Civil and Environmental Engineering, University of California, Irvine

Daniel Fenz, Research Experience for Undergraduate Student, Multidisciplinary Center for Earthquake Engineering Research

Yong Gao, Department of Civil and Environmental Engineering, University of Illinois at Urbana-Champaign

Shubharoop Ghosh, Project Transportation Planner, ImageCat, Inc.

Mark L. Green, Research Assistant Professor, Department of Civil, Structural and Environmental Engineering, University at Buffalo

Mircea Grigoriu, Professor, Department of Civil and Environmental Engineering, Cornell University

Gauri Guha, Graduate Student, Program in Energy, Environmental and Mineral Economics, Pennsylvania State University

Tong-Seok Han, Post Doctoral Researcher, Department of Civil and Environmental Engineering, Cornell University

Bijan Houshmand, Adjunct Associate Professor, Department of Electrical Engineering, University of California, Los Angeles

Charles K. Huyck, Senior Vice President, ImageCat, Inc.

Xianbe Jin, Research Associate, Department of Electrical Engineering, University of Southern California

Woo-Young Jung, Ph.D. Candidate, Department of Civil, Structural and Environmental Engineering, University at Buffalo

Cagdas Kafali, Graduate Student, Department of Civil and Environmental Engineering, Cornell University

Nishade Karunarathne, Research Experience for Undergraduate Student, Multidisciplinary Center for Earthquake Engineering Research

Keith Kesner, Ph.D. Candidate, Department of Civil and Environmental Engineering, Cornell University

Sang-Hoon Kim, Research Associate, Department of Civil and Environmental Engineering, University of California, Irvine

Shigeru Kushiyama, Visiting Research Scholar, Department of Civil and Environmental Engineering, University of California, Irvine; from Hokka-Gakuen University, Japan

Jean-Paul Lavoie, Partner, Geodesy

George C. Lee, Director, Multidisciplinary Center for Earthquake Engineering Research and Samuel P. Capen Professor of Engineering, University at Buffalo

Shu-Yi Liao, Graduate Student, Program in Energy, Environmental and Mineral Economics, Pennsylvania State University; now with California Energy Commission

Li-Yuan Lin, M.S. Student, Department of Civil, Structural and Environmental Engineering, University at Buffalo

Wei Liu, Ph.D. Graduate, Department of Civil, Structural and Environmental Engineering, University at Buffalo; now with Weidlinger and Associates, New York

Babak Mansouri, Project Scientist, ImageCat, Inc.

Scott B. Miles, Graduate Student, Department of Geography, University of Washington

James E. Moore, II, Professor, Departments of Civil Engineering and Public Policy and Management, University of Southern California

Yuko Murachi, Research Associate, Department of Civil and Environmental Engineering, University of California, Irvine

George Mylonakis, Assistant Professor, Department of Civil Engineering, The City College of the City University of New York

Terri Norton, Ph.D. Candidate, Department of Civil Engineering, Florida A&M University

Debo Oladosu, Assistant Professor, School of Environmental Science, Engineering and Policy, Drexel University

Michal J. Orlikowski, Undergraduate Student, Department of Civil and Environmental Engineering, Princeton University

Robert Payne, Research Experience for Undergraduate Student, Multidisciplinary Center for Earthquake Engineering Research

William J. Petak, Professor, School of Policy, Planning and Development, University of Southern California

Adelina Pirijanyan, Undergraduate Student, Department of Civil and Environmental Engineering, University of California, Irvine

Rupa Purasinghe, Professor, Department of Civil Engineering, California State University at Los Angeles

Jincheng Qi, Post Doctoral Researcher, Multidisciplinary Center for Earthquake Engineering Research

Andrei Reinhorn, Professor, Department of Civil, Structural and Environmental Engineering, University at Buffalo

Susan Romero, Undergraduate Student, Department of Civil Engineering, The City College of the City University of New York

Adam Rose, Professor, Department of Geography, Program in Energy, Environmental and Mineral Economics, Pennsylvania State University

Vladimir Rzhevsky, Senior Research Scientist, Multidisciplinary Center for Earthquake Engineering Research

M. Ala Saadeghvaziri, Professor, Department of Civil and Environmental Engineering, New Jersey Institute of Technology

Ramesh Sant, Ph.D. Graduate, Department of Civil, Structural and Environmental Engineering,

University at Buffalo; now with DMJM+Harris, New York

Masanobu Shinozuka, Distinguished Professor and Chair, Department of Civil and Environmental Engineering, University of California, Irvine

Ani Natali Sigaher, Ph.D. Candidate, Department of Civil, Structural and Environmental Engineering, University at Buffalo

Tony Soeller, Research Computing Specialist, Department of Network & Academic Computing, University of California, Irvine

Billie F. Spencer, Jr., Nathan M. Newmark Professor of Civil Engineering, Department of Civil and Environmental Engineering, University of Illinois at Urbana-Champaign

Joseph Stellrecht, Undergraduate Student, Department of Computer Engineering, University at Buffalo

Craig E. Taylor, President, Natural Hazards Management, Inc.

Mai Tong, Senior Research Scientist, Multidisciplinary Center for Earthquake Engineering Research and the Department of Civil, Structural and Environmental Engineering, University at Buffalo

Belan Valencia, M.S. Student, Department of Civil Engineering, California State University at Los Angeles

Miriam Vargas, Undergraduate Student, Department of Civil Engineering, The City College of the City University of New York

Darren Vian, Ph.D. Candidate, Department of Civil, Structural and Environmental Engineering, University at Buffalo

S. Viti, Visiting Researcher, Department of Civil, Structural and Environmental Engineering, University at Buffalo; from the University of Florence, Italy

Detlof von Winterfeldt, Professor, School of Policy, Planning and Development, University of Southern California

Yunli Wang, Ph.D. Candidate, Department of Civil, Structural and Environmental Engineering, University at Buffalo

Gordon Warn, M.S. Student, Department of Civil, Structural and Environmental Engineering, University at Buffalo

Stuart D. Werner, Principal, Seismic Systems and Engineering Consultants

Andrew S. Whittaker, Associate Professor, Department of Civil, Structural and Environmental Engineering, University at Buffalo

Bo Yang, Graduate Student, Program in Energy, Environmental and Mineral Economics, Pennsylvania State University

Tsung Yuan Yang, M.S. Student, Department of Civil, Structural and Environmental Engineering, University at Buffalo

Jin Hak Yi, Visiting Research Associate, Department of Civil and Environmental Engineering, University of California, Irvine; from Korea Advanced Institute of Science and Technology

Xiangjie Zhao, M.S. Graduate, Department of Civil, Structural and Environmental Engineering, University at Buffalo; now with Weidlinger Associates, New York

Youwei Zhou, Graduate Student, Department of Civil and Environmental Engineering, University of California, Irvine

Advances in Seismic Performance Evaluation of Power Systems

by Masanobu Shinozuka, Maria Feng, Xuejiang Dong, Stephanie E. Chang, Tsen-Chung Cheng, Xianhe Jin and M. Ala Saadeghvaziri

Research Objectives

The primary objective of this study is to evaluate the performance of electric power systems before and after a major catastrophic event, such as an earthquake, an accidental or manmade disablement of system components, and more importantly, incorporate the results of the evaluation as an integral part of the overarching framework of MCEER's methodology that will enhance the seismic resilience of communities. Based on our experience in the analysis of the seismic performance of the Los Angeles Department of Water and Power (LADWP) system after the Northridge earthquake, we believe that we have derived a useful set of data and gained significant knowledge on LADWP's system robustness during and after a catastrophic event. By employing a systematic network analysis approach, we are able to analyze the power flow status of the entire Western Systems Coordinating Council (WSCC) grid and determine the seismic performance of the entire system. Based on this knowledge, we are able to further probe the inherent weaknesses in such a system and pinpoint the weak links at the component level. In fact, our earlier studies (Shinozuka, et al., 2002 and 2003) demonstrated that retrofitting transformers sufficiently enhanced the system performance from both a safety and socio-economic point of view.

This paper demonstrates the advances that have been achieved by MCEER's research team and collaborative partners in dealing with electric power systems, since the publication of "Seismic Performance Analysis of Electric Power Systems" in Shinozuka et al., 1999. The advances are prominent in (1) integration of WSCC (Western Systems Coordinating Council) database with EPRI's (Electric Power Research Institute's) IPFLOW (Interactive Power FLOW) computer code for systematic power flow analysis, (2) development of fragility curves for transformers in a transmission network (on the basis of damage information from the 1994 Northridge earthquake and enhanced fragility curves from the test results carried out by this research team), (3) estimation of the likelihood for the power supply and for the number of households without power immediately after an earthquake, (4) development of preliminary performance criteria for

Sponsors

National Science Foundation, Earthquake Engineering Research Centers Program

Research Team

***Masanobu Shinozuka**, Distinguished Professor and Chair, **Maria Feng**, Professor, and **Xuejiang Dong**, Post Doctoral Researcher, Department of Civil and Environmental Engineering, University of California, Irvine*

***Stephanie Chang**, Research Assistant Professor, Department of Geography, University of Washington*

***Tsen-Chung Cheng**, Lloyd F. Hunt Professor of Electrical Engineering and Director, Electric Power Program, **Xianhe Jin**, Research Associate, Department of Electrical Engineering, University of Southern California*

***M. Ala Saadeghvaziri**, Professor, Department of Civil and Environmental Engineering, New Jersey Institute of Technology*

Previous Summaries

***2000-2001**: Saadeghvaziri et al., http://mceer.buffalo.edu/publications/resaccom/0001/rpa_pdfs/04Saad2.pdf*

***1997-1999**: Shinozuka et al., http://mceer.buffalo.edu/publications/resaccom/9799/Ch7shino.pdf*

Collaborative Partners

***Jon Mochizuki** and **Ronald Tognazzini**, Los Angeles Department of Water and Power*

***Hope Seligson**, ABS Consultants.*

power systems, (5) application of a life cycle cost methodology to evaluate seismic mitigation for urban infrastructure systems in general, and power systems in particular, and (6) evaluation of the effect of a disabling event on the performance of a remotely located utility system.

This study evaluates the seismic performance of an electric power system, recommends appropriate seismic rehabilitation measures and estimates the associated socio-economic impact. The LADWP's power system was used as a testbed. Figures 1 and 2 show the LADWP's electric power service areas and the power supply under usual operating conditions. The areas not colored are serviced by Southern California Edison (SCE). To carry out the systems analysis, fragility curves of electrical power equipment, such as transformers in the transmission network, play an important role and are developed on the basis of damage information collected following the 1994 Northridge earthquake. Also, an equipment rehabilitation study is performed in order to examine the extent of the enhancements such rehabilitation work can produce. A systems analysis of LADWP's power system under actual and simulated earthquakes was performed. The analysis was based on an inventory database of the network, together with available fragility information of power equipment and Monte Carlo simulation techniques. This is a unique research work where an actual database from WSCC was used in conjunction with the computer code IPFLOW (version 5.0), licensed by EPRI.

Apart from the vulnerability of transformers, the seismic vulnerability of other equipment, such as circuit breakers and disconnect switches, can be and was integrated into the analysis by using corresponding fragility curves.

To gain a complete understanding of the seismic performance of LADWP's power system, 47 scenario earthquake events were selected and simulated (discussed in detail later in this paper). These are associated with annual "equivalent probabilities" of occurrence so that collectively, they represent the full range of the regional seismic hazard. The results of this analysis produce risk curves for households without power immediately after an earthquake.

For urban infrastructure systems, evaluating the benefits and costs of hazard mitigation measures is complicated by several important considerations. First, electric power, water, and other infrastructure net-

Perceived and actual users of the result of this research consist of utility engineers and managers, regulatory agencies, local, state, and regional emergency response agencies, civil, electrical, mechanical and systems engineers, and power equipment manufacturers. Typically, users include LADWP and SCE (Southern California Edison), California State Office and Emergency Services and Los Angeles City Office of Emergency Response.

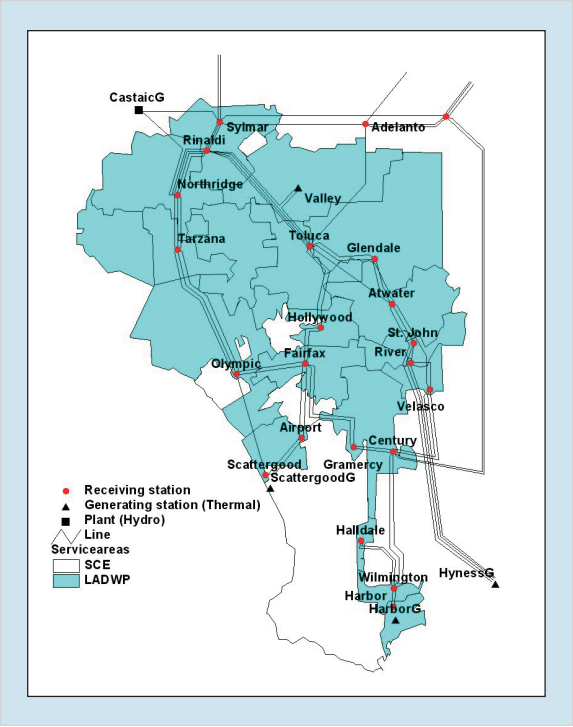

Figure 1. Transmission Network and Service Areas of LADWP's Power System

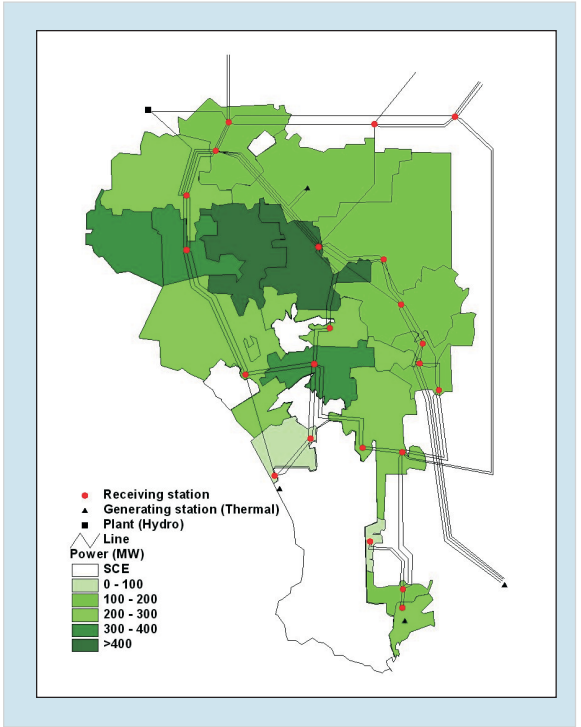

Figure 2. Electric Power Output for Service Areas under Intact Condition

works are spatially distributed across a wide area; hence, evaluations must account for system functionality as well as the spatial correlation of hazard (such as earthquake ground motion) across the area. Second, these systems have long service lives. Analyses must therefore consider how the system itself, as well as the potential impacts of its failure, might change over a period of many decades. Third, infrastructure systems are vital to all sectors of the urban community. Mitigation assessments should therefore include the benefits to both the lifeline infrastructure provider and society as a whole.

This paper applies a life cycle cost methodology for evaluating the effect of infrastructure mitigation techniques for seismic retrofit of LADWP's electric power system. Total life cycle costs include repair cost, utility revenue losses and societal losses in future earthquake disasters.

Development of Fragility Curves

Failure of transformers is one of the most common and significant types of damage to electric power systems due to earthquakes. While transformers are crucial components in an electric power network, their redundancy is not as high as other power equipment due to their very large size and high cost. Therefore, it is important to make a pre-event evaluation of the seismic performance of transformers on the basis of damage information obtained from past earthquakes rather than from laboratory experi-

Links to Current Research

This study develops an analysis procedure to evaluate seismic performance for electric power systems, and can also be integrated with the studies involving other lifeline systems, such as water delivery system and hospital facilities. This research will become an integral part of the methodology for the enhancement of seismic resilience of communities that MCEER's research will ultimately develop. The results can also be used to complement the research on emergency response.

ments. In this research, substantial effort was expended to acquire damage information for transmission level transformers related to the Northridge earthquake identified from one-line diagrams of the LADWP and SCE receiving stations.

The damage information is transformed into empirical fragility curves expressed in the form of two-parameter (median and log-standard deviation) lognormal distribution, as a function of peak ground acceleration (PGA), which represents the intensity of the seismic ground motion at each site. Use of PGA for this purpose is considered reasonable since it is not feasible to evaluate the fragility curves as a function of spectral acceleration. This would require identification of dominant participating natural modes of vibration for each of the large number of transformers and corresponding reliable ground motion time histories. The PGA value at the location of each receiving station is determined by interpolation and extrapolation from the PGA contours (see Wald, 1998, *http://quake.wr.usgs.gov/research/strongmotion/effects/shake/*). In this research, the maximum likelihood method (M. Shinozuka et al., 2000) is employed to estimate the two parameters of the fragility curve resulting in c=0.45g (median) and z=0.42 (log-standard deviation). With these two parameters, the fragility curve for the transformers in the transmission network has been developed and is shown in Figure 3 (in red) with the label Case 1.

Among possible other methods of seismic retrofit, a base-isolation technique was used here as an example. The improvements to the seismic performance of transformers are evaluated based on experimental results involving such a device. The test was performed at the NCREE (National Center for Research of Earthquake Engineering) in Taiwan under the NCREE-MCEER joint research project using NCREE's shaking table (5 m x 5 m in plan and maximum payload 500 kN). The test had additional support from Bridgestone Corporation in Tokyo, Japan. The improvement is measured by the enhancement index defined as:

$$\text{Enhancement Index} = (A_f/A_i)\text{-}1 \quad (1)$$

where A_f and A_i are the maximum acceleration values under fixed-base and base-isolated conditions, respectively, and are both observed at six points along the transmission tank and bushing as discussed below: One point each at the bottom and top of the transformer tank, and four points along the bushing at the following locations as measured

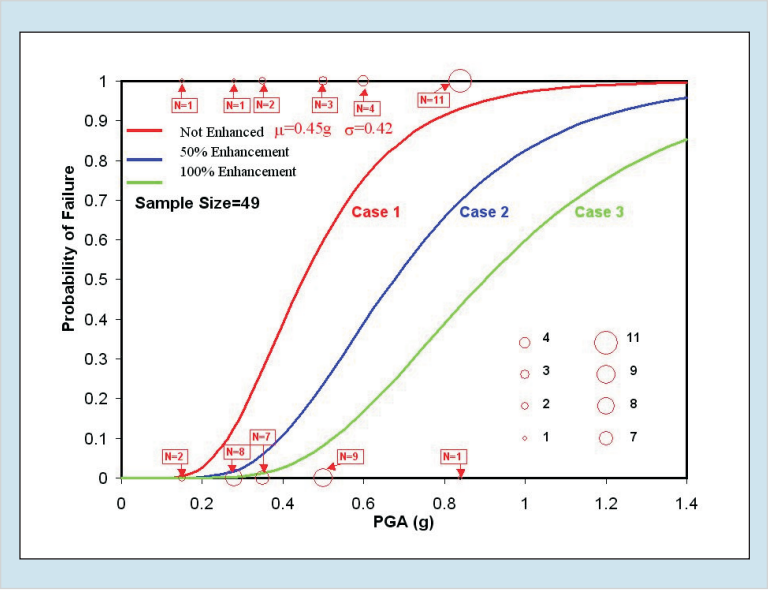

■ Figure 3. Fragility Curves for Transformers in Transmission Network

from the middle flange of the bushing.

- 161 kV bushing: 1st point: -112 (cm), 2nd point: -60 (cm), 3rd point: +88 (cm), 4th point: +197.5 (cm).
- 69V bushing: 1st point: -64 (cm), 2nd point:-30 (cm), 3rd point:+41 (cm), 4th point: +100 (cm)

The experiment used two types of bushings, one for 69 kV and another for 161 kV. Each was attached on the top of a rigid box-shaped frame simulating a transformer tank. In the test, three actual earthquake records were used as input earthquake ground motions: 1940 El Centro, 1994 Northridge (Sylmar) and 1995 Kobe (Takatori). Each of these records is linearly scaled in order to produce five histories with PGA equal to 0.125g, 0.25g, 0.375g, 0.50g and 0.625g, to compute the enhancement index values. However, to avoid potential significant bushing damage caused by large vibrations in the test, the records with high PGAs were not applied during the testing of the fixed-based cases. The maximum PGA for the fixed-based cases is therefore limited to 0.375g, while the maximum PGA for the base-isolated cases is 0.5g (only the Northridge ground motion record at Sylmar Convertor Station has a PGA value of 0.625g.). Each bushing-tank system is subjected to the simulated earthquake records both with and without a base-isolation device. The effectiveness of the enhancement is statistically shown in Figure 4. Table 1 gives the statistical characteristics of the enhancement index from a sample size of 56 for 69 kV and 71 for 161 kV bushings. More detailed statistical analysis is being carried out grouping the acceleration records at each spatial point of measurement. Both Figure 4 and Table 1 show that the improved seismic performance of the transformers is very significant, with a mean value of enhancement index ranging from 1.6 to 3.5. Therefore, in the following analysis, the 50% and 100% enhancement index values are considered to be achievable and are used. However, no change in log-standard deviation is considered. The enhanced fragility curves are also plotted in Figure 3 (blue and green for 50% and 100% enhancement, labeled as cases 2 and 3, respectively).

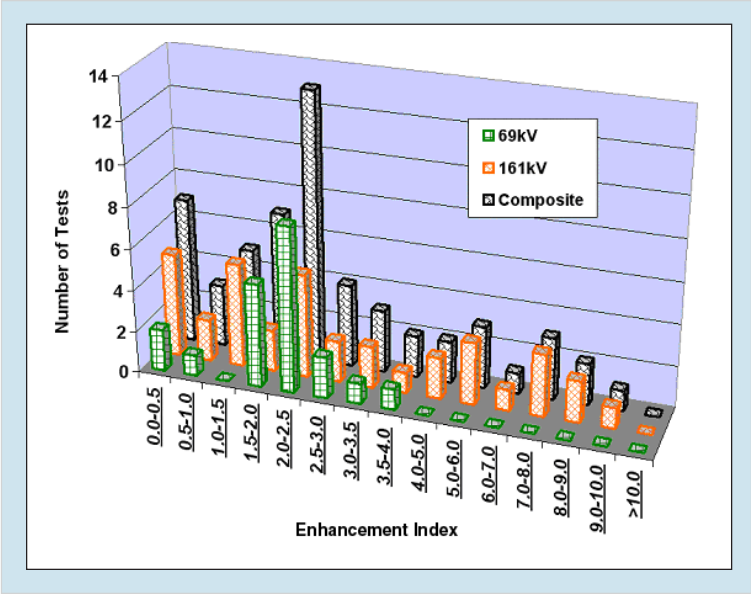

Figure 4. Statistical Distribution of Enhancement of Transformers with the Base-Isolation Device

Table 1. Statistical Characteristics of Enhancement Results

	Mean	Standard Deviation
69kV System	1.611	0.751
161kV System	3.508	2.684
Combined	2.690	2.272

Web Sites

Professor Shinozuka:
http://shino8.eng.uci.edu

Shake Map Home Page:
http://quake.wr.usgs.gov/research/strongmotion/effects/shake

Western Electricity Coordinating Council:
http://www.wecc.biz/main.html

Seismic Performance of LADWP's Power System

The LADWP's network is part of the very large WSCC's (Western Systems Coordinating Council's) power transmission network, which covers 14 western states in the U.S., two Canadian provinces and northern Baja California in Mexico. The present analysis is performed by taking all the receiving stations and transmission facilities covered by the WSCC network into account. Parenthetically, it is noted that the WSCC's network has been expanded to add some additional components and is presently referred to as WECC (Western Electricity Coordinating Council, *http://www.wecc.biz/main.html*). The proposed analysis methodology to predict the seismic performance of the electrical power network is described below:

1. Use 47 scenario earthquakes (13 Maximum Credible and 34 User Defined, *http://shino8.eng.uci.edu/Scenario_Earthquakes/47Scenario.pdf*)
2. For each scenario earthquake, simulate equipment damage using fragility curves with and without rehabilitation
3. Simulate damaged transmission networks
4. Calculate power flow using IPFLOW under network failure criteria
   - Imbalance of Power

$$1.05 < \frac{total\ \ supply}{total\ \ demand} < 1.1 \qquad (2)$$

   - Abnormal voltage

$$\left| \frac{V_{intact} - V_{damage}}{V_{intact}} \right| > 0.1 \qquad (3)$$

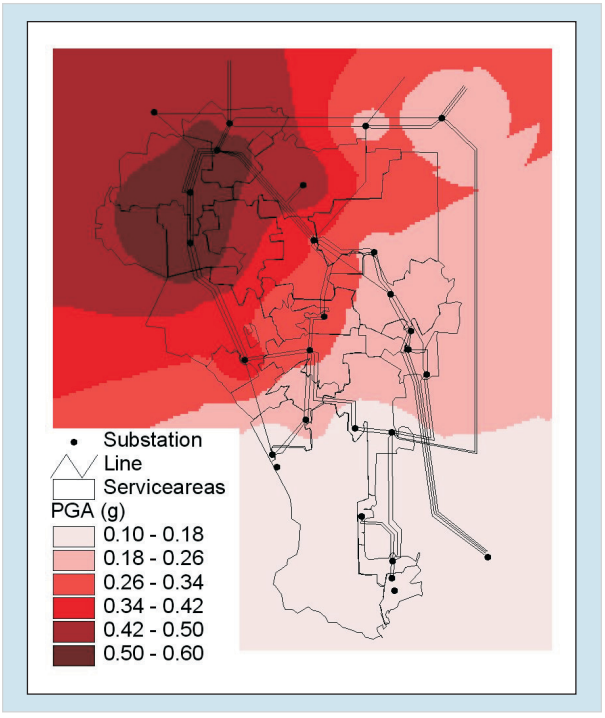

Figure 5. PGA under Northridge Earthquake

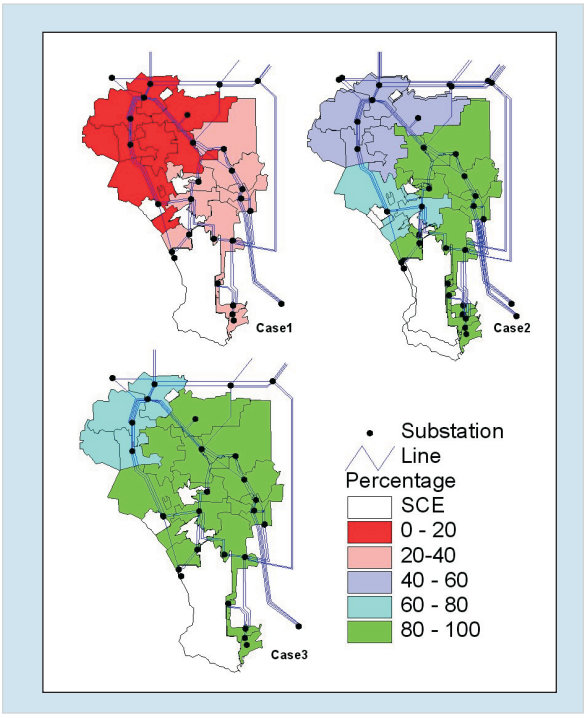

Figure 6. Relative Average Power Output with only Transformers Vulnerable

- Frequency change (IPFLOW does not check this)
- Loss of connectivity

5. Compute reduction in average power supply (total and for each service area)
6. Compute relative number of households without power
7. Develop seismic risk curves (annual probability that system performance will be reduced by more than a specified level due to earthquake)
8. Examine system performance relative to performance criteria with and without rehabilitation
9. Determine effectiveness of rehabilitation

By applying the systems analysis procedures, LADWP's power flow analysis is performed 20 times on the network for each scenario earthquake. Each simulation result represents a unique state of network damage. Figure 5 shows the PGA distribution associated with the Northridge earthquake in LADWP's service areas. Figure 6 shows the ratio of the average power supply of the damaged network to that associated with the intact network for each service area when only transformers are considered as vulnerable. The average is taken over the entire sample size equal to 20. The extent to which the rehabilitation of transformers contributes to improvement of system performance is evident if the power supply ratios under Case 1 (not enhanced), Case 2 (50% enhanced) and Case 3 (100% enhanced) are compared (see Figure 6).

Aside from transformers, there is important electrical equipment in the power network which are also vulnerable to earthquakes, such as circuit breakers and disconnect switches. Figures 7 and 8 show the seismic performance analysis results involving these equipments, using the same fragility characteristics as for the transformers. The results show that if transformers and circuit breakers (Figure 7) or transformers and disconnect switches (Figure 8) are considered to be vulnerable under earthquakes, the power output is significantly reduced throughout LADWP's service areas under the Northridge earthquake.This result matches the actual outcome in the 1994 Northridge earthquake. It is noted that the black-out was short-lived, due to effective restoration management on the part of LADWP. It is also notable that the actual recovery process followed the pattern of power supply restoration in the order similar to Figure 7 or 8 → Case

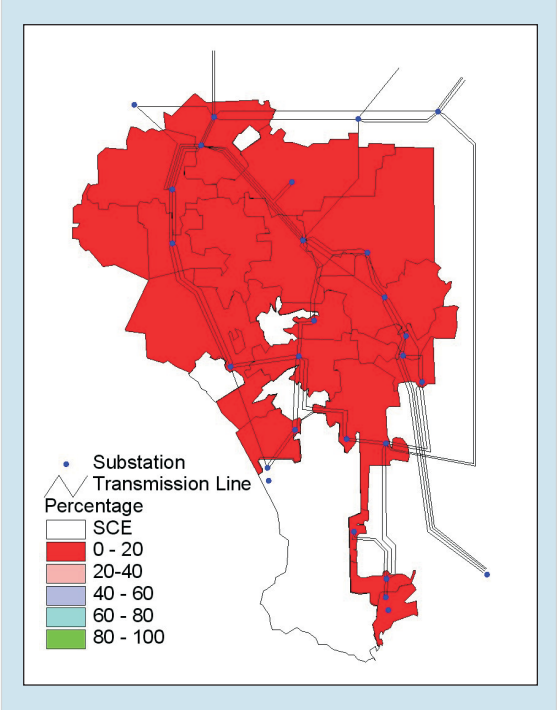

Figure 7. Relative Average Power Output with Transformers, Circuit Breakers Vulnerable

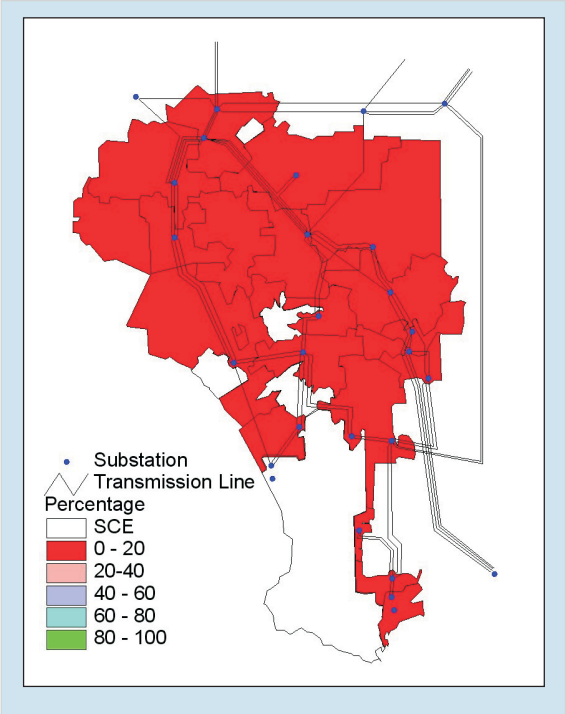

Figure 8. Relative Average Power Output with Transformers, Disconnect Switches Vulnerable

1 (Figure 6) → Case 2 → Case 3. The fact that a black-out condition occurred not only for LADWP's service area but also over several states after the Northridge earthquake demonstrates the far-reaching impact of a local system failure throughout the western grid.

Risk Curves of LADWP's Power System

The locations of LADWP's and SCE's receiving stations relative to faults in and around the Los Angeles area indicates that many are near active faults and have a high possibility of suffering damage should an earthquake occur. In evaluating the risk and costs associated with potential future earthquakes, the performance of the power system in 47 (deterministic) earthquake scenarios was evaluated. These scenarios were developed by Chang et al., 2000, applying a loss estimation software tool, EPEDAT, which was used to generate regional ground motion patterns for a given earthquake epicenter, magnitude, and depth. The 47 events included 13 maximum credible earthquakes on various faults in the Los Angeles region and 34 smaller events of magnitude 6.0 or higher. Based on these analyses, together with their hazard-consistent probabilities, seismic risk of LADWP's power system due to earthquake-induced performance degradation was developed in terms of a risk curve for Case 1 (no enhancement) and Cases 2 and 3 (enhancement index 50% and 100%, respectively), shown in Figure 9.

The percentage of households with and without power supply are computed as follows:

Relative number of households with power:

$$= \frac{\sum_{m=1}^{M} \frac{1}{N} \sum_{n=1}^{N} Rd(m,n) \times Hshld(m)}{\sum_{m=1}^{M} Hshld(m)} \quad (4)$$

Relative number of households without power:

$$= 1 - \frac{\sum_{m=1}^{M} \frac{1}{N} \sum_{n=1}^{N} Rd(m,n) \times Hshld(m)}{\sum_{m=1}^{M} Hshld(m)} \quad (5)$$

where m is the service area number $(1,2,\ldots,M)$, n is the simulation number $(1,2,\ldots,N)$, $Rd\,(m, n)$ is the power output ratio of service area m under simulation n, and $Hshld\,(m)$ is the total households of service area m.

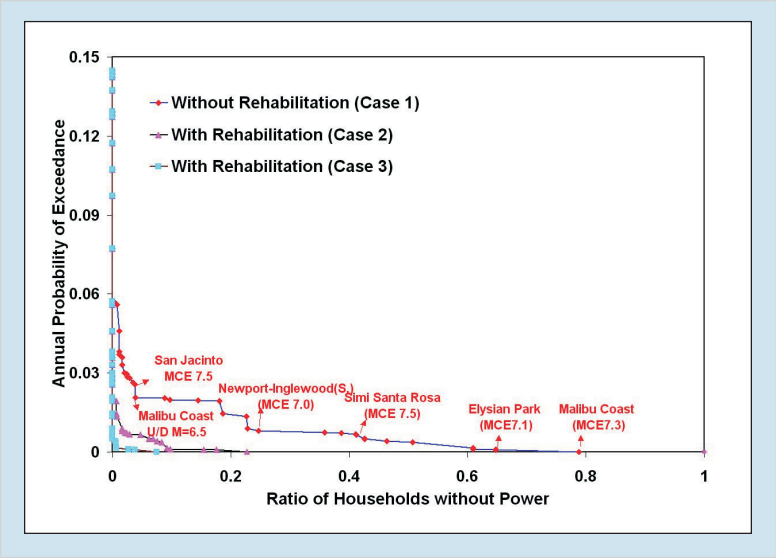

Figure 9. Risk Curves of LADWP's Power System

The risk curve in this study plots the expected annual probability that the system will suffer from a power supply reduction of more than a specified rate, as a function of that rate. Each data point in the figure represents one of the scenario events. The risk curve is useful for economic impact analysis of the Los Angeles area as well as cost and benefit analysis to determine the effectiveness of enhancement technologies. Of equal importance is the use of the risk curve in relation to the development of the performance criteria and their verification as described in the following section.

System Performance Criteria

The performance criteria for power systems listed in Tables 2 and 3 demonstrate a possible format in which the criteria can be given. Table 2 lists criteria to be satisfied in pre-event assessment, and Table 3 lists those in post-event emergency response. These tables also include performance criteria for water and acute care hospital systems. In combination, they conceptually establish the degree of community resilience in terms of robustness, rapidity and reliability. Specific values (in percentages for

Table 2. Statistical Performance Criterion I for Pre-event Assessment and Rehabilitation

	Robustness and Resourcefulness	Reliability
Power	A majority (at least 80%) of households will have continued power supply after earthquake	With a high level of reliability (at least 99% per year).
Water	A majority (at least 80%) of households will have continued water supply after earthquake	With a high level of reliability (at least 99% per year).
Hospital	A majority (at least 95%) of injured or otherwise traumatized individuals will be accommodated in acute care hospitals for medical care	With a high level of reliability (at least 99% per year).

Table 3. System Performance Criterion II for Post-Event Response and Recovery

	Robustness and Resourcefulness	Reliability
Power	A majority (at least 95%) of households will have power supply as rapidly as possible within a short period of time (3 days)	With a high level of reliability (at least 90% of earthquake events).
Water	A majority (at least 95%) of households will have water supply as rapidly as possible within a short period of time (3 days)	With a high level of reliability (at least 90% of earthquake events).
Hospital	All the injured and traumatized individuals will be accommodated in acute care hospitals as rapidly as possible within a short period of time (1 day)	With a high level of reliability (at least 90% of earthquake events).

robustness, rapidity in restoration and reliability) are examples included to better understand the concept. The performance criterion for power systems shown in Table 2 is represented by a point double-circled in Figure 10 (enlarged version of Figure 9), where the robustness corresponds to the annual probability that 80% or more households will have power immediately after any earthquake is equal to 0.99. The risk curve for Case 1 (without rehabilitation) does not satisfy this criterion, but the risk curves for Case 2 and Case 3 (with rehabilitation) do satisfy it. These criteria can also be used to judge the effectiveness of rehabilitation as carried out in this study. Data collection and modeling for rapidity in restoration are much more difficult to pursue. Further research is needed to develop analytical models based on past experience so that performance criteria, such as those shown in Table 3, become meaningful in practice.

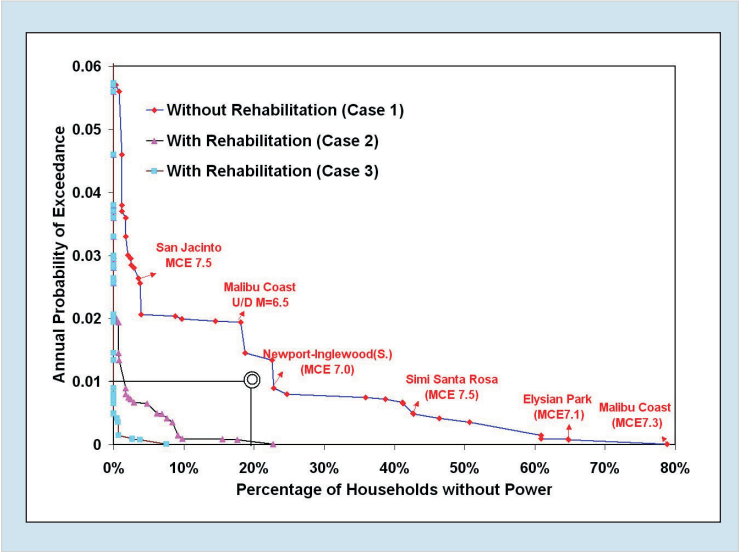

Figure 10. Annual Probability of Exceedance for Households without Power (enlarged view)

Evaluating Mitigation of LADWP's Power System

The evaluation of seismic mitigation for urban infrastructure systems is carried out by applying the life cycle cost method, particularly to LADWP's power system used in this study. The word "mitigation" here is used in a much broader sense than "rehabilitation." The latter refers to specific seismic retrofit of systems and their components, as described below. In contrast to more traditional benefit-cost analysis, the life cycle cost framework readily and transparently accommodates costs that may change over time. For infrastructure systems, this is advantageous for addressing

■ Table 4. Life Cycle Cost Results

	Unmitigated Case	Mitigated Case
Mitigation Cost	$ 0.00	$ 6.54
Repair Cost (discounted)	$ 0.39	$ 0.07
Revenue Loss (discounted)	$ 1.28	$ 0.14
Direct Economic Loss (discounted)	$ 95.52	$ 10.45
Total Life Cycle Costs	$ 97.19	$ 17.19
Total Life Cycle Costs without Direct Economic Loss	$ 1.67	$ 6.75

such issues as infrastructure deterioration and urban growth. Moreover, the framework developed here emphasizes costs that would be imposed on the community, as well as the lifeline agency, in the event of infrastructure failure in a disaster. The framework therefore allows a comprehensive assessment of mitigation benefits. Details of the methodology, along with an application to the Portland, Oregon, water delivery system, can be found in Chang (forthcoming). In this approach, the options of "mitigation" and "no mitigation" are compared in terms of their total life cycle costs. These include repair costs, utility revenue losses, and societal losses in future earthquake disasters. These costs are evaluated for a period of N years, with expected annual costs discounted to their present value. For the mitigation case, life cycle costs also include the cost of the retrofit itself.

In this paper, the case study examines mitigation of high voltage transformers using base isolation. Hence, "mitigation" is synonymous to "retrofit by base-isolation" here. The impact of the mitigation on network performance was assessed by using the results from the power flow analysis of LADWP's power system. The total life cycle cost, C, can be expressed as follows:

$$C = C_s + \sum_t \left(C_{r,t} + C_{v,t} + C_{e,t}\right) \cdot (1+y)^{-t} \qquad (6)$$

where C_s is the cost of the seismic mitigation (retrofitted) measure (assumed to take place in the initial year of analysis), $C_{r,t}$ is expected annual earthquake repair costs in year t, $C_{v,t}$ is expected annual earthquake revenue loss to the utility in year t, C_e is expected annual direct economic loss to the community in year t, and y is a discount rate (assumed to be a real rate of 3 %). The total timeframe of analysis is 50 years. All costs are evaluated in constant dollars, not of inflation. $C_{r,t}$, $C_{v,t}$, and $C_{e,t}$ are each probabilistically aggregated over the 10 or 20 simulations of the 47 earthquake scenarios, as described above.

In the analysis, the mitigated case was represented by a weighted average of the results from the "as-is," "50% performance enhancement," and "100% performance enhancement" analyses. The respective weights are 0.08, 0.12, and 0.80. These weights were based on the confidence levels associated with each performance level in the base isolation testing.

The mitigation case consists of base isolating 109 transformers. Although actual data on the mitigation cost was not available, based

on our research and consultation with LADWP, a rough estimate of $60,000 per transformer was used for this analysis. Seismic mitigation cost C_s is therefore $6.54 million.

Table 4 summarizes the four cost components for the mitigated and unmitigated cases. Mitigation leads to considerable reductions in expected repair costs and revenue loss in future earthquakes. Total discounted costs to the utility agency are reduced from $1.67 million to $0.21 million. However, these savings do not outweigh the cost of mitigation. If societal impacts are disregarded, total life cycle costs with mitigation ($6.75 million) are four times as large as costs in the do-nothing case ($1.67 million), and mitigation does not appear advisable.

However, if direct economic losses are considered, mitigation appears very cost-effective. Direct economic losses are on the order of 50 times as large as the utility's repair and revenue losses combined. If they are included in the analysis, total life cycle costs without mitigation ($97.19 million) are 5.7 times as large as costs with mitigation. Mitigation could reduce discounted, expected direct economic loss by some $85 million. Base isolation of the transformers appears highly cost-effective.

Table 5 presents the results if it is assumed that population and economic activity remain constant over the 50-year period (i.e., no urban growth or productivity increase). The basic finding – that mitigation is cost-effective if societal impacts are considered, but not if they are excluded – is unchanged. In this case, direct economic losses are on the order of 30 times as large as repair and revenue losses combined.

Evaluation of Effect of a Disabling Event on the Performance of a Remotely Located Utility System

A general methodology was also developed in this study to analyze the behavior of large electric utility systems under a catastrophic event, such as a severe earthquake or an intentional disablement of system components. The focus of this analysis is to determine the impact to LADWPs power supply capability if any of the major 500 kV transmission lines in the WSCC grid were disabled, regardless of the reason (earthquake or other hazard) or distance from the Los Angeles area. Two scenarios (A and B) involving disabled 500 kV transmission lines between Washington State and Idaho State (A) and between Washington State and Oregon State (B) are shown in Figure 11 (Scenario A) and Figure 13 (Sce-

Table 5. Life Cycle Cost Results without Urban Growth

	Unmitigated Case	Mitigated Case
Mitigation Cost	$ 0.00	$ 6.54
Repair Cost (discounted)	$ 0.39	$ 0.07
Revenue Loss (discounted)	$ 0.89	$ 0.09
Direct Economic Loss (discounted)	$ 39.38	$ 4.29
Total Life Cycle Costs	$ 40.66	$ 11.00
Total Life Cycle Costs without Direct Economic Loss	$ 1.28	$ 6.70

nario B). A red cross in the WSCC grid in the figures indicates the locations of the interruptions.

In Scenario A, power supply to the service area of LADWP is not affected very much, as shown in Figure 12. The power supply to most service areas is maintained at above 90%. Power supply in only one service area in the middle drops between 85% and 90%. The reason is that the disabled 500 kV transmission line in Scenario A is a more redundant segment in the grid as far as the LADWP power system is concerned. The effect of a power supply reduction to LADWP service areas comes from a power-load balance requirement within the entire WSCC system. For Scenario B, however, the disabled transmission line at the border of Washington and Oregon States is a less redundant component, and influences the LADWP power system through two 500 kV AC transmis-

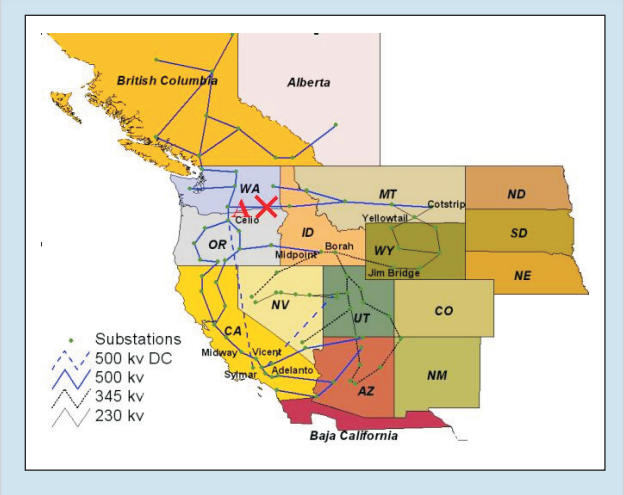

Figure 11. Disabled Location A

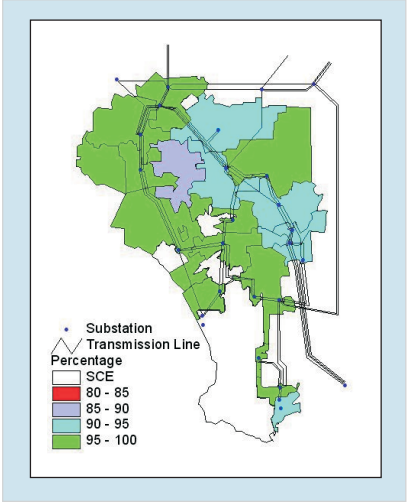

Figure 12. Reduction in Power Supply (A)

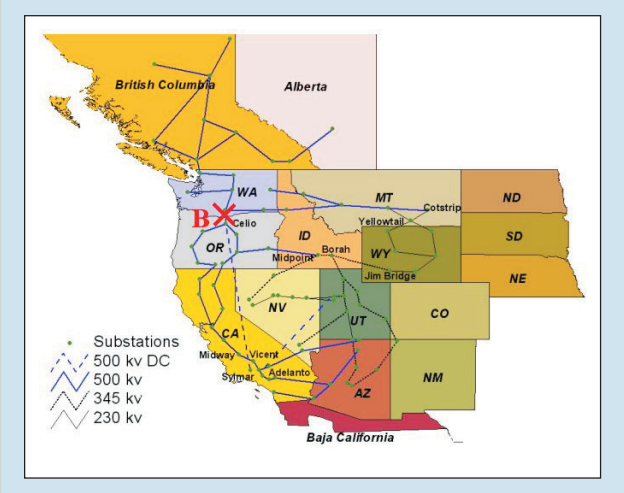

Figure 13. Disabled Location B

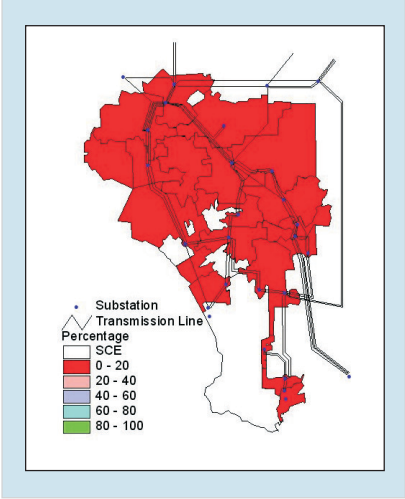

Figure 14. Reduction in Power Supply (B)

sion lines and one 500 kV DC transmission line. From Figure 14, it is seen that the entire LADWP service area is blacked out when this component is disabled. This is indeed a disaster to the LADWP service area, in spite of various redundancy and tolerance built into the system between the Pacific Northwest and Southern California.

Conclusions and Future Research

This study integrated many of the technologies developed by MCEER over the years, including GIS inventory data of the LADWP's electric transmission systems, multiple scenario earthquakes representing the Los Angeles area seismic hazard, fragility analysis of systems, sub-systems and equipment, base isolation techniques for rehabilitation of transformers, systems analysis using WSCC's database and EPRI's IPFLOW computer code, life-cycle cost estimation methods, and preliminary versions of performance criteria definitions and their verification procedures. This integration leads to the capability to evaluate the performance of both power and water systems and the consequences of system interruptions caused by earthquakes. Additional study will be undertaken to further establish performance criteria that can be quantitatively mapped into the response space, in technological, economic, organizational, and social dimensions. Future study will also include the development of probabilistic procedures to estimate the reliability of the seismic resilience of the community. Also, integration with other critical systems such as emergency response organizations, medical care systems (a regionally designated network of acute care hospitals) and highway transportation systems will be carried out to evaluate community resilience. Finally, the application of SCADA in the inverse analysis of power system performance is of significant future interest. This is to improve the time it takes to achieve restoration of system function degraded by the earthquake, which is the rapidity aspect of the resilience criteria.

Acknowledgments

This research was primarily supported by the Earthquake Engineering Research Centers Program of the National Science Foundation, under award number EEC-9701471 to the Multidisciplinary Center for Earthquake Engineering Research. This support is gratefully acknowledged.

References

Chang, S.E. and Seligson, H.A., (2003), "Evaluating Mitigation of Urban Infrastructure Systems," *Sixth U.S. Conference and Workshop on Lifeline Earthquake Engineering (TCLEE)*, Long Beach, California, Aug. 10-13.

Chang, S.E., Shinozuka, M. and Moore, J., (2000), "Probabilistic Earthquake Scenarios: Extending Risk Analysis Methodologies to Spatially Distributed Systems," *Earthquake Spectra*, Vol. 16, No. 3, August, pp. 557-572.

Dong, X.J., (2002), *The Seismic Performance Analysis of Electric Power Systems*, Ph.D Dissertation, University of Southern California, June.

Dong, X.J. and Shinozuka, M., (2003), "Performance Analysis and Visualization of Electric Power Systems," *SPIE's 10 International Symposium on Smart Systems and NDE for Infrastructures*, March 2-6.

Murota, N., (2000), *Earthquake Simulator Testing of Large Scale Electric Transformer Model and Bushing with Base Isolation System*, Masters Thesis, University of California, Irvine.

PowerWorld Corporation, (2000), *User's Guide, PowerWorld Simulator V 7.0*, October.

Saadeghvaziri, M.A. and Feng, M., (2001), "Experimental and Analytical Study of Base-Isolation for Electric Power Equipment," *Research Progress and Accomplishments: 2000-2001*, MCEER-02-SP01, Multidisciplinary Center for Earthquake Engineering Research, University at Buffalo, May, pp. 29-40, *http://mceer.buffalo.edu/publications/resaccom/0001.*

Shinozuka, M. and Dong, X., (2003), "Seismic Performance Criteria for Lifeline Systems," *8th US Japan Workshop on Earthquake Resistant Design of Lifeline Facilities and Countermeasures against Liquefaction*, Tokyo, Japan, December 15-18.

Shinozuka, M. and Eguchi, R., (1997), "Seismic Risk Analysis of Liquid Fuel Systems: A Conceptual and Procedural Framework for Guidelines Development," *Proceedings of The Northridge Earthquake Research Conference*, Los Angeles, California, August 20-22.

Shinozuka, M., Cheng, T.C., Feng, M. and Mau, S.T., (1999), "Seismic Performance Analysis of Electric Power Systems," *Research Progress and Accomplishments 1997-1999*, MCEER-99-SP01, Multidisciplinary Center for Earthquake Engineering Research, University at Buffalo, July, pp. 61-69.

Shinozuka, M., Cheng, T.C., Jin, X., Dong, X. and Penn, D., (2002), "System Performance Analysis of Power Networks," *Seventh U.S. National Conference on Earthquake Engineering (7NCEE)*, Boston, Massachusetts, July 21-25.

Shinozuka, M., Feng, M., Lee, J. and Naganuma, T., (2000), "Statistical Analysis of Fragility Curves," *Journal of Engineering Mechanics*, ASCE, Vol. 126, Issue 12, Dec, pp. 1224-1231.

Shinozuka, M., Rose, A. and Eguchi, R. (eds.), (1998), *Engineering and Socioeconomic Impacts of Earthquakes: An Analysis of Electricity Lifeline Disruptions in the New Madrid Area*, Monograph No. 2, Multidisciplinary Center for Earthquake Engineering Research, University at Buffalo.

Tanaka S., Shinozuka, M., Schiff, A. and Kawata, Y., (1997), "Lifeline Seismic Performance of Electric Power Systems during the Northridge Earthquake," *Proceedings of The Northridge Earthquake Research Conference*, Los Angeles, California, August 20-22.

REDARS 1: Demonstration Software for Seismic Risk Analysis of Highway Systems

by Stuart D. Werner, Jean-Paul Lavoie, Chip Eitzel, Sungbin Cho, Charles Huyck, Shubharoop Ghosh, Ronald T. Eguchi, Craig E. Taylor and James E. Moore II

Research Objectives

The objective of this research is to further develop, apply, program, and disseminate the methodology for seismic risk analysis (SRA) of highway-roadway systems that was developed under FHWA-MCEER Project 106. The methodology's risk-based framework uses models for seismology and geology, engineering (structural, geotechnical, and transportation), repair and reconstruction, system analysis, and economics to estimate system-wide direct losses and indirect losses due to reduced traffic flows and increased travel times caused by earthquake damage to the highway system. Results from this methodology also show how this damage can affect access to facilities critical to emergency response and recovery.

For the past several years, the Multidisciplinary Center for Earthquake Engineering Research has been carrying out highway research under the sponsorship of the Federal Highway Administration. One task from this research has developed a new methodology for deterministic and probabilistic seismic risk analysis (SRA) of highway systems nationwide, and has applied it to the Shelby County, Tennessee highway system (Werner et al., 2000). This methodology will enable users to evaluate and prioritize how various pre-earthquake seismic-risk-reduction strategies (e.g., strengthening of particular bridges, system enhancement) and post-earthquake emergency-response strategies (e.g., traffic management, emergency bypass road construction) will improve post-earthquake traffic flows and reduce associated losses.

During the past year, this SRA methodology has been independently validated (Eguchi et al., 2003), and a plan for developing the methodology into a public-domain software package named REDARS (**R**isks from **E**arthquake **DA**mage to **R**oadway **S**ystems) has been completed (Werner et al., 2003). This software will be programmed, beta-tested, applied to actual highway systems, and disseminated during the remainder of this research project.

However, before undertaking this effort, it was decided to first develop interim demonstration software (REDARS 1). This software, now completed, performs simplified deterministic SRA of the Los Angeles area high-

Sponsors

Federal Highway Administration

Research Team

Stuart D. Werner, *Principal, Seismic Systems & Engineering Consultants*
Jean-Paul Lavoie*, Partner, and* ***Chip Eitzel,*** *Partner, Geodesy*
Ronald T. Eguchi*, President,*
Sungbin Cho*, Senior Transportation Planner,*
Charles Huyck*, Senior Vice President, and*
Shubharoop Ghosh*, Project Transportation Planner, ImageCat Inc.*
Craig E. Taylor*, President, Natural Hazards Management Inc.*
James E Moore II*, Professor, Departments of Civil Engineering and Public Policy and Management, University of Southern California, Los Angeles*

Previous Summaries

2000-2001:
Werner, http://mceer.buffalo.edu/publications/resaccom/0001/rpa_pdfs/07werner_f.pdf

1997-1999:
Friedland et al., http://mceer.buffalo.edu/publications/resaccom/9799/Ch12frie.pdf

way system subjected to scenario earthquakes for which SHAKEMAP ground motion data (TriNet, 2002) are available. Development of this interim software was motivated by the interest of several state highway-transportation agencies, and the need to: (a) provide a simple tool to familiarize these agencies with basic SRA concepts, while the more extensive public-domain software (REDARS 2) is being developed; and (b) enable these agencies to provide early feedback regarding desirable features to include in REDARS 2. This paper summarizes the main features and steps for applying the REDARS 1 interim software, many of which are expected to be included in REDARS 2. Table 1 summarizes the technical features of REDARS 1 and those being included in REDARS 2.

Because REDARS 1 was developed over a short time frame, without beta testing, and with more limited objectives and models than REDARS 2, it is intended for use as a demonstration tool only. However, as such a tool, REDARS 1 provides a rapid and efficient SRA learning vehicle, and also illustrates a wide range of possible types and forms of SRA results.

REDARS 1 Overview

For each set of SHAKEMAP ground motions, REDARS 1 provides SRA results for the Los Angeles area's status-quo highway system (before any repair, seismic upgrade, or traffic-management options are considered.) Then, users can model various repair or seismic-risk-reduction options in REDARS 1, after which the SRA can be rerun to obtain results that show how well these options improve post-earthquake traffic flows and reduce economic losses.

Extent of Mapped Area

The extent of the Los Angeles area that is covered in REDARS 1 is as follows: (a) the northern extremity is just south of CA-126 and the town of Santa Clarita; (b) the southern extremity is just south of the Century Freeway (I-105), which extends from the Los Angeles Airport to the west and the city of Norwalk to the east; (c) the eastern extrem-

This SRA methodology will provide cost and risk information that will facilitate more rational evaluation of alternative seismic risk reduction strategies by decision makers from government and transportation agencies involved with improvement and upgrade of the highway-roadway infrastructure, emergency response planning, and transportation planning. Such strategies can include prioritization and seismic strengthening measures for existing bridges and other components, establishment of design criteria for new bridges and other components, construction of additional roadways to expand system redundancy, and post-earthquake traffic management planning.

■ Table 1. Technical Features of REDARS 1 and REDARS 2 (Werner et al., 2003)

Feature	Demo (REDARS 1)	Public Domain (REDARS 2)
Type of Analysis	Deterministic	Deterministic and Probabilistic
Modularity	Not modular	Will be modular to facilitate adding new or updated seismic-hazard, component vulnerability, or repair/functionality models in future.
Seismic Hazards		
Ground motions	From SHAKEMAP, for actual and hypothetical EQs in Los Angeles area.	Region-specific or imported models.
Others (liquefaction, surface fault rupture and landslide)	No	Liquefaction and surface fault rupture included. Landslide can be added in future.
Bridges		
New or retrofitted bridges	New only	New and retrofitted (when available)
Seismic hazards	Default model for ground shaking hazards only.	Default models for ground-shaking and ground deformation hazards (which can be overridden by separate user-specified fragility model for any bridge in network) .
Repair/functionality models	First-order default model only.	Default model (which can be overridden with user-specified model that better reflects post-EQ repair resources in that particular region.
Other components (tunnels, pavements, embankments, walls, and culverts)	No.	Tunnels and pavements to be included. Other components can be added in future.
Transportation network analysis	User Equilibrium (UE) method, with post-EQ trip demands assumed equal to pre-EQ demands.	UE method with fast numerical algorithms, and with congestion-dependent post-EQ trip demands not necessarily same as pre-EQ demands.
Economic Loss Estimates	First-order (based on travel time delays)	First-order (based on travel time delays)
Variance Reduction (statistical methods to reduce number of simulations needed to attain a given confidence level)	No	Yes
Input Data Wizard (to facilitate input data development)	No	Yes
Decision Guidance Post-Processor	No	Yes

ity is just east of downtown Los Angeles; and (d) the western extremity is the Pacific Ocean.

Earthquakes

REDARS 1 includes SHAKEMAP ground motion estimates within the above-indicated mapped area for: (a) actual earthquake events consisting of the San Fernando (1971), Whittier Narrows (1987), and Northridge (1994) earthquakes; and (b) hypothetical earthquakes estimated for rupture scenarios for the Newport-

Links to Current Research

The fragility models for retrofitted bridges being developed by Shinozuka and others will be incorporated into the REDARS 2 software. In addition, the development of an input data wizard by Eguchi and others at ImageCat will be a valuable addition to REDARS for facilitating the development of highway network input data.

MCEER Team

***Ian G. Buckle**, University of Nevada, Reno*

***Jerry O'Connor,** Multidisciplinary Center for Earthquake Engineering Research*

***Masanobu Shinozuka**, University of California at Irvine*

Inglewood, the Raymond Fault, the 1857 event along the San Andreas Fault, the Santa Monica Fault, and the Whittier Fault.

SRA Methodology

The SRA methodology that is implemented in REDARS 1 is the deterministic element of the general deterministic and probabilistic approach described in Werner et al. (2000). For SHAKEMAP representations of ground motions in the above mapped area, REDARS 1 uses: (a) a rapid-pushover approach (Dutta and Mander, 1998; Mander and Basoz, 1999) to estimate median damage states for each bridge in the highway-roadway network; (b) a default model described in Werner et al. (2000) to estimate bridge traffic states as a function of bridge damage state, number of spans, and number of lanes; (c) a User Equilibrium algorithm to estimate traffic flows and travel times for each post-earthquake system state (Moore et al., 1997); and (d) the Caltrans (1994) model for estimating economic losses as a function of travel-time delay. The following paragraphs summarize these and other elements of the REDARS 1 SRA approach, together with additional features that will be included in REDARS 2.

Ground Motion Uncertainties

There are significant uncertainties in estimating ground motions throughout a spatially distributed highway system, and these uncertainties can have major effects on the estimated bridge damage and economic losses. Because REDARS 1 is deterministic, it cannot directly account for these uncertainties. However, as discussed later in this paper, REDARS 1 does enable the user to manually change the computed ground motions at any bridge site in order to facilitate limited sensitivity studies of the effects of ground motion variations on bridge- and highway-network performance. Of course, the probabilistic element of REDARS 2 will enable ground-motion uncertainties to be modeled directly.

Bridge Damage-State Uncertainties

As originally developed, the rapid-pushover method leads to bridge fragility curves that account for uncertainties in damage-state estimation. Because REDARS 1 is deterministic, it cannot directly account for these uncertainties; i.e., its SRA calculations consider only the 50th percentile damage state estimates from the rapid-pushover method. However, as noted later in this paper, REDARS 1 enables the user to manually change these damage states for any bridge. This will facilitate limited sensitivity studies of effects of damage-state uncertainties on highway-system performance, as well as limited evaluations of the effectiveness of various pre-earthquake seismic upgrade options or post-earthquake repair options. Of course, in contrast to this, the probabilistic element of REDARS 2 represents these uncertainties by directly using bridge–fragility models. (As noted later in this paper, these consist of rapid-pushover models as default curves which can be overridden for any bridge by more refined user-developed curves.)

Bridge Modeling Simplifications

The rapid-pushover method was developed to provide a simplified and rapid approach that uses avail-

able electronic bridge data in the current National Bridge Inventory (NBI) database (FHWA, 1995) for estimating damage to large number of bridges that would ordinarily need to be considered in SRA of a highway system. These simplifications (in which such factors as foundation and abutment response, effects of bridge retrofit, and bridge structural-system response are not included) could have important effects on bridge damage-state estimates.

Although more rigorous bridge damage-estimation procedures are available, their use in SRA applications methods will require additional structural-attribute data beyond that in the NBI database, and will also be more time-consuming to apply for large numbers of bridges. The use of improved damage-state estimation procedures, and development of electronic structural-attribute databases needed to apply these procedures, should be a focus of future research.

In recognition of this issue, REDARS 2 will enable users to input their own fragility curves for any bridge in the system. These curves would be developed beforehand, using whatever level of analytical rigor is deemed appropriate, and would then input these curves into REDARS by manually overriding the default fragility curves. Also, the modular structure of REDARS 2 will facilitate its accommodation of improved bridge-fragility models, as they are developed from future research programs.

Bridge Functionality Model

The model used in REDARS 1 for estimating bridge traffic-states as a function of bridge damage (and time after the earthquake) was originally developed to represent average default conditions throughout the United States. However, it is clear that the ability to implement repairs after a damaging earthquake will vary between different regions of the country, according to available repair resources and past experience in post-earthquake bridge repair. For example, the rapid recovery of the Los Angeles area highway system after the 1994 Northridge Earthquake was undoubtedly due in large part to lessons learned by Caltrans from past earthquakes, and also to their implementation of a bonus-incentive program to accelerate bridge repairs. Such factors are not considered in the REDARS 1 bridge traffic-state model.

In recognition of this issue, REDARS 2 will enable users to override these default models, and instead use their own traffic-state or functionality models that reflect user assessments of their repair experience/resources for the actual highway system being analyzed. This will also enable users to implement sensitivity studies of how changes in the repair process (e.g., deploying additional resources or a bonus-incentive program) can reduce potential losses due to highway-roadway system damage.

Transportation Network Analysis Procedures

Analysis of post-earthquake traffic flows in REDARS 1 is based on a User-Equilibrium (UE) model of transportation-system user behavior, which assumes that all users follow routes that minimize their travel times. In the application of this model in REDARS 1, it is assumed that post-earthquake trip

demands on the highway system are equal to pre-earthquake trip demands.

Past experience has shown that, following a major earthquake, the potential for increased congestion due to earthquake-induced roadway damage and closure can affect post-earthquake trip demands, causing them to be reduced (possibly substantially) relative to pre-earthquake demands. In recognition of this important issue, a new "variable-demand" approach has been developed for estimating post-earthquake trip demands as post-earthquake congestion (which, in turn, will depend on the extent of earthquake damage to the highway-roadway system.) This new model is now being tested, and will be included in the forthcoming REDARS 2 software.

As further discussed later in this paper, REDARS 1 includes an option to add equivalent "detour links", in order to facilitate assessment of the effectiveness of various traffic management strategies in improving post-earthquake traffic flows and travel times. REDARS 2 will also include this option.

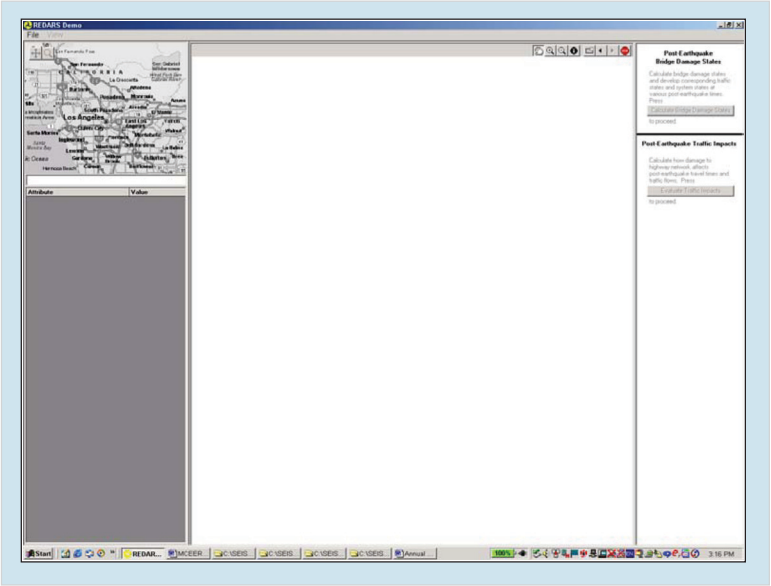

Figure 1. Opening of REDARS 1

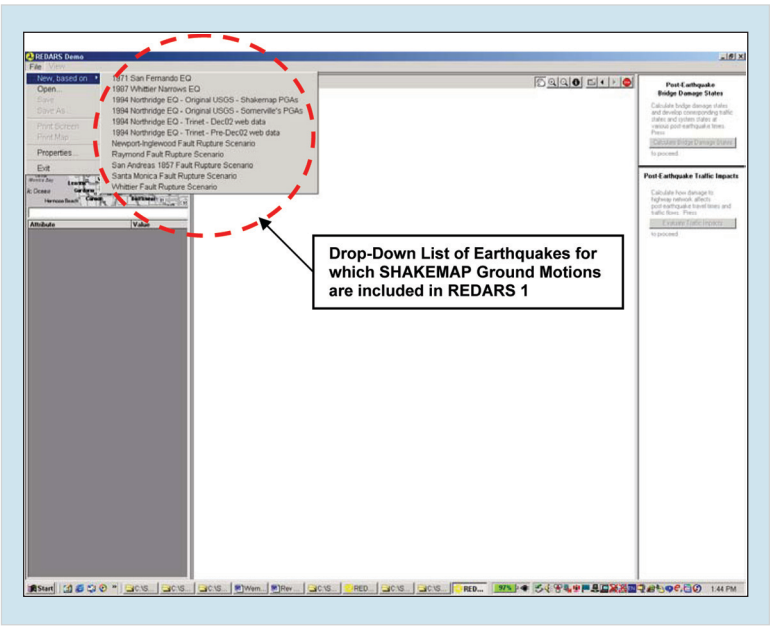

Figure 2. Selection of Earthquake to be Considered in Seismic Risk Analysis

REDARS 1 Implementation

Opening of REDARS 1

REDARS 1 is opened by clicking on the REDARS icon on the user's desktop or in his/her program file. When REDARS 1 is opened, the screen shown in Figure 1 is displayed.

Selection of Scenario Earthquake

The user then selects the scenario earthquake to be analyzed by clicking on "File", and then on "New" as shown in Figure 2. This displays the drop-down menu shown in Figure 2, which lists the various scenario earthquakes for which SRA of the

Los Angeles area highway system can be carried out by REDARS 1.

Displays of Input Data Prior to Initiation of SRA

When an earthquake scenario is selected, REDARS 1 displays the epicenter location as shown in Figure 3. Then, if it is desired to further examine various input data for the SRA, the user can click on "Map Views" in the toolbar for REDARS 1. This produces the drop-down menu shown in Figure 4, which shows that the user can display map views for the following input data: (a) NEHRP soil conditions at each bridge site (see Figures 5 and 6); (b) ground motions (spectral accelerations at periods of 0.3 sec. and 1.0 sec.) at each bridge site (see Figure 7); (c) the pre-earthquake roadway network; and (d) pre-earthquake traffic volumes. In this, Figures 5 and 6 show how legends can be added to these figures, by clicking on ""Map Legends" in the drop-down menu shown in Figure 5.

The user can also access tabular displays of input data for any bridge or link in the highway-system model by clicking on the "Select a Feature" button in the toolbar, and then clicking on the appropriate bridge or link (see Figure 6.) This feature is further described later in this paper.

Computation of Bridge Damage States

The next step in the application of REDARS 1 is to initiate calculation of damage states for all bridges in the system, when the bridges are

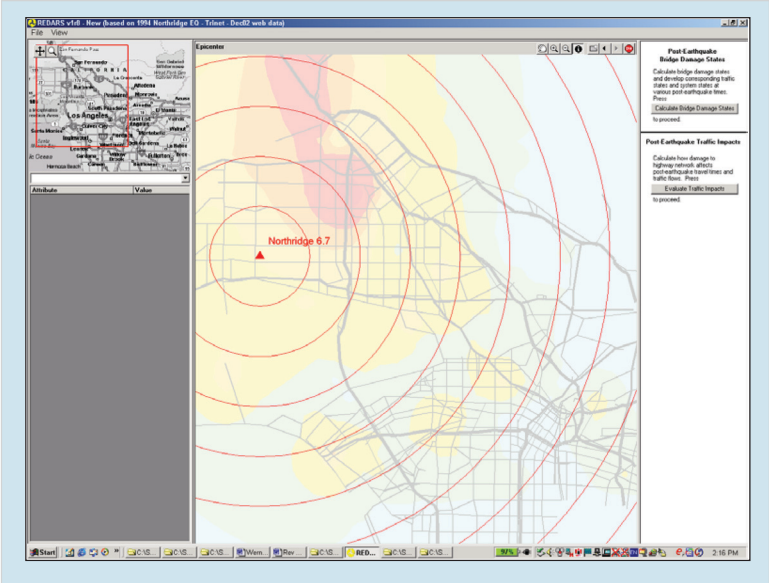

Figure 3. Display of Epicenter for Selected Earthquake

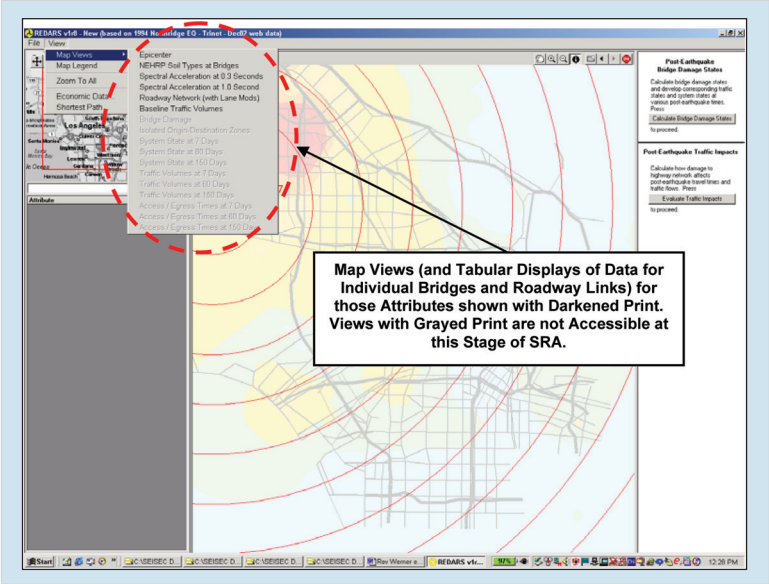

Figure 4. Display of Available Map Views before Initiating SRA Calculations

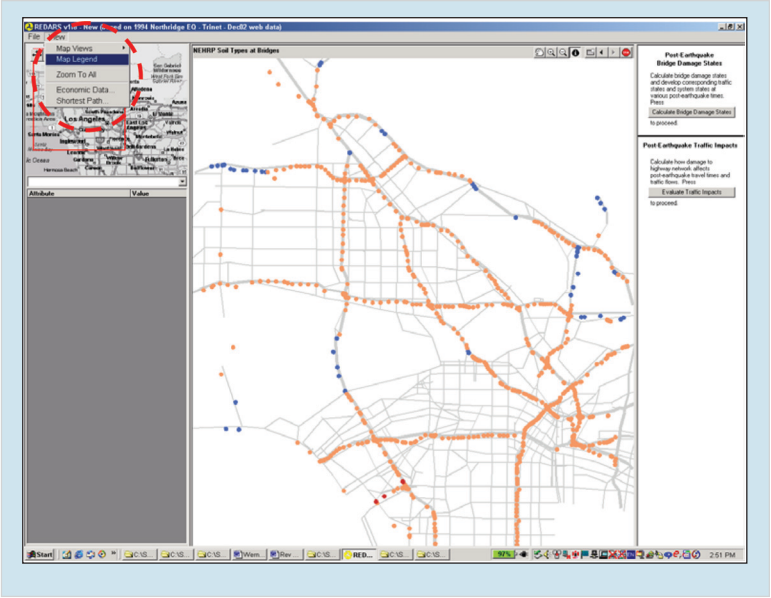

Figure 5. Display of NEHRP Soil Conditions at Each Bridge Site (without map legend) and Access of Map Legends for Various Map Views

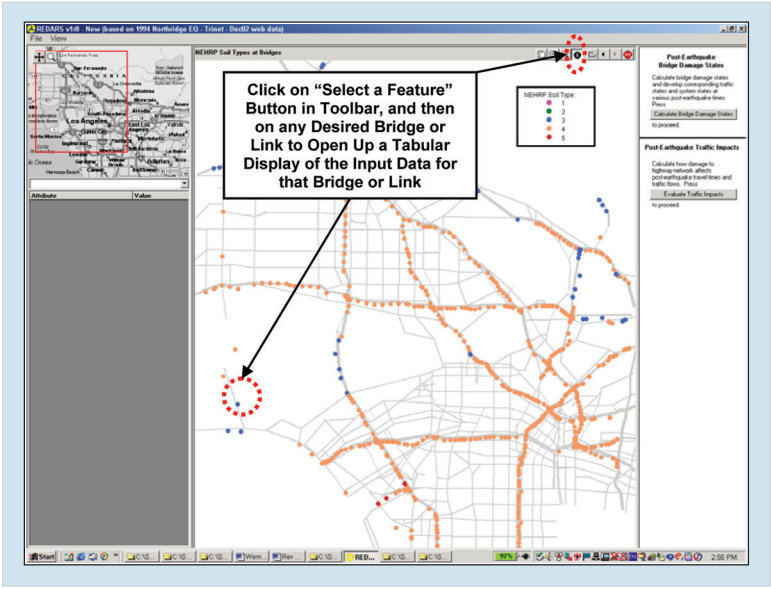

Figure 6. Display of NEHRP Soil Conditions at Each Bridge Site (with Map Legend) and Access of Tabular Displays of Input Data for any Bridge or Link

subjected to the SHAKEMAP ground motions for the selected scenario earthquake. This is accomplished by clicking on the "Calculate Bridge Damage States" button shown in Figure 7.

When these calculations are completed, REDARS 1 automatically provides the following displays for the existing (status-quo) bridges: (a) a map view showing each bridge's damage state; and (b) a tabular summary of the damage-state results. These displays are shown in Figure 8. Figure 8 also shows that the list of map views and data tables that can now be accessed is expanded (relative to the earlier list shown in Figure 4) to also include bridge-damage information.

Transportation Network-Analysis Computation

After computing the bridge damage states, the user will initiate the calculation of the post-earthquake traffic flows and travel times by clicking on the "Evaluate Traffic Impacts" button as shown in Figure 8. As these calculations proceed, their status is continually displayed (Figure 9.)

When the calculations are completed, REDARS 1 automatically provides the following displays: (a) a map view of the bridge damage states and the roadway system state 7-days after the earthquake; and (b) a tabular summary of composite travel-times for the baseline (pre-earthquake) condition and at times

of 7-, 60-, and 150-days after the earthquake; and (c) the economic losses due to the differences between these pre- and post-earthquake travel-times[1]. These displays are shown in Figure 10 for the status-quo highway system. Figure 10 also shows that the list of map views and data tables that can now be accessed is expanded (relative to the prior list shown in Figure 8) to now also include system-states, traffic-volumes, and access-egress times between origin-destination (O-D) zones throughout the region at times of 7-, 60-, and 150-days after the earthquake. Figures 11 and 12 show map views of traffic volumes and access-egress times respectively for the status-quo highway system at 7-days after the earthquake.

Modifications of Map Views

REDARS 1 enables the user to change the location and/or size of the area within the Los Angeles region for which the SRA input data and results are displayed. This is accomplished by clicking on the appropriate button in the REDARS 1 toolbar. Figure 13 shows that these buttons will enable the user to:(a) "pan" (translate the view);(b) enlarge or reduce the size of the area of the region included in the display — by selecting one of the various "zoom" buttons;(c) "identify a feature", which enables the user to select a particular bridge, roadway link, or O-D zone and display locations, attributes, and pre- and post-earthquake performance data; (d) refresh the view shown on the screen (if certain attributes have been manually changed by the user,

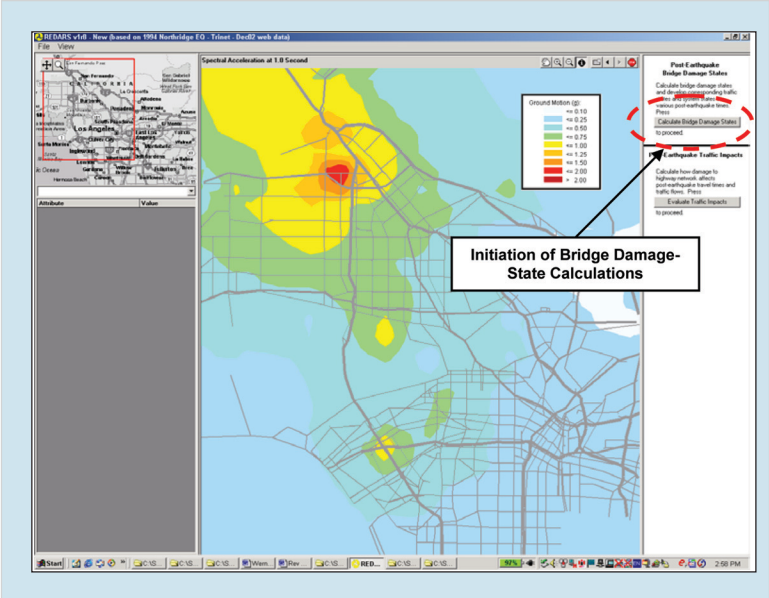

Figure 7. Display of Spectral Ground Accelerations at Period of 1.0 sec. and Initiation of Bridge Damage State Calculations

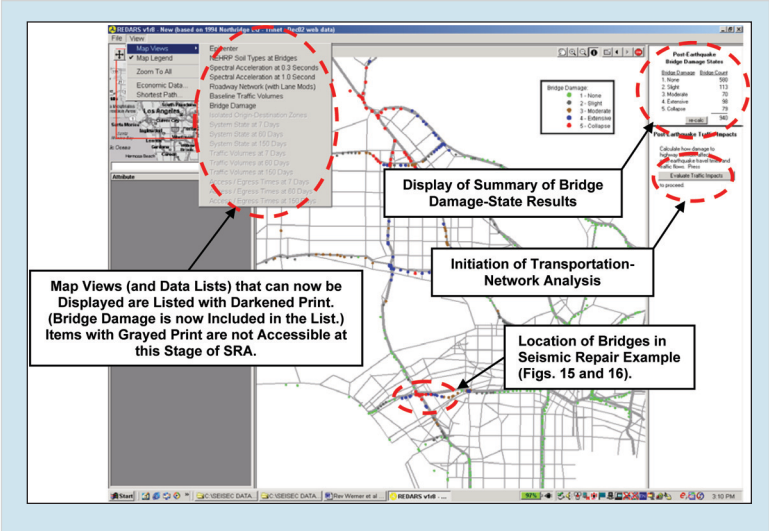

Figure 8. Display of Bridge Damage-States for Status-Quo Highway System and Initiation of Transportation-Network Analysis

[1] The composite system-wide travel time is equal to the sum of the travel times along all links in the REDARS model. It can be computed for the pre-earthquake (undamaged) system state, and then for various post-earthquake system states. Differences between composite travel times computed for the pre- and post-earthquake system states provide a first-order indication of overall effects of earthquake damage to the highway-roadway system, and can be used to estimate economic losses due to earthquake-induced travel-time delays (Werner et al., 2000).

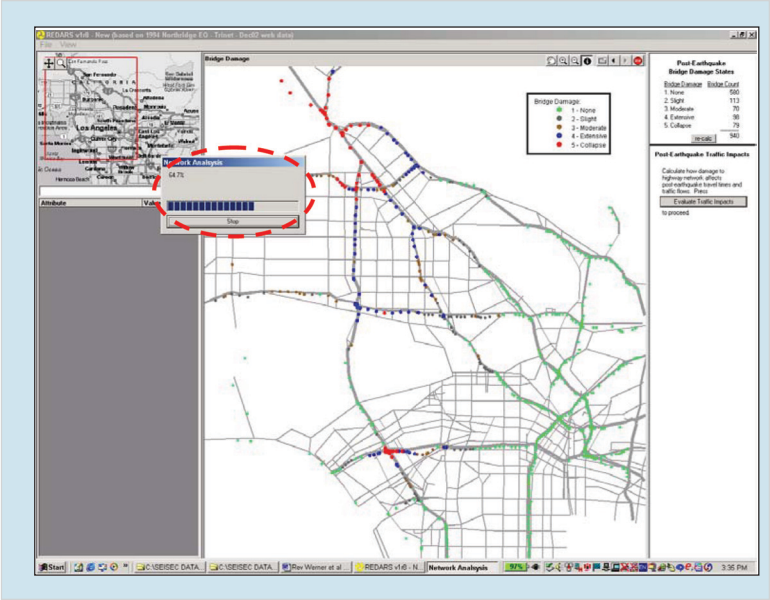

Figure 9. Display of Progress of Transportation-Network Analysis

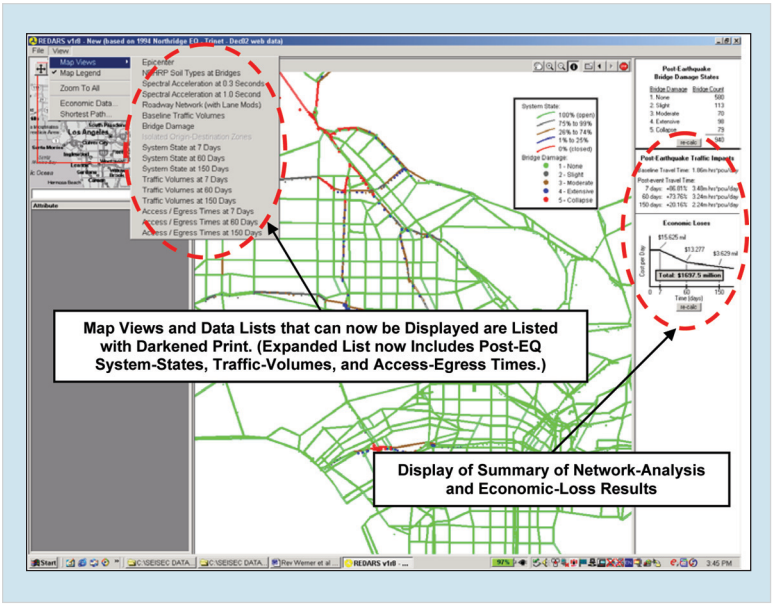

Figure 10 Display of System-State 7-Days after Earthquake for Status-Quo Highway System, after Completion of Transportation-Network Analysis

as described below, and if new SRA calculations have been carried out for the given earthquake); (e) show the previous view or the next view; or (f) stop the display process.

Tabular Display and Editing Features

Figures 14 through 20 describe the steps involved in using REDARS 1 to display and edit SRA results for selected bridges, roadway links, and O-D zones. These features, many of which will be retained in the forthcoming REDARS 2 software, facilitate the use of SRA for guiding seismic-risk-reduction and emergency-response/recovery decisions for highway systems.

Bridges

Figure 14 shows how attribute data for any bridge can be displayed from a map view of bridge damage states. This display is accessed by: (a) clicking on the "select a feature" button in the toolbar; and (b) clicking on the particular bridge in the map view for which data display is desired. This will display a table of bridge attributes and damage states, as shown on the left side of the map view in Figure 14. The elements shown in white background in the table (i.e., the bridge's ground motions and damage state) can be edited by the user, as described below.

Manual Modification of Bridge Damage State: An important benefit of SRA and REDARS will be its usefulness in enabling transportation agencies to evaluate the viability of various emergency-response

options in near-real time after an actual earthquake (including the relative effectiveness of these options in reducing post-earthquake traffic congestion.) One such option will invariably be how to establish priorities/sequences for repair of damaged bridges, according to which of these repair sequences will best improve traffic flows. Another option could be how to establish traffic-management strategies for reducing post-earthquake traffic congestion. The following paragraphs describe features of REDARS that will enable it to support decisions pertaining to post-earthquake bridge-repair priorities. Features of REDARS that will facilitate post-earthquake traffic-management decisions are summarized later in this paper.

To support decisions pertaining to post-earthquake bridge repair sequences, all versions of the REDARS SRA software will be able to use bridge damage states that are input by the user (rather than only relying on computed damage-state using the bridge models included in the software.) In this way, users will be able to incorporate actual bridge damage-state data into REDARS, as these data are obtained from post-earthquake field-reconnaissance surveys. This would involve the following steps: (a) with this actual damage-state data included, use REDARS to estimate post-earthquake traffic flows and economic losses; (b) simulate repair of selected bridges in the system, by manually changing the damage state for these bridges to corre-

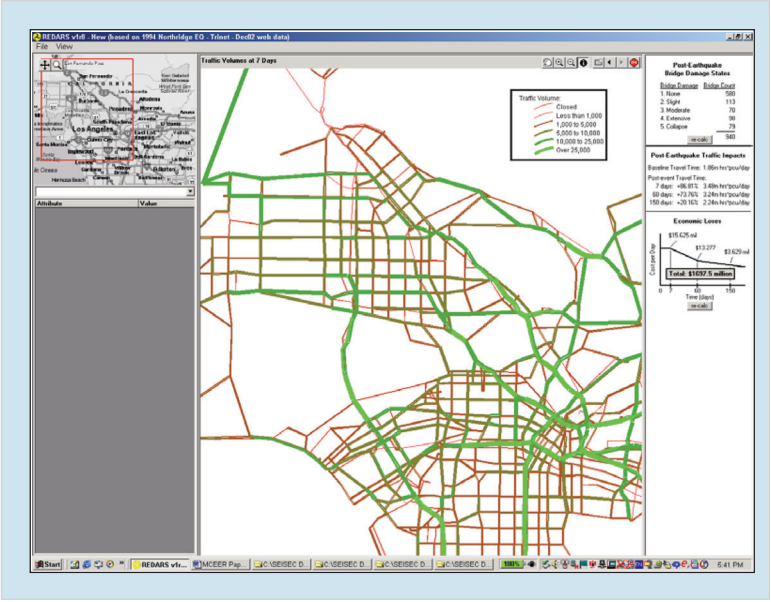

Figure 11. Display of Traffic Volumes for Status-Quo Highway System at 7-Days after Earthquake

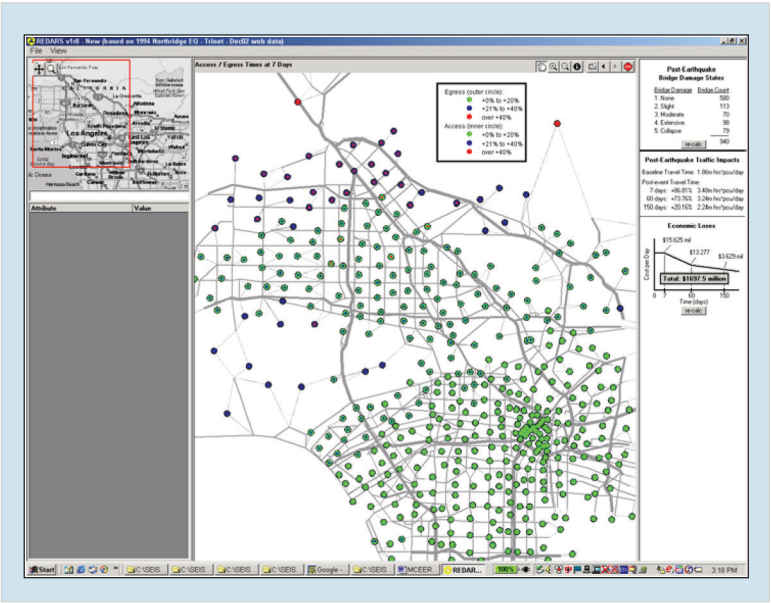

Figure 12. Access-Egress Times between Origin-Destination Zones for Status-Quo Highway System at 7-Days after Earthquake

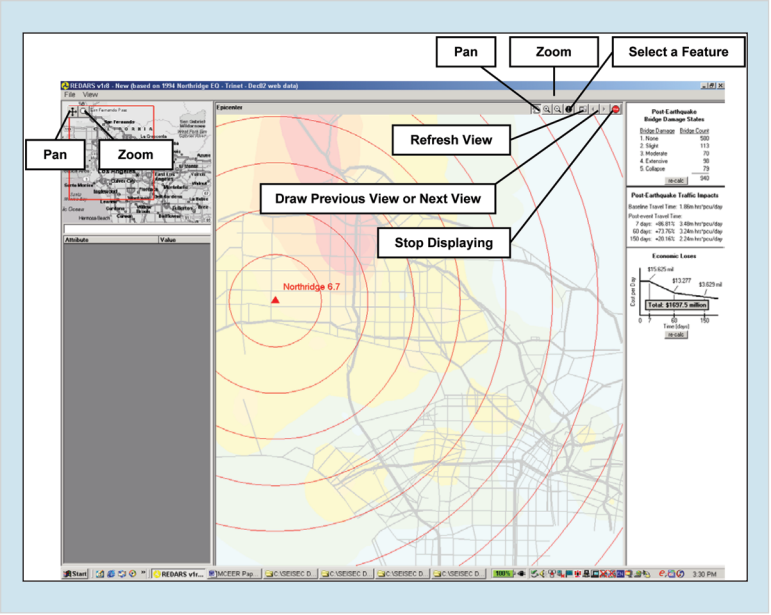

■ Figure 13. Editing of Visual Displays of Input Data and SRA Results

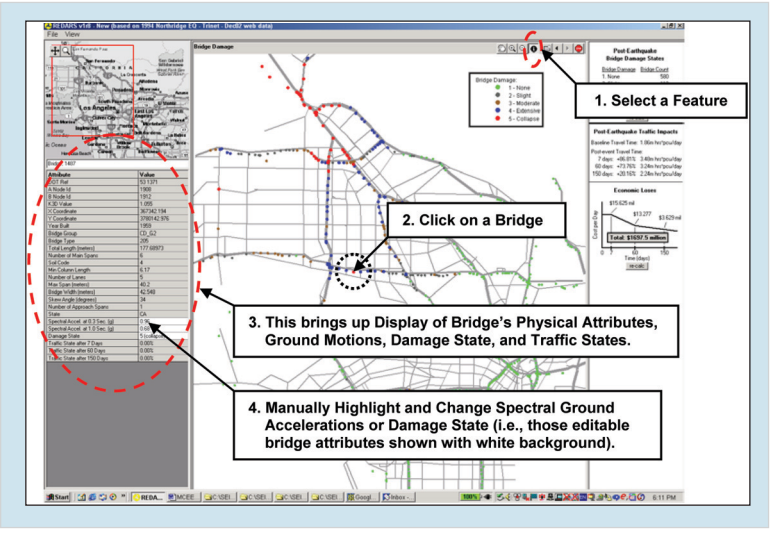

■ Figure 14. Accessing Data for Selected Bridge in Highway System

spond to an undamaged condition; (c) after these simulated repairs are included, use REDARS to re-compute post-earthquake traffic flows and economic losses; (d) compare post-earthquake traffic flows and economic losses from alternative bridge-repair sequences simulated in this way, and also make comparisons with results for the system prior to any post-earthquake repairs; and (e) use these comparisons (and also considering the relative repair-implementation costs) to select a preferred bridge-repair sequence to actually implement.

Figures 15 and 16 show the steps for using REDARS 1 in this way. These steps consist of selecting a particular bridge to be upgraded, displaying its attributes, and manually changing its damage state. To facilitate this process when several closely-spaced bridges are involved, the software displays a list of all bridges that happen to be very near a given bridge that is selected. Then, the attributes for each of these bridges are separately displayed by clicking on the bridge in the list. When the manual modifications of bridge damage states are completed, the user then carries out a new network analysis by clicking on the "recalc" button shown on the right side of Figure 15. This results in the new display of bridge damage states, network analysis results, and economic loss estimates that is shown in Figure 16. Then, new map views of post-earthquake system states, traffic volumes, and access-egress times can be displayed by

appropriate selections from the drop-down menu shown in Figure 10.

To illustrate this process, let us assume that the damaged bridges shown in Figure 15 (which correspond to bridges near the junction of the Santa Monica and San Diego Freeways in Los Angeles) represent actual bridge damage-state data provided by field-reconnaissance teams after an actual earthquake. Let us also assume that the responsible transportation agency (e.g., California Department of Transportation) wishes to evaluate whether to repair these particular bridges before or after implementing repairs of other damaged bridges. To guide this decision, the agency can compare REDARS estimates of economic losses from Figure 15 (prior to repairs of these bridges) vs. those from Figure 16 (after the repairs are in place.) This comparison shows that the economic losses due to earthquake effects on the highway-system traffic flows are reduced by about $51 million when the repairs are implemented. Assessment of the benefits of this repair strategy (i.e., the reduced economic losses) in conjunction with the costs to actually implement the strategy can serve as a basis for deciding whether the repair strategy is viable[2]. Then, this process can be repeated for other plausible bridge-repair sequences, and those sequences with the most favorable costs and benefits would be implemented first.

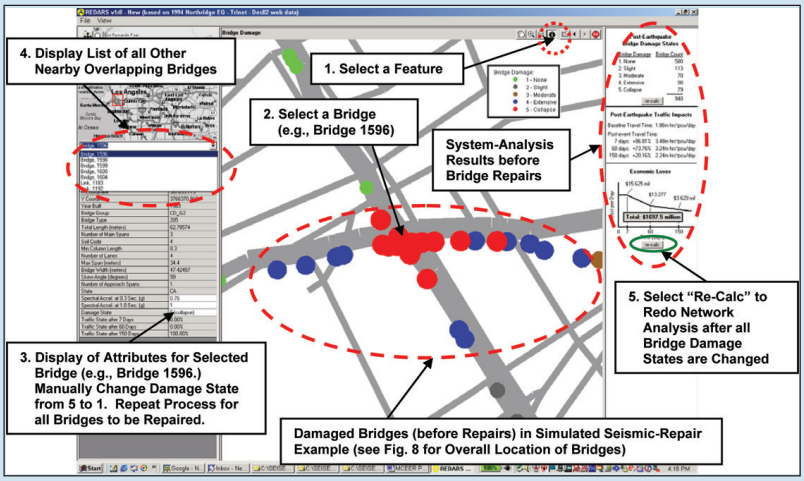

Figure 15. Bridge Seismic-Repair Example (before changing damage states)

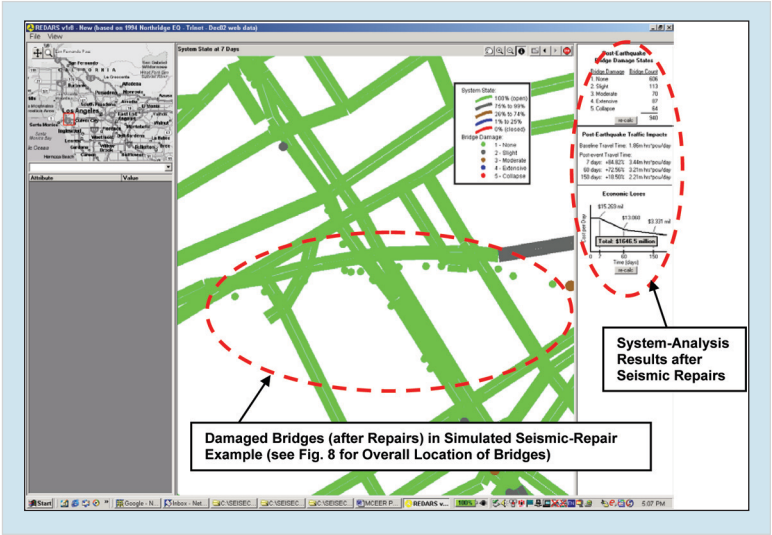

Figure 16. Bridge Seismic-Repair Example (after changing damage states)

[2] Overall economic loss due to increased traffic congestion after an earthquake is only one of many system-performance metrics that can be a basis for decision making. For example, another possible performance metric can be the ability of a given bridge-repair sequence to improve access to/from certain key locations in the region (e.g., key medical facilities, airports, etc.)

Web Sites

The Seismic System for Southern California:
http://www.trinet.org/shake

Manual Modification of Bridge's Input Ground Motions: The above deterministic analysis process is appropriate for rapid application in near-real time after an actual earthquake, in order to guide emergency-response decisions. However, for other types of decisions pertaining to longer-term post-earthquake recovery or to pre-earthquake planning of seismic-risk-reduction programs, probabilistic SRA procedures are much more appropriate, because of their ability to consider effects of uncertainties in: (a) earthquake occurrence, magnitude, and location; (b) seismic-hazards estimation; and (c) estimation of the seismic performance of the highway-system components (e.g., bridges) as well as the overall system itself. Probabilistic SRA of the Shelby County, Tennessee highway system that considers effects of such uncertainties is described in prior reports and technical papers developed under this FHWA-MCEER project (e.g., Werner et al., 2000; Werner, 2001.)

Although REDARS 1 is a deterministic SRA software package, it nevertheless provides a way to consider effects of such uncertainties in a limited way. For example, in addition to guiding user assessments of alternative bridge-repair sequences after an actual earthquake, the ability of REDARS 1 to accommodate manual modifications of bridge damage states can enable a user to roughly assess the sensitivity of highway-system seismic-performance predictions to uncertainties in bridge-damage-state estimates.

Another highly uncertain parameter is the estimation of site-specific ground motions for a given bridge in the highway system. To enable users to carry out a limited assessment of how ground-motion uncertainties can affect SRA results, REDARS 1 can accommodate manual changes to the original computed ground motions (i.e., the ground spectral accelerations at periods of 0.3 sec. and/or 1.0 sec.) at any bridge site.

Figures 17 and 18 show the steps involved in manually changing a given bridge's input ground motions, re-estimating the bridge's damage state, and repeating the network analysis. In the example shown in these figures, the spectral ground acceleration at a period of 1.0 sec. that was applied to a particular bridge (Bridge No. 1487) was manually changed from 0.68 g (which is the estimate from the SHAKEMAP model) to 0.50 g. Such changes of input ground motions can be carried out for any number of bridges in the system. Figure 15 shows that when the input ground motions are changed for any bridge, the prior summary displays of bridge damage states, network-analysis results, and economic-loss estimates no longer appear on the screen.

When all desired ground-motion changes are made for the various bridges in the system, the user proceeds to re-compute the damage states by clicking on the "Calculate Damage States" button shown in the right side of Figure 17. As shown in Figure 16, this results in a new display of bridge damage states. In this example, the assumed change in ground motions for Bridge No. 1487 modified its estimated damage state from 5 (collapse) to 4 (extensive).

Following this, the user clicks on the "Evaluate Traffic Impacts" button shown on the right side of Fig-

ure 18, in order to carry out a new network analysis for this new set of damage states. Then, as described earlier, the user can display new map views of post-earthquake system states, traffic volumes, and access-egress times. Comparisons of these results before and after the ground-motion changes are in place will provide users with a first-order deterministic indication of the sensitivity of the highway-system performance estimates to the variations in ground motion for this particular earthquake event.

Highway-Roadway Network Links

Figure 19 shows how the attribute data for any link in the system can be displayed from a map view of the system state at 7-, 60-, or 150-days after the earthquake. This display is accessed by simply: (a) clicking on the "select a feature" button in the toolbar; and (b) clicking on the particular link in the map view for which data display is desired. This will result in the display of a table of link attributes, as shown on the left side of the map view in Figure 19.

In this link-attribute table, the attributes with a white background — which correspond to "detour lanes" at 7-, 60-, and 150-days after the earthquake — can be manually changed by the user. These parameters, whose initial values are set at 0, are included in REDARS 1 to facilitate assessment of various post-earthquake traffic-management strategies that may be considered, such as: (a) changing of certain roadway links from two-way to one-way traffic; (b) eliminating parking alongside certain roadways, thereby effectively adding one lane each-way to accommodate traffic; and (c) construction of a temporary emer-

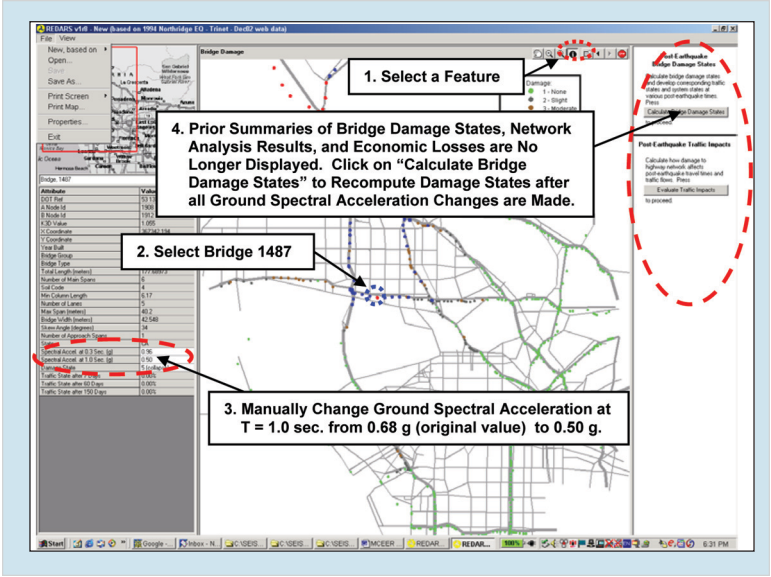

Figure 17. Manual Change of Ground Motion for Selected Bridge: Map View before Recomputation of Bridge Damage State

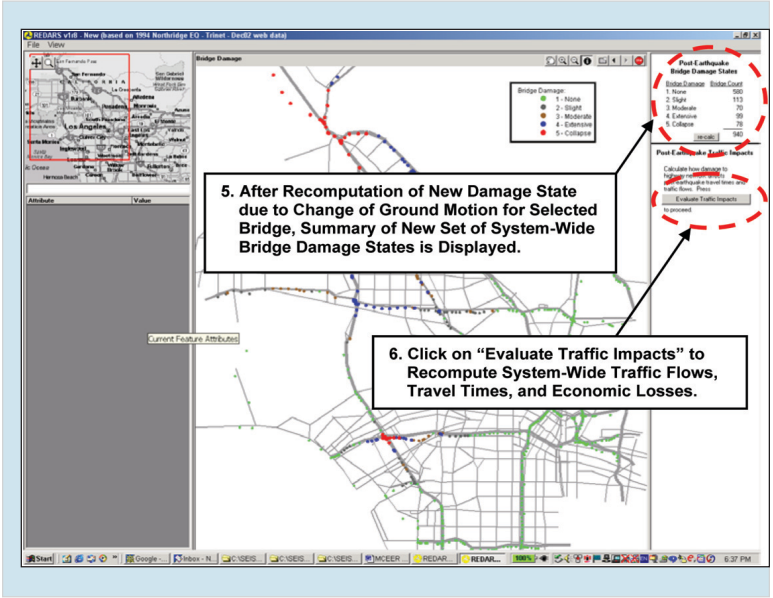

Figure 18. Manual Change of Ground Motion for Selected Bridge: Map View after Recomputation of Bridge Damage State and before Recomputation of Traffic Impacts

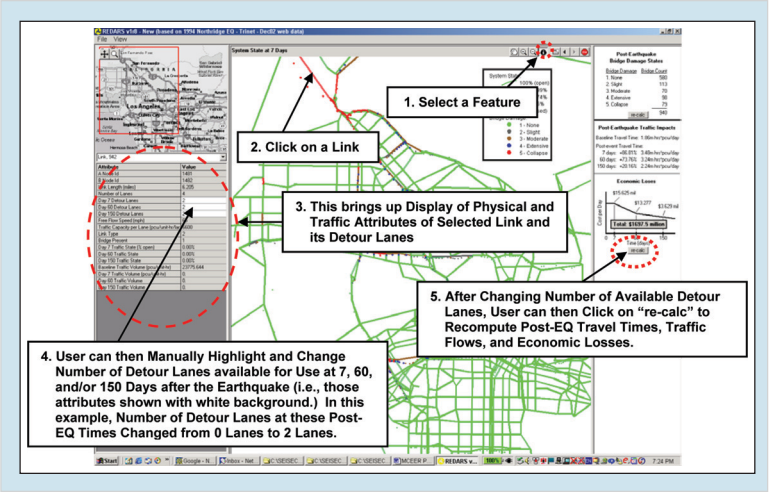

■ Figure 19. Display and Editing of Data for Selected Link in Highway System

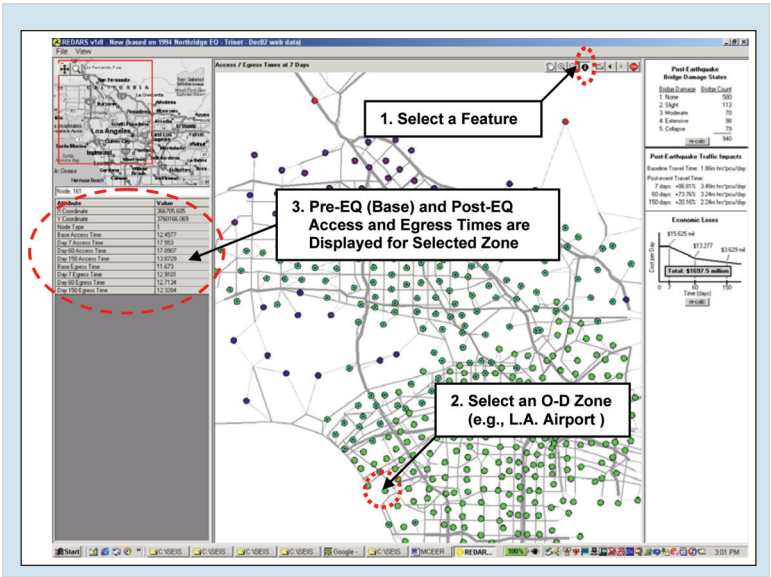

■ Figure 20. Display of Access- and Egress-Times for Selected Origin-Destination Zone

gency detour road alongside a non-redundant roadway segment that has been severely damaged during an earthquake. All of these traffic-management strategies were implemented at various locations throughout the greater Los Angeles area after the 1994 Northridge earthquake (Werner, 1995).

Figure 19 shows that the addition of "detour lanes" to simulate any of the above traffic-management strategies is accomplished by simply inserting an appropriate number of such lanes into the link-attribute table. Then, REDARS 1 uses these changed values to internally compile new system states at 7-, 60-, and 150-days after the earthquake. Next, by clicking on the "recalc" button beneath the summary display of traffic impacts and economic losses, the user enables REDARS 1 to rerun the network analysis, in order to compute new estimates of traffic flows, travel times, and economic losses. When these computations are completed, the user will be able to follow procedures described earlier in this paper in order to display map views for the now-revised system states, traffic volumes, and O-D zone access-egress times.

It is noted that this option in REDARS 1 can facilitate evaluation of alternative traffic-management strategies after an actual earthquake, in much the same way as described earlier in this paper for assessing alternative bridge-repair priorities/sequences. That is, after a given traffic-management strategy is simulated and analyzed in RE-

DARS 1, potential benefits of the strategy can be established by comparing appropriate system-performance metrics (e.g., reductions in economic losses, improved access to key emergency-response locations) before and after the traffic-management strategy is implemented.

Origin-Destination Zones

Another important benefit of the REDARS SRA software is its ability to estimate the extent to which travel times to and from key locations in a region (e.g., medical centers, airports, centers of commerce, government centers, etc.) could be impacted by earthquake damage to the highway-roadway system. Significant disruptions of such travel times could impact the affected region's ability to respond to and recover from the earthquake.

REDARS 1 enables users to develop tabular displays of access- and egress-times to/from any selected O-D zone, for the system's base (pre-earthquake) condition and post-earthquake conditions at times of 7-, 60-, and 150-days after the earthquake. As shown in Figure 20, these displays are developed by: (a) bringing up a map view of access- and egress-times at any of the above post-earthquake times; (b) clicking on the "select a feature" button in the toolbar from that map view; and (c) clicking on the centroid of the particular O-D zone in the map view for which access-time and egress-time results are desired.

Concluding Comments

Prior to our forthcoming development of the detailed public domain REDARS 2 software for deterministic and probabilistic SRA of highway systems, an interim and simplified deterministic demonstration version of the software has been programmed. This software (REDARS 1) will provide users with an introduction to basic SRA concepts and results, as well as an opportunity to provide timely feedback regarding desirable software features to include in REDARS 2. This paper summarizes the main features and steps for applying REDARS 1. It also summarizes and compares various analytical elements of REDARS 1 and REDARS 2, and provides examples of how certain SRA results can be used to guide emergency-response decision-making.

References

Dutta, A. and Mander, J.B., (1998), "Seismic Fragility Analysis of Highway Bridges," *Proceedings of the INCEDE-MCEER Center-to-Center Project Workshop on Earthquake Engineering Frontiers in Transportation Systems*, Tokyo Japan, June 22-23.

Eguchi, R.T., Huyck, C.K., Cho, S., Ghosh, S. and Basoz, N., (2003), *Review of REDARS 1.0 Seismic Risk Analysis Software (Task B1-4)*, ImageCat Inc., January.

Federal Highway Administration (FHWA), (1995), *Recording and Coding Guide for the Structure Inventory and Appraisal of the Nation's Bridges*, Report FHWA-PD-96-001, Office of Engineering, Bridge Division, Bridge Management Branch, Washington DC, December.

Mander, J.B. and Basoz, N., (1999), "Seismic Fragility Theory for Highway Bridges," *Optimizing Post-Earthquake Lifeline System Reliability, Proceedings of the Fifth U.S. Conference on Lifeline Earthquake Engineering,* Seattle WA, Technical Council on Lifeline Earthquake Engineering Monograph No. 6 (Edited by W. M. Elliot and P. McDonough), American Society of Civil Engineers, Reston, VA, pp 31-40, August.

Moore, J.E. II, Kim, G., Xu, R., Cho, S., Hu, H-H. and Xu, R., (1997), *Evaluating System ATMIS Technologies via Rapid Estimation of Network Flows: Final Report*, California PATH Report UCB-ITS-PRR-97-54, December.

TriNet, (2002), *Shakemap Web Site, http://www.trinet.org/shake*, December.

Werner, S.D., (1995), "Transportation Response," *Northridge Earthquake of January 17, 1994, Reconnaissance Report, Vol.1, Earthquake Spectra, Supplement C to Volume 11,* Publication 95-03, April, pp. 356-366.

Werner, S. D., Taylor, C. E., Moore, J. E. II, Walton, J. S. and Cho, S., (2000), *A Risk-Based Methodology for Assessing the Seismic Performance of Highway Systems*, Technical Report MCEER-00-0014., Multidisciplinary Center for Earthquake Engineering Research, University at Buffalo, Buffalo, December 31.

Werner, S.D., (2001), "A Risk-Based Methodology for Assessing the Seismic Performance of Highway Systems", *Research Progress and Accomplishments: 2000-2001,* Report number MCEER-01-SP01, Multidisciplinary Center for Earthquake Engineering Research, University at Buffalo, May.

Werner, S.D., Taylor, C.E., Lavoie, J-P, Eitzel, C., Moore, J.E. II and Walton, J.S., (2003), *Annual Report for Year 3 of Task B1-2, Enhancement and Programming of REDARS Software for Seismic Risk Analysis of Highway Systems*, Seismic Systems & Engineering Consultants, Oakland CA, January.

Effect of Seismic Retrofit of Bridges on Transportation Networks

by Masanobu Shinozuka, Yuko Murachi, Xuejiang Dong, Youwei Zhou and Michal J. Orlikowski

Research Objectives

The objective of this research is to determine the effect earthquakes have on the performance of transportation network systems. To do this, bridge fragility curves, expressed as a function of peak ground acceleration (PGA) and peak ground velocity (PGV), were developed. Network damage was evaluated under the 1994 Northridge earthquake and scenario earthquakes. A probabilistic model was developed to determine the effect of repair of bridge damage on the improvement of the network performance as days passed after the event. As an example, the system performance degradation measured in terms of an index, "Drivers Delay," is calculated for the Los Angeles area transportation system, and losses due to Drivers Delay with and without retrofit were estimated.

Sponsors

California Department of Transportation (Caltrans), Federal Highway Administration

Research Team

Masanobu Shinozuka, *Distinguished Professor and Chair,* ***Yuko Murachi***, *Research Associate,* ***Xuejiang Dong***, *Post Doctoral Researcher,* ***Youwei Zhou***, *Graduate Student,* ***Adelina Pirijanyan***, *Undergraduate Student, Department of Civil and Environmental Engineering, and* ***Tony Soeller***, *Research Computing Specialist, Department of Network and Academic Computing, University of California, Irvine*

Michal J. Orlikowski, *Undergraduate Student, Department of Civil and Environmental Engineering, Princeton University*

Transportation systems, including highways, railroads, airports and harbors, represent a critical component of society's infrastructure systems. They are needed for the welfare of the general public, specifically for commercial, industrial and cultural activities in national as well as international scale, and also to facilitate transportation of search/rescue and medical teams, the injured to hospitals, repair and restoration news and materials, and daily supplies for citizens following disasters. In this respect, under a natural or manmade disaster (e.g., earthquake, flood, etc.), it is critically important that the transportation system remains operational or that its function be repaired or restored as soon as possible. Past experience has shown too often that earthquake damage to highway components (e.g., bridges, roadways, tunnels, retaining walls, etc.) can severely disrupt traffic flow, thus negatively impacting on the economy of a region as well as on post-earthquake emergency response and recovery activities. Furthermore, the extent of these impacts will depend not only on the nature and magnitude of the seismic damage sustained by the individual components, but also on the mode of functional impairment of the highway system as a network resulting from physical damage to its components. In order to estimate the effect of the earthquake on the system

Collaborative Partners

***Li-Hong Shen**, Caltrans*

***W. Phillip Yen**, Federal Highway Administration*

performance of the transportation network, this paper develops an analytical framework to integrate bridge and other structural performance with a transportation network model in the context of seismic risk assessment developed by Shinozuka et al., 2000.

Highway transportation systems comprise numerous structural components and are located in equally complex natural and built environments. Among the engineered components, bridges are potentially the most vulnerable under earthquake conditions. In the previous study by Shinozuka et al., 2000, fragility information expressed as a function of peak ground acceleration (PGA) was utilized. Usually, PGA information is easier to obtain, however, peak ground velocity (PGV) may be an equally capable way to express the fragility information of structures.

The purpose of this research is to develop empirical fragility curves, expressed as a function of the ground motion intensity such as PGA or PGV, and compare them to the degradation of traffic capacity of Caltrans' (California Department of Transportation) network in Los Angeles and Orange County damaged by the 1994 Northridge earthquake. Furthermore, the results are shown with the aid of 3D animations (ArcGIS, 1999, website) to demonstrate post-earthquake traffic behavior. For this purpose, the spatial distributions of PGA and PGV resulting from the 1994 Northridge earthquake are acquired from the TriNet ShakeMap, 2001 (website). The network seismic risk evaluation method is then developed by integrating the seismic hazard represented by the 1994 Northridge earthquake and its associated system performance degradation. In this study, system performance degradation is measured in terms of an index, "Drivers Delay," that is calculated by equilibrium analysis of transportation systems (user optimizing deterministic assignment), on the basis of the 1991 origin-destination survey performed for the region including Los Angeles and Orange County. This index is strictly used as a measure of network degradation under the unchanged origin-destination (OD) matrix. In this sense, it does not precisely represent the network performance relative to the post-earthquake traffic demand. This dynamic aspect of the traffic flow problem is currently under study.

Furthermore, under certain assumptions, the process and progress of bridge repair is simulated by a Monte Carlo method to produce a chronological improvement of post earthquake system performance. These simulations are

A wide spectrum of research, governmental and practicing engineers will be the users of this research. They include researchers in the areas of earthquake and transportation engineering, transportation facilities management and urban planning and economics, governmental agencies, including Caltrans and Federal Highway Administration, and bridge design professionals.

all made utilizing the PGA spatial distribution of 47 selected scenario earthquakes from the regional seismic hazard associated with Los Angeles and Orange County.

In addition, loss due to Drivers Delay is evaluated for the Caltrans freeway network with and without retrofit, and finally, loss due to ground shaking and liquefaction are evaluated for all bridges in Orange County with the aide of HAZUS (National Institute of Building Sciences, 1999) software.

Empirical Fragility Curves

Empirical fragility curves for bridges in the Los Angeles area freeway network are developed from records of damage to Caltrans bridges under the 1994 Northridge earthquake in conjunction with the PGA and PGV values acquired from the TriNet ShakeMap (website).

In this study, the bridges are classified into different subsets according to three distinct attributes:

(a) It is either single span (S) or multiple span (M)

(b) It is built on either hard soil (S_A), medium soil (S_B) or soft soil (S_C) according to the definitions in UBC 1994 (Intl. Conference of Building Officials, 1994)

(c) It has a skew angle θ_1 (less than 20°), θ_2 (between 20° and 60°) or θ_3 (larger than 60°).

To begin with, one might consider the first level hypothesis that the entire sample is taken from a statistically homogeneous population of bridges. The second level subsets are created by dividing the sample either (a) into two groups of bridges, one with single spans and the other with multiple spans, (b) into three groups, the first with soil condition S_A, the second with S_B and the third with S_C, or (c) into three groups depending on the skew angles θ_1, θ_2 and θ_3. The third and fourth level sub-groupings were also considered for the development of corresponding fragility curves under PGA as a ground motion intensity index (Shinozuka et al., 2001).

It is assumed that the curves can be expressed in the form of two parameter lognormal distribution functions, and estimation of the two parameters (median and log-standard deviation) is performed with the aid of the maximum likelihood method. For this purpose, PGA and PGV values are used to represent the intensity of the seismic ground motion.

The likelihood function is expressed as follows:

$$L(c_1,c_2,c_3,c_4,\varsigma)=\prod_{i=1}^{N}\prod_{k=1}^{5}P_{ij}(a_i;E_k)^{x_{ik}} \quad (1)$$

where E_1, E_2, E_3, E_4, and E_5, respectively, indicate the state of no, minor, moderate, major and collapse damage. $P_{ij}(a_i;E_k)$ in turn indicates the probability that a bridge i selected randomly from the sample will be in the damage state E_k when subjected to ground motion intensity expressed by PGA or PGV $=a_i$. x_{ik} equals 1 or 0 depending on whether or not the damage state E_k occurs for the i-th bridge subjected to a_i. N is the total number of bridges inspected after the earthquake.

Under the current lognormal assumption, fragility curves take the following analytical form

$$F_j(a_i;c_j,\varsigma_j)=\Phi\left[\ln\left(\frac{a_i}{c_j}\right)\Big/\varsigma_j\right] \quad (2)$$

Links to Current Research

The analysis procedure to evaluate topological degradation of transportation networks can be integrated into the urban lifeline system research being performed for power and water lifelines as well as to complement emergency response activities.

Web Sites

Professor Shinzuka:
http://shino8.eng.uci.edu

U.S. Department of Homeland Security:
http://www.fema.gov/hazus

ESRI: GIS and Mapping Software:
http://www.esri.com

The Seismic System for Southern California:
http://www.trinet.org/shake/

where Φ [ ] is the standardized normal distribution function, parameters c_j and ς_j are the median and log-standard deviation of the fragility curves for the damage state of "at least minor," "at least moderate," "at least major," and "collapse" identified by j=1,2,3 and 4, respectively. From this definition of fragility curves, and under the assumption that the log-standard deviation is equal to ς common to all the fragility curves, one obtains;

$$P_{i1} = P(a_i, E_1) = 1 - F_1(a_i; c_1, \varsigma) \quad (3)$$

$$P_{i2} = P(a_i, E_2) = F_1(a_i; c_1, \varsigma) - F_2(a_i; c_2, \varsigma) \quad (4)$$

$$P_{i3} = P(a_i, E_3) = F_2(a_i; c_2, \varsigma) - F_3(a_i; c_3, \varsigma) \quad (5)$$

$$P_{i4} = P(a_i, E_4) = F_3(a_i; c_3, \varsigma) - F_4(a_i; c_4, \varsigma) \quad (6)$$

$$P_{i5} = P(a_i, E_5) = F_4(a_i; c_4, \varsigma) \quad (7)$$

The maximum likelihood estimations c_{0j} for c_j and ς_{0j} for ς_j are obtained by solving the following equations,

$$\frac{\partial \ln L(c_1, c_2, c_3, c_4, \varsigma)}{\partial c_j} = \frac{\partial \ln L(c_1, c_2, c_3, c_4, \varsigma)}{\partial \varsigma} = 0 \quad (j = 1,2,3,4) \quad (8)$$

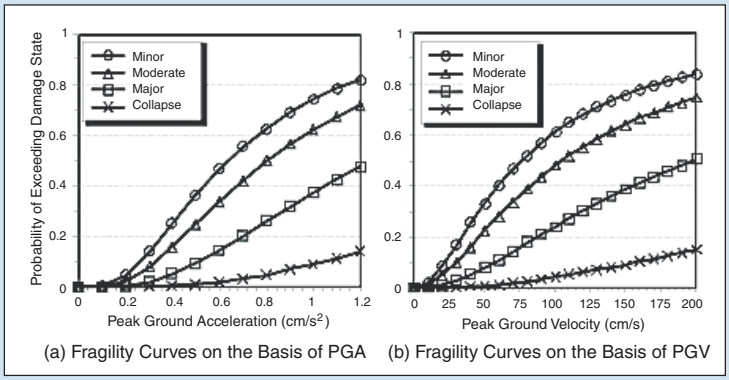

■ Figure 1. Fragility Curves for Caltrans' Bridges (First Level (Composite))

by implementing a straightforward optimization algorithm. The median values and log-standard deviations of all levels of attribute combinations are listed in Table 1. Note that if an element of a matrix in Table 1 is labeled N/A, it indicates that no sub-sample was found for the particular combination of bridge attributes signified by the element. The family of fragility curves corresponding to the first level is plotted in Figure 1. The curve with a "minor" designation represents, at each PGA or PGV value a, the probability that "at least a minor" state of damage will be sustained by a bridge (arbitrarily chosen from the sample of bridges) when it is subjected to PGA or PGV a. The same meaning applies to other curves with their respective damage state designations.

Methodology

Highway System: Assessing Structural Component and Network Damage

Highway transportation systems comprise numerous structural components and are located in equally complex natural and built environments. Among the engineered components, bridges are the most vulnerable under earthquake conditions. Thus, bridges are the only structures considered to be seismically vulnerable in this analysis. For the purpose of simulation, every bridge in the study region is considered to be an independent structure and determination of the degree of damage to each bridge can be treated as an independent statistical experiment.

■ Table 1. Median and Log-standard Deviation at Different Levels of Sample Sub-division

Damage State	PGA(m/s²)		PGV(cm/s)	
	c	ζ	c	ζ
Min	0.64	0.70	76	0.98
Mod	0.80	0.70	106	0.98
Maj	1.25	0.70	200	0.98
Col	2.55	0.70	555	0.98

(a) First level (Composite)

Span	Damage State	PGA(m/s²)		PGV(cm/s)	
		c	ζ	c	ζ
S*	Min	0.89	0.66	129	0.98
	Mod	1.15	0.66	188	0.98
	Maj	1.76	0.66	357	0.98
	Col	N/A	0.66	N/A	0.98
M*	Min	0.56	0.66	63	0.92
	Mod	0.70	0.66	87	0.92
	Maj	1.09	0.66	163	0.92
	Col	2.16	0.66	428	0.92

*S: Single, M: Multiple

(b) Second level (Span)

Skew	Damage State	PGA(m/s²)		PGV(cm/s)	
		c	ζ	c	ζ
θ_1†	Min	0.82	0.76	108	1.07
	Mod	1.10	0.76	164	1.07
	Maj	1.86	0.76	343	1.07
	Col	3.49	0.76	833	1.07
θ_2†	Min	0.60	0.71	70	0.98
	Mod	0.72	0.71	90	0.98
	Maj	1.15	0.71	173	0.98
	Col	3.18	0.71	769	0.98
θ_3†	Min	0.42	0.52	42	0.75
	Mod	0.52	0.52	56	0.75
	Maj	0.74	0.52	96	0.75
	Col	1.26	0.52	212	0.75

†θ_1: less than 20°, θ_2: between 20° and 60°, θ_3: larger than 60°

(c) Second level (Skew)

Soil	Damage State	PGA(m/s²)		PGV(cm/s)	
		c	ζ	c	ζ
S_A‡	Min	0.87	0.75	110	1.03
	Mod	1.10	0.75	151	1.03
	Maj	1.51	0.75	234	1.03
	Col	N/A	0.75	N/A	1.03
S_B‡	Min	0.64	0.71	65	0.81
	Mod	0.84	0.71	91	0.81
	Maj	1.24	0.71	145	0.81
	Col	N/A	0.71	N/A	0.81
S_C‡	Min	0.61	0.69	74	0.98
	Mod	0.76	0.69	102	0.98
	Maj	1.22	0.69	199	0.98
	Col	2.35	0.69	523	0.98

‡S_A: hard soil, S_B: medium soil, S_C: soft soil

(d) Second level (Soil)

These fragility curves are utilized to generate, in Monte Carlo simulation, the state of damage for each Caltrans bridge in Los Angeles and Orange County under postulated scenario earthquakes, and hence, the following analysis applies only to the bridge prior to the post-Northridge retrofit.

The performance of the highway transportation system in the Los Angeles metropolitan area following the Northridge earthquake demonstrated some system resiliency that was achieved by enlisting and integrating some unaffected secondary highways and artillery streets into the expressway network. Therefore, in this analysis, the alternate routes are considered to exist although they have lesser traffic capability in terms of both free flow speed and capacity compared to those associated with the segment or the link of the expressway they replaced. Table 2 shows a loss of traffic capability depending on the degree of the state of the link damage. The link damage repre-

■ Table 2. Change in Road Capacity and Free Flow Speed

State of Link Damage	Capacity Change Rate	Free Flow Speed Change Rate
No Damage	100%	100%
Minor Damage	100%	75%
Moderate Damage	75%	50%
Major Damage	50%	50%
Collapse	50%	50%

sents the worst state of damage to the bridges in that link (i.e., bottleneck hypothesis; if, for example, at least one of the bridges in a link suffers major damage, and if that is the greatest state of damage, the link has the major damage.). The values in Table 2 are hypothetical and future research is needed to validate them.

Calculating a Comprehensive System Performance Index: Drivers Delay

In order to define the network performance as a whole after an earthquake, a comprehensive index of performance is introduced. Following the method documented by Shinozuka et al., 2000, the index used here is the "Drivers Delay." This is defined as the increase in total daily travel time for all travelers, including commuters and commercial vehicles, caused by earthquake induced delays. Essentially, it is the difference between the total daily travel for all network travelers on the damaged network and that of the original undamaged network.

$$TT = \sum_a x_a t_a(x_a) \tag{9}$$

$$Delay = \sum_a x'_a t'_a(x'_a) - \sum_a x_a t_a(x_a) \tag{10}$$

Equation (9) exhibits the calculation of the total daily travel time for all network users, in hours per day; as defined earlier, x_a is the flow on link a (in Passenger Car Units per day), and t_a is the travel time on link a (in hours per Passenger Car Unit). Thus, the product of the two yields the total daily travel time for all network travelers on link a. The summation over all the links yields the total daily travel time on the entire network. Equation (10) exhibits the calculation of the Drivers Delay. The notation in Equation (10) is the same as in Equation (9) except that the primed variables denote the damaged network, and the unprimed variables refer to the original undamaged network. Note that "Drivers Delay," when calculated this way, has units of hours per day. In order to obtain a total "Drivers Delay" with units of hours, this expression must be integrated over all the days that a delay persists.

The travel time on a link is calculated by utilizing a link performance function developed by the United States Bureau of Public Roads, 1964:

$$t_a = t_a^0\left[1+\alpha\left(\frac{x_a}{C_a}\right)^{\beta}\right] \tag{11}$$

where t_a^0 is the travel time at zero flow on link a (this is simply the link's length divided by the speed limit); C_a is the "practical capacity" of the link, and α and β are variable parameters. Ordinarily, and in this study, α =0.15 and β =4.0. It is important to note that this empirically derived expression asserts that the travel time on a link carrying 100% of capacity is 15% greater than the free flow time.

Determining the flow on each link depends on the availability of

origin-destination (OD) data. Given the difficulty of collecting such a set of traffic flow data over a regional dimension, the OD data are developed only occasionally over the years and hence lags behind the change in traffic patterns. Therefore, traffic flow characteristics are approximates. In this context, we developed a method by which a large OD matrix can be reduced to a manageable size following Shiraki, 2000. This method relies upon the Thiessen function (an ArcGIS software) where the number of OD locations are reduced to the number of the nodes of the freeway network, each representing OD information within the Thiessen polygon developed around that node (see Figure 2). This significantly reduces the matrix dimension and makes the OD matrix usable in the PC-based near-real-time traffic flow simulation. Upon producing a useable origin-destination matrix, the flow between links must be solved using an equilibrium analysis.

Using the methods discussed here, it is possible to develop a rudimentary measure of a system's performance as a network given any state of damage to its components (bridges).

Determining Effects of Repair Efforts

Earlier, it was noted that the calculated value of Drivers Delay was actually in terms of hours per day, and it would be necessary to integrate the delay over the time that it persists in order to have a measurement of the total delay. Notably, the Drivers Delay is not constant over the time it persists. Repair efforts

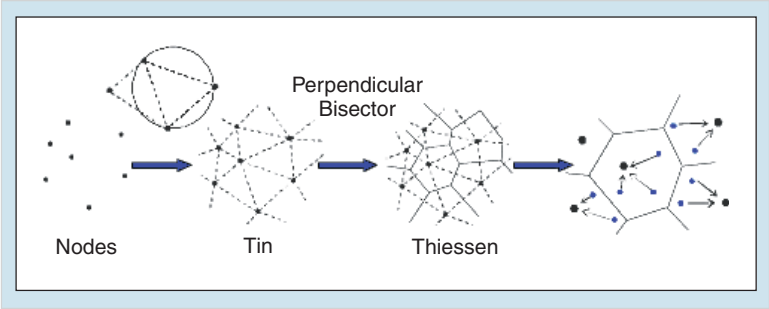

Figure 2. Making Thiessen Polygon

improve the state of damage to the network, thus decreasing Drivers Delay over time. In this connection, this paper accounts for the bridge repair process. Unfortunately, this is fairly difficult, as there is not much consistent and systematic data on the processes by which repair is conducted, and little documentation made available on the priorities selected by the engineers involved in the operation. Highway repair is conducted by and large using the best judgment of the engineers and management involved, and hence this process is not easily modeled. Nonetheless, a model is developed for this simulation to provide some numerical insight to the problem.

In this paper, the repair process is modeled as the time to complete a repair for each individual bridge damaged is assumed to be a random variable uniformly distributed over travels ($t_{i,min}$ and $t_{i,max}$) in which i=1, 2, 3 and 4 represent minor, moderate, major and collapse states of damage, respectively. For example, $t_{i,min}$ = 10 days and $t_{i,max}$ = 150 days indicates a bridge that sustained a state of minor damage requires most optimistically 10 days and most pessimistically 150 days to complete repair. Otherwise, repair time takes a uniformly distrib-

uted value between these two values, (see Figure 3). Chances are uniformly distributed for completion. Other values of subscript *i* apply most optimistic and pessimistic times to bridges subjected to different damage states. The size and importance of bridges are not factored into this simplistic analysis, and are the subject of future study.

Notice that the functions do not necessarily assume that all bridges can be repaired on Day 0, nor do they assume that the slopes (daily probabilities of repair), are the same. The choice of the parameters of the optimistic and pessimistic repair scenarios, (essentially, the first and last possible days a bridge of a given damage state can be repaired), are left to the best judgment of those developing the model. It is important to note that there are numerous ways that the repair of the system could be probabilistically modeled. For instance, link flow data could have been used to estimate the priorities for bridge repair. The method used here is chosen because there seems to be a correlation between the damage state of a bridge and the amount of time for a repair contract to be awarded, and for simplicity in simulation.

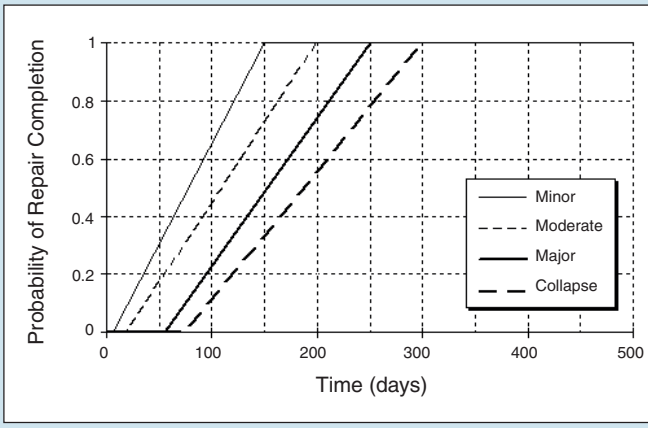

Figure 3. Probability Distribution of Functions used to Model Repair Processes

The repair process is simulated by another use of the Monte Carlo technique. Day 0 represents the day of the earthquake – when the system has the greatest extent of damage. The data available includes the damage state of each bridge, as well as the damage state of the link and the Drivers Delay. The bridge damage data is the relevant information for performing the repair simulation. Considering some arbitrary amount of time after the event, one can perform a Monte Carlo simulation in the same way as before with the repair distributions to determine if each bridge is repaired. This is done by considering each bridge one at a time. Based on the bridge's damage state, the time since the event, and the appropriate repair function for the damage state, one can use a random number generator to decide if the bridge is repaired. If the random value falls above the function for the given time since the event, it is not repaired; if it falls beneath the function, it is repaired. In this simulation, a repaired bridge shifts from its previous damage state directly to the no damage state, and its record is modified to reflect that change. This process is then repeated for every bridge in the study region. The result is a system with an entirely different state of damage. Link damage state and the Drivers Delay must be recalculated to reflect the changes to the system.

Developing a Risk Measure

Given the possibility of performing multiple simulations for a study

region, measures of risk for a spatially distributed highway system can be developed using methods introduced in Chang et al., 2000. Using a number of earthquake scenarios, and calculating their probabilities of exceedance, risk curves can be produced for the system. A risk curve is a plot of the probability of exceeding a certain hazard level versus a measure of damage (in this case, Drivers Delay). A set of these is produced in the case study described later in this paper.

Application

Network Model

Figure 4 displays the freeway and state highway network considered in this study. The study is limited to the freeway network in Los Angeles and Orange County in the Los Angeles Metropolitan Area.

This network model consists of 118 nodes and 185 links. The total number of bridges in this network is 2,727. The network is defined in terms of nodes and links, where nodes consist of locations where two or more highways intersect (usually interchanges), as well as locations where a highway crosses the boundary of the study area. A link is defined by a line (not self-intersecting) between two nodes with no other nodes in between. The link characteristics are described by free flow speed and flow capacity. The free flow speed for a link is based upon its speed limit, which is considered to be 65 miles per hour on the freeway, and 35 miles per hour on the highway. This is done for analytical simplicity, and can be adjusted for regional differences. Similarly, the practical capacities for freeway and highway links are assumed to be 2,500 and 1,000 passenger car units per hour, respectively.

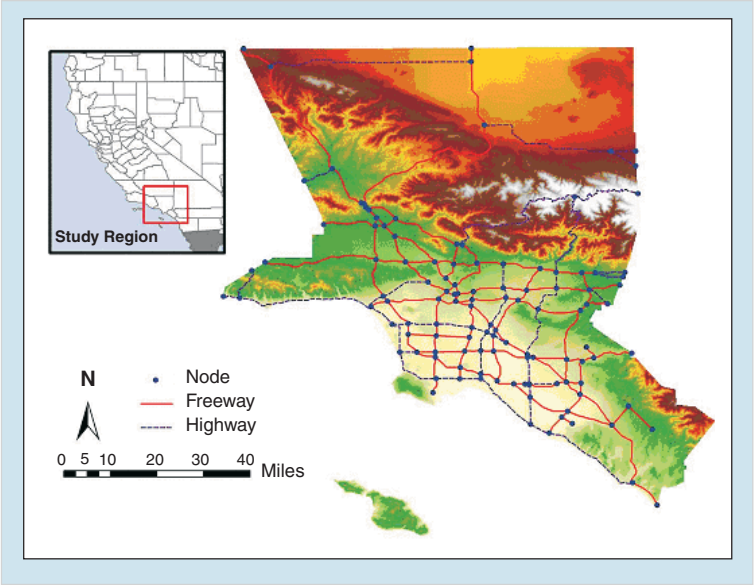

Figure 4. Los Angeles Area Highway Network

Fragility curves for the bridges in the study region are represented by the family of those corresponding to the first level population as shown in Figure 1. The spatial distribution of PGA and PGV values for the 1994 Northridge earthquake are acquired from the TriNet ShakeMap. The bridge damage state is determined by Monte Carlo simulation based on the fragility information. The state of damage thus simulated for each bridge determines the link capacity as shown in Table 2 where the worst state of the bridge damage in the link determines the state of the link damage.

The origin-destination data used in this paper consists of 1991 southern California origin-destination survey results for 1,527 traffic analysis zone. The reader is referred to SCAG report (Southern California Association of Governments, 1993) for details. As mentioned in

the section on Methodology, Thiessen polygons are used to convert the 1991 SCAG survey data to node OD data of the freeway network shown in Figure 4.

Traffic Analysis

To perform the traffic equilibrium analysis numerically, the method of user optimizing deterministic assignment described earlier is used with the aid of the incremental assignment technique. Figures 5 and 6 show the average result over 10 simulations, including average damage state and average speed ratio. A speed ratio η for each link, representing one measure of system performance degradation, is defined as:

$$\eta_a = \frac{S'_a}{S_a} \qquad (12)$$

where, η_a is the speed ratio on link a, $S_a$is the flow speed on link a under intact condition, and S'_a is the flow speed on link a under damaged condition.

In the 1994 Northridge earthquake, Goltz (1994) reported that bridges collapsed on I-10 (Santa Monica Freeway), on I-5 (Golden State Freeway), at I-5/SR-14 (Antelope Valley) intersection, and on SR-118 (San Fernando Valley). In the simulation, major or moderate damage to links are recognized at I-405, I-101 and I-210, as well as these four links (e.g., I-10, I-5, SR-14, and SR-118). The differences between the actual damage states and simulated results is caused by the fragility curves used in this study, where the bridges are assumed to have a statistically homogenous vulnerability to earthquake damage, which do not reflect the attributes of bridges such as skew, number of spans and soil conditions. When compared to the results based on PGA and PGV, only one different damage state is seen at I-5 and I-10. This is caused by the spatial distribution of PGA and PGV, and is not significant.

Figures 7 and 8 display the result of post-earthquake ground motion intensity and traffic behavior in 3D animations. The legends in Figures 7 and 8 are the same as in Figures 5 and 6. These 3D animations show

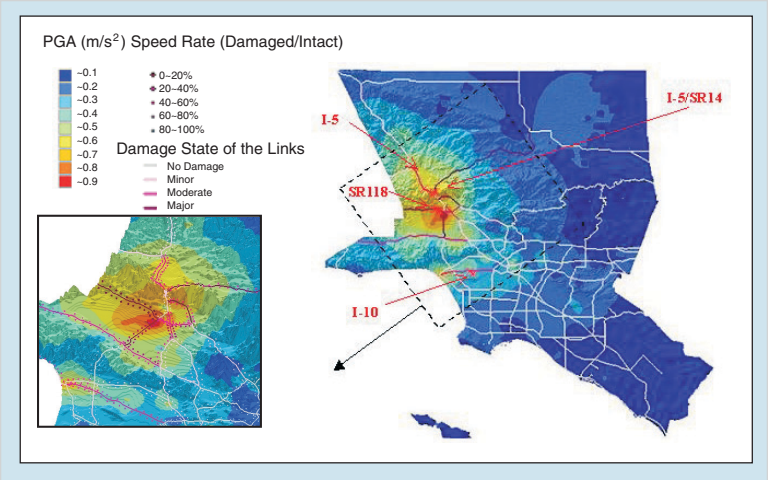

■ Figure 5. The 1994 Northridge Earthquake PGA Distribution, Average Damage State of Links, and Average Speed Ratio of Links (Using Fragility Curves on the Basis of PGA)

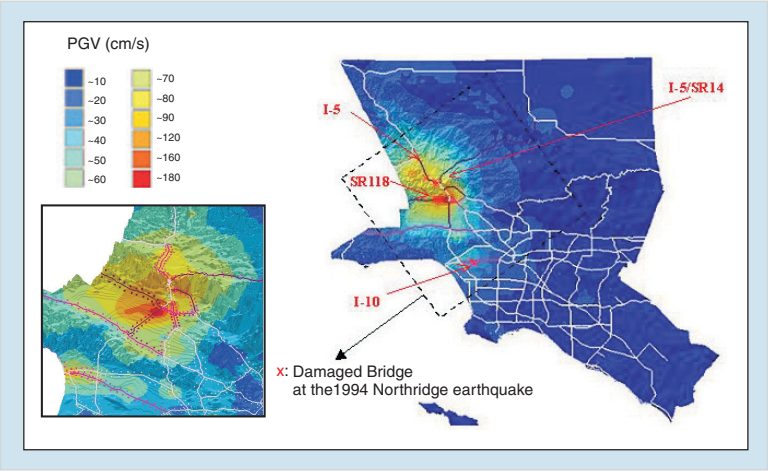

■ Figure 6. The 1994 Northridge Earthquake PGV Distribution, Average Damage State of Links, and Average Speed Ratio of Links (Using Fragility Curves on the Basis on PGV)

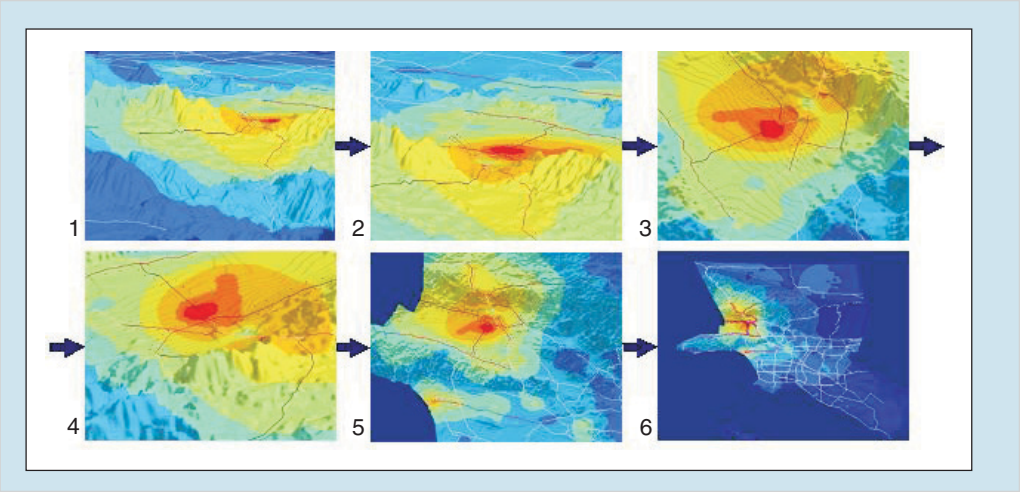

Figure 7. 3D Animation for the 1994 Northridge Earthquake (PGA)

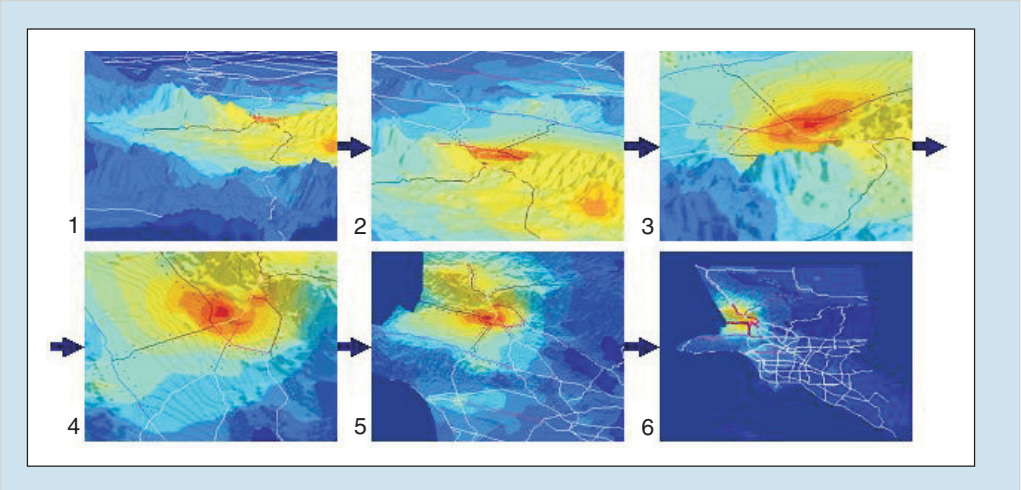

Figure 8. 3D Animation for the 1994 Northridge Earthquake (PGV)

the detail of traffic congestion in the damaged area, and thus are useful for developing pre-event emergency response strategies.

The computed average Drivers Delay is shown in Table 3. The total travel time under intact conditions is $8.90*10^5$ hours. Drivers Delay based on PGA and PGV increased 78% and 73% from the total travel time under intact condition, respectively. Drivers delay based on PGV was 7% shorter than based on PGA, which is not a significant difference. This shows that if PGA or PGV are used consistently, the difference between the actual data and simulation network analysis is insignificant.

Table 3. Average Drivers' Delay

Case	Total Travel Time $*10^5$ (hours)	Drivers' Delay $*10^5$ (hours)	Drivers' Delay (min/PCU)
Simulation Based on PGA	15.87	6.97	14.30
Simulation Based on PGV	15.40	6.50	13.34

*Total number of PCU (Passenger Car Unit) = 2,921,668

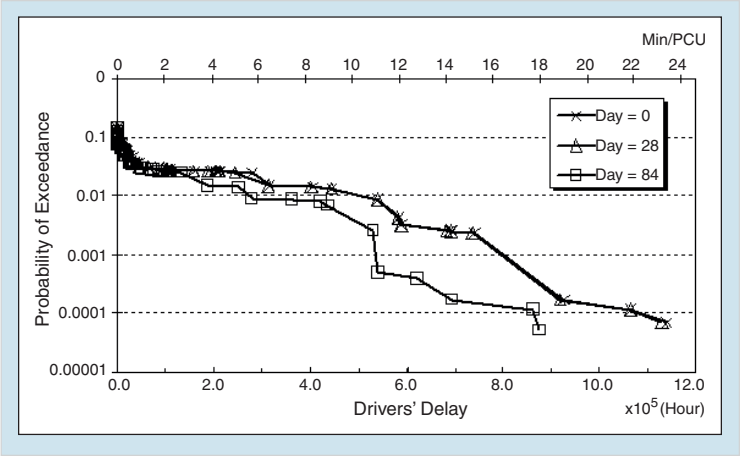

Figure 9. Risk Curves, Separated by Time after Event

Risk Curves for Repair Efforts

A set of 47 earthquake scenarios were considered, consistent with Chang et al., 2000. The spatial PGA distributions for the selected event scenarios are modeled using the USC-EPEDAT (Early Post Earthquake Damage Assessment Tool) software, jointly developed by University of Southern California and EQE, adapting original EPEDAT (Eguchi et al., 1997) to the present study.

The simulation is conducted by executing ten runs for each of the 47 earthquake scenarios.The Drivers Delay results are then averaged to offset the variability inherent in the implementation of the Monte Carlo method. The resulting data from each scenario's simulation includes: the damage caused to the network by the earthquake, the resulting Drivers Delay, and the variation of the Drivers Delay over time after the event. Using the Drivers Delay data, and the calculated probabilities of exceedance for each scenario event, risk curves are developed for the system.

Figure 9 plots the system risk curves for the Drivers Delay on Day 0, 28, and 84. Though there is a good deal of noise in the Day 84 curve, it is apparent that the probability to exceed large Drivers Delays is virtually eliminated 12 weeks after an event.

Loss Estimation

Similar simulations are performed for 47 scenario earthquakes using the fragility curves as a function of PGA with and without retrofit. The effect of retrofit is demonstrated by the ratio of the median values of the fragility curves for a retrofitted column to that of the column before retrofit (Shinozuka et al., 2002). This ratio is referred to as fragility "enhancement." The fragility enhancement shows 55%, 75%, 104%, and 143% improvement for the minor, moderate, major and collapse damage, respectively. It is assumed that the fragility enhancement thus obtained applies to the development of fragility curves with the retrofit for the empirical fragility curves (Figure 1 (a)). Figure 10 represents the fragility curves with and without retrofit. Figure 11 plots the risk curves for Drivers Delay with and without retrofit. The results of Drivers Delay based on enhanced fragility are

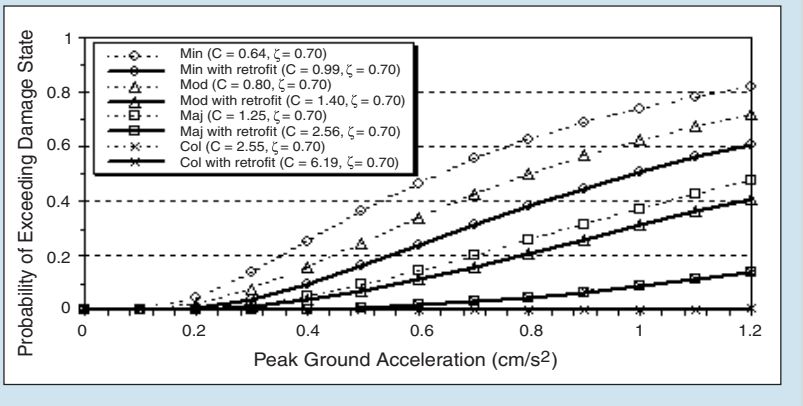

Figure 10. Fragility Curve, with and without Retrofit

reduced almost 90% over the results from without retrofit.

Furthermore, using these results, loss due to Drivers Delay is computed on the bases of $50 per one hour delay. Table 4 shows the results simulated for the representative scenario earthquakes. Estimated losses with retrofit are less than 10% of those without retrofit, and thus shows that the effect of retrofit is significant. Particularly, in the simulation for Malibu Coast, almost $50 million loss is avoided every day after the bridges are retrofitted, if repair is not made and if the same OD matrix is used.

A preliminary estimation of direct loss due to ground shaking and liquefaction is performed with the aid of HAZUS (National Institute of Building Sciences, 1999) software. In this estimation, 1,307 bridges, including local bridges in Orange County, are studied. Using HAZUS software, together with information available elsewhere for scenario earthquakes defined by MM (moment magnitude) and the liquefaction susceptibility map shown in Figure 12, permanent ground displacement (PGD) for lateral spread and ground settlement is evaluated. Integrating PGD, fragility curve, damage ratio, replacement value

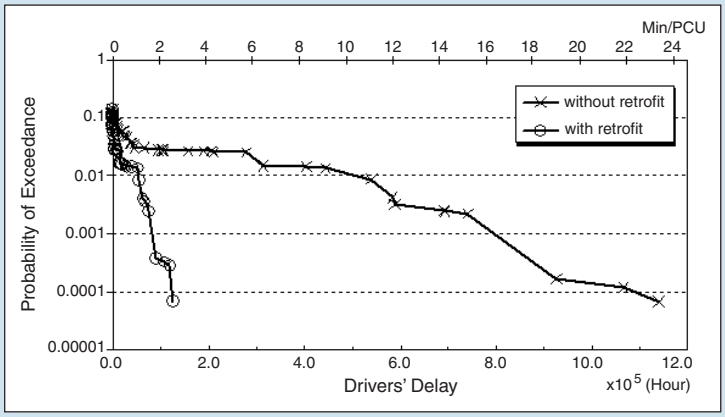

Figure 11. Risk Curves for Drivers Delay with and without Retrofit

Table 4. Daily Loss Due to Drivers' Delay ($M)

Scenario Earthquake	Without Retrofit	With Retrofit
Newport-Inglewood(S.) M7.0	4.74	0.27
Newport-Inglewood(N.) M7.0	10.60	0.98
Elysian Park M7.1	15.73	1.02
Malibu Coast M7.3	56.94	6.25

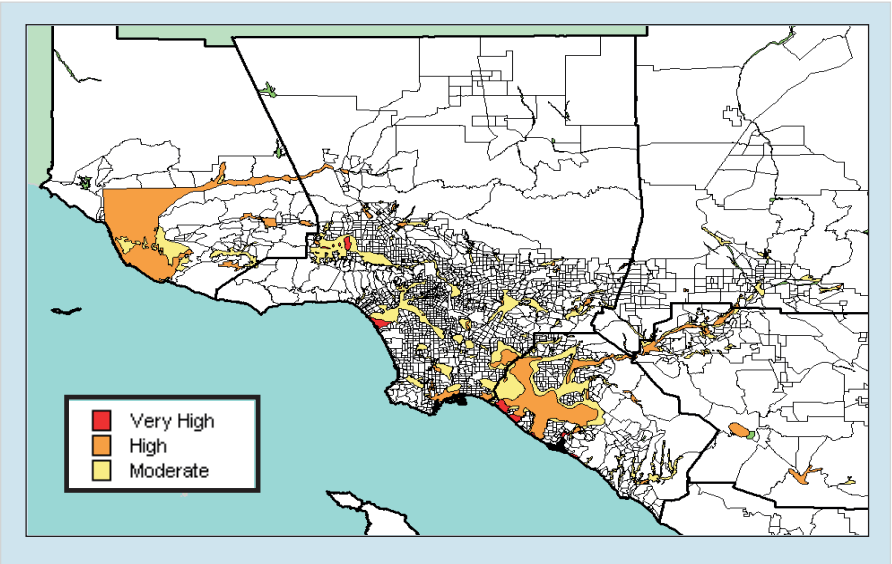

Figure 12. Liquefaction Susceptibility Map from EPEDAT (Eguchi et al., 1997)

■ Table 5. Loss Due to Ground Shaking and Liquefaction ($M)

Scenario Earthquake	Ground Shaking	Liquefaction	Ground Shaking & Liquefaction
Newport-Inglewood(S.) MM7.5	39.70	20.99	60.69
Newport-Inglewood(S.) MM6.9	29.27	15.97	45.24
Elysian Park MM6.7	16.63	9.40	26.03

and probability of liquefaction, loss due to liquefaction is estimated. The reader is referred to HAZUS Users' Technical Manual for the details. For the present analysis, the soil type is assumed to be stiff, and ground water depth is assumed to be five feet for the all bridges. Average replacement values of $150 per deck area (square foot) obtained from Caltrans data is used. Loss due to ground shaking plus liquefaction is estimated by simply adding both losses to be conservative and the results are shown in Table 5. From the table, losses due to liquefaction are almost 55 % of loss due to ground shaking, and thus the effect of liquefaction is significant.

Conclusions and Future Research

This study empirically developed four fragility curves associated with four different states of damage to Caltrans bridges using damage data compiled from the 1994 Northridge earthquake. Two-parameter lognormal distribution functions were used to represent the fragility curves. ShakeMap data were used for PGA and PGV at each bridge site.

Integrating the fragility information into the Monte Carlo analysis of traffic flows, degradation of traffic capacity of Caltrans' network in Los Angeles and Orange County damaged by the Northridge earthquake was evaluated. The simulation results were compared to the actual performance of Caltrans' network in the aftermath of the earthquake. Both simulation results were very reasonable, and it was concluded that the choice of ground motion intensity, whether PGA or PGV, does not significantly influence the network simulation results. Visual insight provided by the 3D animation of simulated traffic flow was useful in developing pre-event emergency response strategies.

A probabilistic model was developed to evaluate the effect of bridge damage repair on the improvement of the transportation network performance as days passed after the event. Notably, given the low probabilities of exceeding even moderate Drivers Delays, as evidenced by the risk curves, it can be said that the system exhibits remarkable resilience. This model could benefit from further work by considering the attributes of bridges, such as skew and number of spans, on the model repair processes.

Losses due to Drivers Delay with and without retrofit were computed by assuming the loss of $50 per one hour delay. The results show that the effect of retrofit was significant. Losses due to ground shaking and liquefaction were estimated with the aid of HAZUS software as a first step to incorporate PGD in the analysis. The effect of liquefaction is an important factor to be taken into account in the transportation network simulation.

Future study will emphasize the following subjects: dynamic aspects of traffic flow problems relative to

post-earthquake traffic demand; link damage definition and related link occupancy; modeling the repair process as a function of the size and importance of bridges; and perform uncertainty analysis to take advantage of the integrated insight acquired through this and other studies on modeling, numerical analysis and statistical interpretation.

References

ArcGIS 8.2, (1999), ESRI Inc., *http://www.esri.com.*

Chang, S.E. Shinozuka, M. and Moore, J., (2000), "Probabilistic Erathquake Scenarios: Extending Risk Analysis Methodologies to Spatially Distributed Systems," *Earthquake Spectra*, Vol.16, No.3, pp-557-572.

Eguchi, R.T., Goltz, J.D., Seligson, H.A., Flores, P.J., Blais, N.C,. Heaton T.H. and Bortugno, E., (1997), "Real-time Loss Estimation as an Emergency Response Decision Support System: the Early Post-Earthquake Response Tool (EPEDAT)," *Earthquake Spectra*, Vol.13, 1997, pp. 815-832.

Goltz, J.D., (1994), *The Northridge, California Earthquake of January 17, 1994: General Reconnaissance Report*, Technical Report NCEER-94-0005, March 11, 1994.

Intl. Conference of Building Officials, (1994), *Uniform Building Code.*

National Institute of Building Sciences, (1999), *Earthquake Loss Estimation Methodology: HAZUS 99 (SR2) Technical Manual*, Developed by Federal Emergency Management Agency, Washington DC, *http://www.fema.gov/hazus*.

Shinozuka, M., Shiraki, N. and Kameda H., (2000), "Performance of Highway Network Systems under Earthquake Damage," *Proceedings of the Second International Workshop on Mitigation of Seismic Effects on Transportation Structures*, Taiwan, Sep. 13-15, 2000, pp. 303-317.

Shinozuka, M., Feng, M.Q., Kim, H., Uzawa, T. and Ueda, T., (2001), *Statistical Analysis of Bridge Fragility Curves*, unpublished MCEER Technical Report, *http://shino8.eng.uci.edu/journalpapers.htm*.

Shinozuka, M., Kim, S.H., Kushiyama S. and Yi, J.H., (2002), "Fragility Curves of Concrete Bridges Retrofitted by Column Jacketing," *Journal of Earthquake Engineering and Engineering Vibration*, Vol. 1, No. 2, Dec. 2002, *http://shino8.eng.uci.edu/journalpapers.htm.*

Shiraki, N., (2000), *Performance of Highway Network Systems under Seismically Induced Traffic Delays*, M. S. Thesis, Kyoto University, Kyoto, Japan.

Southern California Association of Governments, (1993), *1991 Origin-destination survey*, Los Angeles, CA.

TriNet ShakeMap, (2001), *http://www.trinet.org/shake/.*

US Bureau of Public Roads, (1964), *Traffic Assignment Manual*.

Performance Estimates in Seismically Isolated Bridges

by Gordon P. Warn and Andrew S. Whittaker

Research Objectives

The objectives of this research are two fold. First, to evaluate the accuracy and efficacy of the static analysis procedure for calculating displacements at the center of rigidity of seismically isolated bridge structures subjected to earthquake excitation. Two key assumptions of the current static analysis procedure set forth by the American Association of State Highway and Transportation Officials (AASHTO) Guide Specifications for Seismic Isolation Design are investigated, namely, linearly increasing displacements for periods greater than 1-second and the effect of bidirectional horizontal shaking on the displacement estimate can be ignored. Second, to propose an improved testing protocol for prototype seismic isolators for seismic loading. This improved prototype testing protocol will be determined based on the observed energy demands imposed on seismic isolators from numerical simulation of maximum earthquake shaking.

Sponsors

Federal Highway Administration

Research Team

Gordon P. Warn, *M.S. Candidate, and* ***Andrew S. Whittaker****, Associate Professor, Department of Civil, Structural and Environmental Engineering, University at Buffalo*

A key step in predicting the performance of a seismically isolated bridge during earthquake shaking is estimating the maximum displacement response of the isolation system. Once the isolators are sized to accommodate the gravity and earthquake loads, service-level displacements, and maximum earthquake displacements, the isolators are evaluated by full-scale prototype testing. The *AASHTO Guide Specification for Seismic Isolation Design* (AASHTO, 1999) provides both an equation for estimating maximum displacements and procedures for prototype testing.

The AASHTO equation for calculating displacements in seismically isolated bridges (Equation 3a in the Uniform Load Method) is based on work in the 1980s with a focus on building structures. The equation assumes linearly increasing displacements in the constant-velocity region of the design spectrum and accounts for the effects of energy dissipation (hysteretic or viscous) using properties of the equivalent viscoelastic system. The seismic input is assumed to be unidirectional for the AASHTO calculation. The AASHTO equation is:

$$d = \frac{10 A S_i T_{eff}}{B} (inches) \qquad (1)$$

Web Sites

PEER Strong Motion Database:
http://peer.berkeley.edu/smcat/

SAC Steel Project Database:
http://nisee.berkeley.edu/data/strong_motion/sacsteel/ground_motions.html

where d is the calculated displacement at the center of rigidity of the isolation system in inches, A is an acceleration coefficient in g; S_1 is a coefficient related to the site soil profile; T_{eff} is the effective period of the isolation system at the design displacement in seconds; and B is a coefficient related to the system damping.

Given the importance of Equation 1 in the design of seismic isolation systems for bridges (and buildings), it is appropriate to question its accuracy. Legitimate questions related to the characterization of the spectrum (the definition of the constant velocity range), the effect of bidirectional earthquake input on the calculation of maximum displacement, and the use of conservative (small) values for the damping factor B have been posed.

This research will lead to answers to these questions. Another result of this research will be a new equation for calculating maximum displacements if it is shown that Equation 1 is either unconservative (under-predicts maximum displacements) or too conservative (grossly over-predicts maximum displacements). Such a new equation would better characterize the design spectrum over a broad period range (perhaps using the NEHRP characterization of a design spectrum), account for bidirectional seismic input, and make use of the improved values of B per the work of Ramirez et al., 2000.

Prototype testing assesses the adequacy of a production seismic isolator. Inappropriate procedures for prototype testing will lead to inaccurate assessments of isolator performance. Procedures for evaluating the response of a seismic isolator should be closely tied to the demands imposed on the isolators and isolation system during extreme or maximum earthquake shaking. Some procedures adopted in the past decade for evaluating the performance of seismic isolators have been overly onerous or excessive leading to inappropriate conclusions. Data from the response-history analysis being conducted in support of the maximum-displacement studies described above are being mined to provide new knowledge of the energy-related demands on seismic isolators and seismic isolation system during maximum earthquake shaking.

Research Approach

A summary of the approach used for this research is presented first, followed by a more detailed explanation of the individual components. First, ground motions were collected and organized into several bins to facilitate response-history analysis. Both unidirectional and bidirectional response-history

Results of this investigation will provide bridge design engineers and isolation hardware suppliers with useful information for prototype testing requirements of seismic isolator units. Other potential users of the results of this research beyond the academic community include the AASHTO, state highway agencies, and building design engineers.

analysis was performed considering linear and nonlinear systems using seven bins of ground motions. Results of the response-history analyses are being used to determine: (1) the increase in horizontal displacement of an isolator due to bidirectional seismic excitation and (2) review the accuracy of the AASHTO equation and suggest modification to the current equation, and (3) the energy demand imposed on individual isolators and isolation systems subjected to a maximum earthquake event.

A total of 72 earthquake ground motion pairs were utilized for this study. Ground motions were organized into seven bins, four of which are based on moment magnitude and distance-to-fault. Acceleration time histories were extracted from two sources. The first, the Pacific Earthquake Engineering Research (PEER) database (PEER, 2000), and the second, the SAC Steel Project database, (SAC, 1997). The ground motion bins are denoted: (1) Near-Field, (2M) Large-Magnitude Small-Distance (3) Large-Magnitude Large-Distance, (4) Small-Magnitude Small-Distance, (5) Small-Magnitude Large-Distance, (6) Near-Field Soft-Soil and (7) Large-Magnitude Soft-Soil. Bin names qualitatively represent the parameter values used to group the ground motions, noting, that descriptions of Bins (2M) through (5) were first adopted by Krawinkler (2001). Information regarding the seven bins of ground motions used in this study is presented in Table 1.

Elastic response spectra were generated for each ground motion component used in this study. All spectra were generated for 5% critical damping. Short period mean spectral accelerations ranged from approximately 1.1g for the near-field bin (Bin 1) to 0.18g for small-magnitude small-distance bin (Bin 5). This range of spectral demand is representative of seismic hazard zones throughout the United States. Mean and median spectra were generated assuming the spectral acceleration data follow a normal and lognormal distribution, respectively. For brevity, mean and median spectra generated for each bin have not been shown.

A simple SDOF oscillator was assumed for linear response-history analysis. The SDOF oscillator was characterized using the following parameters: ζ the critical viscous damping ratio and T_n the natural period of vibration. Four values of the critical damping ratio were con-

Table 1. Ground Motion Bins

Bin	Name	Number of Records	Moment Magnitude	Distance to Fault (km)	Soil Type	Soil Classification
1	NF	24	6.7 – 7.4	<10	D	NEHRP
2M	LMSD	20	6.7 – 7.4	10 – 30	A,B,C	USGS
3	LMLD	20	6.7 – 7.3	30 – 60	A,C	USGS
4	SMSD	20	5.8 – 6.5	10 – 30	A,C	USGS
5	SMLD	20	5.8 – 6.5	30 – 60	A,C	USGS
6	NF-SS	20	6.5 – 7.3	1.2 – 36	E,F	NEHRP
7	LM-SS	20	6.9 – 8.1	2.6 – 385	E,F	NEHRP

sidered: 0.05, 0.10, 0.20 and 0.30. The natural period of vibration, T_n, was varied from nearly zero to 4.0 seconds for each level of damping considered.

For unidirectional response-history analysis, the equation of motion was solved numerically to obtain the displacement response using each ground motion component and is presented in mass normalized form as

$$\ddot{u}(t)+\left(\frac{4\cdot\pi\cdot\zeta}{T_n}\right)\cdot\dot{u}(t)+\left(\frac{2\cdot\pi}{T_n}\right)^2\cdot u(t)=-\ddot{u}_g(t) \qquad (2)$$

where T_n and ζ are the natural period and critical damping ratio as previously defined; $\ddot{u}(t)$ is the acceleration response; $\dot{u}(t)$ is the velocity response; $u(t)$ is the displacement response; and $\ddot{u}_g(t)$ is the earthquake ground acceleration. For each ground motion, the maximum of the displacement response was recorded for each set of parameters, ζ and T_n. For bidirectional response-history analysis the equation of motion, shown previously, was solved for each ground motion component individually and the horizontal displacement response calculated as the square-root-sum-of-squares of each orthogonal displacement at every time step. The maximum of the horizontal displacement response was then recorded for each set of parameters, ζ and T_n.

For nonlinear response-history analysis, a mathematical model of a simple isolated bridge structure was utilized. This model represents the simplest of isolated bridge structures and assumes both the superstructure and the substructure to be rigid. This simple bridge model enables a clear understanding of the effect of bidirectional excitation on isolation systems. Properties for the model bridge (i.e., mass, length, width) were based on a single span of a multi-span bridge proposed in an Applied Technology Council report (ATC, 1986). The isolators were modeled using a coupled-plasticity representation (Huang, 2000). Defining parameters of this model are based on a unidirectional bilinear characterization of the isolator. A schematic of this bilinear characterization and design parameters is shown in Figure 1. The second-slope stiffness can be related to the second-slope period using the following equation

$$T_d=2\cdot\pi\sqrt{\frac{W}{K_d\cdot g}}\quad (seconds) \qquad (3)$$

where W is the weight acting on the isolator; g is the gravitational acceleration constant; T_d is the second-slope period; and K_d is the second-slope stiffness.

Isolator parameters (i.e., normalized characteristic strength and second slope period) were varied to ensure broad applicability of results for isolated bridges in the United

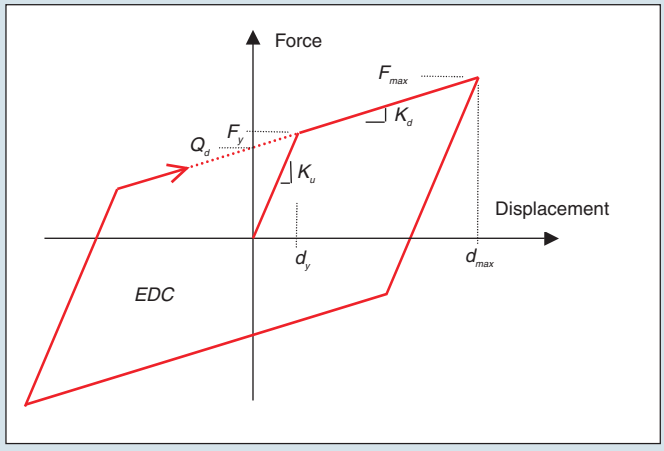

Figure 1. Unidirectional Bilinear Characterization of an Isolation Bearing

States. Four values of the characteristic strength Q_d/W (normalized by the weight acting on the isolator) were chosen and ranged from 0.03 to 0.12. Similarly, five values of the second-slope period, T_d, were chosen and ranged from 1.5 seconds to 4.0 seconds resulting in twenty combinations of isolation parameters.

Both unidirectional and bidirectional excitation where considered for nonlinear response–history analysis. For unidirectional excitation, 144 response-history analyses were performed for each of twenty combinations of isolator parameters for a total of 2880 simulations. For bidirectional excitation, 72 ground motions pairs were used for nonlinear response-history analysis for a total of 1440 simulations. Displacement and force data were also processed to calculate the energy dissipated by seismic isolators during earthquake excitation.

Shown in Figure 2 are sample results of nonlinear response-history analysis considering unidirectional and bidirectional excitation with isolator parameters, $Q_d/W = 0.09$ and $T_d = 4.0$ seconds. The ground motion components used for these analyses are from the Northridge earthquake, Canoga Park station (CNP106_ AT2.txt and CNP196_ AT2.txt) and are part of ground motion bin 2M. Two important results of bidirectional excitation are shown in Figure 2. The first being the effect on unidirectional isolator properties (i.e, Q_d) and the second the increase in displacement along the x-direction horizontal axis. Due to the coupled behavior of the isolator response, the contribution of plastic force in the x-(horizontal) direction varies due to ground motion demands in the perpendicular y- (horizontal) direction. The result of the bidirectional analysis is shown in Figure 2 by the solid black line. A reduction in the plastic force along one axis results in an increase in isolator displacement along that axis thus increasing the displacement of the isolator in the horizontal x–y plane. This observation is similar to that reported in Huang (2000) and Mosqueda (2001).

Results of both the unidirectional and bidirectional nonlinear response-history analysis are being used to determine the increase in horizontal displacement due to bidirectional excitation. Two factors contribute to this increase in horizontal displacement, the first contribution is due to the phasing of the earthquake ground motion components, and the second is a result of the coupled behavior of the isolators. One approach to quantify this increase is in the form

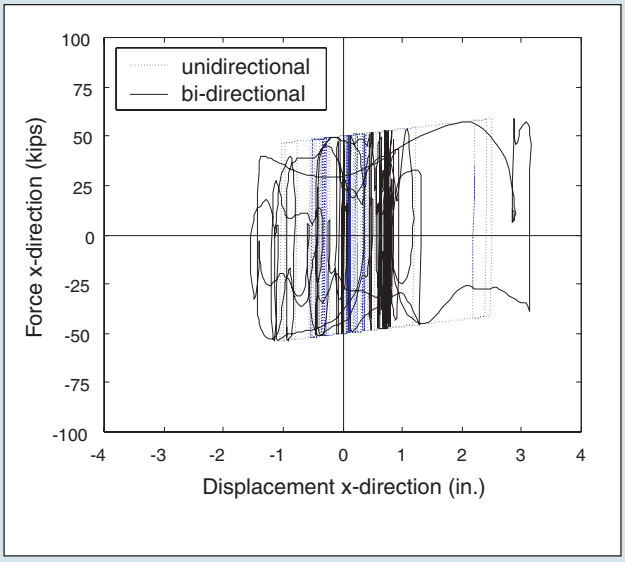

Figure 2. Sample Results of Nonlinear Response-History Analysis for Unidirectional and Bidirectional Excitation using Ground Motions: CNP106 and CNP 196

"The final results from this research will be used to develop an improved equation for calculating maximum displacements in seismically isolated bridges"

of a unidirectional displacement multiplier, α_{xy}.

This multiplier has been defined to be the average of the ratio of the maximum horizontal displacement of the isolated bridge considering bidirectional excitation to the maximum displacement of the isolated bridge considering unidirectional excitation. The equation for the unidirectional displacement multiplier is shown below

$$\alpha_{xy} = average\left(\frac{d_{xy}^{i}}{d_{x}^{i}}\right) \qquad (4)$$

where d_{xy}^{i} is the maximum horizontal displacement of the center of rigidity of the isolation system determined from bidirectional response-history analysis using the i^{th} ground motion pair for a particular bin of ground motions; and d_{x}^{i} is the maximum displacement of the center of rigidity of the isolation system determined from unidirectional response-history analysis using the first component of the i^{th} ground motion pair.

An investigation of the energy dissipated by an individual seismic isolator during earthquake excitation was undertaken to assess current prototype testing requirements for bridge seismic isolators. Results of the unidirectional and bidirectional nonlinear response-history analyses were utilized to determine the energy dissipated by seismic isolators during earthquake excitation. Results of this investigation have been presented in the form of normalized energy dissipated (*NED*) given by Equation 5

$$NED = \frac{\int F \cdot dU}{EDC} \qquad (5)$$

where, F is the restoring force corresponding to an incremental distance dU. Integration of $F{\cdot}dU$ gives the cumulative energy dissipated by the seismic isolator from the nonlinear response-history analysis determined using numerical integration of the force-displacement response of the isolator. For bidirectional response-history analysis the total cumulative energy dissipated was calculated as the sum of the cumulative energy dissipated in each of the two horizontal orthogonal directions, namely

$$E = \int F_x \cdot dU_x + \int F_y \cdot dU_y \qquad (6)$$

The *EDC*, energy dissipated per cycle, was calculated assuming one fully reversed cycle to the maximum displacement determined from response-history analysis using Equation 7

$$EDC = 4 \cdot Q_d \cdot \left(d_{max} - d_y\right) \qquad (7)$$

where, Q_d is the characteristic strength of the isolator; d_{max} is the maximum displacement obtained from response-history analysis; and d_y is the yield displacement that is assumed to be negligible. For bidirectional excitation the *EDC* was calculated using the maximum horizontal displacement, determined as the maximum of the square-root-sum-of-squares response.

Research Results

Results of the unidirectional and bidirectional response-history analyses performed for this study are being mined to determine maximum isolator displacements and the cumulative energy dissipated by seismic isolators during earthquake excitation. In the case of bidirectional analysis the response in each horizontal orthogonal direction were combine at every time step to determine the square-root-sum-of-squares response from which the maximum horizontal isolator displacement was determined. Maximum unidirectional and bidirectional displacements are being used to evaluate Equation 3a (Equation 1 of this paper) of the AASHTO Guide Specifications Seismic Isolation Design, Uniform Load Method (AASHTO, 1999).

Design displacements were calculated using the AASHTO Uniform Load Method for each of the twenty isolation systems considered in this study using the mean 1-second spectral acceleration for each of the seven bins of ground motions and damping coefficients from two sources: (1) Table 7.1 – 1 from the AASHTO Guide Specifications and (2) Table 3 – 3 from Ramirez et al. (2000). Presented in Figure 3a are design displacements obtained using the AASHTO approach with the damping coefficients from AASHTO and the 1-second spectral acceleration from the mean spectrum of Bin 1; $A{\cdot}S_i$=1.0g which assumes a site coefficient of unity corresponding to a stiff soil or rock site. Displacements are observed to increase with increasing effective period for all system strengths considered. This is due to the conservative values of the damping coefficient assumed by AASHTO, which are limited to a value of 2 for 50 percent damping or greater. Referring to Figure 3b, using the AASHTO approach with damping coefficients per Ramirez et al, an increasing trend is observed for the systems with the lowest strength, namely Q_d/W=0.03.

For each of the other three system considered (all with greater strength), significantly different

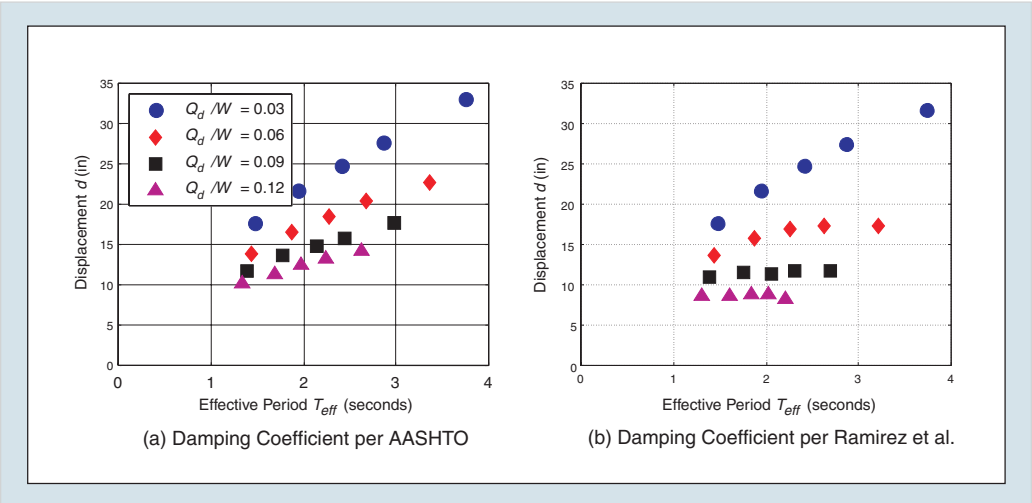

Figure 3. Calculated Displacements for Twenty Isolation Systems using AASTHO Equation 3a and the Mean Spectrum from Bin 1 (AS_i=1.0g)

trends are observed with increasing effective period. These trends are simply explained from the values of the damping coefficients per Ramirez et al., which are not limited at 50 percent damping but increasing to a value of 4.65 for 100 percent damping. This result implies that using properties of the equivalent viscoelastic system for hysteretic systems with greater strengths to accounting for the effects of energy dissipation may be inappropriate. Further studies on this subject are now underway.

Shown in Figure 4 is a comparison between displacements calculated using the AASHTO approach utilizing both definitions of the damping coefficient with the mean results of unidirectional and bidirectional response-history analysis considering ground motions from Bin 1. In Figure 4, d is the displacement calculated using the AASHTO approach and the mean, 5% damped elastic spectrum determined from Bin 1 ground motions; d_x is the mean of the maximum displacements obtained from unidirectional nonlinear response-history analysis; and d_{xy} is the mean of the maximum horizontal displacements obtained from bidirectional nonlinear response-history analysis. Referring to Figure 4a, it is observed that the AASHTO approach conservatively estimated the maximum displacement for unidirectional excitation (top plot of Figure 4a) for almost all isolation systems considered. However, the displacements obtained using the AASHTO method under predict the maximum displacement for all systems considered when compared to the results of bidirectional analysis, d_{xy} (middle plot of Figure 4a). A comparison between the displacements obtained from the AASHTO approach using damping coefficients per Ramirez et al. (2000) and the mean of the maximum displacements from unidirectional response-history analysis are shown in the top plot of Figure 4b. It is clear that for isolation systems with Q_d/W=0.03 the AASHTO displacement calculated using damping coefficients per Ramirez et al. are conservative. However for systems with higher strengths the displacements are unconservative. Comparing the AASHTO displacements to the results of bidirectional response-history analysis (middle plot of Figure 4b), it is clear that the AASHTO approach significantly underestimates the maximum isolator displacement. Shown in the bottom two plots of Figure 4 is a comparison of the AASHTO calculated displacements multiplied by a unidirectional displacement multiplier, α_{xy}, and the results of bidirectional response-history analysis. Values of the unidirectional displacement multiplier have not been presented here, however, values ranged from approximately 1.0 to 1.2 for Bin 1 using the definition given by Equation 4. These results suggest that the displacements obtained using the AASHTO approach multiplied by a unidirectional displacement multiplier lead to unconservative estimates of the maximum displacement. In light of this observation, alternative definitions for α_{xy}, are being explored.

Sample results of the work on energy dissipated by seismic isolators during earthquake excitation are presented in Figure 5. Plotted in Figure 5a, is the mean normalized energy dissipated by an individual isolator for each of the isolation systems considered based

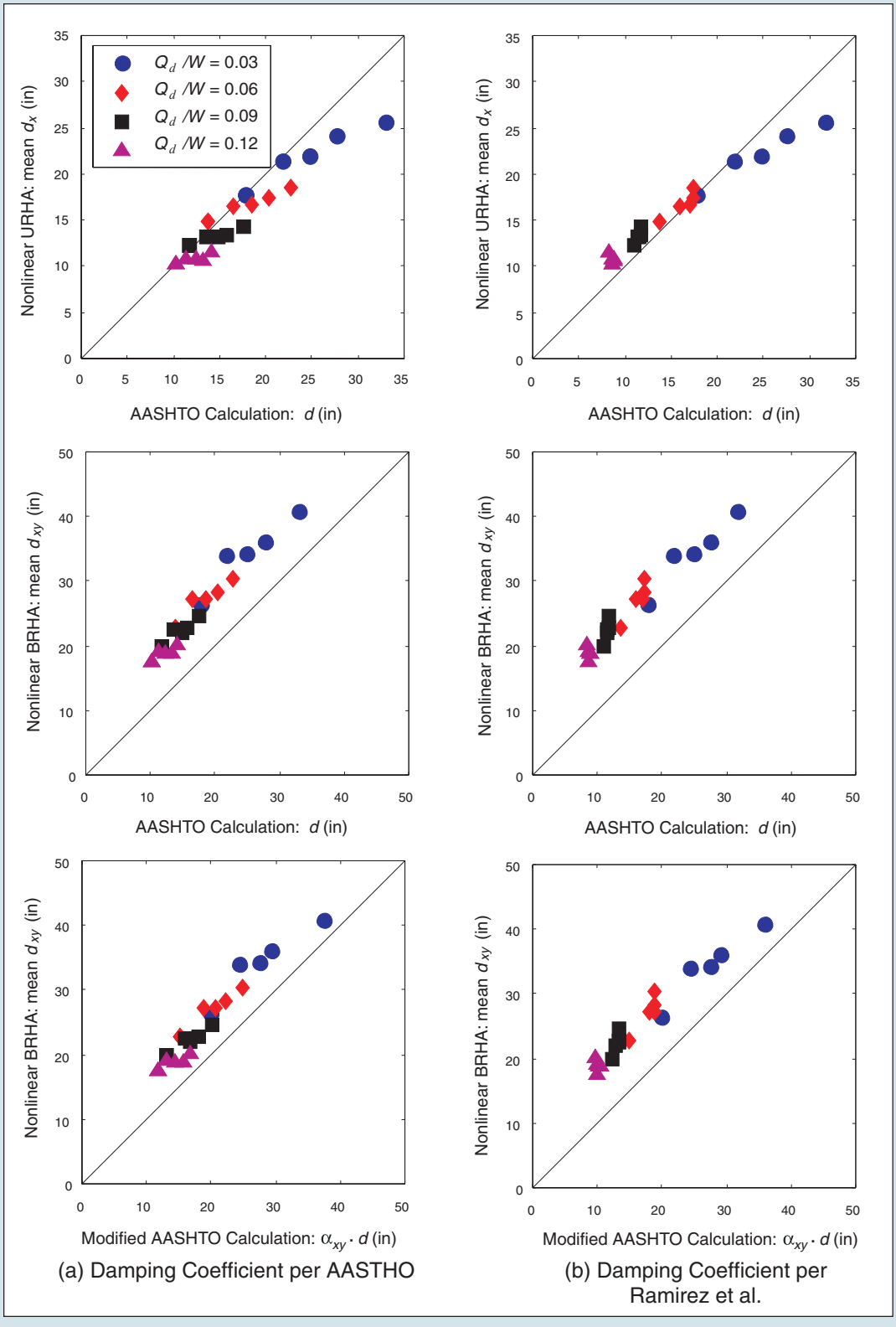

■ Figure 4. Comparison of Displacements Obtained from AASHTO Equation 3a using the Mean Spectrum of Bin 1 (AS_i=1.0g) and Nonlinear Response-History Analysis

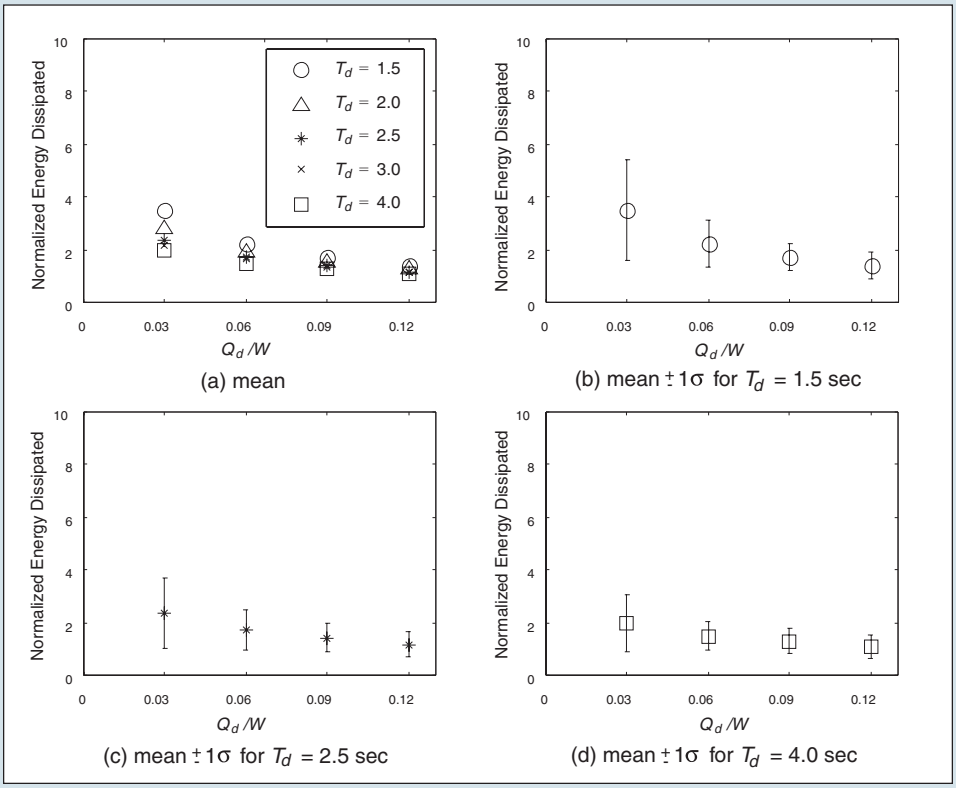

■ Figure 5. Normalized Energy Dissipated Based on the Results of Unidirectional Response-History Analysis using Bin 2M Ground Motions

on unidirectional excitation using ground motions from Bin 2M. Mean values have been reproduced in Figures 5b, 5c, and 5d including sample standard deviation information (shown by the error bars) for isolation systems with second-slope periods of, 1.5, 2.5, and 4.0 seconds, respectively. Figure 5a shows a decreasing trend in normalized energy dissipated with increasing characteristic strength (normalized by the weight acting on the isolator) for each value of the second-slope period considered. Similar trends were observed for analyses performed using the remaining six bins of ground motions. If only isolators with Q_d/W=0.06 (or greater) and T_d = 2.5 seconds (common isolator properties) are considered, the normalized energy dissipated is observed to be approximately two or less. These sample results suggest that on average the current procedures for the prototype testing of seismic isolators impose far greater demands than would be observed due to an extreme or maximum earthquake event.

Conclusions

Results presented in this report are only preliminary final results and conclusions will be presented upon completion of the research (Warn, 2003). Conclusions based

on the results of research conducted to date indicate the following:

1. Both linear and nonlinear response-history analysis indicate bidirectional earthquake excitation significantly increases maximum horizontal isolator displacements over those calculated assuming unidirectional excitation.
2. The 1999 AASHTO and 1996 HITEC prototype-testing requirements impose far greater demands on an isolator unit than the demands observed from numerical simulation of maximum earthquake shaking.

Final results will be used to develop an improved equation for calculating maximum displacements in seismically isolated bridges. This improved equation will account for bidirectional seismic input through the use of a displacement amplification factor similar to the unidirectional displacement multiplier presented here. Finally, an improved testing protocol for prototype seismic isolators subject to seismic loading will be proposed. This improved testing protocol will likely be in the form of a number of sinusoidal cycles to the total design displacement at a specified (dynamic) frequency.

References

AASHTO, (1999), *Guide specifications for seismic isolation design*, American Association of State Highway and Transportation Officials (AASHTO).

ATC, (1986), *Seismic Design Guidelines for Highway Bridges,* Applied Technology Council (ATC), Report ATC-6.

HITEC, (1996), *Guidelines for the Testing of Seismic Isolation and Energy Dissipating Devices*, CERF Report: HITEC 96-02, Highway Innovative Technology Evaluation Center, Washington, DC.

Huang W.-H., Fenves G.L., Whittaker, A.S. and Mahin, S.A, (2000), "Characterization of Seismic Isolation Bearings for Bridges from Bi-directional Testing," *Proceedings of the 12th World Conference on Earthquake Engineering*, New Zealand.

Krawinkler, (2001), Private Communication.

Mosqueda, G., (2001), *Experimental and Analytical Studies of the Friction Pendulum System for the Seismic Protection of Bridges,* CE 299 Report, Department of Civil and Environmental Engineering, University of California at Berkeley.

PEER, (2000), *Strong Motion Database, http://peer.berkeley.edu/smcat/.*

Ramirez, O.M., Constantinou, M.C., Kircher, C.A., Whittaker, A.S., Johnson, M.W. and Gomez, J.D., (2000), *Development and Evaluation of Simplified Procedures for Analysis and Design of Buildings with Passive Energy Dissipation Systems.* Technical Report MCEER-00-0010, Multidisciplinary Center for Earthquake Engineering Research, University at Buffalo.

SAC, (1997), *Suites of Earthquake Ground Motions for Analysis of Steel Moment Frame Structure*, Report SAC/BD-97/03, Woodward-Clyde Federal Services, SAC Steel Project.

Warn, G., (2003), *Performance Estimates in Seismically Isolated Bridge Structures,* M.S. Thesis, University at Buffalo, May.

Developing Fragility Curves for Concrete Bridges Retrofitted with Steel Jacketing

by Masanobu Shinozuka and Sang-Hoon Kim

Research Objectives

The ultimate goal of this research is to improve highway system performance in earthquakes by evaluating the effectiveness of retrofitting bridges with column jacketing. The objective of the study is to determine if steel jacketing increases the ductility capacity of bridge columns and hence improves the fragility characteristics of the bridge. Analytical fragility curves are used to adjust the empirical fragility curves obtained for the unretrofitted bridges using seismic damage data collected following past earthquakes. The adjustment was carried out by increasing the median values of the empirical curves through comparison with the median values of the corresponding fragility curves obtained analytically, both before and after being retrofit.

Sponsors

Federal Highway Administration and Caltrans

Research Team

***Masanobu Shinozuka**, Distinguished Professor and Chair, **Sang-Hoon Kim**, Research Associate, **Jin Hak Yi**, Visiting Research Associate (from the Korea Advanced Institute of Science and Technology) and **Shigeru Kushiyama**, Visiting Research Scholar (from Hokka-Gakuen University, Japan), Department of Civil and Environmental Engineering, University of California, Irvine*

Several recent destructive earthquakes, particularly the 1989 Loma Prieta and 1994 Northridge earthquakes in California, and the 1995 Kobe earthquake in Japan, have caused significant damage to highway structures. The investigation of this damage gave rise to a serious review of existing seismic design philosophies and led to extensive research activities on the retrofit of existing bridges as well as the development of seismic design methods for new bridges. This study presents an approach to the fragility assessment of bridges retrofitted by steel jacketing of columns with substandard seismic characteristics.

This study presents the results of an in depth fragility analysis of typical bridges in California that have been strengthened using steel jacketing of bridge columns. A computer code was developed and used to calculate the bilinear hysteretic parameters of the bridge columns before and after steel jacketing. Nonlinear dynamic time history analysis was used to evaluate the responses of the bridges before and after column retrofit under sixty ground acceleration time histories developed for the Los Angeles area by the Federal Emergency Management Agency (FEMA) SAC (SEAOC-ATC-CUREe) steel project (Somerville et al., 1997). Monte Carlo simulation was used to study fragility curves represented by lognormal distribution functions with two parameters (fragility parameters consisting of median and log-standard deviation) and developed as a function of

Collaborative Partners

***Li-Hong Shen**, Caltrans*

***W. Phillip Yen**, Federal Highway Administration*

peak ground acceleration (PGA). Fragility curves of the bridges before and after column retrofit were compared and the results show that steel jacketing significantly improved the seismic performance of bridges.

Retrofit of the Concrete Columns

Concrete columns commonly lack flexural strength, flexural ductility and shear strength, especially in the bridges designed under older codes. The main causes of these structural inadequacies are lap splices in critical regions and/or premature termination of longitudinal reinforcement.

A number of column retrofit techniques, such as steel jacketing, wire pre-stressing and composite material jacketing, have been developed and tested. Although advanced composite materials and other methods have been recently studied, steel jacketing is the most common retrofit technique.

Steel Jacketing

An experiment was performed by Chai et al., 1991 to investigate the retrofit of circular columns with steel jacketing. In this experiment, for circular columns, two half shells of steel plate rolled to a radius slightly larger than the column are positioned over the area to be retrofitted and are site-welded up the vertical seams to provide a continuous tube with a small annular gap around the column. This gap is grouted with pure cement. Typically, the jacket is cut to provide a space of about 50 mm (2 inches) between the jacket and any supporting member. This is to prevent the possibility of the jacket acting like a compressing reinforcement by bearing against the supporting member at large drift angles. The jacket is effective only in passive confinement and the level of confinement depends on the hoop strength and stiffness of the steel jacket.

Moment-Curvature Relationship

Confining Effect of Transverse Reinforcement

Chai et al., 1991 also observed that confinement of the concrete columns can be improved if transverse reinforcement layers are

Analytical fragility curves computed for various damage states in this study make intuitive sense relative to the bridge's design, retrofit and performance in past earthquakes. This research provides information necessary to the design profession from the performance design perspective, and paves the way for ensuing analysis to determine the level of enhancement of transportation network performance due to the retrofit. This research is thus beneficial to bridge engineering, transportation engineering and management professionals.

placed relatively close together along the longitudinal axis by restraining the lateral expansion of the concrete. This makes it possible for the compression zone to sustain higher compression stresses and much higher compression strains before failure occurs. Unfortunately, however, it cannot be applied to existing bridges to enhance the performance of columns by adding transverse reinforcement layers.

Compression Stress-Strain Relationship for Confined Concrete

Confinement increases the compression strength and ultimate strain capacity of concrete. Many different stress-strain relationships have been developed for confined concrete. Most of these are applicable under certain conditions. A recent model applicable to all cross-sectional shapes and all levels of confinement (Shinozuka et al., 2003b) is used here for the analysis together with key equations from Priestley et al., 1996.

Bridge Analysis

Description of Bridges

Two example bridges used for the analysis are shown in Figures 1 and 2. Bridge 1 has the overall length of 34 m with three spans. The superstructure consists of a longitudinally reinforced concrete deck slab 10 m wide and is supported by two pairs of columns (and by an abutment at each end). Each pair has three columns of circular cross section with 0.76 m diameter. The

Links to Current Research

The analysis method described here is for developing fragility curves for retrofitted bridges. The method can also be applied to other lifelines, such as power and water systems, as well as hospital facilities, where fragility curves are being developed.

In the economic dimension, this study provides a basic cost-benefit analysis procedure for seismic retrofit of bridges.

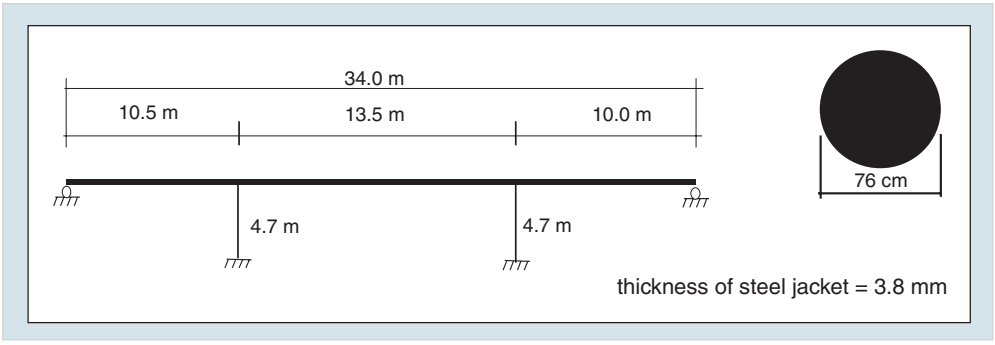

Figure 1. Elevation and Column Section of Bridge 1

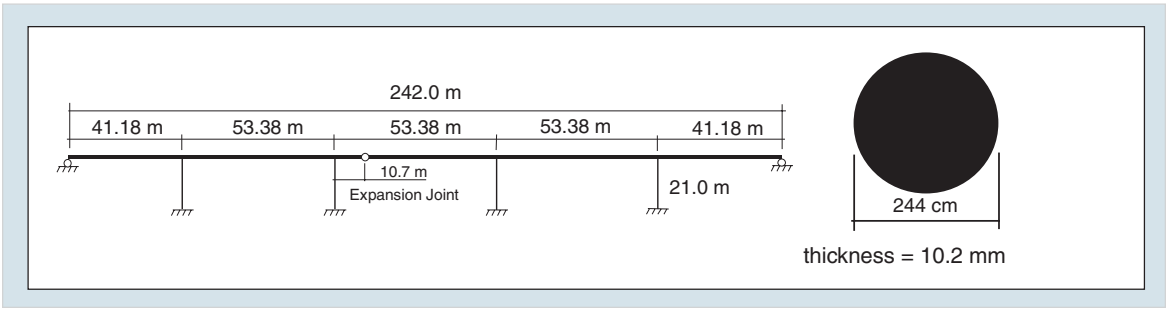

Figure 1. Elevation and Column Section of Bridge 1

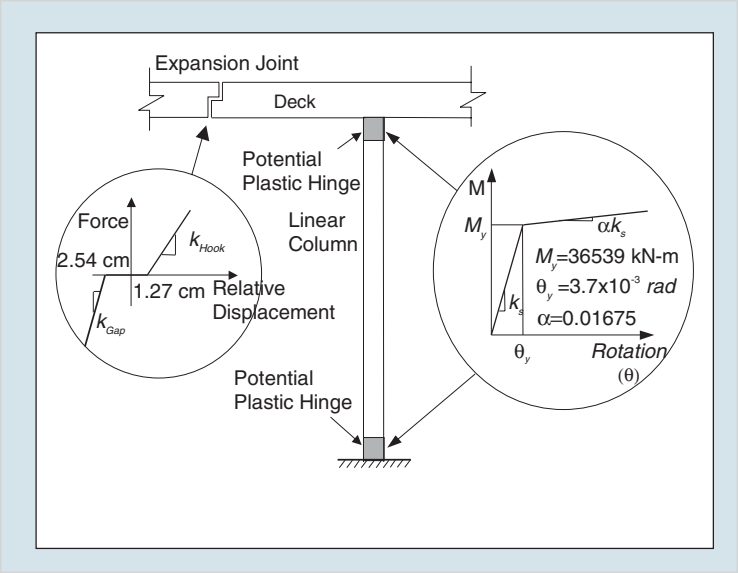

Figure 3. Nonlinearities in Bridge Model

overall length of Bridge 2 is 242 m with five spans, with an expansion joint in the center span. This bridge is supported by four columns of equal height of 21 m between the abutments at the ends. Each column has a circular cross section of 2.44 m diameter. The deck has a three-cell concrete box type girder section 13 m wide and 2 m deep.

A column is modeled as an elastic zone with a pair of plastic zones at each end of the column. Each plastic zone is then modeled to consist of a nonlinear rotational spring and a rigid element depicted in Figure 3. The plastic hinge formed in the bridge column is assumed to have bilinear hysteretic characteristics. For Bridge 2, the expansion joint is constrained in the relative vertical movement, while freely allowing horizontal opening movement and rotation. The closure at the joint, however, is restricted by a gap element when the relative motion of adjacent decks exhausts the initial gap width of 2.54 cm (Shinozuka et al., 2003a). A hook element sustaining tension only is used for the bridge retrofitted by restrainers at expansion joints and the opening is restricted by the element when the relative motion exhausts the initial slack of 1.27 cm. Springs are also attached to the bases of the columns to account for soil effects, while two abutments are modeled as roller supports. To reflect the cracked state of a concrete bridge column for the seismic response analysis, an effective moment of inertia is employed, making the period of the bridge correspondingly longer.

Thickness of Steel Jacketing

The thickness of the steel jacket is calculated from the following equation (Priestley et al., 1996).

$$t_j = \frac{0.18(\varepsilon_{cm} - 0.004)Df'_{cc}}{f_{yj}\varepsilon_{cm}} \quad (1)$$

where ε_{cm} is the strain at maximum stress in concrete, ε_{sm} is the strain at maximum stress in steel jacket, D is the diameter of circular column, f'_{cc} is the compressive strength of confined concrete and f_{yj} is the yield stress of steel jacket.

Nonlinear Dynamic Analysis

Nonlinear time history analysis has been performed using SAP 2000 Nonlinear (2002) for the example bridges under sixty Los Angeles earthquake time histories (selected for FEMA/SAC project) to develop fragility curves before and after retrofitting the column with the steel jacket.

These acceleration time histories were derived from past records with some linear adjustments and consist of three groups (each with 20 time histories) with probabili-

ties of exceedence of 10% in 50 years, 2% in 50 years and 50% in 50 years, respectively (*http://quiver.eerc.berkeley.edu:8080/studies/system/motions*). A typical acceleration time history in each group is plotted in the same scale to compare the magnitude of the acceleration in Figure 4.

Moment-Curvature Curves and Damage States

Nonlinear response characteristics associated with the bridge are based on moment-curvature curve analysis taking axial loads as well as confinement effects into account. The moment-curvature relationship used in this study for the nonlinear spring is bilinear without any stiffness degradation. Its parameters are established using the computer code developed by Kushiyama (Shinozuka et al., 2002) and by Caltrans (*COLx*).

These moment-curvature curves for a column of Bridge 1 are plotted together in Figure 5. In the present study, Kushiyama's curves are used for the dynamic analysis. The result shows that the curve after retrofit gives a much better performance than before retrofit by 2.6 times based on curvature at the ultimate compressive strain.

The parameter used to describe the nonlinear structural response in this study is the ductility demand. The ductility demand is defined as θ/θ_y, where θ is the rotation of a bridge column in its plastic hinge under the earthquake ground motion considered and θ_y is the corresponding rotation at the yield point.

A set of five different damage states are also introduced following the Dutta and Mander (1999) recommendations. These five damage states and the corresponding drift limits for a typical column are given in Table 1. For each limit state, the drift limit can be transformed to peak ductility capacity of the columns for the purpose of this study. Table 2 lists the values for Bridges 1 and 2.

Details for the section of the column, stress-strain relationship, distribution of axial force, P-M interaction diagram, moment-curvature curve and moment-rotation curve for a column before and after retrofit are given in Shinozuka et al., 2003b.

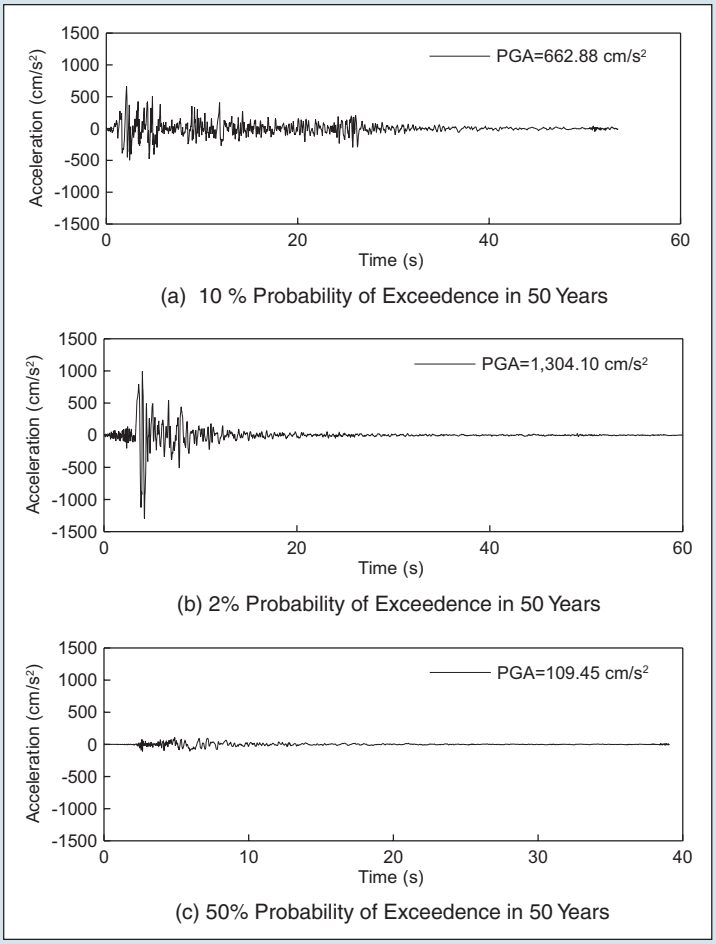

Figure 4. Acceleration Time Histories Generated for Los Angeles

Table 1. Description of Damage States

Damage State	Description	Drift Limits
Almost no	First yield	0.005
Slight	Cracking, spalling	0.007
Moderate	Loss of anchorage	0.015
Extensive	Incipient column collapse	0.025
Complete	Column collapse	0.05

Table 2. Peak Ductility Demand of Columns of Example Bridges

Damage State	Bridge 1		Bridge 2	
	Before Retrofit	After Retrofit	Before Retrofit	After Retrofit
Almost no	1.0	1.0	1.0	1.0
Slight	1.4	2.4	1.5	2.3
Moderate	3.1	7.9	3.5	7.5
Extensive	5.3	14.8	6.0	14.3
Complete	10.7	32.1	12.3	30.9

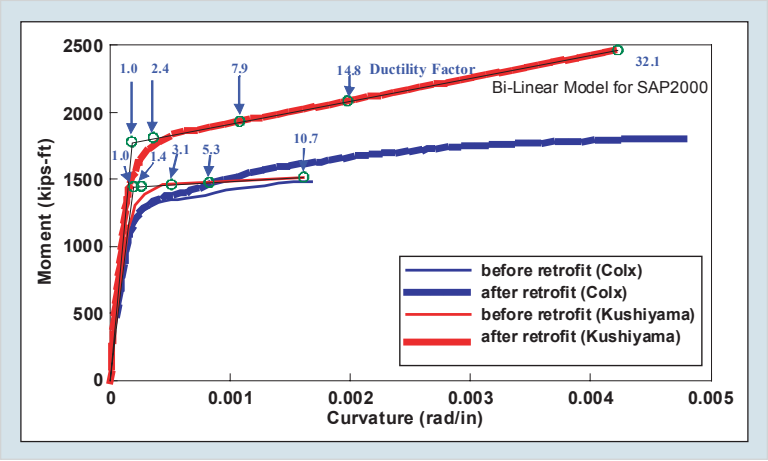

Figure 5. Moment-curvature Curves for Column of Bridge 1

Bridge Response

Typical responses at column bottom end of Bridge 1 are plotted in Figure 6. As expected, the rotation after retrofit is generally smaller than before, while the accelerations do not necessarily behave similarly and are quite different each other. Some higher fluctuations in the acceleration response appear after retrofit because the column becomes stiffer than before. The same trend is observed for Bridge 2.

Typical responses at the expansion joints of Bridge 2 are of interest and plotted in Figure 7 to show the difference in structural behavior in terms of relative displacement between right and left girders for the cases without and with considering gap and hook elements. The effect of the restraints is significant and can be seen by comparing Figures 7(a) and (b).

Fragility of Analysis of Bridges

It is assumed that the fragility curves can be expressed in the form of two-parameter lognormal distribution functions, and the estimation of the two parameters (median and log-standard deviation) is performed with the aid of the maximum likelihood method. A common log-standard deviation, which forces the fragility curves not to intersect, can also be estimated. The following likelihood formulation described by Shinozuka et al., 2002 is introduced for this purpose.

Although this method can be used for any number of damage states, it is assumed here for simplicity that there are four states of damage from none to severe. A family of three fragility curves exists in this case where events E_1, E_2, E_3 and E_4, respectively, indicate none, minor, moderate and major damage. $P_{ik} = P(a_i, E_k)$ in turn indicates the probability that a bridge i, selected randomly from the sample, will be in the damage state E_k when subjected to ground motion intensity expressed by PGA = a_i. All fragility curves are then represented by

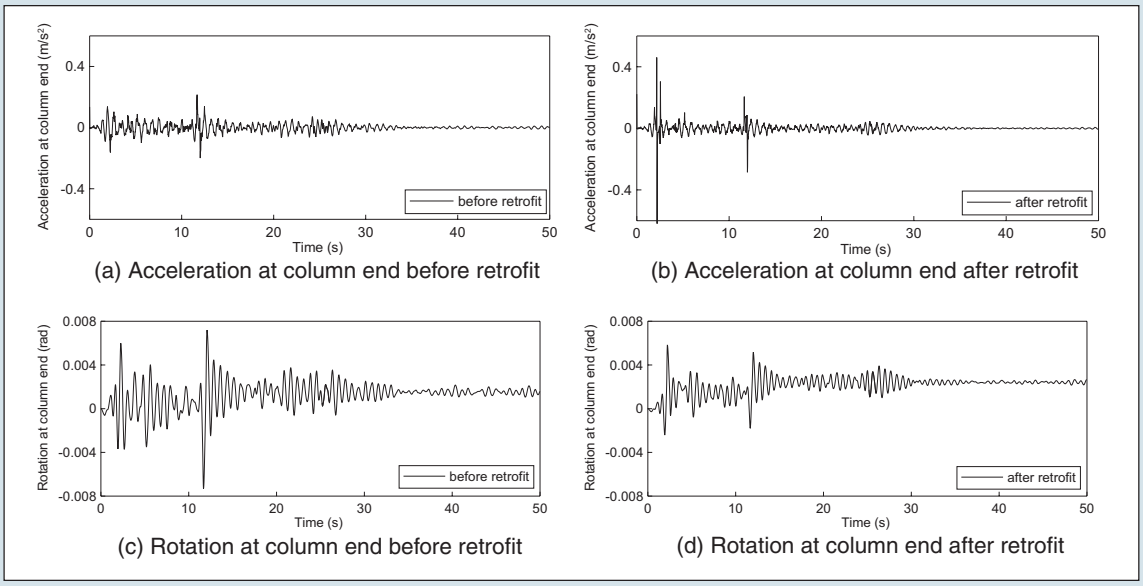

■ Figure 6. Responses at Column End of Bridge 1

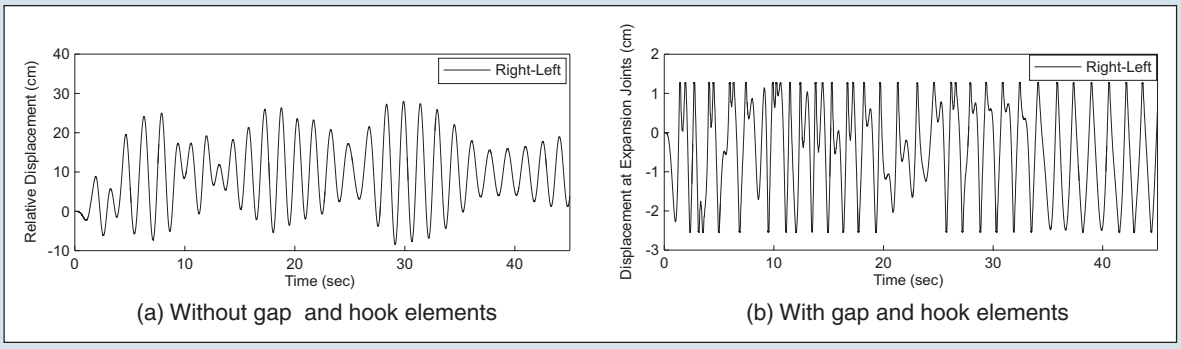

■ Figure 7. Displacement at Expansion Joints of Bridge 2

$$F_j(a_j;c_j,\varsigma_j)=\Phi\left[\frac{\ln(a_i/c_j)}{\varsigma_j}\right] \quad (2)$$

where Φ(.) is the standard-normal distribution function, c_j and ζ_j are the median and log-standard deviation of the fragility curves for the damage states of "at least minor," "at least moderate" and "major" identified by j = 1, 2 and 3. From this definition of fragility curves, and under the assumption that the log-standard deviation is equal to ζ common to all the fragility curves, one obtains;

$$P_{i1}=P(a_i,E_1)=1-F_1(a_i;c_1,\varsigma) \quad (3)$$

$$P_{i2}=P(a_i,E_2)=F_1(a_i;c_1,\varsigma)-F_2(a_i;c_2,\varsigma) \quad (4)$$

$$P_{i3}=P(a_i,E_3)=F_2(a_i;c_2,\varsigma)-F_3(a_i;c_3,\varsigma) \quad (5)$$

$$P_{i4}=P(a_i,E_4)=F_3(a_i;c_3,\varsigma) \quad (6)$$

Web Sites

Professor Shinozuka:
http://shino8.eng.uci.edu

Time Histories:
http://quiver.eerc.berkely.edu:8080/studies/system/motions

The likelihood function can then be introduced as

$$L(c_1,c_2,c_3,\varsigma)=\prod_{i=1}^{n}\prod_{k=1}^{4}P_k(a_i;E_k)^{x_{ik}} \tag{7}$$

where

$$x_{ik}=1 \tag{8}$$

if the damage state E_k occurs in the i-th bridge subjected to $a = a_i$, and

$$x_{ik}=0 \tag{9}$$

otherwise. Then the maximum likelihood estimates c_{0j} for c_j and ζ_0 for ζ are obtained by solving the following equations,

$$\frac{\partial \ln L(c_1,c_2,c_3,\varsigma)}{\partial c_j}=\frac{\partial \ln L(c_1,c_2,c_3,\varsigma)}{\partial \varsigma}=0 \quad (j=1,2,3) \tag{10}$$

by implementing a straightforward optimization algorithm.

Fragility Curves

Figure 8 shows a typical fragility curve, based on 60 time histories, along with the 60 point pairs indicating whether the damage state was sustained or not. A total of 60 diamonds are plotted on the two axes at $x_i = 0$ for the state of 'no damage' and $x_i = 1$ for the state of 'slight damage.' The corresponding fragility curves are derived on the basis of these diamonds in conjunction with Eqs. 2 through 10.

The fragility curves for Bridges 1 and 2 associated with these damage states are plotted in Figures 9 and 10, respectively, for before and after retrofit as a function of peak ground acceleration. Note that the same log-standard deviation value for the pair of fragility curves in Figures 9 and 10 is obtained by considering the two cases (before and after retrofit) together and calculating the optimal values from Eq. 10 for these fragility curves. This is because the bridge with jacketed columns is expected to be less vul-

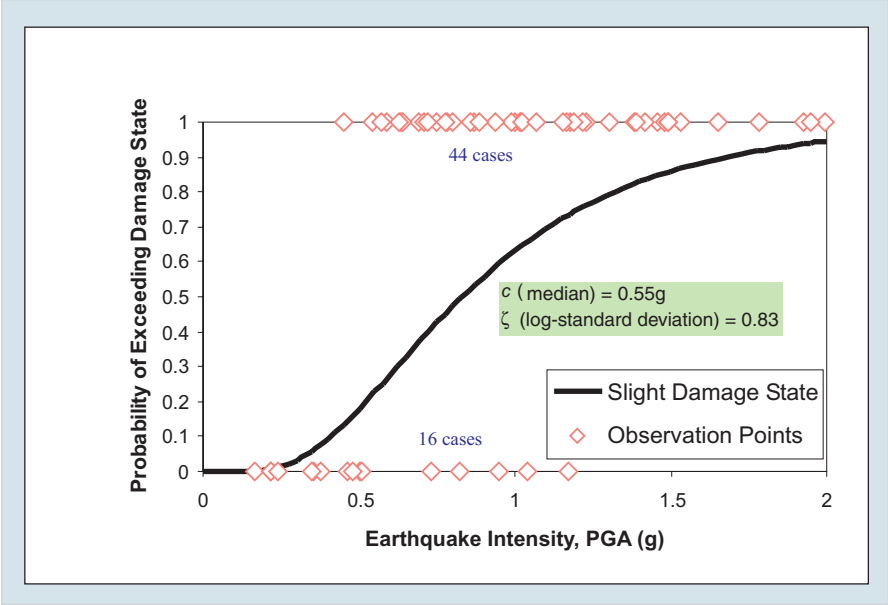

Figure 8. Fragility Curve for Slight Damage State

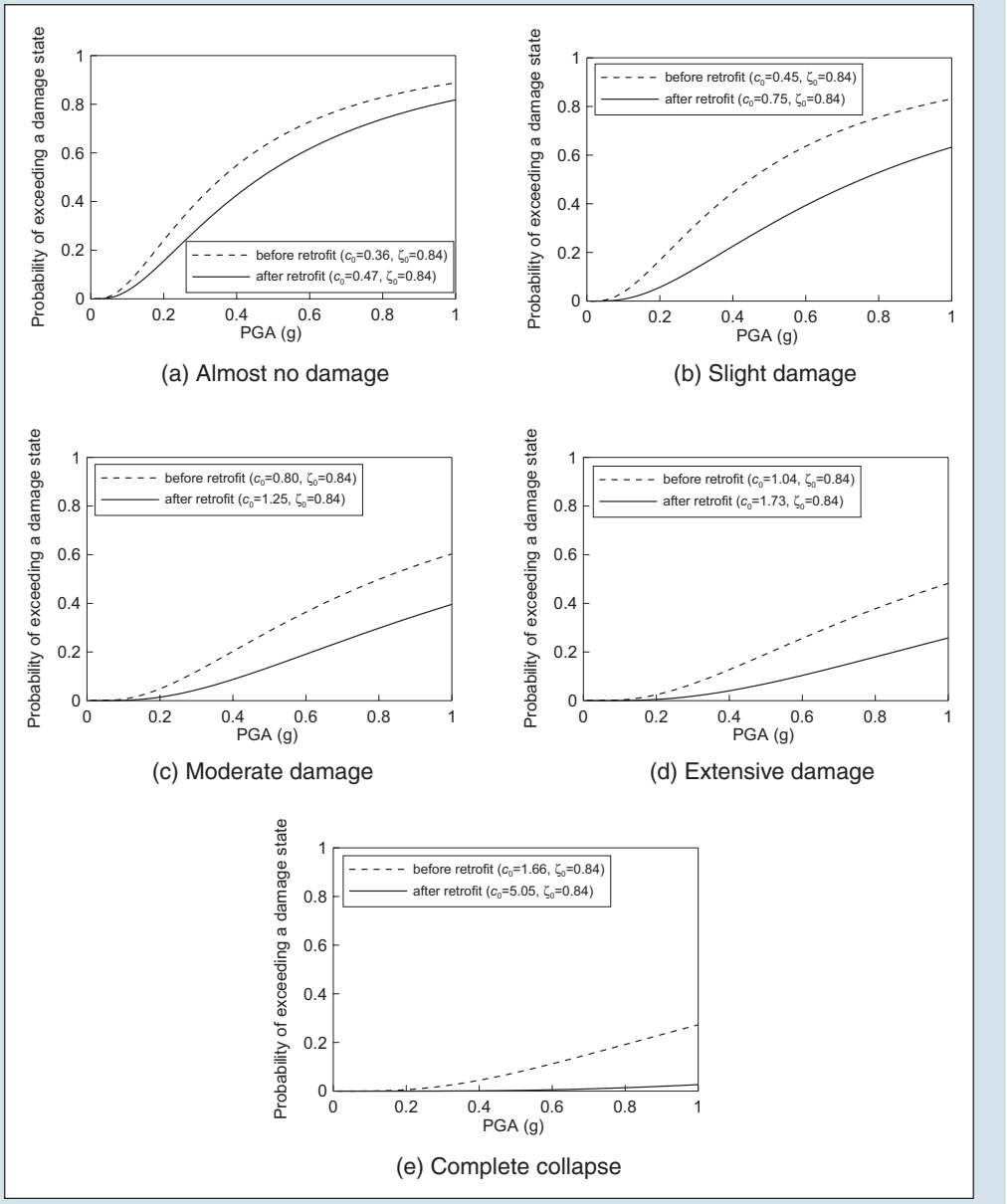

Figure 9. Fragility Curves of Bridge 1

nerable to ground motion than the bridge without column jacketing and, therefore, the pair of these fragility curves should not theoretically intersect.

Effect of Steel Jacketing

The damage state of a bridge in this study is defined by the maximum value of the peak ductility demands observed among all the column ends. In this context, comparison between the two curves in Figures 9 and 10 indicates that the bridge is less susceptible to damage from the ground motion after retrofit than before. The simulated fragility curves demonstrate that, for all levels of damage states, the

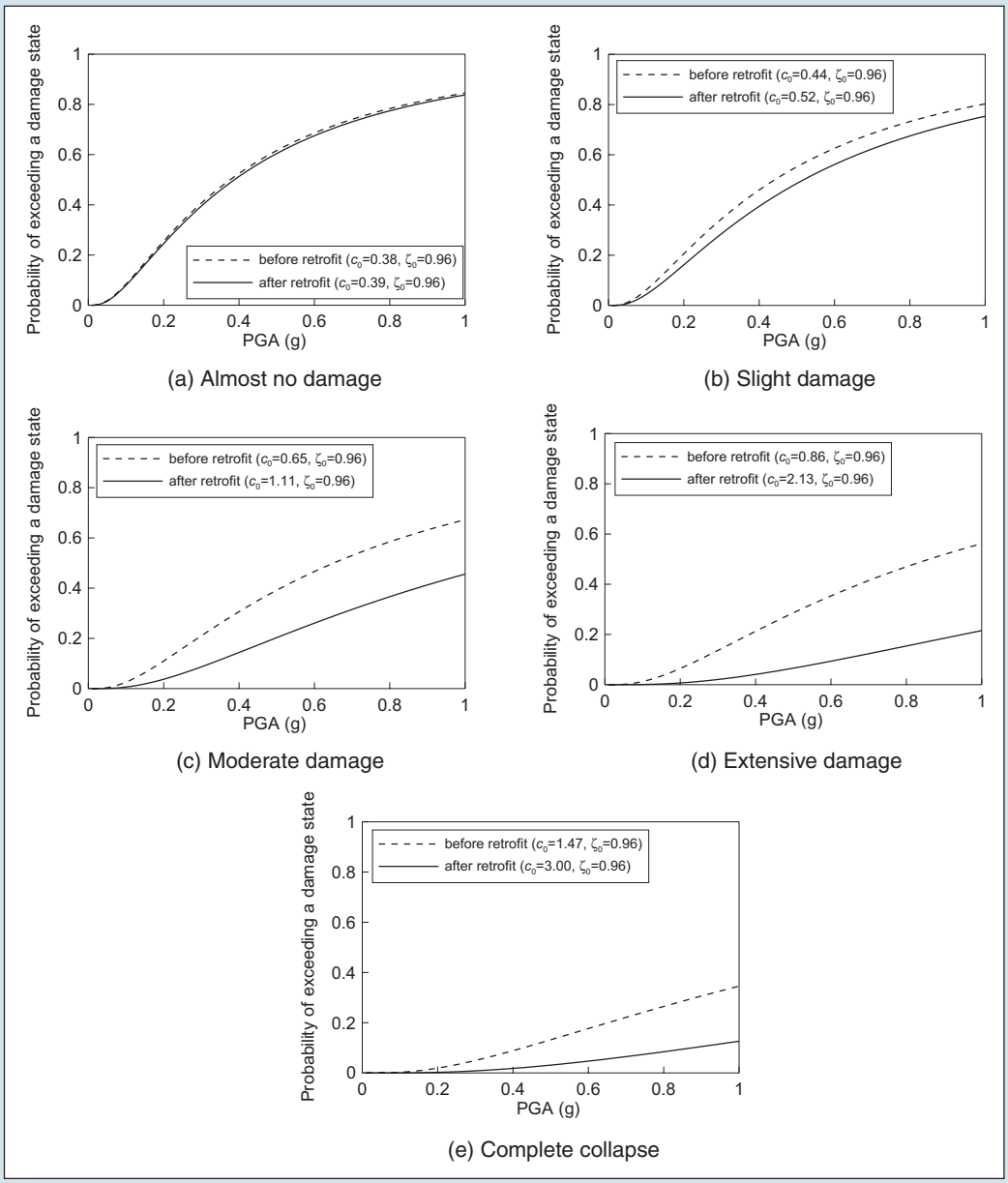

■ Figure 10. Fragility Curves of Bridge 2

median fragility values after retrofit are larger than the corresponding values before retrofit. This implies the following: for Bridge 1, on average, there is a smaller number of damage states after it has been retrofitted. Tables 3 and 4 list the number of damage states both before and after retrofit for Bridge 1 and Bridge 2, respectively. The results in Tables 3 and 4 are consistent with the observation that fragility enhancement is more significant for more severe states of damage. It shows that column retrofit greatly improves the seismic

performance of bridges; Bridge 1 is up to three times less fragile (complete damage) and Bridge 2 is 2.5 times (extensive damage) less fragile after retrofit in terms of the median values.

The effect of retrofit is demonstrated by comparing the ratio of the median value of the fragility curve for the retrofitted column to that for the unretrofitted column. This ratio is referred to as fragility "enhancement." Considering Bridges 1 and 2 with circular columns and the corresponding sets of fragility curves before and after retrofit, the average fragility enhancement over these bridges at each state of damage is computed and plotted as a function of the state of damage. An analytical function is interpolated as the "enhancement curve" and is plotted through curve fitting as shown in Figure 11. This curve shows 20%, 34%, 58%, 98% and 167% improvement for each damage state described on the *x* axis in Figure 11.

It is assumed that the fragility enhancement obtained from this function also applies to the development of the fragility curves after the retrofit for the empirical fragility curves (Figure 12) associated with expressway bridges in Los Angeles and Orange County, California subjected to the Northridge earthquake.

Assuming that Dutta and Mander's damage states (1999) are interchangeable with Caltrans definitions so that "slight = minor," "moderate = moderate," "extensive = major," and "complete = collapse," three enhanced empirical fragility curves after retrofit for minor, moderate and major damage are plotted in Figures 13, 14 and 15, respectively, for use in expressway network performance analysis.

Table 3. Number of Damage States for Bridge 1

Damage States	Before Retrofit	After Retrofit
Almost none	56	53
Slight	51	44
Moderate	41	28
Extensive	34	15
Complete	17	2

sample size=60

Table 4. Number of Damage States for Bridge 2

Damage States	Before Retrofit	After Retrofit
Almost none	51	50
Slight	47	41
Moderate	37	22
Extensive	30	10
Complete	14	4

sample size=60

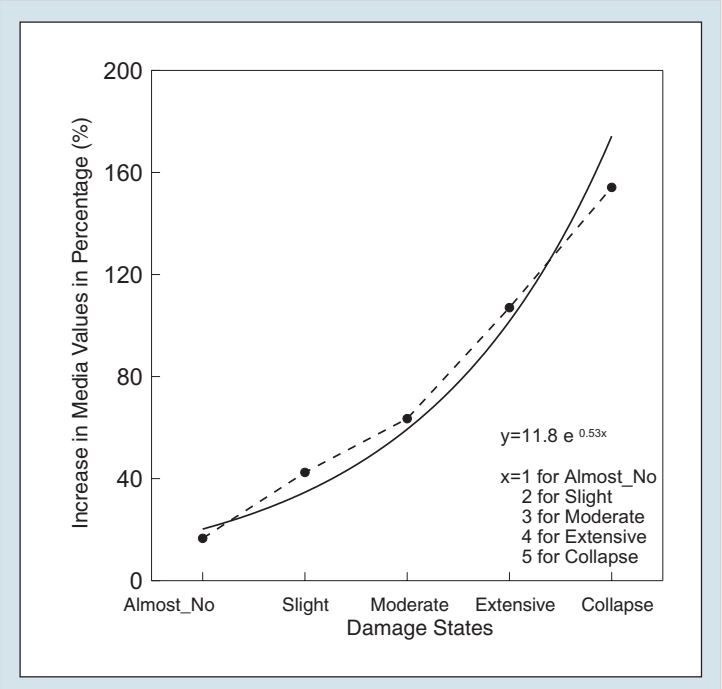

Figure 11. Enhancement Curve for Circular Columns with Steel Jacketing

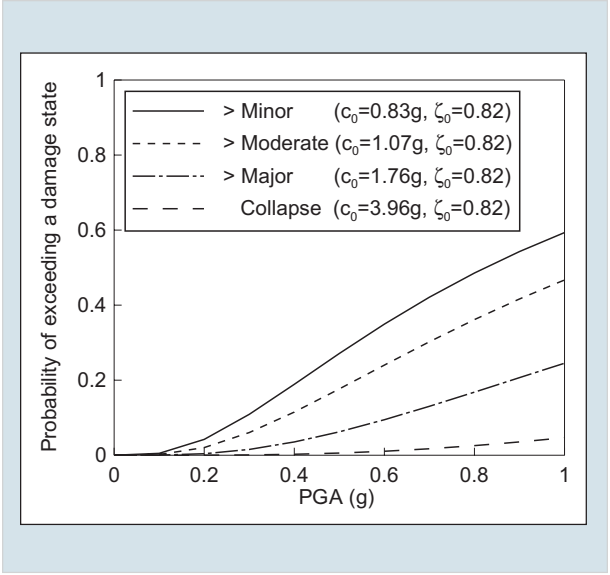

Figure 12. Empirical Fragility Curves of Caltrans' Bridges (Developed by Shinozuka et al., 2001)

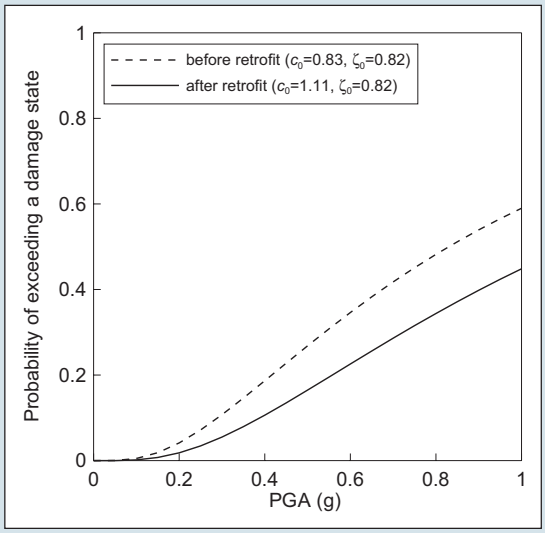

Figure 13. Enhanced Empirical Fragility Curves for Minor Damage after Retrofit

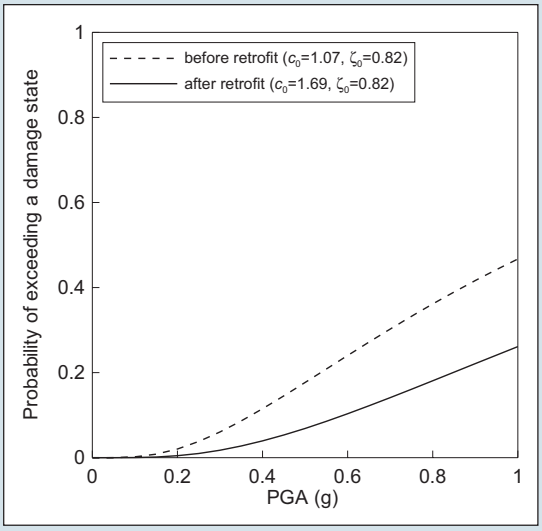

Figure 14. Enhanced Empirical Fragility Curves for Moderate Damage after Retrofit

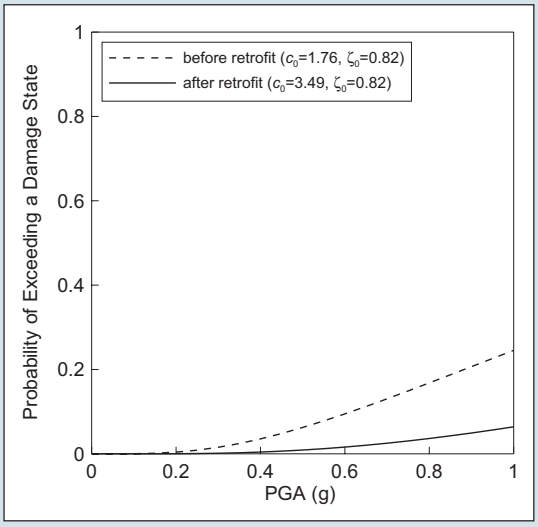

Figure 15. Enhanced Empirical Fragility Curves for Major Damage after Retrofit

Fragility Curves for Retrofit with Restrainers

Fragility curves for Bridge 2 are also developed to demonstrate the effect of retrofit at expansion joints by extending seat width in Figure 16 and installing restrainers (modeled as the hook element introduced in Figure 3) designed for anchor force capacity in Figure 17. These two figures show excellent improvement for both retrofit methods at the expansion joints. However, this observation might not always apply, depending on the specific bridge characteristics. Further study is in progress.

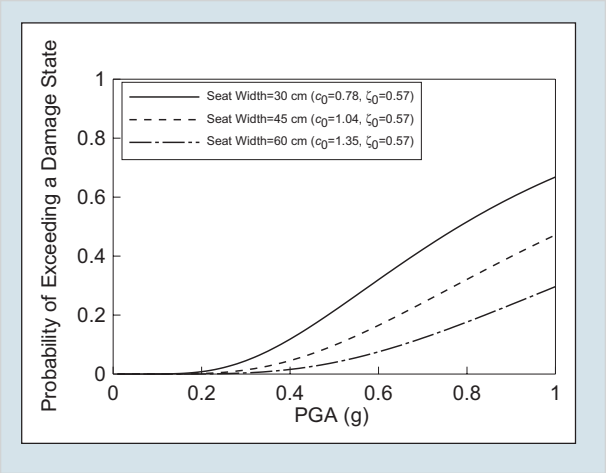

■ Figure 16. Fragility Curves for Expansion Joint Retrofitted by Extenstion of Seat Width

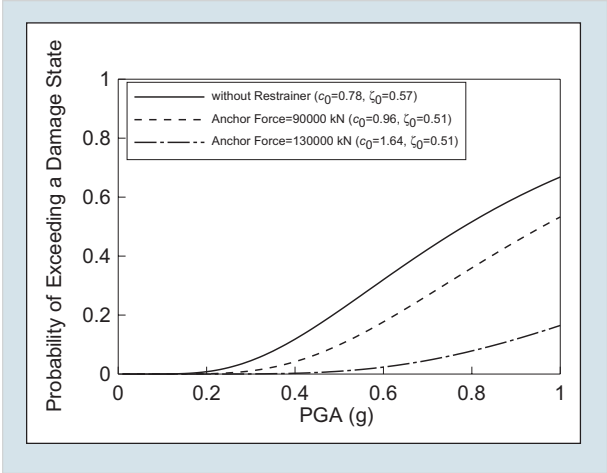

■ Figure 17. Fragility Curves for Expansion Joint Retrofitted by Restrainers

Conclusions and Future Research

This research presents a fragility analysis of two typical bridges in California before and after column retrofit with steel jacketing. The analytical fragility curves are constructed as a function of peak ground acceleration utilizing nonlinear dynamic analysis to investigate the effect of the column retrofit. Two-parameter lognormal distribution functions are used to represent the fragility curves by using the maximum likelihood procedure. Each event of bridge damage is treated as a realization from a multi-outcome Bernoulli-type experiment.

The following are conclusions drawn from the study.

1. Simulated fragility curves after column retrofit with steel jacketing show excellent improvement (less fragile) when compared to those before retrofit by as much as three times based on median PGA values.
2. After retrofit, the number of damaged bridges substantially decreases; especially for severe damage states defined in this study.
3. An "enhancement curve" is proposed and applied to develop fragility curves after retrofit on the basis of empirical fragility curves.
4. Fragility curves developed for retrofit with restrainers provide useful information to the seismic design practice by quantifying the improvement due to retrofit.
5. On the strength of the results obtained in this and others studies, uncertainty analysis will be performed in relation to fragility characteristics.

References

Chai, Y.H., Priestley, M.J.N. and Seible F, (1991), "Seismic Retrofit of Circular Bridge Columns for Enhanced Flexural Performance," *ACI Structural Journal,* Vol. 88, No. 5, pp. 572-584.

Dutta, A. and Mander, J.B., (1999), "Seismic fragility analysis of highway bridges," *Proceedings of the Center-to-Center Project Workshop on Earthquake Engineering in Transportation Systems*, Tokyo, Japan.

Priestley, M.J.N., Seible, F. and Calvi, G.M., (1996), *Seismic Design and Retrofit of Bridges*, John Wiley & Sons, Inc., pp. 270-273.

SAP2000, (2002), *User Manual*, *Computers and Structure*, Vol. 7.44, CA.

Shinozuka, M., Feng. M.Q., Kim, H.-K., Uzawa, T. and Ueda, T., (2001), *Statistical Analysis of Fragility Curves,* unpublished MCEER Technical Report, Multidisciplinary Center for Earthquake Engineering, *http://shino8.eng.uci.edu/techniclpapers.htm*.

Shinozuka, M., Kim, S.-H., Yi, J.-H. and Kushiyama, S., (2002), "Fragility Curves of Concrete Bridges Retrofitted by Column Jacketing," *Earthquake Engineering and Engineering Vibration*, *http://shino8.eng.uci.edu/journalpapers.htm*, Vol. 01, No. 2.

Shinozuka, M. and Kim, H.-K., (2003a), "Effects of Seismically Induced Pounding at Expansion Joints of Concrete Bridges," Accepted for Publication, *Journal of Engineering Mechanics*, ASCE, *http://shino8.eng.uci.edu/journalpapers.htm*.

Shinozuka, M., Kim, S.-H., Kushiyama, S, (2003b), "Fragility Curves of Seismically Retrofitted Bridges with Column Jacketing," to be submitted for publication, *Journal of Engineering Mechanics*, ASCE, *http://shino8.eng.uci.edu/journalpapers.htm*.

Somerville, P., Smith, N., Punyamurthula, S. and Sun, J., (1997), *Development of Ground Motion Time Histories for Phase 2 of the FEMA/SAC Steel Project*.

Advanced Technologies for Response Modification of Hospital Buildings

by Michel Bruneau (Coordinating Author), Andrei M. Reinhorn, Amjad Aref, Sarah L. Billington, Michael C. Constantinou, George C. Lee and Andrew S. Whittaker

Research Objectives

The objective of this research is to develop a better understanding of the applications of advanced technologies to protect critical facilities from the effects of earthquakes. A broad range of advanced technologies are under investigation, from those close to implementation to others that require long-term investigation. Results from these analytical and experimental studies will be used in fragility studies to probabilistically quantify the relative merits and potential benefits of implementing these technologies. Eventually, the results will be quantified and included in decision support methodologies that integrate both engineering and social science aspects.

Retrofitting hospitals using advanced technologies can make it possible to meet or exceed the high level of performance expected of these facilities following an earthquake. The initial expense of these technologies may be high, but increased implementation based on sustained research efforts is expected to reduce costs in the future to the point where they will be the same or less than conventional retrofitting techniques.

MCEER's diversified research activities investigate a broad range of advanced technologies, from some near to implementation with a high probability of acceptance, to those requiring long-term investigation with high potential payoff. Together, these technologies provide the necessary diversity to tackle complex loss reduction problems, and the flexibility required to rapidly adjust the research directions when data collected from new earthquakes suddenly changes perceptions and long held beliefs about what constitutes acceptable solutions.

A first approach strives to provide satisfactory seismic performance by introducing discrete control devices. The intent is to provide the highest level of control without the need for repairs or replacements following a major earthquake. Because there is not yet a consensus on how this can be best achieved, other new technologies are being developed to modify the existing solutions, enhance their effectiveness, provide better overall control, and ensure fail-safe mechanisms. Such new technologies must be aggressively investigated as they may provide the best solution, in some

Sponsors

National Science Foundation, Earthquake Engineering Research Centers Program

Research Team

***Michel Bruneau**, Professor, **Andrei Reinhorn**, Professor, **Amjad Aref**, Assistant Professor, **Michael Constantinou**, Professor and Chair, **George C. Lee**, Samuel P. Capen Professor of Engineering, **Andrew Whittaker**, Associate Professor, **S. Viti**, Visiting Researcher and Professor (from the University of Florence, Italy), **Mai Tong**, Senior Research Scientist, Department of Civil, Structural and Environmental Engineering, University at Buffalo*

***Sarah Billington**, Assistant Professor, and **Tong-Seok Han**, Post Doctoral Researcher, Department of Civil and Environmental Engineering, Cornell University*

Research Team continued on page 2

Research Team (cont.)

Graduate Students:

***Jeffrey Berman**, Ph.D. Candidate, **Woo-Young Jung**, Ph.D. Candidate, **Wei Liu**, Ph.D. Graduate (now with Weidlinger Associates, New York), **A. Natali Sigaher**, Ph.D. Candidate, **Darren Vian**, Ph.D. Candidate, **Michael Astrella**, M.S. Student, **Hiram Badillo**, M.S. Student and **Tsung Yuan Yang**, M.S. Student, Department of Civil, Structural and Environmental Engineering, University at Buffalo*

***Keith Kesner**, Ph.D. Candidate, Cornell University*

instances the only solution, to achieve the high level of seismic performance sought for critical buildings in regions of high seismicity.

A second approach focuses on the use of infill panels. These may be particularly suitable in regions where the implementation of advanced devices is less probable, due to lack of earthquake awareness, or to engineer preference for material-based solutions over device-based approaches (for various reasons). All the infill systems studied hold the promise that they could be implemented (among many possible solutions) without reinforcing the beams and columns in an existing building. This makes them particularly interesting solutions for hospital retrofit for two reasons. First, they would greatly reduce the cost of retrofits, and second and more importantly, recognizing that hospitals undergo frequent re-organization of floor space usage, these infills could be moved just like the non-structural partitions they would replace (although not as easily and likely not without some input from an engineer). While this is an ultimate goal, it is important to recognize that other more general studies are required prior to establishing and validating this full-portability concept; it remains, however the ideal to be pursued.

Research work on both these approaches is facilitated by the use of a demonstration hospital. The demonstration hospital serves as a standard mathematical model for MCEER researchers to integrate work on characterization and retrofit of structural and non-structural components and systems. Development of the models was just recently completed. Therefore, some of the seismic retrofit strategies summarized in this paper were accomplished without the benefit of these models. However, in future phases of this research, the demonstration hospital will serve to assess the effectiveness of the new proposed strategies both in enhancing seismic performance of the structural systems, and assessing their adequacy in providing greater levels of protection to the non-structural elements, equipments, and contents. Details of the models are described in the next subsection, followed by descriptions of specific retrofit strategies under investigation.

Design engineers and researchers can use the technologies investigated and developed in this research to improve the seismic resilience of critical facilities. Results will be integrated into a decision support methodology to aid hospital administrators in selecting the most appropriate strengthening techniques for their specific situation, to assess loss of performance/capabilities and time to recovery, and to determine cost/benefit of using these technologies. The demonstration hospital can be used as a baseline analytical tool in undergraduate and graduate courses in earthquake engineering.

MCEER Demonstration Hospital

The MCEER Demonstration Hospital is an existing facility in the San Fernando Valley in Southern California. The hospital facility was constructed in the early 1970's to meet the seismic requirements of the 1970 Uniform Building Code (ICBO, 1970). For the intended purpose of the demonstration hospitals, the framing system of the existing facility was modified slightly to a rectangular plan profile and the penthouse was eliminated. The vertical shafts in the building for mechanical and vertical transportation systems were replaced by typical floor framing. The resulting building is termed West Coast 1970s (or WC70).

The Uniform Building Code (UBC) was used for seismic design in California from the late 1920's until the 2000 International Building Code was introduced in 2001. In the late 1960's, the Uniform Building Code was substantially revised. Limits on allowable displacements in buildings were introduced in the 1964 edition of the UBC. This change led to substantial increases in the required elastic lateral stiffness, and subsequently the lateral strength, of moment-frame buildings such as the existing facility. As such, the stiffness and strength of 1970's moment-frame construction are significantly greater than those constructed in the 1960's. To enable investigators tasked with developing retrofit strategies for structural components and systems to prepare solutions for weak and flexible buildings similar to those constructed on the West Coast in the 1960's, the authors developed a framing system that complied with the gravity-load and seismic requirements of the 1964 Uniform Building Code. That framing system was designed for the same gravity loads as those used for the design of the existing facility. The resulting framing system is termed West Coast 1960's (or WC60).

Medical facilities on the West Coast have been designed for earthquake effects for more than 60 years. Such effects were not considered in the design of East Coast medical facilities until the 1990's. As such, there is a large inventory of medical facilities on the East Coast that have minimal resistance to earthquake effects. To facilitate the preparation of retrofit strategies for a typical (vulnerable) 1970's East Coast medical facility, beam and column sizes for the third framing system were developed to comply with the requirements of the 1970 Building Code of New York. This code had no seismic design requirements, and framing systems that complied with the Code were designed for gravity and wind loads only. The framing system was designed for the same gravity loads as WC70 and WC60. The resulting framing system is termed East Coast 1970's (or EC70).

Mathematical models of the three buildings have been developed on one or more analysis platforms: SAP2000NL, IDARC, and OpenSees.

Previous Summaries

2000-2001:
Vian et al., http://mceer.buffalo.edu/publications/resaccom/0001/rpa_pdfs/08bruneau4.pdf

Constantinou et al., http://mceer.buffalo.edu/publications/resaccom/0001/rpa_pdfs/10Lee-ketter-2.pdf

Lee et al., http://mceer.buffalo.edu/publications/resaccom/0001/rpa_pdfs/12lee-hosp_graphics.pdf.

***1999-2000**:*
Shinozuka et al., http://mceer.buffalo.edu/publications/resaccom/9900/Chapter2.pdf

1997-1999:
Reinhorn et al., http://mceer.buffalo.edu/publications/resaccom/9799/Ch3reinh.pdf

Lee et al., http://mceer.buffalo.edu/publications/resaccom/9799/Ch4lee.pdf

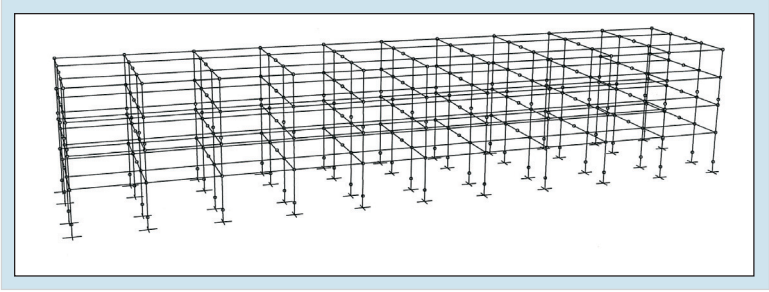

Figure 1. Isometric View of the Hospital Building Framing

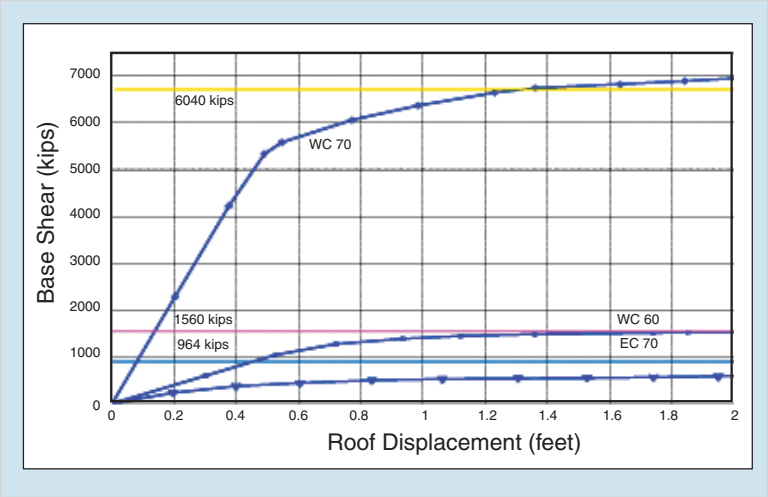

Figure 2. Base Shear Versus Roof Displacement Relationships for WC70, WC60, and EC60

Figure 1 is an isometric view of the framing of the hospital facility.

The three mathematical models were analyzed to establish the model frequency and fundamental period in each direction. The fundamental periods in the longitudinal and transverse directions for WC70, WC60, and EC60 are (0.87 sec., 0.82 sec.), (1.76 sec., 1.86 sec.), and (2.06 sec., 2.05 sec.), respectively. Approximately 85% of the total mass participated in these modes, in the two principal directions of the building.

Nonlinear static analysis and simple plastic analysis was undertaken to establish the maximum lateral strength of the three buildings. Sample results are shown in Figure 2 for the three buildings under lateral loading in the transverse direction, for nonlinear static analysis (curves denoted WC70, WC60 and EC70) and plastic analysis (horizontal lines denoted 6040 kips, 1560 kips and 964 kips). Plastic analysis predicts the ultimate lateral strength of the frames well for WC70 and WC60.

Structural Retrofit Strategies

Concepts considered by MCEER researchers are presented in the following sections, with brief descriptions of progress to date and potential advantages.

Steel Infills

The seismic retrofit of existing buildings is a difficult task due to many factors, such as, the cost of closing the building for the duration of the retrofit work or having to heavily reinforce existing framing due to the increased demands the retrofit strategy may place on it. Light-gauge steel plate shear walls could provide engineers with an effective option for the seismic retrofit of older buildings. The concept is to create a system that is strong enough to resist the necessary seismic forces and yet light enough to keep the existing structural elements from needing reinforcement. Additionally, if these systems could be installed quickly and eliminate the need to disrupt the occupants of existing structures, they would be even more desirable, especially in the context of a hospital retrofit.

Steel plate shear infills are proposed to achieve these goals. These can be designed to buckle in shear and form a diagonal tension field. Subsequent yielding of the infill in tension provides the opportunity to dissipate seismic energy.

A design procedure for steel plate shear walls based on the plastic analysis of an accepted analytical model developed by Thorburn et al., 1983 and Timler and Kulak, 1983 was created. The analytical model represents the steel plate shear wall

using a series of inclined, tension only, strips. The design procedure involves the selection of the infill thickness at a given story using:

$$t = \frac{2V_s\Omega_s}{F_Y L 2\sin 2\alpha} \qquad (1)$$

where V_s is the story shear, F_y is the infill yield stress, L is the bay width, Ω_s is the system overstrength factor, and α is the angle of inclination of the tension field with respect to vertical. Details regarding this design procedure can be found in Berman and Bruneau, 2003.

Using the MCEER Demonstration Hospital, two different types of light-gauge steel plate shear wall prototypes were designed as seismic retrofit alternatives (Berman, 2002). The first type used a 20 gauge (1.0 mm or 0.0396 in.) flat infill plate of steel (at the first floor) and the second used a corrugated infill, type B steel deck, of 22 gauge (0.75 mm or 0.0295 in) material. These thicknesses were found assuming that one bay of every gravity frame line in the north-south direction of the demonstration hospital would receive an infill.

Using these infill thicknesses, three light-gauge steel plate shear wall test specimens were designed. The first two, specimens F1 and F2, used the flat plates with different connections to the boundary frame. F1 made use of an industrial strength epoxy, while F2 used a welded connection. Figure 3 shows specimen F1 prior to testing. A third specimen, C1, was fabricated using the corrugated infill of type B steel deck with an epoxy connection to the boundary frame. Figure 4 shows specimen C1 prior to testing.

Specimen F1 suffered a failure of the epoxy connection prior to yielding of the infill and therefore, did not dissipate a significant amount of energy. Specimen C1 was tested successfully to a displacement ductility of three prior to significant strength degradation. The hysteresis curves for specimen C1 are shown in Figure 5. Due to the corrugated profile of specimen C1, local buckling developed when the corrugations were in compres-

Links to Current Research

The seismic retrofit technologies and response modification methods investigated in this effort will be incorporated into integrated decision support systems under development by Alesch, Dargush, Grigoriu, Petak and von Winterfeldt.

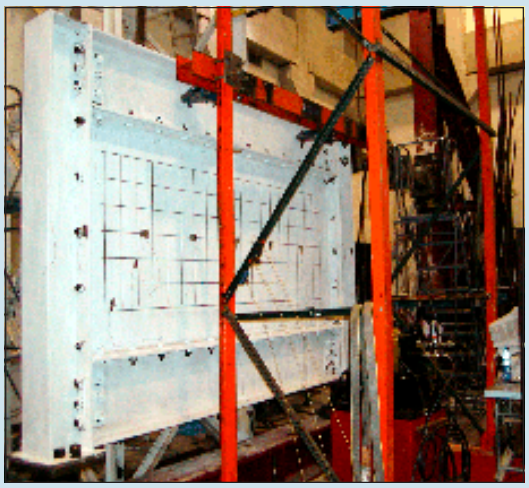

Figure 3. Specimen F1 Prior to Testing

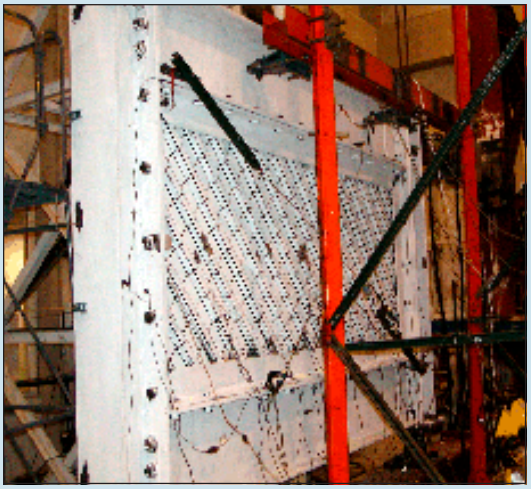

Figure 4. Specimen C1 Prior to Testing

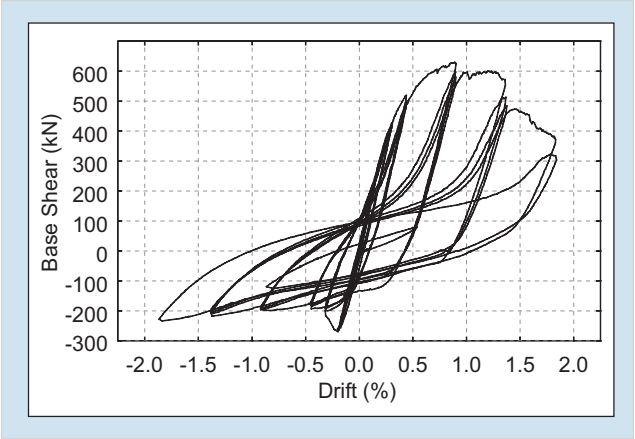

Figure 5. Hysteresis for Specimen C1

Figure 6. Fracture of Infill for Specimen C1

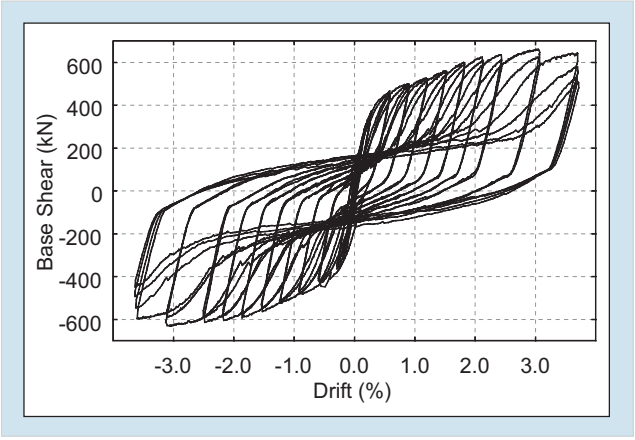

Figure 7. Hysteresis for Specimen F2

sion. After cyclic loading, the fractures developed along the local buckling lines, causing the strength of the specimen to degrade rapidly. An example of the infill fractures is shown in Figure 6.

Specimen F2 was tested to a displacement ductility of 12 prior to losing significant strength. As shown in Figure 7, the hysteresis loops were pinched but stable and exhibited behavior similar to that of a concentrically braced frame with slender braces. Ultimate failure of the specimen resulted from fractures that propagated from the terminus of the welds connecting the infill to the boundary frame (an example is shown in Figure 8). Though these fractures developed early in the testing, they did not effect the behavior until a displacement ductility of 12 had been achieved. From strain gauge data, the demands induced on the columns and beams of the boundary frame were minimal, meaning this system could be implemented in a retrofit situation without having to heavily reinforce the existing framing.

These tests showed that light-gauge steel plate shear walls can be a useful alternative for the seismic retrofit of buildings. They are effective in minimizing the impact of the retrofit on the existing framing while adding substantial strength, stiffness, and ductility. Further research will investigate their impact on the behavior of secondary systems.

Figure 8. Fracture at 3.5% Drift for Specimen F2

Advanced Composite Infills

The following sections describe the conceptual designs of three infill panels that have been investigated analytically and experimentally to assess their performance as seismic retrofitting strategies.

Multi-layer PMC Infill Panel

A multi-layer system is introduced as a main concept to increase energy dissipation and stiffness of steel frames. This multi-layer system allows in-plane shear deformation and, therefore, sliding along specific layers to take place upon loading the frame. The panel is tailored to experience damage at specific layers, thereby energy dissipation will be produced within the infill panel when these layers exhibit in-plane shear deformations. As shown in Figure 9, the conceptual design of the polymer matrix composite (PMC) infill panel system consists of three panels forming the entire wall thickness: first, an inner panel composed of a core material and core shell; second, outer panels that consist of outer shells at both sides of the inner panel; and third, visco-elastic honeycomb layers at the interface between these two panels. The role of the inner panel is to increase structural rigidity. In turn, the outer panels are designed to transfer applied lateral force to the visco-elastic honeycomb layers as well as to resist large contact forces at the interface with the steel columns. Upon testing, this multi-layer infill provided significant stiffness enhancements and moderate energy dissipation. However, the interface layers can be designed to meet specific drift limitations, or to provide damping via the damage introduced at the interface layers.

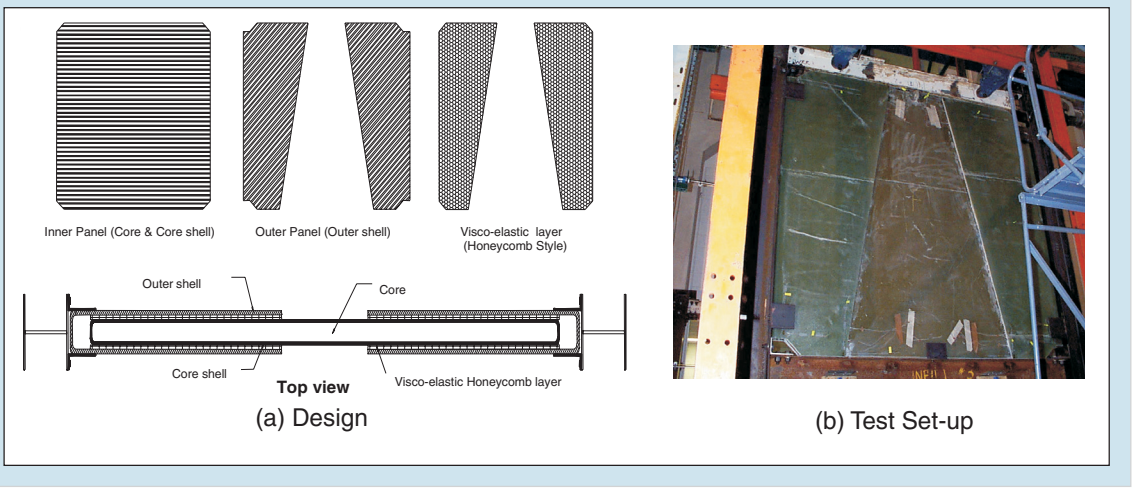

Figure 9. Configuration of the Multi-layer PMC Infill Panel System

Collaborative Partners

An-Cor Industrial Plastics

Armstrong World Industries

Enidine, Inc.

Kuraray Company, Ltd. Japan

Office of Statewide Health Planning & Development (OSHPD)

Sumitomo 3M LTD, Japan

Multi–panel Infill Panel

A multi–panel PMC infill panel is designed to have higher damping, by introducing a combination of 3M visco-elastic solid and polymeric honeycomb materials. This system provides significant damping for seismic protection of buildings.This multi-panel PMC infill wall comprises two separate components as shown in Figure 10. A sandwich design is considered as the infill panel to reduce the weight, sound, and vibration as well as to improve the structural rigidity of the composite panel, and the damping panels are designed to exhibit shear deformation at the interface layers between fiber reinforced polymer (FRP) plates by the relative motion of the top and bottom beams.As such, the geometry of the damping panels is designed to have three PMC laminates, and the damping materials are located at the interface between them. In this case, the interaction of this system with the steel frame produces both stiffness and damping following different drift values. By designing the proper vertical interface layers, this system can dissipate seismic excitations. The design parameters along with simplified analysis tools are available for the designer to tailor the panels to achieve the desired damping characteristics.

Multi-Box Infill Panel

Light and flexible building systems often require specific design features for limiting earthquake damage.With the same mechanical concept used in the multi–panel system, a tube–type infill structure is designed to have three PMC box panels as shown in Figure 11.In this case, significant increase in the damping of a steel frame may be expected by larger damping area at the interface between the box panels.The significant advantage of this system is that it provides energy dissipation without adding any significant stiffness to the steel frame. Thus, by minimizing the stiffness associated with this infill panel, semi-rigidly connected frames and similar classes of frames will not exhibit failure at the column-beam

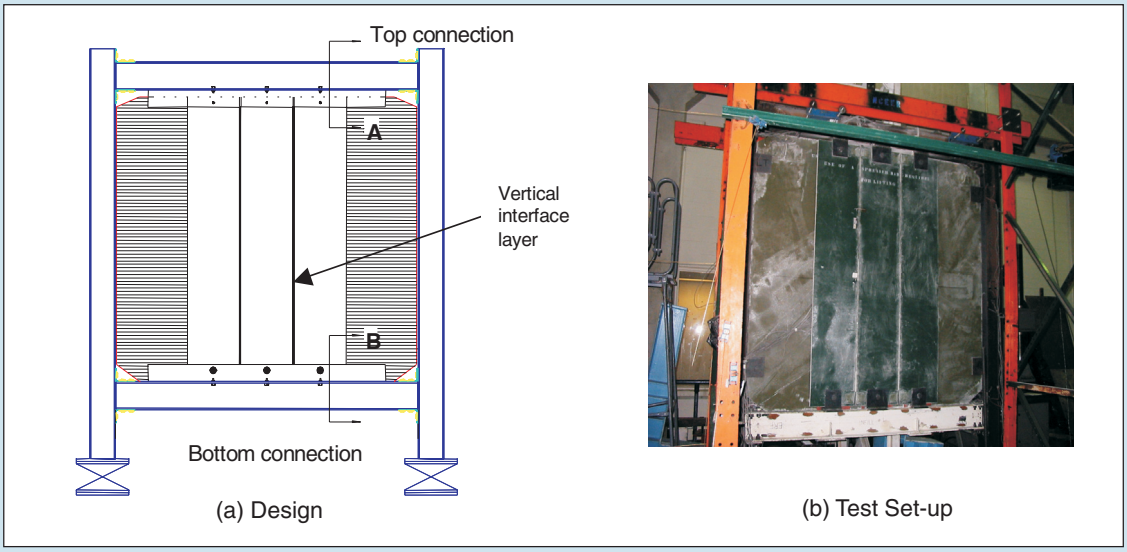

Figure 10. Configuration of the Multi-Panel Infill System

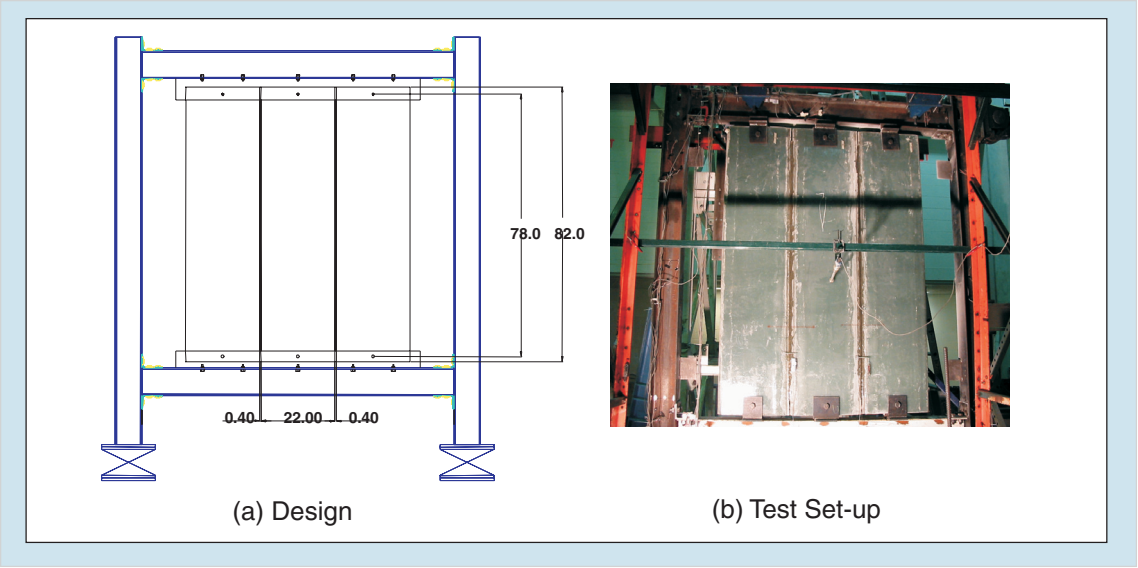

Figure 11. Configuration of the Multi-Box Infill Panel System

connection because this infill is flexible and does not attract significant forces at the joints. The main emphasis here is to provide the required damping without imparting any adverse damage to the joints of the structural system. Moreover, because these box panels may be designed not to fill the entire space between the columns, interruptions to the floor plan can be minimized.

Precast Infill Panels Made with Engineered Cementitious Composite Materials

An infill system that utilizes engineered cementitious composites materials (ECC) is being developed for the protection of critical structures. The ECC materials, used in lieu of traditional building materials, are advantageous due to their pseudo-strain hardening response in tension (Figure 12(a)) (Li, 1998 and Li and Leung, 1992). This ductile response results in greater amounts of energy dissipation in steel reinforced ECC structural applications when compared to traditional reinforced concrete materials (Fischer and Li, 2002). The infill system under development utilizes precast ECC infill panels with bolted, pre-tensioned connections between the infill panels and at connections to the existing structure. Additional details of the research are presented in Kesner, 2003.

The primary (non-structural) advantage of the proposed infill system lies in the inherent flexibility of the system's use and ease of installation. The use of bolted connections allows for the easy removal or relocation of infill panels in response to changes in facility use. The two-piece infill sections allow for installation in an existing frame with minimal equipment and interference with ongoing facility use. Additional flexibility in use is provided by the ability of partially infilled frames to increase the strength, stiffness and energy dissipation of a structural frame. Partial frame infills minimize the impact the retrofit has on the existing

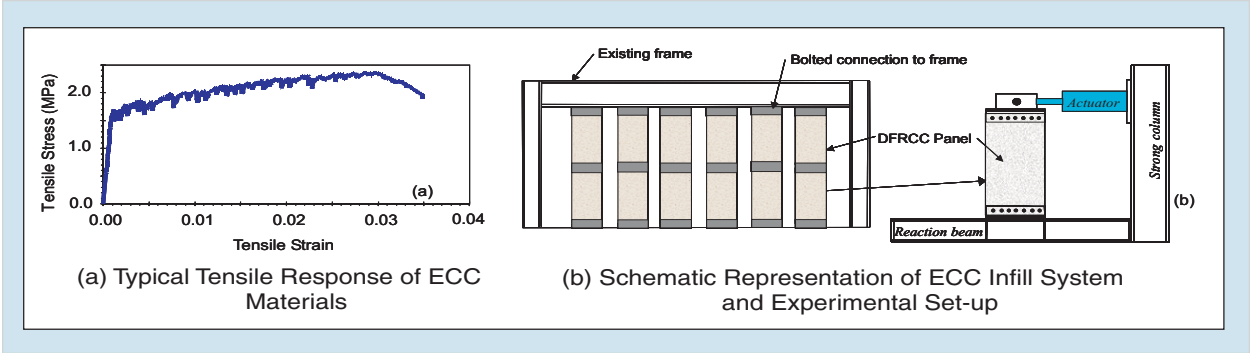

(a) Typical Tensile Response of ECC Materials

(b) Schematic Representation of ECC Infill System and Experimental Set-up

Figure 12. ECC Infill System

structure and on existing secondary systems.

To evaluate the beam-type infill system, panel connection tests and large-scale infill panel tests were conducted (Kesner, 2003). The panel connection tests identified appropriate levels of bolt pretensioning for the retrofit connections as well as slip coefficients useful for design. The infill panel tests were conducted as single panel tests (Figure 12(b)) with each tested panel representing one half of a beam-type infill section. The effect of different ECC mix designs, alternate reinforcement details and two different panel shapes on cyclic response of the panel was examined. Each panel was subjected to symmetric cyclic loading to increasing drift levels. Load-displacement response, the amount of energy dissipated by the panels, cracking behavior, and panel failure mechanisms were of particular importance for the testing. Figure 13 compares the load-drift response of an ECC panel with welded wire fabric reinforcement (WWF), an ECC panel with WWF and a single deformed reinforcing bar on the perimeter of the panel, and a concrete panel with WWF and a deformed perimeter bar. The perimeter bar clearly adds strength and energy dissipation capacity to the panels. The ECC panels showed clear advantages over the concrete panel in terms of increased strength, drift capacity, and energy dissipation. The enhanced performance of the ECC is a consequence of the strain hardening of the ECC in tension in combination with mild reinforcement. Further details of the experimental program and results are given in Kesner, 2003.

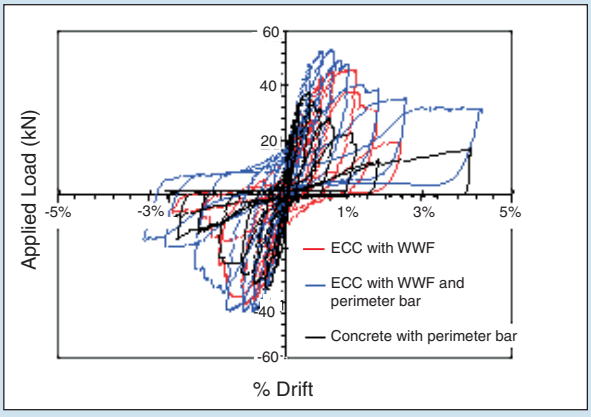

Figure 13. Selected Experimental Results of Single-Panels

To examine the response of the beam-type infill system in steel framed structures, a series of finite element analyses were performed. The goal of the analyses was to verify the ability of an infilled frame to satisfy performance limits for critical structures as presented in FEMA 273, 1999. Various analyses

were conducted to examine the effect of the infill addition on the strength and stiffness of the frame, to examine load distribution through the panels, and to determine if infill additions resulted in localized yielding in the frames that they are retrofitting. A constitutive model for ECC did not exist and was therefore developed and implemented for this research (Han et al., 2002). Details of the analyses are given in Kesner, 2003.

The simulation results indicated that the beam-type infill panel systems could significantly increase the strength and stiffness of the frame, as well as the energy dissipation during cyclic loadings. Typical simulation results are shown in Figure 14. The variation in frame response when different numbers of infill sections are used demonstrates the variety of solutions and strength/stiffness options this retrofitting system offers. Yielding in the frame occurred at similar levels (all in the base of the frame) whether there was an infill system in place or not. This indicates that the infill addition can simultaneously protect the frames and increase stiffness. Additional analyses showed that a panel geometry that tapers toward the center of the beam-type infill gives a similar response as the rectangular panels while using less material (Kesner, 2003). Tapered panels allow for even more flexibility in the use of this system in terms of having more options for existing non-structural components to "penetrate" the bay where the infill is placed.

Based upon the results of the experiments and numerical simulations, the concept of precast ECC infill panels appears viable. The laboratory testing of the ECC infill

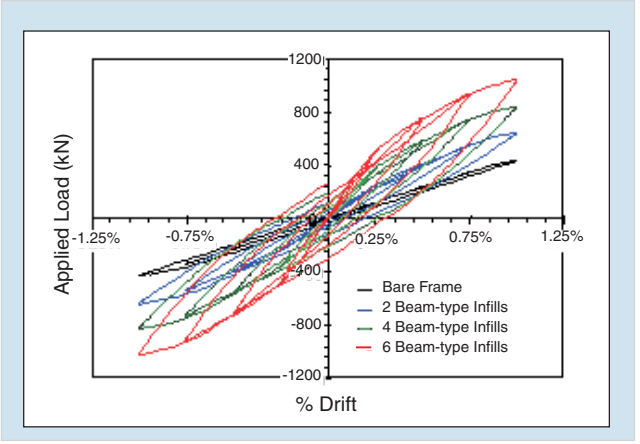

Figure 14. Simulated Load-Drift Response from a Bare Steel Frame and Frames with ECC Infill Panels

panels demonstrated the strength, stiffness and energy dissipation levels that can be obtained from such infill panels. The panel strength and drift capacity can be tailored through variations in panel reinforcement, ECC material and panel geometry. The simulation results indicated that a variety of levels of increased strength, stiffness and energy dissipation are possible with various amounts of beam-type infills.The increase in strength, stiffness and energy dissipation of the ECC infilled frames can be achieved with minimal impact on the use of the existing structure.

Global Retrofit of Structures by Weakening and Damping

A new procedure for global retrofit of existing structures subjected to seismic excitation is proposed.The main features of this procedure are to reduce maximum acceleration and associated forces in buildings by reducing their strength (weakening). The global weakening retrofit, which takes the opposite approach from conventional retrofitting procedures, is

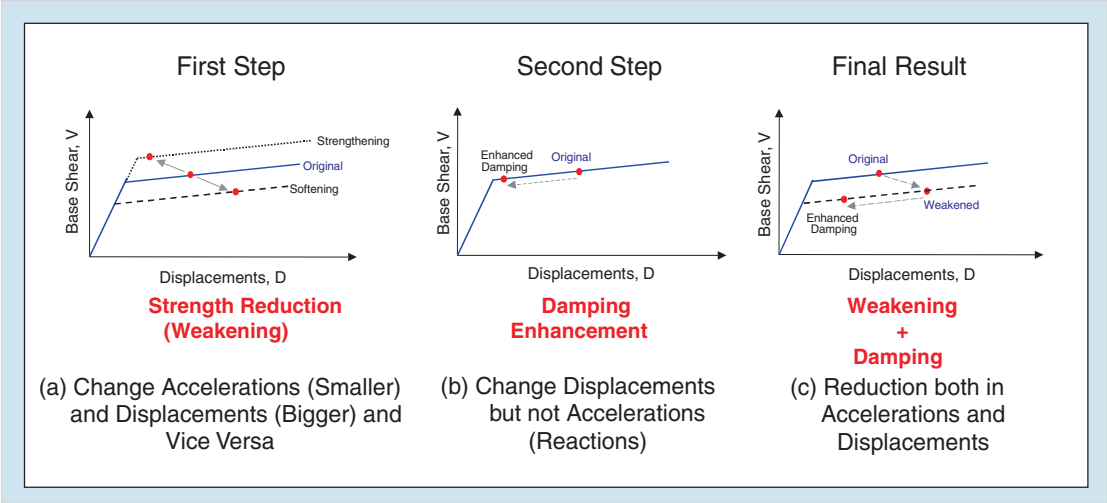

Figure 15. Strength Reduction and Damping Enhancement

particularly suitable for buildings that have overstressed components and foundation supports or weak brittle components. Moreover, such retrofit may protect secondary systems sensitive to high accelerations. However, by weakening the structure, large deformations are expected. By adding supplemental damping devices, it is possible to control the deformation to be within desirable limits. A structure retrofitted with this strategy will have, therefore, a reduction in both the acceleration response and deformations, depending on the amount of additional damping introduced. An illustration of the above strategy is performed by evaluating the inelastic response of the structure through a spectral procedure, modified to fit structures with additional damping. The results are compared with a dynamic nonlinear analysis. Both methods show that the retrofit solution is feasible and simplified techniques can be used for evaluation.

Conventionally, seismic performance can be improved by both increasing the strength and ductility capacity of the structure, or by decreasing the level of excitation. In this retrofit strategy, both strength capacity and demand are reduced as well as the deformation response and ductility demands. The process is done in two different steps (see Figure 15). The first step consists of weakening the structure, which leads to a decrease in strength capacity and with it, a decrease in the acceleration demand. This is also associated with an increase in the ductility demand. The second step consists of adding viscous damping to reduce the ductility demand (see Figure 15).

The structural "weakening" can be easily obtained by releasing selected connections in the structure. The properties of the modified connections depend on the materials and the construction practices used in the building. In this paper, it is suggested to replace selected fixed connections with hinges by releasing the bolts or strategically removing welds. The enhancement of damping can be achieved by adding structural braces with built-in devices such as viscoelastic, fluid viscous, friction devices or

unbonded braces (Reinhorn et al., 1995 and Constantinou et al., 1998).

To illustrate the retrofitting technique, the four-story steel frame structure from the MCEER demonstration hospital (shown in Figure 1) is evaluated. The evaluation of the structure's response is performed using an inelastic spectral analysis, based on approximated inelastic design spectra (Reinhorn, 1997). This analytical procedure, used for undamped or lightly damped structures (Ramirez et al., 2000), was modified for highly damped structures. The results obtained for the spectral inelastic response and those provided by an inelastic dynamic analysis show the same characteristics for the modified structure. The seismic excitation is derived according to FEMA 273 and with the information provided by NSHMP (National Seismic Hazard Mapping Program) for the hospital's location. Three probabilities of occurrence, 10%, 5% and 2% in 50 years, are assumed in this study, corresponding to a PGA of 0.50 g, 0.63 g and 0.77g, respectively. The influence of the retrofit method is shown in Figure 16. The base shear is reduced by weakening, while the displacements are reduced by added damping. Figure 17 illustrates the influence of low vs. high damping. The robustness of the response should be noted, i.e., the maximum force/acceleration response is almost the same, independent of the hazard level. At the same time, the displacement is bounded to smaller values than in the original structure.

While this is work in progress, it is clear from the above evaluation that this retrofit strategy can globally affect the structural system undergoing inelastic deformations in reducing both accelerations and displacements. The reduction of displacements leads to a reduction in the global damage inflicted to the structure. The reduction in accelerations can affect the functionality of the non-structural components and of the equipment, thus improving the resilience of the hospital in case of severe earthquakes. Performance targets and design criteria may be developed, along with practical, implementable construction solutions.

Web Sites

ECC Technology Network:
www.engineeredcomposites.com

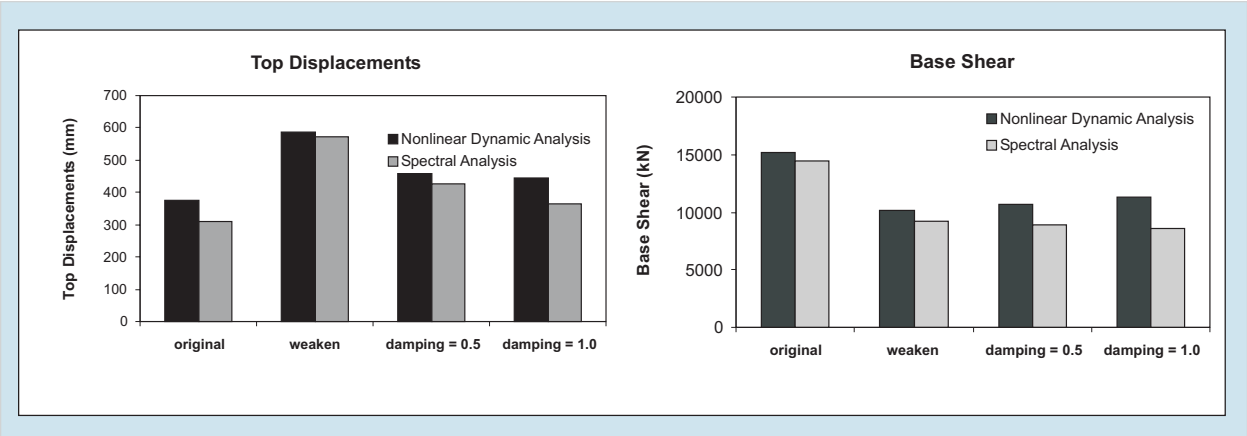

Figure 16. Performance of Weakened-Damped Structure Evaluated by Spectral Method and Time Analysis

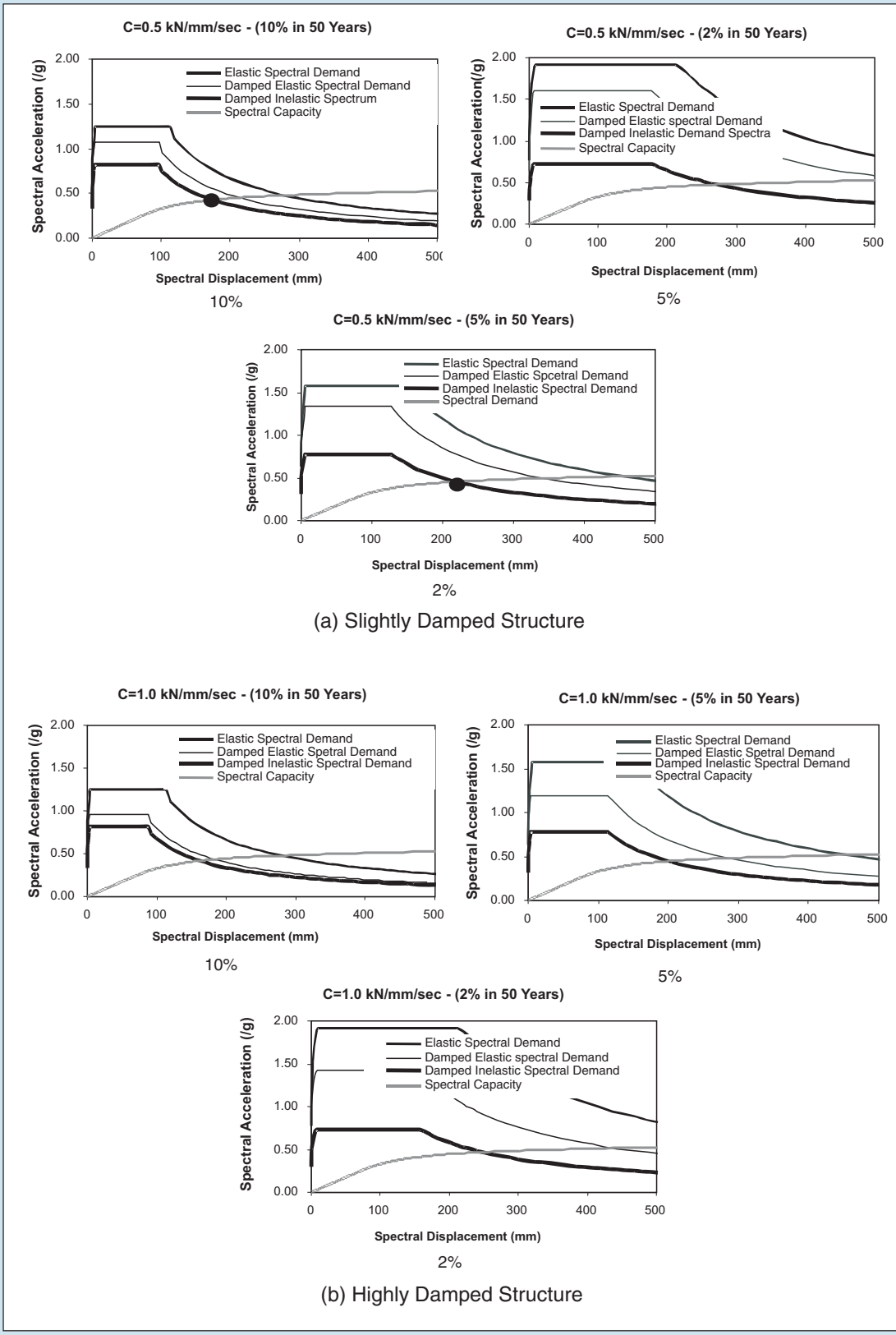

■ Figure 17. Performance of Damped-Weakened Retrofitted Structure for Different Hazards

Semi-Active Response Modification Systems – Combined RSPM and Passive Damping Hybrid Control System

RSPM (Real-time Structural Parameter Modification) is a semi-active nonlinear control system for reducing structural seismic responses. Figure 18 illustrates how the combined system works. The system includes a passive damper and a controlled stiffness unit. The passive damper is always engaged to dissipate energy, but the stiffness unit is connected or disconnected based on a pre-set threshold. It is disconnected initially until a response threshold value—termed the open distance, is reached. If the relative displacement (the absolute value) becomes larger than the open distance, the stiffness unit is engaged to control the response. If, at any instant, the displacement (absolute value) becomes smaller than the threshold, the RSPM stiffness unit is disconnected. The semi-active control mechanism is activated only when the stiffness unit is connected. The devices are normally combined as a pair of tension and compression units working as a push-and-pull set.

The internal semi-active control of the stiffness unit is based on maximized accumulation and removal of energy. In the simple case of a linear stiffness unit, the control force is governed by

$$R = \begin{cases} k_d(S_d(t) - S_d(\underline{t}_i)) & \underline{t}_i < t \le \underline{t}_{i+1} \\ 0 & t = \underline{t}_{i+1} \end{cases} \qquad (2)$$

where S_d is the net stroke from the last controlled switching point; $\underline{t}_i$ is the i^{th} control point at which a switching command is executed and the device force is released.

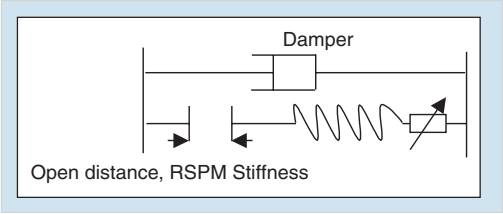

Figure 18. Combined RSPM and Passive Damping Hybrid Control System

The hybrid system has been analyzed through an existing building with a potential pounding problem (Lee et al., 2002). The math-science building of the University of California at Los Angeles (UCLA) is a seven-story moment resistant steel frame structure. One seismic hazard is possible collision of the building with an adjacent building, the "Math-science addition." The gap in the north-south direction between these two buildings is only six inches. The combined RSPM and passive damping devices are considered between the roofs of the two buildings to reduce the roof displacement response. Another requirement is to reduce the acceleration response level. For this purpose, a pure damping device may be more effective in reducing acceleration. Therefore, the RSPM and damping device are combined to take advantage of their respective strengths.

In a simple lumped mass model comparison, Figure 19 shows the response levels under 'LA' earthquake with RSPM or with only linear viscous damping control. The response reduction effects of the control systems are normalized as the percentage of the controlled response over the non-controlled response level. A lower curve implies a better response reduction

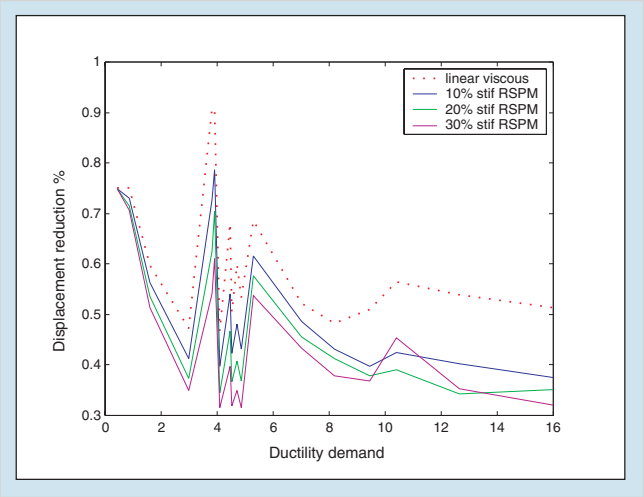

Figure 19. Comparison of Response Levels

effect. As shown in the figure, the passive damping devices will become less effective as the structural yielding (ductility demand) increases. This is primarily due to the increased energy dissipation from the structural ductility and a slower velocity response increase rate. In the nonlinear structural responses, as a trade off effect of structural member yielding, the displacement response will typically grow at a faster rate than the velocity and acceleration responses. Under such a condition, the displacement-based RSPM control illustrates a clear advantage over the velocity-based passive dampers.

In summary, semi-active control strategies may be able to provide a larger control capability for seismic induced structural response reduction. In particular, they are better able to balance the difficult structural control requirements, such as limiting acceleration levels and controlling story responses, thus reducing structural response in both elastic and inelastic ranges.

Dampers

MCEER investigators have made important contributions to the development of existing guidelines or specifications for structures with damping systems: FEMA 273/274 *Guidelines for the Seismic Rehabilitation of Buildings*, published in 1998, FEMA 356 *Prestandard and Commentary for the Seismic Rehabilitation of Buildings*, *NEHRP 2000 Provisions for Seismic Regulations for New Buildings*, published in 2001 and *NEHRP 2003 Provisions for Seismic Regulations for New Buildings*, to be published in 2004.

While the technical basis for the methods of analysis and design of buildings with damping systems in FEMA 273/274/356 and 2000 NEHRP were primarily developed at MCEER prior to 2000, the lack of verification studies prevented these methods from gaining the design professional acceptance needed to move the procedures into model codes and standards.

MCEER researchers, under the direction of Technical Subcommittee 12 of the Building Seismic Safety Council, have completed and published verification studies that demonstrate the validity of the MCEER-developed methods of analysis and design (Ramirez et al., 2001, 2002a, 2002b, and to appear; Whittaker et al., to appear). Based on this work, these methods have reached Chapter status in the 2003 NEHRP Provisions and have been accepted for inclusion in ASCE Standard 7-05, *Minimum Design Loads for Buildings and Other Structures*, that is scheduled for publication in 2005. All future building codes, starting with the next edition of the International Building Code,

will refer to the ASCE Standard for methods of analysis and design.

The evaluation and verification studies performed at MCEER included studies of numerous models of structures with damping systems and several three-story and six-story multistory steel buildings with damping systems. However, all studies concentrated on seismic excitations with far-field, and stiff soil or rock characteristics. The verification studies were extended with MCEER funding in 2002-2003 to include near-field and soft soil excitations. These additional studies have just been completed. The results demonstrate that the developed methods of analysis and design are also appropriate and accurate for near-field and soft soil seismic excitations.

Finally, MCEER researchers have completed, published and patented (see Sigaher and Constantinou, 2003 and Constantinou, 2002) work on the Scissor-Jack Seismic Energy Dissipation System. The first application of this new technology is pending following the call for bids on the Cyprus Olympic Committee Building, a six-story reinforced concrete building with 52 scissor-jack-damper assemblies.

Next Steps and Conclusions

The research projects described in this paper are just one component of MCEER's integrated research plan. Successful execution of this plan depends on close interaction between various tasks. First, reliable seismic time-histories representative for eastern North America, and their associated level of reliability, must be developed to complement the available western North America suites of earthquake records (Papageorgiou, 2001). The resulting seismic input feeds directly into the fragility studies as well as the geotechnical, structural and non-structural evaluation and retrofit research tasks.

Second, seismic evaluation and retrofit of structural systems interacts in a close manner with fragility curve development, providing new retrofit schemes based on advanced technologies that can be used in the fragility studies to probabilistically quantify the relative merits and potential benefits of alternative retrofit schemes. The fragility studies also return to the evaluation and retrofit studies valuable information on seismic performance that can be used to focus the seismic retrofit research activities. A similar interdependency exists for the research on non-structural systems, to an even greater degree. Fragility studies, enhanced through interaction with evaluation and retrofit studies, provide key information to develop reliable cost-benefit analysis decision tools. Research dependency also exists, in a very close interactive loop, between cost-benefit analyses and social studies on implementation and incentives, as both rely on each other's data to converge to a respective solution.

The development of decision support methodologies that can integrate both the engineering and social science aspects needed to achieve quantification of resilience is a key research activity that ties all of these tasks together. These activities are described in an another paper in this Volume.

An important subsequent task in continuation of the research activi-

ties reported in this paper will be research on response modification devices and strategies to protect non-structural systems. The objectives will be to investigate how various types of response modification strategies can help modify floor responses (maximum displacements, velocities, and accelerations). This will allow limits to be established within which structural retrofit solutions can (or cannot) provide adequate seismic protection to non-retrofitted non-structural equipment, and to determine the type of floor responses that can be controlled with these various structural retrofit strategies.

Acknowledgments

This research was primarily supported by the Earthquake Engineering Research Centers Program of the National Science Foundation, under award number EEC-9701471 to the Multidisciplinary Center for Earthquake Engineering Research. This support is gratefully acknowledged.

References

Berman, J., (2003), *Experimental Investigation of Light-Gauge Steel Plate Shear Walls for the Seismic Retrofit of Buildings*, MCEER-03-0001, Multidisciplinary Center for Earthquake Engineering Research, University at Buffalo.

Berman, J. and Bruneau, M., (2003), "Plastic Analysis and Design of Steel Plate Shear Walls," *Journal of Structural Engineering*, ASCE (in press).

Constantinou, M.C., (2002), Highly Effective Energy Dissipation Apparatus, inventor: Michael C. Constantinou, assignee: Research Foundation of State University of New York, United States Patent 6,438,905, issued August 28, 2002.

Constantinou, M.C., Soong, T.T. and Dargush, G.F., (1998), *Passive Energy Dissipation Systems for Structural Design and Retrofit*, MCEER-98-MN01, Multidisciplinary Center for Earthquake Engineering Research, University at Buffalo.

FEMA-273, (1999), *NEHRP Guidelines for Seismic Retrofit of Buildings*, Federal Emergency Management Agency, Washington, DC.

Fischer, G. and Li, V.C., (2002), "Effect Of Matrix Ductility On Tension Stiffening Behavior of Steel Reinforced Engineered Cementitious Composites," *ACI Structural Journal*, Vol. 99, No. 1, pp. 104-111.

Han, T.S., Feenstra, P.H. and Billington, S.L., (2002), "Simulation of Highly Ductile Fiber-Reinforced Cement-based Composites," *ACI Structural Journal*, accepted for publication, November.

Kesner, K.E., (2003), *Development of Engineered Cementitious Composite Materials for Seismic Retrofit and Strengthening Applications*, Ph.D. Dissertation, Cornell University, 337 pp.

Lee, G.C., Tong, M., Wu, Y. H., Hwang, S. and Hart, G., (2002), "Application of a Semi-Active Seismic Protective System in an Existing Building in Los Angeles," *Proceedings, 7NCEE*, Boston, MA, July 21-25, 2002.

References (Cont'd)

Li, V.C., (1998), "Engineered Cementitious Composites – Tailored Composites Through Micromechanical Modeling," *Fiber Reinforced Concrete: Present and the Future*, N. Banthia, A. Bentur, and A. Mufti, eds., Canadian Society for Civil Engineering, Montreal, pp. 64-97.

Li, V.C. and Leung, C., (1992), "Steady-State and Multiple Cracking of Short Random Fiber Composites," *Journal of Engineering Mechanics*, Vol. 118, No. 11, pp. 2246-2264.

Papageorgiou, A.S., Halldorsson, B. and Dong, G., (2001), "Earthquake Motion Input and Its Dissemination Via the Internet," *Research Progress and Accomplishments: 2000-2001*, MCEER-01-SP01, Multidisciplinary Center for Earthquake Engineering Research, University at Buffalo.

Ramirez, O.M., Constantinou, M.C., Kircher, C.A., Whittaker, A.S., Johnson M.W. and Gomez, J.D., (2000), *Development and Evaluation of Simplified Procedures for Analysis and Design of Buildings with Passive Energy Dissipation Systems*, Technical Report MCEER-00-0010, Multidisciplinary Center for Earthquake Engineering Research, University at Buffalo, December.

Ramirez, O.M., Constantinou, M.C., Kircher, C.A., Whittaker, A.S., Johnson, M.W., Gomez, J.D. and C.Z. Chrysostomou, (2001), *Development and Evaluation of Simplified Procedures for Analysis and Design of Buildings with Passive Energy Dissipation Systems*, Technical Report MCEER-00-0010, Revision 1, Multidisciplinary Center for Earthquake Engineering Research, University at Buffalo, November.

Ramirez, O.M., Constantinou, M.C., Gomez, J., Whittaker, A.S. and Chrysostomou, C.Z., (2002a), Evaluation of Simplified Methods of Analysis of Yielding Structures with Damping Systems," *Earthquake Spectra*, Vol. 18, No. 3, pp. 501-530.

Ramirez, O.M., Constantinou, M.C., Whittaker, A.S., Kircher, C.A. and Chrysostomou, C.Z., (2002b), "Elastic and Inelastic Seismic Response of Buildings with Damping Systems," *Earthquake Spectra*, Vol. 18, No. 3, Aug. 2002, pp. 531-547.

Ramirez, O.M., Constantinou, M.C., Whittaker, A.S., Kircher, C.A., Johnson, M.W. and Chrysostomou, C.Z., (to appear), "Validation of 2000 NEHRP Provisions Equivalent Lateral Force and Modal Analysis Procedures for Buildings with Damping Systems," *Earthquake Spectra*.

Reinhorn, A., (1997), "Inelastic analysis technique in seismic evaluation," *Proceedings of the International Workshop on Seismic Design Methodologies for the next Generation of Codes*, Bled/Slovenia, June 24-27.

Reinhorn, A., Li, C. and Constantinou, M.C., (1995), *Experimental and Analytical Investigation of Seismic Retrofit of Structures with Supplemental Damping: Part 1 – Fluid Viscous Damping Devices*, NCEER-95-0001, National Center for Earthquake Engineering Research, University at Buffalo.

Sigaher, A.N. and Constantinou, M.C., (2003), "Scissor Jack Damper Engergy Dissipation System," *Earthquake Spectra*, Vol.19, No.1, Feb. 2003, pp. 133-158.

Thorburn, L.J., Kulak, G.L., and Montgomery, C.J., (1983), *Analysis of Steel Plate Shear Walls*, Structural Engineering Report No. 107, Department of Civil Engineering, University of Alberta, Edmonton, Alberta, Canada.

Timler, P.A. and Kulak, G.L., (1983), *Experimental Study of Steel Plate Shear Walls*, Structural Engineering Report No. 114, Department of Civil Engineering, University of Alberta, Edmonton, Alberta, Canada.

Whittaker, A.S., Constantinou, M.C., Ramirez, O.M., Johnson, M.W. and Chrysostomou, C.Z., (to appear), "Equivalent Lateral Force and Modal Analysis Procedures of the 2000 NEHRP Provisions for Buildings with Damping Systems," *Earthquake Spectra*.

Decision Models: Approaches for Achieving Seismic Resilience

by Daniel J. Alesch (Coordinating Author), Gary F. Dargush, Mircea Grigoriu, William J. Petak and Detlof von Winterfeldt

Research Objectives

Decisions about enhancing seismic safety in critical facilities requires more than engineering choices about which technology is most appropriate. Such decisions are made in the context of organizational goals and strategy, financial capacity, choices about how safe is safe enough, and driving forces in the social, economic, and political environment. This project is aimed at devising integrated decision-assisting models for helping executives and engineers make informed choices about alternatives approaches to improving seismic safety. The platforms integrate state of the art understanding of structural response, alternative means for mitigating the risk, normative decision-assisting models, and behavioral models of organizational choice and decision processes.

The Challenge

One of the fundamental long-term goals of earthquake engineering research in general and MCEER in particular is to enable the development of disaster-resilient communities. The development of innovative engineering technologies, and the associated design guidelines, is certainly beneficial in this regard. However, to prove effective, the new technologies must be implemented and corresponding enhancements to engineering design codes must be adopted. The processes involved in technology implementation and code adoption go far beyond strictly engineering concerns. It is essential to also give simultaneous consideration to the organizational, economic, social, political and legal aspects of the problem.

This multidisciplinary coupling significantly complicates the situation and necessitates the development of a new generation of decision support methodologies that can help organizations cope with the complexity of the decision-making process. These organizations may include companies interested in developing markets for new technologies, critical care facility owners required to meet legislated levels of seismic performance, local communities faced with prioritizing rehabilitation projects and federal agencies responsible for resource allocation. In all of these cases, the organizations are confronted with a myriad of decisions that must be made

Sponsors

National Science Foundation, Earthquake Engineering Research Centers Program

Research Team

***Daniel J. Alesch**, Professor Emeritus, Department of Public and Environmental Affairs, University of Wisconsin-Green Bay*

***William J. Petak**, Professor, **Detlof von Winterfeldt**, Professor, and **Robert Chen**, Ph.D. Candidate, School of Policy, Planning and Development, University of Southern California*

***Mircea Grigoriu**, Professor, and **Cagdas Kafali**, Graduate Student, Department of Civil and Environmental Engineering, Cornell University*

***Gary F. Dargush**, Professor, **Mark L. Green**, Research Assistant Professor, **Ramesh S. Sant**, Ph.D. Graduate (now with DMJM+Harris, New York), **Xiangjie Zhao**, M.S. Graduate (now with Weidlinger Associates, New York), **Yunli Wang**, Ph.D. Candidate, **Li-Yuan Lin**, M.S. Student, Department of Civil, Structural and Environmental Engineering, University at Buffalo*

Previous Summaries

***2000-2001**:*
Alesch and Petak
http://mceer.buffalo.edu/publications/resaccom/0001/rpa_pdfs/02Alesch_final.pdf

Constantinou et al.,
http://mceer.buffalo.edu/publications/resaccom/0001/rpa_pdfs/10Lee-ketter-2.pdf

1999-2000:
Shinozuka et al.,
http://mceer.buffalo.edu/publications/resaccom/9900/Chapter2.pdf

in the presence of a broad range of physical and sociotechnical uncertainties.

Consider, for example, the owner of a single acute care facility in California required to comply with the provisions of legislation known throughout California as Senate Bill 1953. The facility may consist of a stand-alone building constructed all at one time. More likely, however, it consists of multiple loosely-coupled buildings or one old, original structure that has had a series of additions built onto it. Major options include the decision to: (a) not retrofit and face the consequences; (b) not retrofit, but lobby to change the legislation; (c) tear down the facility and rebuild; (d) convert the facility from acute care to an alternative use; (e) retrofit the facility to meet minimum requirements; (f) retrofit to a higher level of performance; and/or (g) request extensions for compliance. Then, within each of these global options, many lower level decisions must be made. For example, within the retrofit options (e) and (f), many possibilities exist for the primary structure, including traditional and non-traditional (i.e., base isolation, passive energy dissipation, semi-active control) retrofit strategies. For option (f), consideration to upgrade the performance of secondary systems may also be relevant. Due to the current state of critical health care in California, there are important financial implications associated with all of these options. Beyond this, there is also a temporal dimension that further complicates the decision-making process.

What is a proper course of action for this owner? Clearly, some systematic analysis is needed. One possibility is to construct computational models in order to study the situation. These models may range from structural dynamics models for assessing the behavior of various retrofit options to organizational models that characterize the performance of health care delivery and financial viability of the healthcare organization. A collection of models could then be used for the analysis of a selected number of alternatives. Perhaps sensitivity studies could also be

The decision-assisting platforms are intended to help illuminate the consequences of choice for both engineering consultants and their clients. Since clients must consider a wider range of variables than their engineers when making choices about seismic safety, the models are intended to couple organizational and engineering concerns into one or more models to help create recommendations for seismic safety that meet the needs of all the critical stakeholders. Stakeholders may include companies interested in developing markets for new technologies, critical care facility owners required to meet legislated levels of seismic performance, local communities faced with prioritizing rehabilitation projects and/or federal agencies responsible for resource allocation.

conducted. The difficulty with this approach relates to the combinatorial nature of the decision space. The associated computational complexity of this problem effectively prohibits full exploration. Alternative methodologies are needed to find good solutions; the effort to develop such methodologies drives this part of this research effort.

Goals and Approach

MCEER investigators working on this effort are focused on helping to meet the need for effective methodologies to assist organizational decision makers and those who advise them. The investigators' activities are aimed at remedying the fact that no integrated decision-assisting tool exists that can be used by hospital owners and consulting engineers to address complex issues and problems associated with seismic retrofit of acute care facilities within today's complex healthcare decision environment. The investigators' goal is to devise one or more decision-assisting platforms that will help to illuminate the consequences of choices in complex, multi-dimensional environments.

We have adopted a multidisciplinary approach to address a multidisciplinary problem. The team includes two structural engineers, one decision scientist, two specialists in organizational behavior and decision-making, a research assistant professor and a significant number of graduate students. Team members are working simultaneously on two approaches to decision-assisting platforms, each of which is fundamentally different from the other. One approach is based on decision analysis models, but goes beyond them to integrate information on earthquakes and their effects. The other approach is based on conceptually new models employing methods that allow for simulating the robustness, through time, of each of a very large number of alternative mitigations for a specific simulated structure. That model will work toward integrating organizational decision criteria, whereas the former works from decision criteria toward an integration of earthquakes and structural response. At the same time, two groups of researchers are collecting data for their respective decision-assisting platforms and further developing their models, while other researchers are focused directly on the question of how hospital owners and administrators make choices about enhancing seismic safety in a turbulent decision environment. Based on information obtained from interviews with administrators in a diverse set of acute care hospitals in California, these researchers are working to characterize the decision environments within which hospital owners and managers must make difficult choices about how to comply with SB 1953 regulations. They are identifying variables that affect the choices made by the owners and managers. They are attempting to integrate, or otherwise link, actual decision criteria employed by real-world managers with the two fundamental decision-assisting platforms being developed by the other research teams in this project.

Investigators and their graduate students face significant obstacles in their attempts to link the various models to create a powerful set of decision-assisting tools. No precedents exist as guides. By the end

Links to Current Research

The decision support systems under development in this effort will incorporate the seismic retrofit technologies and response modification methods developed in a parallel effort being carried out by Bruneau, Reinhorn and others.

of summer 2003, the investigators expect to have completed a "proof of concept" test for linking the behavioral and engineering models being developed as a basis for the two fundamental platforms. Should the proofs of concept show that direct linkages can be made between the behavioral decision-making model and the engineering aspects of the platforms, work will progress in the coming year to advance those linkages. Should the tests prove less than encouraging, efforts will be made in the coming year to create more loosely-coupled linkages between the models. In that case, the behavioral model may simply provide constraints that preclude some seismic retrofitting approaches from being employed in some specific instances, while indicating which other approaches might work well.

The approach being taken by this research team reflects the three-level MCEER approach. It links basic research to tools for application and it embraces the multidisciplinary approach deemed essential to addressing complex socio-technical problems. Initial work focused on research in modeling both normative and behavioral decision-making, developing appropriate understanding of critical facility structural demands and response, and on means for evaluating the effectiveness of a wide range of alternative means for mitigation. In the past year, work has begun on integrating the component parts to create the desired decision-assisting platforms. Coordination meetings provide a checkpoint for addressing technical and communication issues and for assessing the effectiveness of team communication processes.

The team's strategy is to work on two decision-assisting platforms simultaneously. The approach is intended to generate timely practical payoffs while, at the same time, providing for basic research that, if it proves out as expected, will lead to cutting edge methods for evaluating alternative means for mitigating earthquake forces on structures. The "sure-fire" approach is based on approaches to decision science, behavioral models of organizational decision-making, and structural analysis that are advanced, but that are lodged primarily in the mainstream of practice. The parallel approach is based on emergent models integrating evolutionary modeling with the contemporary computing power to test the robustness of many structural mitigations against many seismic forces. By simultaneously working on two approaches, the research team ensures that at least one practical, timely decision-assisting platform will be generated, with the likely probability of generating two extremely useful platforms, each with its own strengths and capabilities.

The following sections describe the four component parts of the decision platforms project.

Decision Analysis Approach Framework

This section describes one of two decision analysis frameworks currently being developed to support seismic rehabilitation decisions. This framework combines a probabilistic model of ground shaking, engineering fragility curves, statistical estimates of potential damage costs, and a financial model of the costs and benefits of rehabilitation.

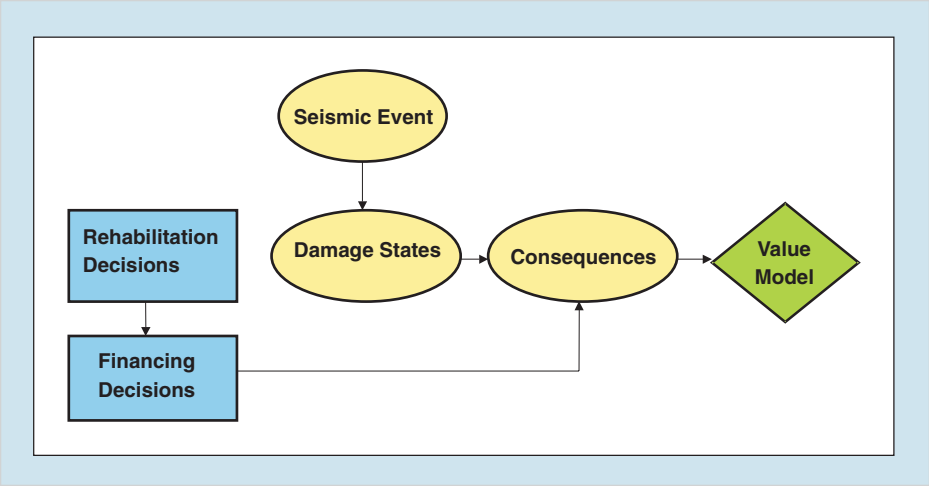

Figure 1. Decision Analysis Framework

Users of the analysis can choose among many important model parameters, including loan terms for financing the rehabilitation cost, the time horizon of ownership of the hospital building, the discount rate, and many more. The overall framework is shown in Figure 1.

The rectangles in Figure 1 are decision nodes, which include the alternatives under the decision maker's control. For example, when considering whether to rehabilitate a building, the rehabilitation decision node would consist of the decision alternatives "No Rehabilitation," "Life Safety Rehabilitation," and "Limited Downtime Rehabilitation" (see Benthien and von Winterfeldt, 2002). In most real rehabilitation decisions, the decision maker also has financial options, which are described by the decision node "Financing Decision." This node includes decision alternatives described by the time horizon considered, amount of the rehabilitation cost that the decision maker chooses to finance, the terms of the loan, and the discount rate.

The ellipses are chance nodes. They include events outside the decision maker's control. The seismic event chance node includes the degree of ground shaking (measured as peak ground acceleration or spectral acceleration) at each of a series of specified time intervals (typically annually for up to 50 years or the useful lifetime of the building). Probability distributions are assessed over the degree of ground shaking using data from the USGS and the Southern California Earthquake Center (see Benthien and von Winterfeldt, 2002).

The second uncertainty concerns the damage states, given a specific degree of ground shaking. The decision analysis model considers five possible states: "No Damage," "Green Tagged," "Yellow Tagged," "Red Tagged," and "Total Loss." Fragility curves are obtained for a particular structure, using fragility curves from the HAZUS Manual (Federal Emergency Management Agency, 1999). These fragility curves are only a starting point; they will usually be adapted based on engineer-

ing knowledge of the specific structure. The fragility curves are translated into conditional probabilities of damage states, given a level of ground shaking.

Given damage states, there still is some uncertainty about the consequences of the seismic event. The major uncertainties are the cost of repairs and the possible lives lost or injuries due to the damage. In some cases, e.g., acute care hospitals, there will also be uncertainty about the downtime during repairs and the resulting costs, e.g., lost revenue and reduced access to hospital care during the down time. The analysis also considers other, more certain consequences of the rehabilitation decision at this point. First, the analysis considers the cost of retrofitting (including financing costs). Furthermore, the analysis considers possible non-seismic benefits of rehabilitation. For example, acute care hospitals may be able to incorporate more contemporary service designs into hospital design during retrofit.

In the past year, the decision analysis approach was refined substantially by adding a module for decisions to finance rehabilitation projects. This module includes two major parameters: the percentage of the rehabilitation cost that is to be financed and the discount rate. These parameters have an important effect on the model results. With larger loans and larger discount rates, rehabilitation decisions become less attractive. In addition, the model has been expanded to include life loss and non-seismic benefits of rehabilitation.

To evaluate the retrofitting alternatives, the decision analysis approach includes a value model for possible consequences. This value model consists of two stages. In the first stage, all consequences are converted to a common unit (either utilities or economic cost equivalents). Next a multiattribute utility model is used to aggregate across consequences (see Keeney and Raiffa, 1976, Clemen and Reilly, 2001). In the simplest case, we use the sum of the equivalent economic costs and benefits to gauge the value of retrofitting. Since the consequences are time dependent, they are discounted at the rate specified by the decision maker.

Either of two generic decision analysis approaches can be used to combine the probabilistic information embodied in Figure 1 with cost and benefits information to help decision making. The first is a simulation approach in which the costs and benefits are estimated for each combination of peak ground accelerations, damage states and rehabilitation options. This approach results in probability distributions over net present value (NPV) for the different rehabilitation options. This approach is very useful for exploring the tails of the probability

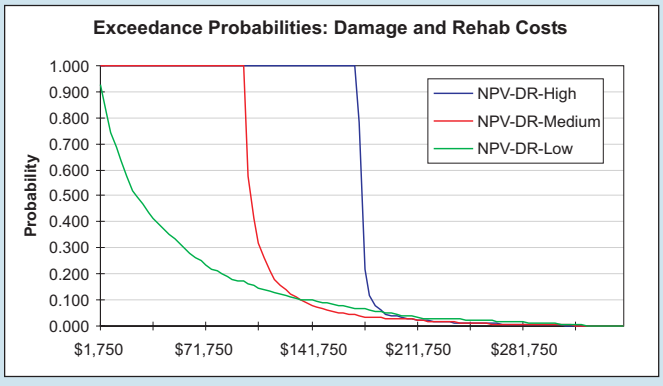

Figure 2. Typical Simulation Output

distributions and for exploring extreme events.

The other approach is to translate the probabilistic information in Figure 1 into a decision tree, to assign costs and benefits at the end of the tree, and to calculate expected values or expected utilities. While this approach does not easily address extreme values, it lends itself to exploring the sensitivities of many of the probabilities, costs, and benefits.

We used both approaches in past applications. For the simulation approach, we used the software "Crystal Ball" by Decisioneering (2002). For the decision tree approach, we used the software package Decision Analysis by TreeAge (DATA), version 3.5 (TreeAge Software, 1998), to create the decision tree and run all analyses. Figure 2 shows a typical output of the simulation, in the form of exceedance probability curves over the total equivalent costs (retrofitting plus damage costs) for three retrofitting alternatives (low, medium and high). Figure 3 shows a segment of a typical decision tree. The real tree in this case is fairly large and cannot be displayed on a page. After running the analysis, the DATA program displays the expected costs at each node of the tree, so the decision maker can determine both the expected costs at the root decision node and anywhere else in the tree.

The decision tree approach was applied to homeowners' decisions to rehabilitate hillside homes in the Los Angeles area (see von Winterfeldt, Roselund and Kitsuse, 2000) and both the decision tree and the simulation approach was applied to rehabilitating apartment buildings with tuck-under garages (Benthien and von Winterfeldt, 2002; von Winterfeldt, Gosh, and Gupta, in preparation).

Both applications led to similar conclusions. The results are very sensitive to the time horizon of ownership (favoring rehabilitation for longer time horizons, but not for shorter ones), the financial terms (favoring rehabilitation for low, subsidized interest rates, but not for normal market level interest rates), the ability to recover some of the rehabilitation cost with increases in property values or rent increases, and the degree of concern with losses of human lives.

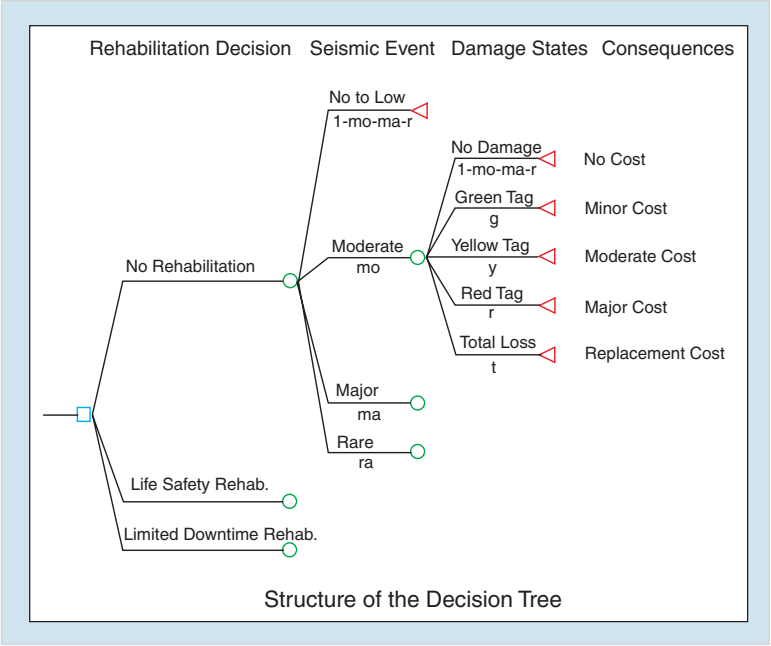

Figure 3. Generalized Structure of the Decision Tree

Seismic Hazard, Fragility Surfaces, and Cost-Benefit Analysis

This component of the proposed framework is designed to be integrated with the other components of the model described in the previous section. It uses probabilistic models to characterize the seismic hazard for a community, describes the seismic performance of the critical systems in a community by fragility surfaces, and evaluates retrofit strategies for these systems using cost-benefit analysis.

During the past year, the work focused on (1) generating life cycle seismic hazard scenarios, (2) essentials of a methodology for generating seismic ground accelerations at a collection of sites, (3) methodology for generating fragility surfaces for structural/nonstructural components of an individual health care facility, and (4) preliminary cost-benefit analyses based on this and the decision approach framework. These developments will be used in the selection of an optimal strategy (apart from organizational constraints) for seismic rehabilitation of structural/nonstructural systems of the demonstration hospital project.

The essentials of the approach are outlined in the following sections.

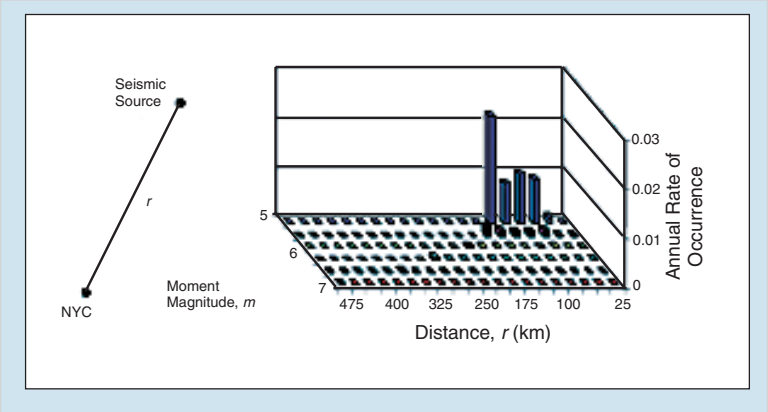

Figure 4. Seismic Activity for New York City

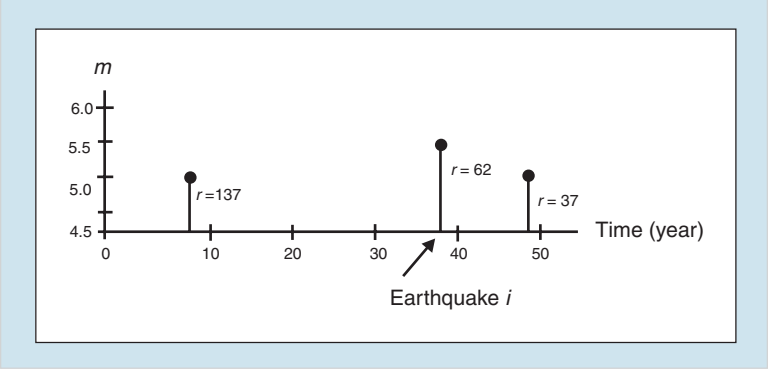

Figure 5. Sample of the Seismic Hazard in New York City for τ =50 years

Seismic Hazard

Suppose that the seismic hazard needs to be evaluated for a community over a time interval measured in years, for example, $\tau = 10, 20,$ or 50 years. The definition of the seismic hazard for this community is based on the following models.

1. Seismic activity model. Tectonic considerations and/or seismic ground acceleration records can be used to identify all relevant seismic sources, that is, seismic sources causing damaging earthquakes, and calculate the annual rate of earthquake occurrence as a function of the seismic source to site distance r and the earthquake magnitude m. Figure 4 shows this function for New York City (NYC).

A sample of the seismic hazard for New York City for $\tau = 50$ years in shown in Figure 5.

The sample provides the times of all seismic events in τ and the magnitude m as well as the source to site distance r for each event.

2. Seismic ground acceleration models. Two models are used to specify the probability law of the ground acceleration process at a collection of sites in a community.
   - The specific barrier model characterizes the properties of the seismic ground acceleration at individual sites as a function of the earthquake magnitude m, seismic source to site distance r, soil conditions, and other parameters.
   - The coherence function model describes the relationship between ground motions caused by a seismic event at various sites in a community.

The Monte Carlo algorithm for generating samples of the seismic ground motions at various sites in a community is based on the specific barrier and the coherence models, and involves two steps:

1. Generate samples of the seismic hazard for a community similar to the sample in Figure 5. The generation is based on the histogram in Figure 4 and properties of Poisson processes.
2. Generate samples of the ground motion at all sites in a community for the values (m, r) generated in the previous step. Figure 6 shows such a sample.

The generation is based on the definition of the ground motion process delivered by the specific barrier and the coherence function models, and Monte Carlo methods for generating samples of stochastic processes.

Fragility Surfaces

We have seen that for each (m, r), soil condition, and some other parameters, it is possible to generate ground motion samples at all sites of interest in a community.

Consider a structural or nonstructural system located at a site in a community for which one or more levels of performance criteria have been specified. Each level of performance can be associated with a damage state. The objective is to calculate the probability that the system reaches a damage state as a function of magnitude m and source to site distance r, that is, the *fragility surfaces* for this system. The calculation of these surfaces involves four steps:

1. Select a value for the pair (m, r). Only values of these parameters that have a non-zero probability of occurrence need to be considered. These values result from the annual rate of earthquake occurrence (Figure 4).
2. Generate n ground motion samples at the system site, and calculate the system response to these simulated samples of the ground acceleration.
3. Estimate the value of the fragility surface at (m, r) by the ratio n_f/n, where n_f denotes the number of response samples that do not meet a particular performance criterion.

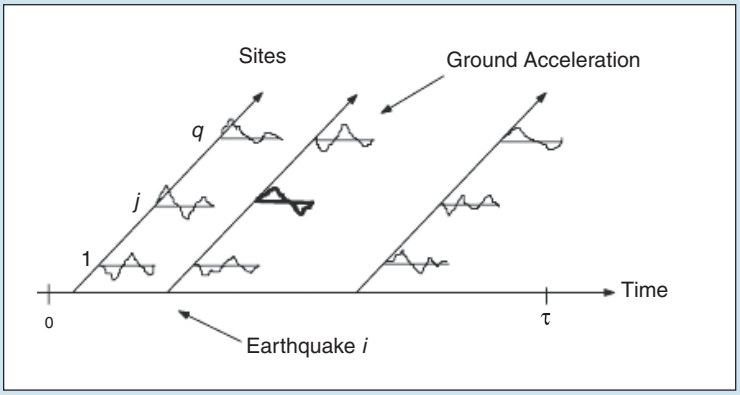

Figure 6. Ground Motion Samples for All Sites in a Community

4. Repeat the calculations in the above steps for all relevant values of (m, r) and a particular performance criterion. Match a surface, referred to as fragility surface, defined on the space of parameters (m, r) to the estimates n_f/n in step 3. A family of fragility surfaces corresponding to various performance criteria can be developed following this algorithm.

Cost-Benefit Analysis

The input to cost-benefit analysis consists of (1) a time horizon τ, (2) seismic hazard at the site of interest (Figure 5), and (3) cost functions including, for example, retrofit and repair costs, loss of use, and loss of life, as well as some potential monetary benefits of retrofit such as increased efficiency in treatment, staffing, and logistics.

Suppose that a system experiences an earthquake with magnitude m occurring at a seismic source at distance r from the system site. Following the earthquake, the system enters a damage state $d_s(m, r)$ with a probability $p_s(m, r)$ given by the system fragility surfaces. Suppose also that the system is repaired so that it is brought to its initial state immediately following this earthquake. Denote by c_s, the cost of bringing the system from damage state $d_s(m, r)$ to its initial state. This elementary cost structure presented here for illustration can be augmented to include the components mentioned above.

Consider now samples of the seismic hazard at the system site, as shown in Figure 5. Let (m_i, r_i) denote the values of (m, r) corresponding to earthquake i in a sample of the seismic hazard. The corresponding damage states $d_s(m_i, r_i)$ and their probabilities $p_s(m_i, r_i)$ result from the system fragility surfaces. Denote by c_s the repair cost associated with the damage state $d_s(m_i, r_i)$. Since damage state s has probability $p_s(m_i, r_i)$, the repair cost for the seismic event i is $C_i = \sum_s c_s d_s(m_i, r_i)$. The total cost for this sample of the seismic hazard is $C = \sum_i C_i$. The cost C is a random variable, whose properties can be estimated from a collection of seismic hazard samples. Figure 7 shows hypothetical histograms of C corresponding to various retrofit strategies.

These histograms have similar expectations but very different tails, suggesting that the use of expected cost as a decision tool for selecting an optimal retrofit strategy can yield unsatisfactory results.

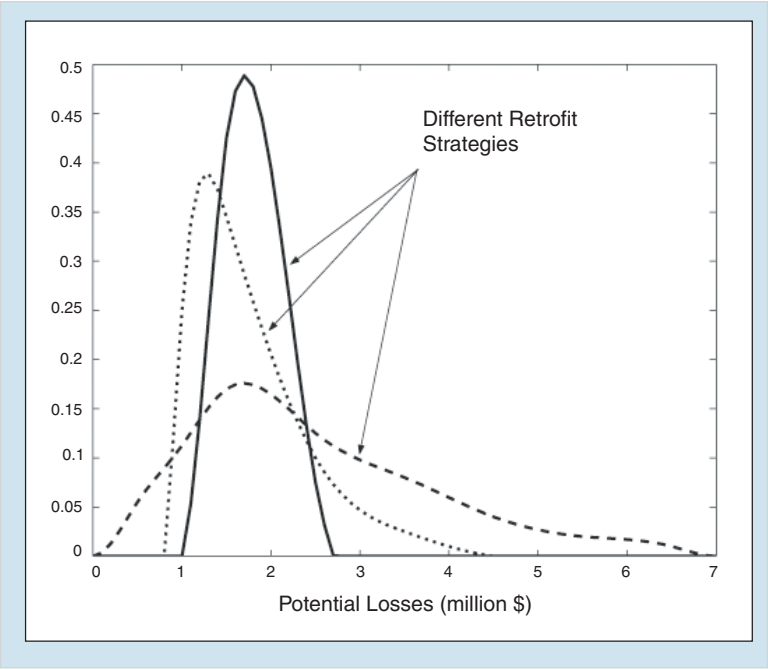

Figure 7. Histograms of Total Cost C

Evolutionary Methodology as a Basis for a Decision Support Platform

Complex Adaptive Systems and Evolutionary Methodologies

Over the past two decades, there has been increasing interest in the concept of *complex adaptive systems*, originally formulated by Holland (1975). These systems typically involve the complicated nonlinear interaction of many components or agents, which aggregate in a hierarchical manner in response to an uncertain or changing environment. As a result, complex adaptive systems evolve over time through self-organization and ultimately acquire collective properties not exhibited by the components or agents acting alone. Classical examples are the human central nervous system, the local economy or a rain forest. Notice, however, that many of these same characteristics are essential for the development of disaster-resilient communities. This suggests that computational approaches suitable for studying complex adaptive systems may be quite appropriate for use in multidisciplinary seismic decision support.

By bringing ideas from biological evolution to bear on the problem, Holland (1962, 1975) also developed a unified theory of adaptation in both natural and artificial systems. Besides providing a general formalism for studying adaptive systems, this led to the development of a variety of *evolutionary methodologies*, including *genetic algorithms*. These computational approaches have enjoyed considerable success in recent years over a wide range of applications in science and engineering (Goldberg, 1989; Mitchell, 1996). These are essentially naturally parallel noncalculus based optimization procedures that can readily accommodate a disparate collection of models.

Genetic algorithms are particularly effective for finding robust solutions to combinatorial problems in the presence of environmental uncertainties. Consequently, evolutionary methods hold significant promise as an excellent framework for the development of a new class of decision support tools toward earthquake hazard mitigation. In the following section, an initial application of this approach for seismic retrofit of structures with passive energy dissipation devices is considered.

"The approach taken by this research team is to link basic research to tools for application and to use a multidisciplinary approach to address complex socio-technical problems."

Evolutionary Aseismic Design and Retrofit

This section includes a brief overview of the proposed computational framework for aseismic design and retrofit. The primary objective is to develop an automated system that can evolve robust designs under uncertain seismic environments. This evolutionary design process involves a sequence of generations. In each generation, a population of individual structures is defined and evaluated in response to ground motions that are realized in association with the geophysical environment. Cost and performance are used to evaluate the fitness of each structure in the population. These fitness values, along with random genetic opera-

tors modeling selection, crossover and mutation processes, define the makeup of the next generation of structures. In our system, performance is judged by conducting nonlinear transient dynamic analysis using an explicit state-space transient dynamics computer code (tda). The implementation of the genetic algorithm controlling the design evolution is accomplished within a modified version of the computer code Sugal (Hunter, 1995).

In the area of seismic passive energy dissipation systems, Singh and Moreschi (1999, 2000, 2002) developed the first genetic algorithm applications, while further information on several different aspects of the present evolutionary aseismic design approach can be found in Dargush and Sant (2000, 2002), Dargush et al. (2002), Zhao (2002) and Dargush and Green (2002).

For illustrative purposes, we will now consider an example of a twelve-story steel frame retrofit with passive energy dissipators. Three different types of dampers are available: metallic plate dampers, linear viscous dampers, and viscoelastic dampers (e.g., Soong and Dargush, 1997). For each type, four different sizes are possible. We utilize a four-bit genetic code to represent the devices in each floor. Consequently, a 48-bit chromosome is employed to completely specify the dampers present in any particular structure. Then for this problem, the set of attainable structures contains roughly 2^{48} members. Exhaustive search of the decision space is clearly not possible.

Currently, a two-surface cyclic plasticity model is applied for the primary structural system and metallic plate dampers, while a coupled thermoviscoelastic model with inelastic heat generation is used for the viscoelastic dampers. The mathematical models employed for these elements are defined in Dargush and Soong (1995) and Dargush and Sant (2002). In addition, the viscous dampers are strictly linear Newtonian devices and all of the bracing elements associated with the passive dampers are assumed to be perfectly rigid. In order to establish acceptable performance for a structure, limits are imposed on interstory drift and story acceleration for each story.

We employ the USGS Gutenberg-Richter seismicity database for eastern North America (Frankel, 1995; Frankel et al., 1996) to model the seismic environment. The entire geographical region is subdivided into bins, with each bin representing 0.1 degrees of longitude and latitude. The USGS database then provides Gutenberg-Richter parameters a and b for each bin such that the number N of earthquakes per year of magnitude greater than or equal to M can be written as $\log N = a - bM$. We simulate the seismic environment by running Poisson processes in each bin to determine significant events that may occur during the intended life cycle of the structure. Whenever a significant event occurs, the ground motion generation algorithm defined by Papageorgiou (2000) is used to produce an appropriate synthetic accelerogram for the specified magnitude and epicentral distance.

For this twelve-story structure, let W_i and k_i represent the ith story weight and story elastic stiffness, respectively. The baseline frame model has story weights $W_1 = \ldots = W_6 = W$, $W_7 = W_8 = 0.75W$, $W_9 = \ldots = W_{12}$

$=0.5W$ and stiffnesses $k_1 = \ldots = k_6 = k$, $k_1 = \ldots k_{12} = 0.25k$. Notice that there is a strong discontinuity at the seventh story. After selecting the parameters W and k, the first two natural frequencies are 0.50Hz and 1.10Hz. Additionally, the story yield forces are also specified in terms of the parameter W as follows:

$$F_1^{yL} = \ldots = F_6^{yL} = 0.20W,$$

$$F_7^{yL} = \ldots = F_{12}^{yL} = 0.05W$$

We now assume that this steel structure is located on firm ground near Memphis, TN. The base structure without dampers survives only 29% of the significant earthquakes. In our retrofit options, we permit all three damper types: triangular plate metallic dampers (tpea), viscous dampers (visc), as well as, viscoelastic dampers (ve). In order to restrict the search to more practical designs, we introduce a recessive gene concept in the genetic algorithm to prohibit structures that utilize more than two different damper types. Hypothetical device cost data for various size dampers are set with each increment in damper size corresponding roughly to a doubling of the damping capacity. There is, of course, considerable subjectivity introduced in setting the relative cost-performance relations for the different damper types. However, we should emphasize that this is only a model problem intended to illustrate the methodology.

Figure 8 presents a snapshot of the overall graphical system. Included is a map that locates the generated seismic events, a database of candidate structures, and reliability plots of robust designs that have evolved through the automated design process. In particular, the upper left diagram provides a detailed view of the earthquakes generated throughout the New Madrid fault zone surrounding Memphis within a portion of one simulation. The variation of mean fitness of the

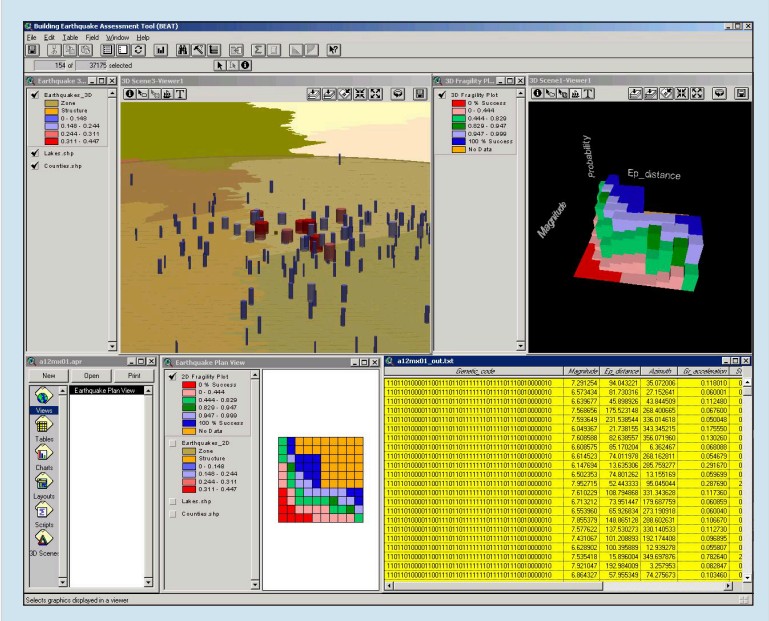

Figure 8. Evolutionary Aseismic Design and Retrofit – Graphical Interface

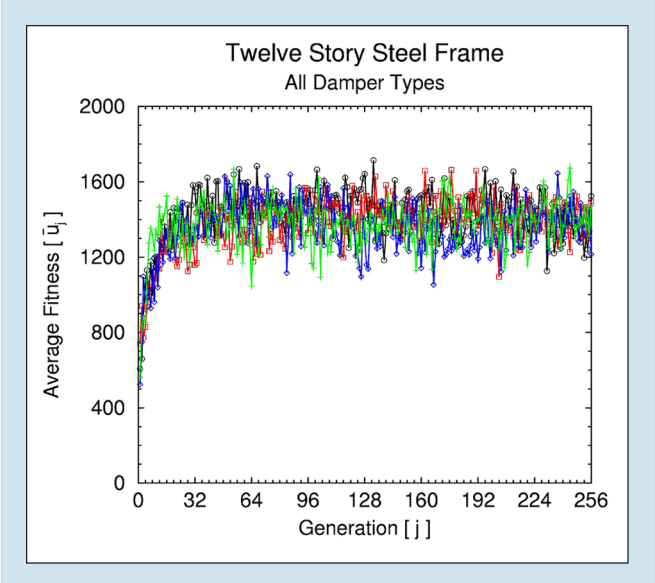

Figure 9. Average Fitness Variation for Twelve Story Steel Frame

population versus generation number is shown in Figure 9 for four separate simulations. As the system evolves, the population becomes enriched with robust structures. However, the mean fitness does not increase in a monotonic fashion due to the inherent uncertainty of the seismic environment and the continual search for better structures. Several robust designs that evolved over 256 generations are shown in Figure 10. Color indicates the damper type and the radius of the rings corresponds to damper size. Notice that each of these designs experienced over four hundred earthquakes with survival rates well above 90%. Interestingly, all three of these robust designs attempt to compensate for the structural discontinuity at the seventh story by introducing large viscoelastic dampers that provide increased damping and stiffness.

Results for this and a range of other structures suggest that the proposed evolutionary methodology is capable of identifying robust design alternatives while explicitly accounting for the uncertainty in the environment. Furthermore, this approach can be readily extended to other retrofit options, including those associated with secondary systems. Current work focuses on the development of efficient versions of the code for massively parallel computer architectures, on the incorporation of a knowledge base to help guide the evolutionary process and on the enhancement of the graphical user interface. Furthermore, beginning in Year 6, we are extending the methodology to examine proof-of-concept models for combined physical and sociotechnical decision support capabilities.

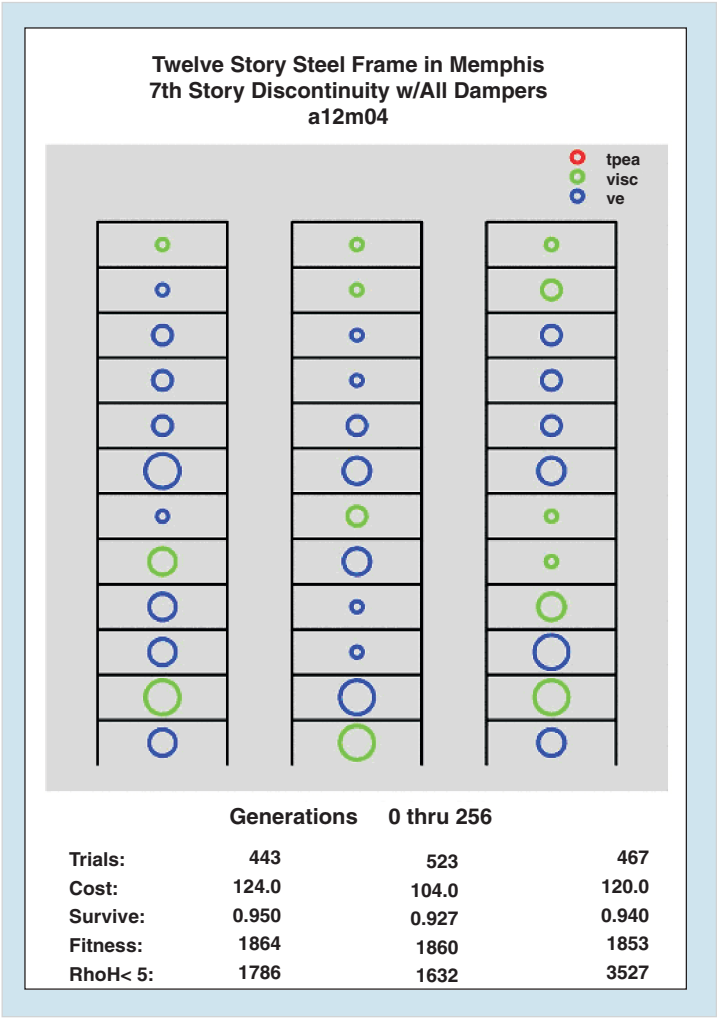

■ Figure 10. Robust Design Configurations for Twelve Story Steel Frame

Behavioral Models of Organizational Decision Making about Enhancing Seismic Safety for Acute Care Hospitals

In another effort, researchers are focusing their attention on organizational and institutional impediments to implementing precautions for enhanced seismic safety and means for overcoming those im-

pediments, with a special focus on acute care hospitals. Their goal is to work with other investigators in this area to integrate what is known about organizational decision making and policy and program implementation into the decision-assisting frameworks being developed by other members of the team. Like the other members of the team, their work places special emphasis on mitigating seismic hazards in older acute care hospitals but is expected to have general application as well.

The Approach

Each of the team members working on decision-assisting models is coming at the problem from a different perspective, but each has the intent of coupling their work with that of other team members to create a truly effective tool. One approach stems from decision science. It is essentially based in normative theory; that is, it is based on how one "should" make choices. Another is empirically-based in engineering and earth science; it feeds directly into the decision science-based model. A third approach is also empirically-based on structural response and the effects of various kinds of damping systems, but employs a novel simulation approach that allows a large number of different mitigation strategies to be tested against a large array of ground-shaking events. The fourth approach is also empirically-based; it focuses on describing what happens in connection with policy implementation under various sets of circumstances. Those circumstances involve the design of policies and programs, the conditions within which implementing organizations find themselves when considering actions to improve seismic safety, and characteristics of the institutional arrangements within which programs are administered and decisions are made by those affected by policies and programs. At the same time, however, they must necessarily focus on characteristics of organizations that affect the decisions they make about how to respond to externally imposed policies and programs.

Initially, investigators worked to develop an understanding of obstacles to implementation, including characteristics of the policy itself and the dynamics of policy and program administration through various levels of government and agencies. For that initial work, they relied heavily on an extensive and intensive review of the literature. Following their initial work, they initiated an extensive case study of SB 1953 in California.

Highlights from the Work

The researchers talked extensively with professionals and have generated several very important propositions concerning enhancing seismic safety in older hospitals. First, individual healthcare organizations respond to SB 1953 very differently from one another. Some organizations are moving ahead in a timely fashion to comply. Others are doing as little as possible to comply. Still others apparently do not plan to comply. Some hospitals have been closed. Second, the response of individual healthcare organizations to the requirements of SB 1953 has less to do with their concern with seismic safety than it does with a myriad of other concerns, concerns that are in some

"The goal of this effort is to provide significantly enhanced means for facilitating development of workable strategies to enhance the seismic safety of hospitals."

cases unique to individual hospitals and, in others, common to most. The institutional and organizational decisions about what to do about SB 1953 are driven by the context within which the individual organizations must make their choices.

Hindsight is not always 20-20, but, in retrospect, it has been possible to identify characteristics of the policies embodied in SB 1953 and its regulations that, had they been different, could have contributed to smoother and less painful implementation for the healthcare organizations and, perhaps, even the organization charged with administering the provisions of the Act. The lessons learned from the retrospective examination can be informative for subsequent policy development.

Finally, the research on organizational decision-making emphasizes the dynamics of policy and program implementation. Changing circumstances affect the solution set perceived by organizational decision makers. Rapidly changing, highly dynamic settings for critical systems, like acute healthcare, demand policy making that is temporally responsive to the needs of those delivering critical services.At the same time, the investigators are concerned that most traditional behavioral organizational decision making theory is based on static situations or on comparative statics; the researchers are coming to believe that decision-assisting models, if they are to be most helpful, must be compatible with dynamic organizational processes and rapidly changing premises and perceived options.

Future Research

In summary, researchers are working on the basic problem of developing decision-assisting platforms from both ends – engineering and decision-making – while paying careful attention to how they might effectively merge their efforts in the middle.They are working as an multidisciplinary team to learn the extent to which they can integrate one or both of the basic platforms models with what is being learned about how acute care organizations actually make decisions about seismic retrofit. To the extent that it can be accomplished, it will provide significantly enhanced means for facilitating development of workable strategies for enhancing seismic safety in hospitals. Moreover, the array of potential applications of such a platform would make it a significant contribution to the field of decision-making under conditions of extreme complexity and uncertainty.

In the coming years, research on organizational decision making in older, acute care hospitals will be integrated into the two decision analysis systems being developed. A proof of concept test is being designed and conducted to learn the extent to which an organizational decision making component can be integrated into the respective models. Depending on the outcome of those tests, the team will work to integrate the models fully into the platforms. If the tests are not encouraging, the teams will seek other means for loosely-coupling the behavioral decision-making models to the current platforms so the information they have generated can be used as criteria for evaluating alternatives.

Acknowledgments

This research was primarily supported by the Earthquake Engineering Research Centers Program of the National Science Foundation, under award number EEC-9701471 to the Multidisciplinary Center for Earthquake Engineering Research. This support is gratefully acknowledged.

The authors also wish to thank the University at Buffalo, Center for Computational Research (CCR).

References

Benthien, M. and von Winterfeldt, D., (2002), *Using Decision Analysis to Improve Seismic Rehabilitation Decisions: A Framework and an Application,* Working Paper No. 3-2002, Institute for Civic Enterprise, University of Southern California, Los Angeles.

Clemen, R. and Reilly, T., (2001), *Making Hard Decisions with Decision Tools*, Duxbury Press, Pacific Grove, CA.

Dargush, G.F. and Green, M.L., (2002), "Evolutionary Aseismic Design and Retrofit," *KEERC-MCEER Joint Seminar*, Buffalo, NY.

Dargush, G.F. and Sant, R.S., (2000), "Computational Aseismic Design and Retrofit: Application to Passively Damped Structures," *Mitigation of Earthquake Disaster by Advanced Technologies-2*, Las Vegas, NV, MCEER-01-0002, Multidisciplinary Center for Earthquake Engineering, University at Buffalo, pp. 175-185.

Dargush, G.F. and Sant, R.S., (2002), "Computational Aseismic Design and Retrofit with Application to Passively Damped Structures," *Seventh U.S. Nat. Conf. Earthquake Engrg.*, EERI, Boston, MA.

Dargush, G.F. and Soong, T.T., (1995), "Behavior of Metallic Plate Dampers in Seismic Passive Energy Dissipation Systems," *Earthquake Spectra*, Vol. 11, 545-568.

Dargush, G.F., Green, M.L. and Zhao, X., (2002), "Evolutionary Aseismic Design of Passively Damped Structural Systems," *International Conference on Advances and New Challenges in Earthquake Engineering Research*, Harbin, China, August 2002.

Decisioneering, Inc., (2002), *Crysal Ball Users Manual*.

Federal Emergency Management Agency, (1999), *HAZUS99-SR1, Technical Manual*. Chapter 5, Federal Emergency Management Agency, Washington, DC.

Frankel, A., (1995), "Mapping Seismic Hazard in the Central and Eastern United States," *Seismological Research Letters*, Vol. 66, pp. 8-21.

Frankel, A., Mueller, C., Barnhard, T., Perkins, D., Leyendecker, E.V., Dickman, N., Hanson, S. and Hopper, M., (1996), *National Seismic-Hazard Maps: Documentation*, U.S. Geological Survey, Open-File Report 96-532, 110 pp.

Goldberg, D.E., (1989), *Genetic Algorithms in Search, Optimization and Machine Learning*, Addison-Wesley, Reading, MA.

Holland, J.H., (1962), "Outline for a Logical Theory of Adaptive Systems," *J. Assoc. Comp. Mach.*, Vol. 3, 297-314.

Holland, J.H., (1975), *Adaptation in Natural and Artificial Systems*, MIT Press, Cambridge, MA, 2nd Edition, 1992.

Hunter, A., (1995), *Sugal Programming Manual*, Version 2.1, University of Sunderland, England.

References (Cont'd)

Keeney, R.L. and Raiffa, H., (1976), *Decisions with multiple objectives*, Wiley, New York.

Mitchell, M., (1996), *An Introduction to Genetic Algorithms*, MIT Press, Cambridge, MA.

Papageorgiou, A., (2000), "Ground Motion Prediction Methodologies for Eastern North America," *Research Progress and Accomplishments, 1999-2000*, MCEER-00-SP01, Multidisciplinary Center for Earthquake Engineering Research, University at Buffalo.

Singh, M.P. and Moreschi, L.M., (1999), "Genetic Algorithm-based Control of Structures for Dynamic Loads," *Proc. IA-99*, Osaka University, Japan.

Singh, M.P. and Moreschi, L.M., (2000), "Optimal Seismic Design of Building Structures with Friction Dampers," *Proc. US-China Millennium Symposium Earthquake Engrg.*, Beijing, China.

Singh, M.P. and Moreschi, L.M., (2002), "Optimal Placement of Dampers for Passive Response Control," *Earthquake Engrg. Struct. Dyn.*, 31, 955-976.

Soong, T.T. and Dargush, G.F., (1997), *Passive Energy Dissipation Systems in Structural Engineering*, Wiley, London and New York.

Treeage Software, Inc., (1998), *DATA™ 3.5 Users Manual*, Williamstown, MA.

von Winterfeldt, D., Roselund, N. and Kituse, A., (2000), *Framing earthquake retrofitting decisions: The case of hillside homes in Los Angeles*, PEER Report 2000/03, Pacific Earthquake Engineering Research Center, University of California, Berkeley, CA.

von Winterfeldt, D., Gosh, S., and Gupta, C., (in preparation), A Simulation Model for Sesmic Rehabilitation Decisions.

Zhao, X., (2002), *Evolutionary Aseismic Design with Supplemental Viscous Dampers*, M.S. Thesis, University at Buffalo, NY.

Developing an Integrated System for Seismic Risk Analysis of Critical Hospital Facilities

by George C. Lee, Masanobu Shinozuka and Mai Tong

Research Objectives

This paper describes an approach used to develop retrofit strategies for hospitals and other critical facilities in low to moderate seismic hazard zones, where strong earthquakes are infrequent, but if they should occur, the consequences would be high. Hospitals in New York State and other urban centers in the eastern U.S. fall into this category, where seismic retrofit requires information on the impact of losing medical services after a destructive earthquake. A team of MCEER researchers is currently developing an approach to address this task. It is a truly multidisciplinary effort, with team members from a variety of disciplines including engineering, seismology, structural dynamics, risk and reliability analysis, manufacturing process engineering, computer simulation, urban and regional planning, and economics. When this research task is completed, it will be united with MCEER's general hospital project to develop seismic retrofit strategies.

Making a decision to seismically retrofit a hospital facility in New York State typically involves different considerations than for facilities located in California. This is primarily because earthquakes are not as likely in New York State, whereas, other natural and manmade hazards and threats are perceived to have equal or even higher risks. Following the five-step decision making process for performing a systems evaluation of a hospital, in New York State described by Lee et al., 2001, the benefits of choosing a seismic retrofit must be objectively compared with other options such as creating a risk plan, developing emergency response procedures, using risk aversions or simply accepting the risks. The core of this analysis process is the quantitative modeling of the relationship between the hospital operation and its supporting resources (human and facilities) as illustrated in Figure 1. The Forrest model is considered to be a suitable tool for presenting a system model of the relationships within a hospital.

Building on last year's research effort on seismic retrofit strategies for hospitals in New York and throughout the Eastern United States (Lee et al., 2001), a framework for a multi-layer platform has been developed by the research team. This platform focuses on the resources provided by facility

Sponsors

National Science Foundation, Earthquake Engineering Research Centers Program

Research Team

***George C. Lee**, Director and Samuel P. Capen Professor of Engineering, **Mai Tong**, Senior Research Scientist, **Vladimir Rzhevsky**, Senior Research Scientist, and **Jincheng Qi**, Post Doctoral Researcher, Multidisciplinary Center for Earthquake Engineering Research*

***Wei Liu**, Ph.D. Graduate, (now with Weidlinger Associates, New York), Department of Civil, Structural and Environmental Engineering, University at Buffalo*

***Joseph Stellrecht**, Undergraduate Student, Department of Computer Engineering, University at Buffalo*

***Masanobu Shinozuka**, Distinguished Professor and Chair, Department of Civil and Environmental Engineering, University of California, Irvine*

Previous Summaries

2000-2001:
Lee et al., http://mceer.buffalo.edu/publications/resaccom/0001/rpa_pdfs/12lee-hosp_graphics.pdf

MCEER Team

***Apostolos Papageorgiou**, Professor, Department of Civil, Structural and Environmental Engineering, University at Buffalo*

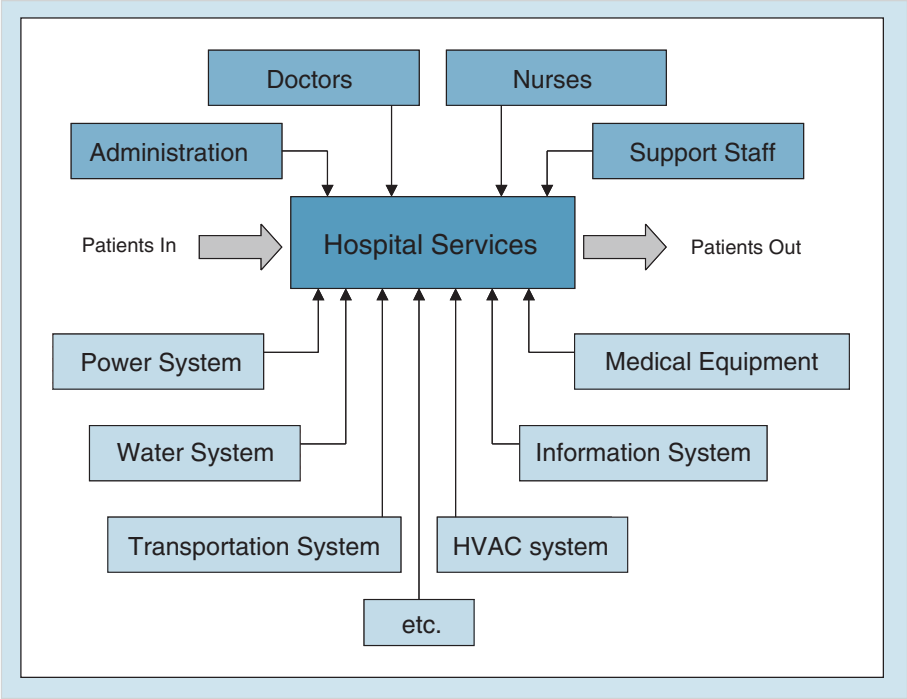

Figure 1. Model of the Relationship between Hospital Operation and Supporting Resources

systems, such as power, water, HVAC, equipment, etc. It is an important step towards developing a comprehensive evaluation procedure for a hospital network system. Currently, a specific case study is being carried out in a hospital located in Central New York State.

Seismic Impact to Hospital Operations

In many moderate seismic zones such as New York State, critical hospital facilities face risks of facility system breakdowns caused by an earthquake. In contrast to California, the probability that a significant earthquake will occur in these moderate seismic zones is not as likely, but the cost of collapse could be much higher due to the lack of protective measures. It follows that the consequences of building damage or collapse may range from slight to complete collapse, and damage to or caused by nonstructural components may also fall in a wide range. Therefore, as we have encountered in all five

Hospital administrators, building owners and other stakeholders in regions of minor to moderate seismicity can use the evaluation system for retrofit strategies to make optimal risk management decisions. Resources for hazard mitigation of all types are limited, and a decision-making method based on solid cost-benefit principles will be a valuable tool in planning for multi-hazards, including earthquakes.

hospitals studied in New York State, the decision to proceed with seismic retrofit or emergency preparations requires a true understanding of the seismic risk factors associated with the hospital and how such an earthquake would impact daily operations. As we proposed in 1999, (reference?) to acquire true risk information, a systematic way to evaluate the seismic hazard impact to the hospital operation is needed. This evaluation method could then also be applied to other natural hazards.

As described in Lee et al., (2001), a hospital is a service organization where medical services are provided to patients. For each medical service provided to a patient, many supporting resources are needed, including human resources (medical doctors, nurses, staff, administrators) and physical facility resources (power, water, HVAC, medical gas, information, medical supplies). Figure 1 shows how an earthquake will impact a hospital's ability to deliver medical services. First, a hazard event will directly impact the structural system, the lifeline systems, medical facilities and medical services in terms of structural damage, limitation or shortage of supplies, and increased patients; second, the structural responses will result in non-structural systems damage; third, the lifeline system damage will influence the proper operation of medical equipment; and fourth, collectively, the damage or inoperability of the building structure, lifelines, and/or medical equipment will impact the overall delivery of medical services.

To understand the impact of an earthquakefrom the occurrence of the hazard event to the medical services, a multi-layer integrated platform is developed to assess and evaluate the seismic risk.

Collaborative Partners

***Thomas Jung**, State of New York Department of Health, Bureau of Architectural and Engineering Facility Planning, Troy, New York*

***Joe Middleton**, Bassett Hospital, Cooperstown, New York*

***Brian Sitzman** and **Ron Curtis**, Cannon Design*

Columbia Presbyterian Medical Center, New York, New York

Erie County Medical Center, Buffalo, New York

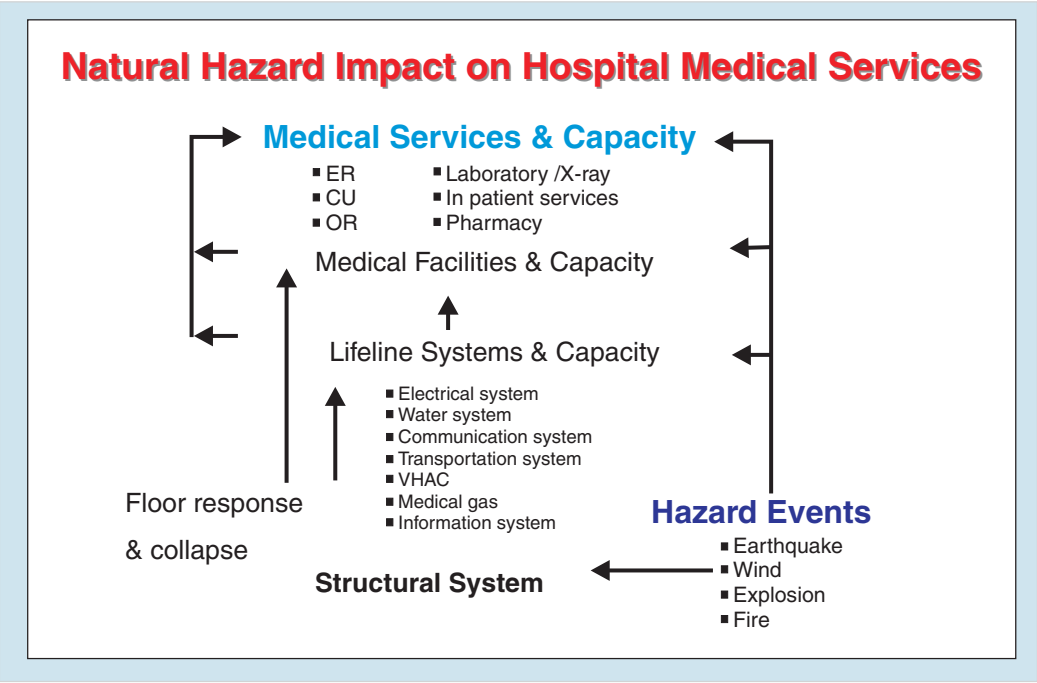

Figure 2. Hazard Impact on Hospital Services

A Platform for Risk Evaluation of Critical Hospital Facilities

The platform for risk evaluation of critical facilities is intended to integrate the structural and major non-structural systems in a hospital and provide seismic risk analysis for the integrated facility. As illustrated in Figure 3, the platform consists of five category layers: hazard, structural system, major non-structural systems, risks and business services. In the following subsections, the functions of each layer are described.

Hazards

Hazards are the cause of disaster consequences. In order to quantitatively assess different hazards, a uniform data process is used. The process requires three types of data inputs: physical parameters, characteristics and influential factors. Physical parameters provide the quantitative values of the hazard conditions such as ground acceleration, velocity and displacement for an earthquake hazard. For each selected physical parameter, there is a corresponding list of characteristics that further describe its condition. For instance, in seismic hazard assessment, the peak amplitude, frequency components and duration of ground acceleration are three critical characteristics of the hazard conditions. A given physical parameter and its critical characteristics provide the basis for a quantitative assessment of the hazard. However, final determination often depends on external, or influential factors. For seismic hazards, influential factors include the source of ground motion, fault, distance from the epicenter, site effects, and so on.

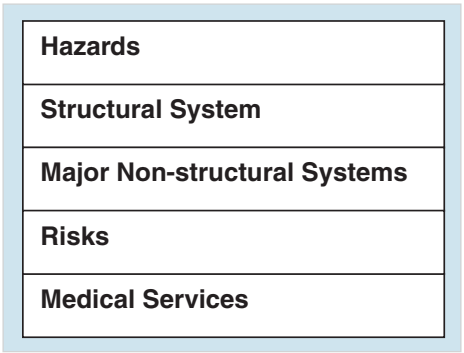

Figure 3. Five Layers of the Integrated Platform

Structural System

The structural integrity and safety is the basic warranty for the functionality of all major non-structural systems and medical services in the hospital. In general, the structural layer deals with essential information from the major load carrying members such as the columns and beams and their material, size, construction quality, and spatial distribution. A structural system model, such an a finite element (FE) model, can be derived from the basic structural member information. Such a model can be used to evaluate the structural integrity under various given hazard loads. Or, it can be used to generate floor or area responses to evaluate the response of supported nonstructural systems.

In the structure layer, the design seismic load plays a key role in the structural evaluation. In the IBC 2000 code, hospital structures are classified in seismic use group III, and have the highest importance factor, 1.5. In contrast, for ordinary buildings in seismic use group I, the importance factor is 1.0. For seismic rehabilitations, FEMA 356 (pre-standard and commentary for the seismic rehabilitation of buildings) offers the BSO (basic seismic objective) performance levels defined as OP (operational) for earthquakes of 50% exceedance probability in 50 years, IO (immediate occupancy) for earthquakes of 20% exceedance probability in

50 years, LS (life safety) for earthquake of 10% exceedance probability in 50 years (BSE-1), and CP (collapse prevention) for earthquakes of 2% exceedance probability in 50 years (BSE-2). According to FEMA 356, rehabilitation design for BSO is expected to produce earthquake performance similar to that desired for new buildings in seismic use group I. Therefore, for hospital buildings, the design seismic load level is approximately 50% more than for ordinary, or regular, buildings.

The evaluation of a hospital structure performed under different hazard conditions is compared to certain pre-determined requirements. In California, under the SB 1953 bill, OSHPD (Office of Statewide Health Planning and Development) is requiring hospitals to determine the structural and non-structural system performance categories, and plan for necessary upgrades.There are five SPC (structural performance categories).This technical classification of structural performance requirements may be a useful reference for hospitals in other lower seismic hazard zones.

Major Non-structural Systems

This layer deals with detailed information about major non-structural systems, including:

- Power system
- Water system
- HVAC system
- Gas, medical gas and vacuum system
- Fire alarm and suppression system
- Communication system
- Internal transportation and egress system
- Information and data network system
- Architectural components
- Medical equipments

Although the general working principles of the above systems are the same in all hospitals, each hospital has its own unique adaptation that makes them different from the systems in another hospital. Since damage is often directly related to these differences, it is necessary to develop a hospital-specific detailed function stream flow diagram for each of the above systems along with a collection of relevant component information.

In order to understand how a component's failure influences the overall function of the system, a logic tree approach is often used to build system operability. For each component, its operation is normally dependent on several other components. By classifying these subordinate components as logic OR (redundant) and AND (essential), a system logic tree can be formed. The dependency relationship of the system to its components is thus established.

Among the non-structural components, medical equipment is a special group. They are directly related to specific medical services, and are more delicate than most components of utility systems. Therefore, protection of medical equipment will be different from that of other utility systems. In surveying several NY State hospitals, it was found that most of the medical equipments are portable. In addition, their operability most often depends on three factors: building integrity, utility supply and information networking.

Links to Current Research

This task is pursued in parallel with the other larger efforts related to acute care facilities (Alesch, Bruneau, and others). The detailed hospital facility model developed herein will characterize facilities in low to moderate seismic zones, which will complement those being developed primarily for hospitals in California.

Web Sites

MCEER Hospital Project:
http://mceer.buffalo.edu/hospitals/
(Choose the Introduction tab for an overview of the project. For user controlled information, please contact Mai Tong at mtong@mceermail.buffalo.edu.)

Risks

Risks are various types of potential failure or damage. The facility-related risks can be generally assessed through survival analysis. The results of earlier studies have been published in Shinozuka, 2001; Porter et al., 1993, Grigoriu and Waisman, 1998 and Shinozuka et al., 2000. A component's failure acceleration is described as follows (Shinozuka, 2001 and Porter et al., 1993)

$$A = A_m \varepsilon_R \varepsilon_U \qquad (1)$$

where A_m is the median failure acceleration, ε_R represents the inherent randomness of A, and ε_U represents the uncertainty. Both ε_R and ε_U are assumed to be unit median lognormal random variables with logarithmic standard deviation (SD), β_R and β_U.

The seismic risk of a component is measured by its fragility - the conditional probability of "failure" under a given level of seismic hazard level a (intensity of motion at the support).

$$P_{fc} = \Phi\left[\frac{ln(a/A_m) + \beta_U \Phi^{-1}(Q)}{\beta_R}\right] \qquad (2)$$

where Φ is the normal cumulative distribution function. The logarithmic SD of fc is

$$\beta_c = \sqrt{\beta_R^2 + \beta_U^2} \qquad (3)$$

For instance, the fragility of a major electrical transformer under seismic hazard is a function of failure probability vs. PFA (peak floor acceleration). This function varies according to the level of confidence. However, if many uncertain factors are not clearly identified, such as, the footing condition, the anchor condition, and the quality of internal components in the transformer example, then the fragility function may largely vary between low to high levels of confidence. Identifying these uncertain factors and applying proper engineering assessment and judgment may decrease the variance of the fragility function. In this regard, detailed information in the facility model plays an important role.

The system fragility can be formed by using the logic tree (fault tree) based on the dependency relationship established for components and subsystems. In particular, for each AND and OR relationship, the combined fragility will be

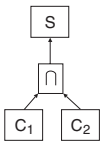

$$P_s = 1 - (1-P_{c1})(1-P_{c2})$$

$$P_s = P_{c1}P_{c2}$$

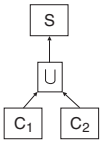

where P_{c1} and P_{c2} are the fragilities of the components C_1 and C_2.

Annual probability of failure P_{fa} due to earthquake of any intensity

$$P_{fa} = \int_0^\infty \frac{-dH(a)}{da} P_{fc}(a)da \qquad (4)$$

where H(a) is a hazard function (measured in the occurrence probability of exceedance) of a given level of hazard (motion at support) a (measured in g).

For seismic hazard, California hospitals are required by OSHPD to evaluate their critical non-structural components and systems according to a five level NPC (Non-structural Performance Category).

Medical Services

This layer deals with patient service operations in the hospital. It analyzes the patient distribution and the services provided in each department (internal medicine, surgery, radiology, eye & throat, etc.) Using correlation and input-output analyses, one of the main features is to evaluate the dependency of medical services to the utility systems. The utility demands are delivered by the physical utility systems. The demands themselves are not attributes of the physical utility systems, rather they are requirements to the physical utility systems and are directly associated with the patient services. Therefore, demands are determined in the patient service model.

The medical services are dependent on time and spatial factors. The corresponding utility demands will vary during the day, month or season. Also, they are distributed into designated areas (OR, ER, ICU, etc.). Furthermore, during and immediately after a disaster, the type of medical services can be significantly changed by the destructive nature of the disaster. In some cases, even without any limitation of material supply, the operational capacity of a hospital may not be sufficient to meet the overloaded demand caused by the disaster.

One of the research areas in this layer is the change in the dependency relationship between normal and emergency conditions. As observed in many cases, medical service procedures adopted in an emergency situation can be significantly different from normal procedures; therefore, the input-output relationship established in the normal situation is no longer valid for emergency medical service analysis. However, for a longer period of time, within a probabilistic confidence interval, the relationship may still be applicable for certain analysis.

On Going Case Study

Figure 4 shows a plan view of the hospital building that is currently being studied. This hospital is undergoing a major renovation and expansion as of 2003. Several seismic structural retrofit options are

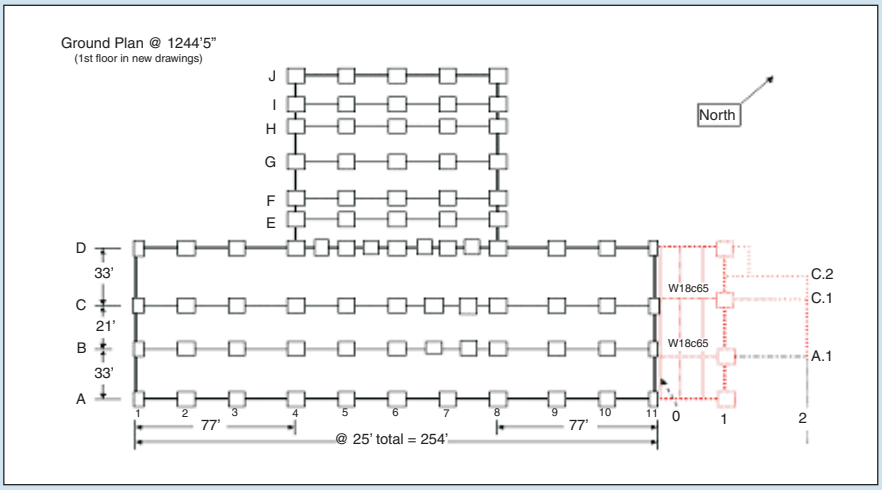

Figure 4. Hospital Building Plan View - Case Study

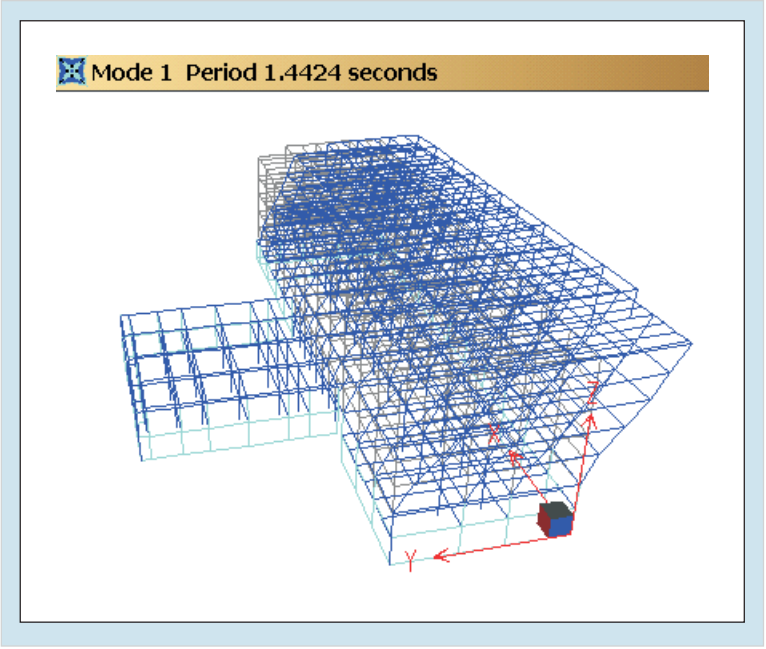

Figure 5. First Mode of the Hospital Structure

under consideration to improve the main medical building's resistance to seismic hazards. One option is to add steel shear walls in both directions of the building; another is to increase the section area and reinforcement of several columns. In order to determine the benefits offered by these options and provide design load and capacity requirements, a time history analysis has been performed.

The dynamic analysis obtained from the finite element model indicates that the first major mode is in the short direction and the corresponding fundamental period is about 1.5 seconds (see Figure 5). When a design earthquake following IBC2000 is applied to the structure, several major columns appear to be severely overstressed, and should be strengthened by seismic retrofit.

However, it was found that after the structural retrofit, the seismic risks to the non-structural systems may become higher, since the strengthened building structure will have a shorter fundamental period; therefore, the non-structural systems may be subject to higher floor responses under the same earthquake.

Conclusion and Future Research

The studies related to protecting hospitals in New York State from earthquake disasters have so far developed the analytical and computational capabilities for analysis of structural and non-structural components; a GIS-based database for seismic hazard assessment, and several hospital structural models that include the property characteristics of the structures.

Some data on medical equipment and non-structural components has been collected and stored in a database. The database lacks information on the deterioration of property characteristics of these equipments and non-structural components. A future effort will concentrate on collecting this information and adding it to the database, with an emphasis on their impact to the seismic risks of hospital facilities.

Acknowledgments

This research was primarily supported by the Earthquake Engineering Research Centers Program of the National Science Foundation, under award number EEC-9701471 to the Multidisciplinary Center for Earthquake Engineering Research. This support is gratefully acknowledged.

References

Grigoriu, M. and Waisman, F., (1998), "Seismic Reliability and Performance of Nonstructural Components," *Proceedings of the Seminar on Seismic Design, Retrofit and Performance of Nonstructural Components, ATC-29-1*.

Lee, G.C., Tong, M. and Okuyama, Y., (2001), "Retrofit Strategies for Hospitals in the Eastern United States,"*Research Progress and Accomplishments 2000-2001*, MCEER-01-SP01, Multidisciplinary Center for Earthquake Engineering Research, University at Buffalo, pp. 141-148.

Porter, K., Johnson, G.S., Zadeh, M.M., Scawthorn, C.R. and Eder, S.J., (1993), *Seismic Vulnerability of Equipment in Critical Facilities: Life-safety and Operational Consequences*, Technical Report NCEER-93-0022, Multidisciplinary Center for Earthquake Engineering Research, University at Buffalo, 380 p.

Shinozuka, M., (2001), *Seismic Risk Assessment of Non-structural Components in Hospitals*, FEMA/USC Hospital Project, December.

Shinozuka, M., Feng, M.Q., Lee, J. and Naganuma, T., (2000), "Statistical Analysis of Fragility Curves," *ASCE Journal of Engineering Mechanics*, Vol. 126.

Resilient Disaster Response: Using Remote Sensing Technologies for Post-Earthquake Damage Detection

by Ronald T. Eguchi

Research Objectives

The objectives of this research are to characterize urban building damage, using a comparative analysis of remote sensing imagery acquired before and after an earthquake event, and to develop preliminary damage detection algorithms for locating collapsed urban structures.

Remote sensing technologies are emerging as useful post-earthquake damage evaluation tools. Recent studies in Japan, Europe and the U.S. demonstrate that satellite-based imagery can identify broad zones of damage following significant earthquake events. For example, Wesnousky et al. (2001) identify the damage caused by widespread liquefaction and fire-following effects on low-resolution remotely sensed data. Damage sustained in urban environments has more recently been identified through visual inspection of optical (Matsuoka and Yamazaki, 1998; Chiroiu et al., 2002; Huyck et al., 2002; Mitomi et al., 2002; Yusuf et al., 2002; Saito and Spence, 2003) and SAR (Aoki et al., 1998, Huyck et al., 2002; Yusuf et al., 2002) coverage.

For several years, a Multidisciplinary Center for Earthquake Engineering Research (MCEER) team has been investigating the use of remote sensing technologies for earthquake damage detection and emergency response (Eguchi et al., 1999; Eguchi et al., 2000; Tralli, 2001; Huyck and Adams, 2002; Huyck et al., 2002). Research has focused on various aspects of damage detection, including: the distinction between extreme levels or states of damage versus non-damage; the quantification of damage states on a regional basis (Mansouri et al., 2002); and the assessment of damage sustained by individual buildings.

The following paper describes methodological progress in the characterization of urban building damage using optical and Synthetic Aperture Radar (SAR) remote sensing imagery. Preliminary damage detection algorithms are introduced for the 1999 Marmara earthquake in Turkey, demonstrating the ability of advanced technologies to determine the scale of a disaster. A quantitative assessment is made of the magnitude and extent of building collapse in the city of Golcuk, which builds on reconnaissance information presented by Eguchi et al. (2000a) in a previous publication of MCEER research accomplishments (see also Eguchi et al., 2000b).

Sponsors

National Science Foundation, Earthquake Engineering Research Centers Program

Research Team

Ronald T. Eguchi, *President,* ***Charles, K. Huyck****, Senior Vice President,* ***Beverley J. Adams****, Project Scientist, and* ***Babak Mansouri****, Project Scientist, ImageCat, Inc.*

Bijan Houshmand, *Adjunct Associate Professor, Department of Electrical Engineering, University of California, Los Angeles*

Masanobu Shinozuka, *Distinguished Professor and Chair, Department of Civil and Environmental Engineering, University of California, Irvine*

Previous Summaries

***2000-2001**:*
O'Rourke et al., http://mceer.buffalo.edu/publications/resaccom/0001/rpa-pubs/14orourke.pdf.

1999-2000:
Eguchi et al., http://mceer.buffalo.edu/publications/resaccom/9900/chapter7.pdf.

1997-1999:
Eguchi et al., http://mceer.buffalo.edu/publications/resaccom/9799/

Collaborative Partners

***Fumio Yamazaki**, University of Tokyo*

***Masashi Matsuoka**, Earthquake Disaster Mitigation Research Center*

Architectural Institute of Japan

Japanese Geotechnical Institute

Japan Society of Civil Engineers

European Space Agency

NIK Insaat Ticaret, Ltd.

In terms of benefits to emergency responders, urban damage functions generated from remote sensing coverage promise an accelerated *rate* of response, while guiding the *scale* of response efforts and resource allocation. They further provide critical information to international aid agencies, supporting logistical planning and deployment of equipment.

Technical Summary

Following an earthquake, such as the 1999 Marmara event, change detection techniques based on high-resolution remote sensing data provide an overview of the post-disaster scene, a method of rapid damage assessment, and critical information for directing rescue and recovery efforts. Figure 1 introduces the methodological approach that forms the basis of this research. The flowchart indicates that damage arising from a disaster is detected in the form of 'changes' between a temporal sequence of images acquired 'before' and 'after' the event. This comparative analysis is facilitated by pre-processing the imagery, which also minimizes the occurrence of false positives. The data is registered and georeferenced within a common coordinate system. Although visual inspection of changes between pre- and post-event scenes may provide an initial focus for recovery efforts, quantitative techniques promise a more detailed damage record, which will fully support emergency response efforts. Temporal changes are therefore computed using a range of mathematical operators, such as subtraction and correlation. The final step involves comparing these measures of change with 'ground truth' damage data, which are used to assess model performance by establishing associations between spectral changes in remote sensing coverage, and damage states observed in the field.

Methodology

Based on the previously outlined approach (see Figure 1), change detection algorithms were developed for the city of Golcuk, which is the most densely populated urban center in the Kocaeli province of Turkey. From Figure 2, Golcuk is situated on the south shore of Izmit Bay, approximately 10km west of the earthquake epicenter. The city experienced extensive damage during the 17th August 1999 event, due to the 4-5 meters of surface rupture and associated shaking that oc-

The results of this research will ultimately help emergency response officials, and building and safety engineers, by providing more reliable methods of assessing post earthquake damage. Characterizing urban building damage using optical and SAR remote sensing imagery will help to determine the scale of the disaster, guide the rate and scale of the response efforts and provide critical information to international aid agencies, supporting logistical planning and deployment of equipment.

curred (Lettis et al., 2000). According to Coburn et al. (1999, cited in Rathje, 2000), 30-40% of structures experienced full or partial collapse, due in many cases, to soft first stories.

As shown in Table 1, remotely sensed SPOT panchromatic and ERS intensity and complex images were acquired 'before' and 'after' the earthquake event. The performance of both optical and SAR sensors was investigated, since each are subject to distinct advantages and limitations, related to spectral wavelength and spatial and temporal resolution. Further details are given in Table 1. As noted above, the minimum requirement for change detection is a single 'before' and 'after' scene. In the case of ERS SAR data, a sequence of images ('Before 1' [B1], 'Before 2' [B2], 'After 1' [A1] and 'After 2' [A2]) was acquired. 'Before-before' [B1,B2] and 'after-after' [A1,A2] pairings are 'baseline' cases. They encapsulate the effect of seasonality, shadowing and differences in illumination, which although causes of change, are distinct from damage sustained by the built environment. In terms of preprocessing, the optical

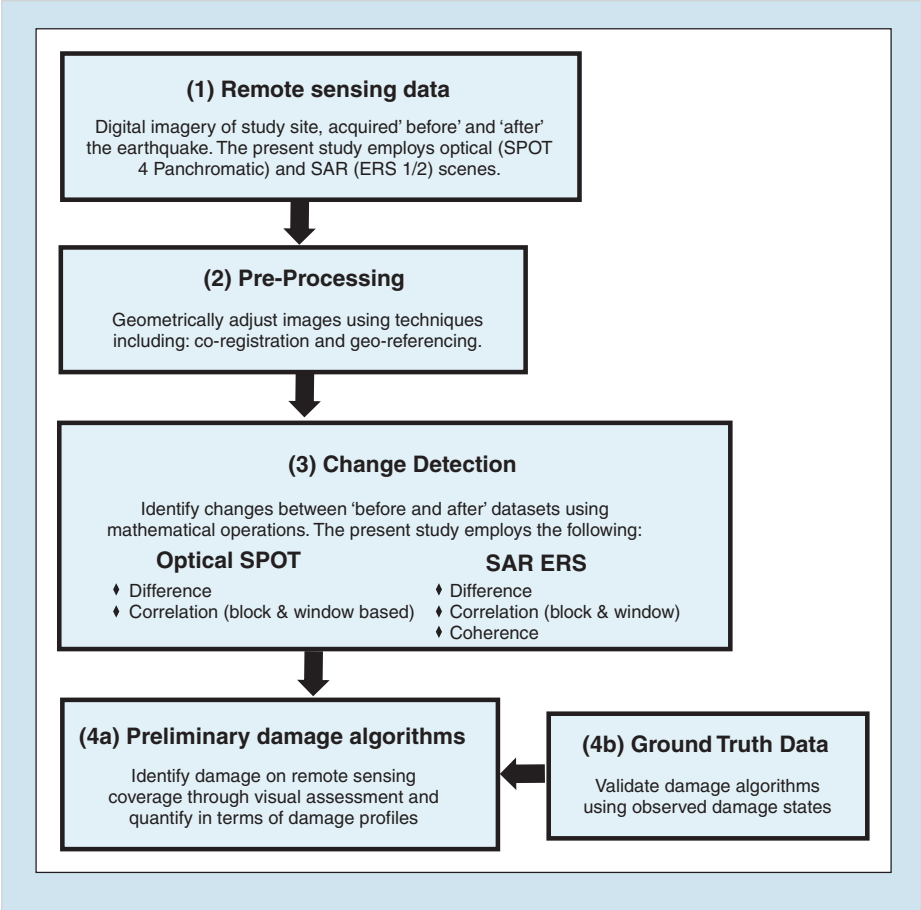

Figure 1. Flowchart Summarizing the Sequence of Methodological Procedures Involved in Damage Detection using Optical SPOT and ERS SAR Imagery

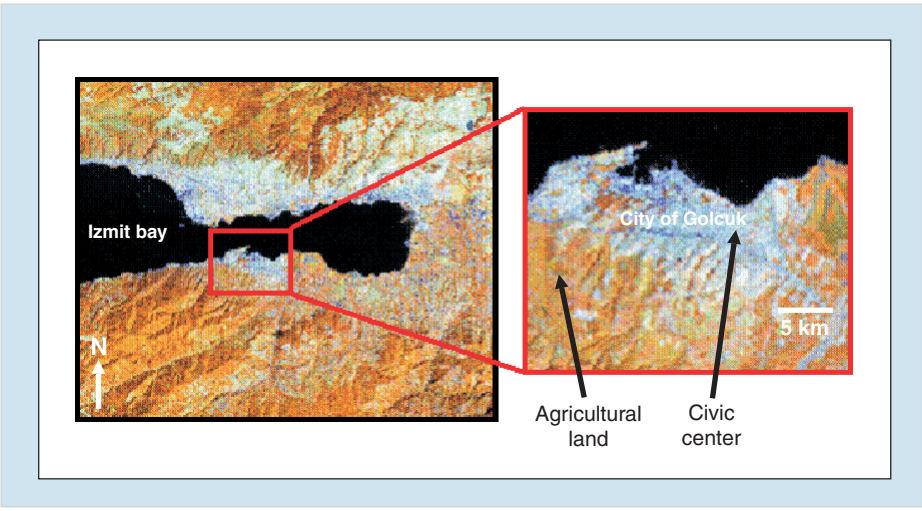

Figure 2. Landsat 5 RGB Image (Red: Band 4, Green: Band 5, and Blue: Band 3) Acquired on September 18, 1999, Showing Izmit Bay in Turkey, and the Golcuk Study Site where Widespread Building Damaged was Sustained during the 1999 Marmara Earthquake (Data Courtesy of ESA)

■ Table 1 Specification of Optical and SAR Imagery of Golcuk, Acquired 'Before' and 'After' the 1999 Marmara Earthquake

Sensor	Satellite	Image ID	Acquisition Date	Advantages	Limitations
Optical	SPOT 4	B1	7/15/99	Images are easy to understand & interpret	Obscured by cloud & smoke
		A1	8/20/99	Imagery is comparable to human vision	Limited to daylight hours
					Low revisit frequency
SAR	ERS 2	B1	3/20/99	Day and night imaging capability	Image interpretation is complicated, as SAR records backscatter
		B2	4/24/99	Penetrates cloud & smoke	Subject to considerable noise
	ERS 1	A1	9/10/99	High revisit frequency	Sideways looking sensor causes layover issues
	ERS 2	A2	9/11/99		

and SAR datasets were co-registered. The SPOT imagery was provided in a geo-referenced format, while a complex template matching technique was developed and applied to the ERS scenes.

A range of change detection measurements were explored for the SPOT panchromatic data: (1) simple difference (dif) between intensity values; and (2) sliding window-based (cor) and modulated block correlation (bk_cor) indices, computed between the 'before' and 'after' images. In the case of SAR intensity and complex data, a wider selection of indices were calculated, comprising: (1) simple difference between intensity values; (2) sliding window-based and modulated block correlation indices between intensity images; and (3) coherence (coh) or complex correlation between complex images.

The next methodological step compares indices of change with 'ground truth' damage data collected by a Japanese reconnaissance team that visited Turkey shortly after the earthquake (AIJ, 1999). The AIJ team adopted the zone-based sampling strategy in Figure 3a, using administrative boundaries corresponding with the street network. Within each zone, damage states were recorded for a sample of buildings. The damage classification is a variation of the European Macro-seismic Scale (EMS98), which divides damage sustained by masonry and reinforced concrete buildings into the following five categories (see AIJ, 1999):

- Grade 1: Negligible to slight damage
- Grade 2: Moderate damage
- Grade 3: Substantial to heavy damage
- Grade 4: Very heavy damage
- Grade 5: Destruction/collapse

This information was used to produce the damage state map in Figure 3b, which expresses the percentage of collapsed structures (Grade 5) as a function of the total number of observations (Grades 1-5). For analytical purposes, these percentages are divided into the following standard categories: A (0-6.25% of buildings totally collapsed); B (6.25-12.5%); C (12.5-25%); D (25 – 50%); and E (50-100%). There is an additional 'Sunk' zone corresponding with an area that experienced significant subsidence after the earthquake, which is situated in the northeast corner of Figure 3b.

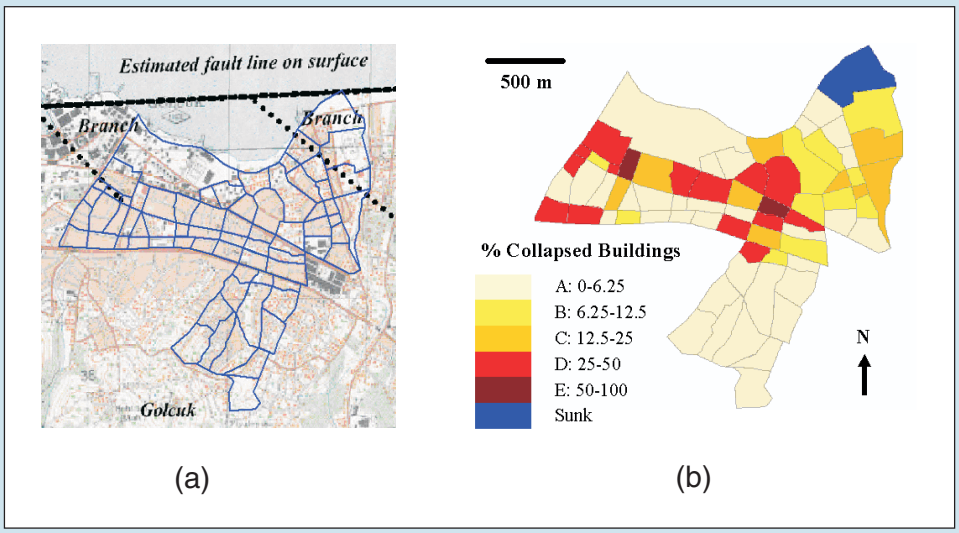

■ Figure 3. Ground Truth Data for Golcuk: (a) Street Network Used as a Basis for Defining the 70 Sample Areas (Shown in Blue) Employed during the AIJ Damage assessment; (b) the 70 Zones are Color-Coded to Represent the Distribution of Collapsed Structures and the Location of the Subsided (Sunk) Area (Data Courtesy of AIJ, 1999)

Finally, a set of algorithms was generated to quantify spectral changes linked to earthquake damage. So called 'damage profiles' are an exploratory tool, which demonstrate broad trends between building damage states and the magnitude of temporal variations in the remote sensing coverage. For the optical dataset, results are generated for the difference, sliding window and block correlation datasets. A mean value was computed for each of the 70 ground truth zones, and these responses aggregated by damage state. The result is a central measure of tendency and standard deviation (plotted as error bars) for each damage state. Given the availability of multiple 'before' and 'after' images for SAR, preliminary tests were completed to ascertain the optimum permutation for distinguishing between damage states A-E. To isolate earthquake-related damage from extraneous changes, the SAR profiles also include the baseline scenario (for example, [A1, A2]). These algorithms are 'preliminary' in the sense that they are empirically-based and applied to a single event. Subsequent research will enable further development of theoretical bases underpinning the models, leading to more widespread application of the approaches presented here to other earthquakes.

Results

Visual Characterization

As a precursor to the quantitative evaluation, Figures 4 and 5 show a sample of the image-based intensity, difference and correlation data from which the optical and SAR damage profiles are derived. Comparing Figure 4a-b provides a rudimentary visual distinction between the basic optical reflectance characteristics of Golcuk 'before' and 'after' the earthquake event. The images are annotated to highlight key areas of change. In Figure 4a, circle one (C1) identifies a stretch of the shore where several wharf structures were located prior to the earthquake. Circle two (C2) demarcates an area of the coastline where

Links to Current Research

The development of new technologies that quantify post-earthquake damage in near real-time is a critical step towards improving contemporary response and recovery procedures. These technologies will enhance community resilience, by:

- *helping emergency officials to identify severely impacted areas in near real-time;*
- *contributing to decision support systems that must prioritize response activities based on need, opportunity and available resources; and*
- *aiding the communication of critical response information using wireless technologies.*

significant ground subsidence was observed. Circle three (C3) encompasses part of Golcuk that was populated with 3-4 story buildings. In Figure 4b, which shows the post-earthquake image of Golcuk, the major wharf structure (C1) is no longer present. There is a marked decrease in reflectance around C2, where a large parcel of land subsided and was subsequently inundated. Finally, significant building collapse is evident in C3, with this region of the city appearing brighter yet poorly defined on the 'after' scene.

The difference scene in Figure 4c is color-coded to highlight regions of Golcuk exhibiting pronounced differences in reflectance, which may be related to earthquake damage. Changes are concentrated in the central urban area of the city. Strongly negative values arise where there is a marked increase in reflectance between the 'before' and 'after' scene. With reference to the damage map in Figure 3b, these areas clearly correspond with zones exhibiting severe building damage (D-E). This result suggests that debris piles associated with collapse exhibit a higher spectral return than the standing structure. Although considerable damage was also sustained to the west of Golcuk, reduced differences may be due to suppressed reflectance values where smoke from the burning Tupras oil refinery was present in the upper atmosphere. Positive differences are limited to the coastal stretch that experienced subsidence, where reflectance values have fallen following widespread inundation.

Results for the block and window-based correlation (Figure 4d-e) are overlaid with a base map of Golcuk. For visualization purposes, all values are displayed as positive, since the magnitude rather than the direction of change is of interest. Areas exhibiting low levels of correlation are synonymous with pronounced changes between the images. For both block and sliding window-based results, these areas (displayed in red) are concentrated in central Golcuk (see annotation C1). As with the difference values, comparison with the damage map (Figure 3b) confirms that building collapse was widespread throughout this region of the city. A low level of correlation around the subsidence zone (C2) may be explained by the change in reflectance following inundation, while low correlation offshore (C3) is probably due to the random or chaotic patterns of surface reflectance associated with wind-driven wave action.

Figure 5 depicts the SAR intensity responses for Golcuk. Due to the noisy/speckled nature of SAR data, difference scenes are difficult to interpret. Instead, a comparison is best drawn between the constituent 'before' and 'after' scenes in Figure 5a-d. Reflectance is consistently high throughout the city. Comparison with the damage map in Figure 3b confirms that these bright areas within the vector overlay correspond with urban coverage of the city center, where there is a concentration of multistory buildings that act as high return corner reflectors. In contrast, the low backscatter associated with: the flat principal road through the city; less densely occupied areas with fewer corner reflectors; and surrounding agricultural land, produce a darker response. Together with these spatial trends, a general observation is

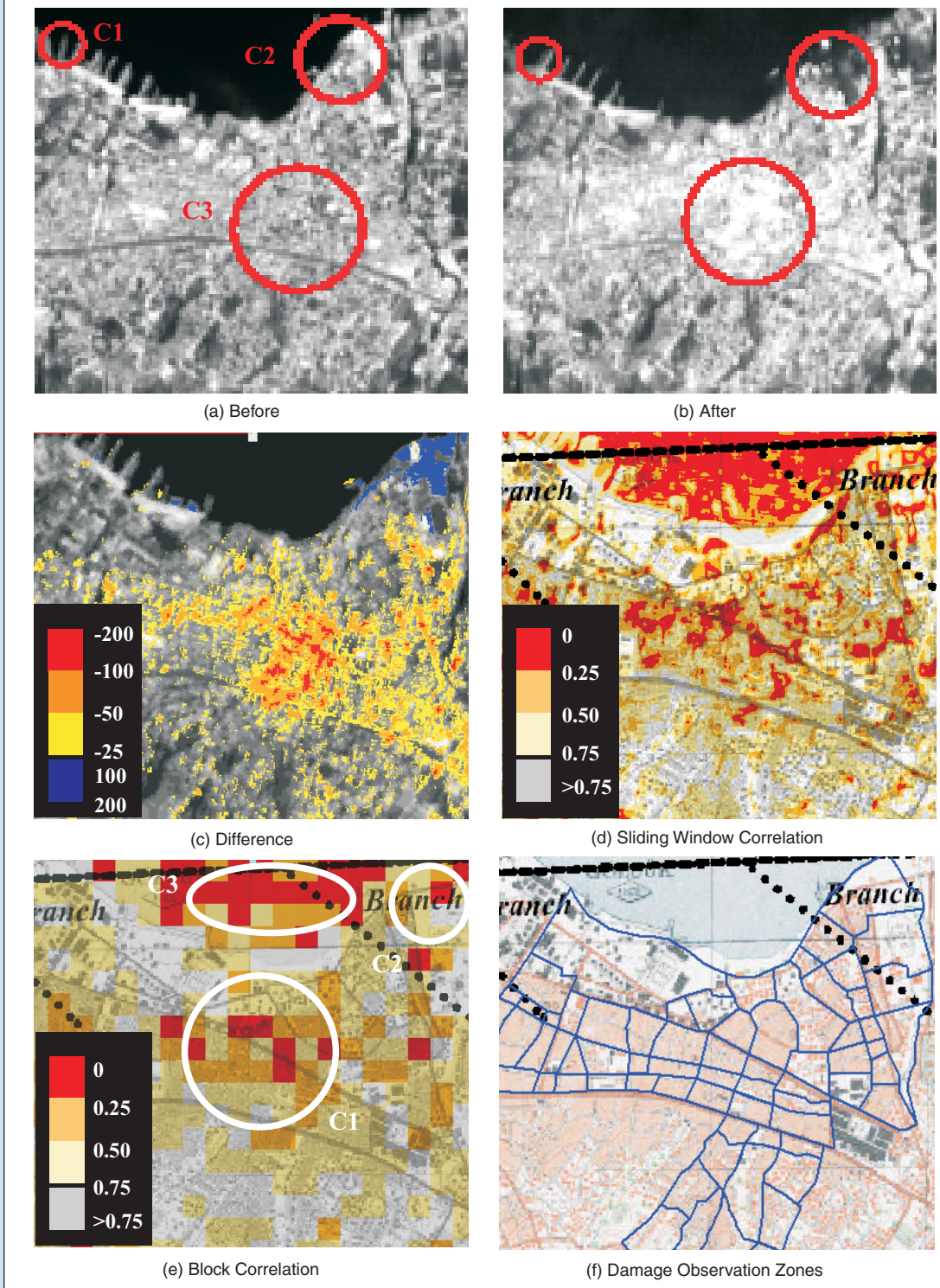

■ Figure 4. Panchromatic SPOT4 Coverage of Golcuk, Showing (a) 'Before' Image; (b) 'After' Image; (c) Difference Values; (d) Sliding Window Correlation; (e) Block Correlation; and (f) the 70 Sample Zones in which AIJ Observed Building Damage (See text for discussion of annotations)

Web Sites

Multidisciplinary Center for Earthquake Engineering Research:
http://mceer.buffalo.edu

Bogazici University, Kandilli Observatory and Earthquake Research Institute:
http://www.boun. edu.tr/graduate sciences_and_engineering/kandilli_observatory_earthquake_research_ institute.html

Earthquake Disaster Mitigation Research Center:
http://www.edm.bosai.go.jp/english.htm

warranted concerning scene brightness. [B1] is markedly brighter than [B2], and although the 'after' scenes are also comparatively bright, little difference is evident between them. This variation may reflect the temporal interval between data acquisition. For [B1,B2] this is approximately 1 month, whereas for [A1,A2] it is just one day. Changes in ambient conditions, such as atmospheric diffusion, may vary considerably over these time spans.

The correlation images in Figure 5e-h depict the permutation with optimal distinguishing capability [B2,A1], together with the baseline case [A1,A2]. For visualization purposes, the data was thresholded at $0.2 < cor < 0.6$, with intermediate values displayed across an 8-bit (a 0-255) range using a linear contrast stretch. Block correlation statistics were further classified into categories of: low ($0 < bk\_cor < 0.2$); moderate ($0.2 < bk\_cor < 0.4$); high ($0.4 < bk\_cor < 0.6$); and very high ($bk\_cor > 0.6$). Low correlation values (see annotation C1) are evident throughout central areas of Golcuk. Comparison with the damage map (Figure 3b) suggests correspondence with high levels of building collapse. Low correlation outside the urban area is concentrated around Izmit Bay (C2), where changing conditions of the water surface causes pronounced differences in backscatter. In a general sense, block correlation levels within central Golcuk are consistently higher in the baseline scenes, compared with the 'before'-'after' permutations. As such, it appears that earthquake related changes exceed natural levels of variation.

Figure 5i-j shows the 'before'-'after' and baseline coherence images for Golcuk. Results suggest that low coherence is present throughout both urban and rural areas. The apparent increase in coherence levels throughout the baseline scene coh[A1,A2], compared with coh[B2,A1], probably reflects the reduced temporal interval between data acquisition.

Damage Profiles

Figure 6 presents quantitative damage profiles for the optical and SAR datasets. The panchromatic imagery yields an encouraging trend between difference and damage state (Figure 6a). As the percentage of collapsed buildings increases from class A to E, the offset between 'before' and 'after' scenes is increasingly pronounced. For category A, where 0-6.25% of structures collapsed, values tend towards zero. In contrast, values for category E, where 50-100% collapsed, reach Dif[B1,A1] ~ -50DN. The positive difference of Dif[B1,A1] ~ 80DN exhibited by the 'Sunk' category demonstrates the ability of damage profiles to distinguish between various types of earthquake-related damage. SPOT correlation profiles (Figure 6b-c) follow a similar tendency towards decreasing levels of correlation as the degree of building damage increases from class A-E. Together, these trends suggest that the transition from standing structures ('before') to debris piles ('after') produces a distinct signature throughout visible regions of the spectrum.

The SAR intensity difference profile for dif[B2,A1] in Figure 6d exhibits an upward trend, as the percentage of collapsed structures increases with the transition from category A to E. In absolute terms,

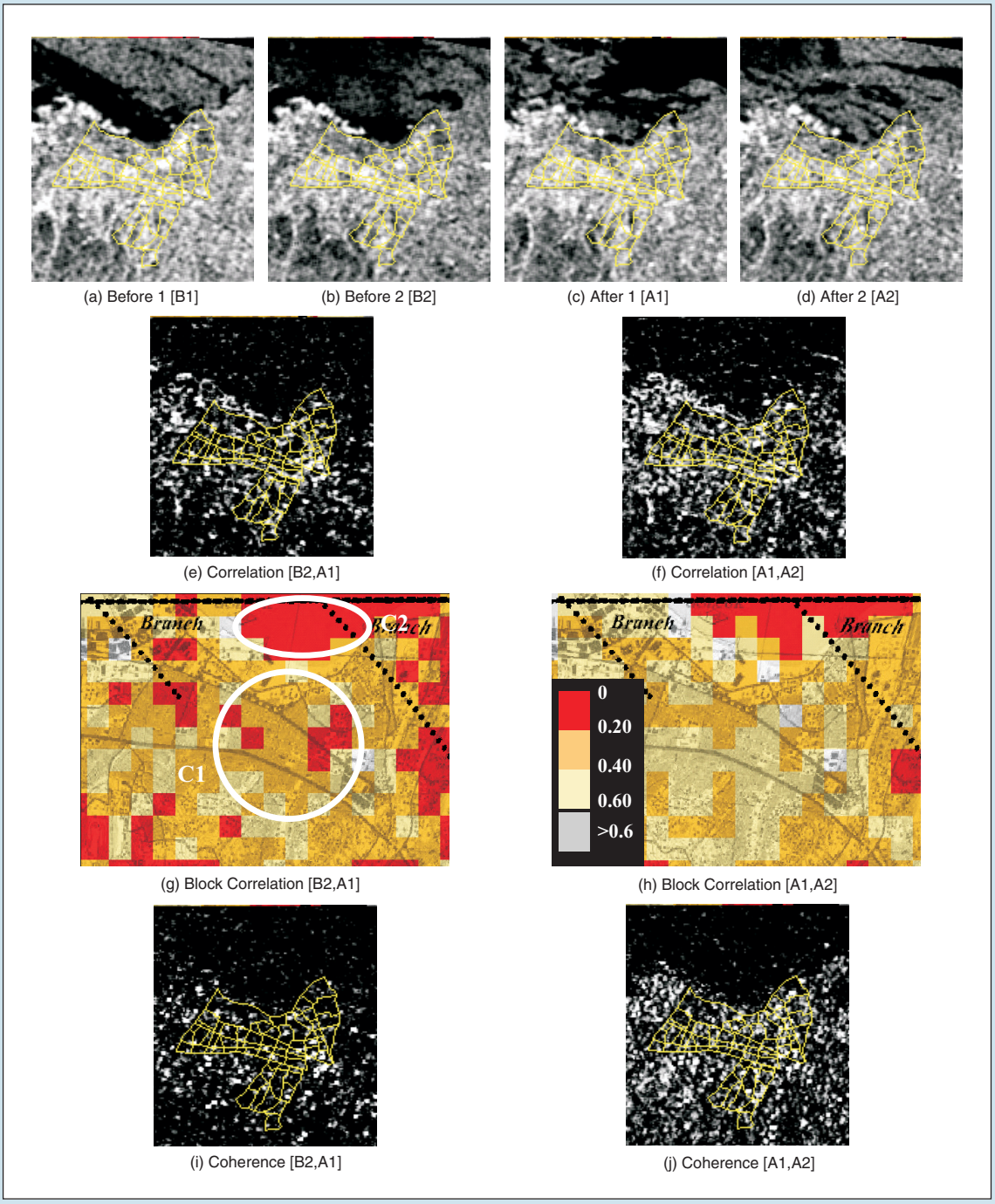

■ Figure 5. SAR ERS Coverage of Golcuk, Showing (a-b) 'Before' Images; (c-d) 'After' Images; (e) Sliding Window-Based Correlation between Images 'Before 2' and 'After 1' [B2.A1]; (f) Correlation between Baseline Images 'After 1' and 'After 2' [A1,A2]; (g-h) Block Correlation for [B2,A1] and [A1.A2]; and (i-j) Coherence for [B2,A1] and [A1,A2]

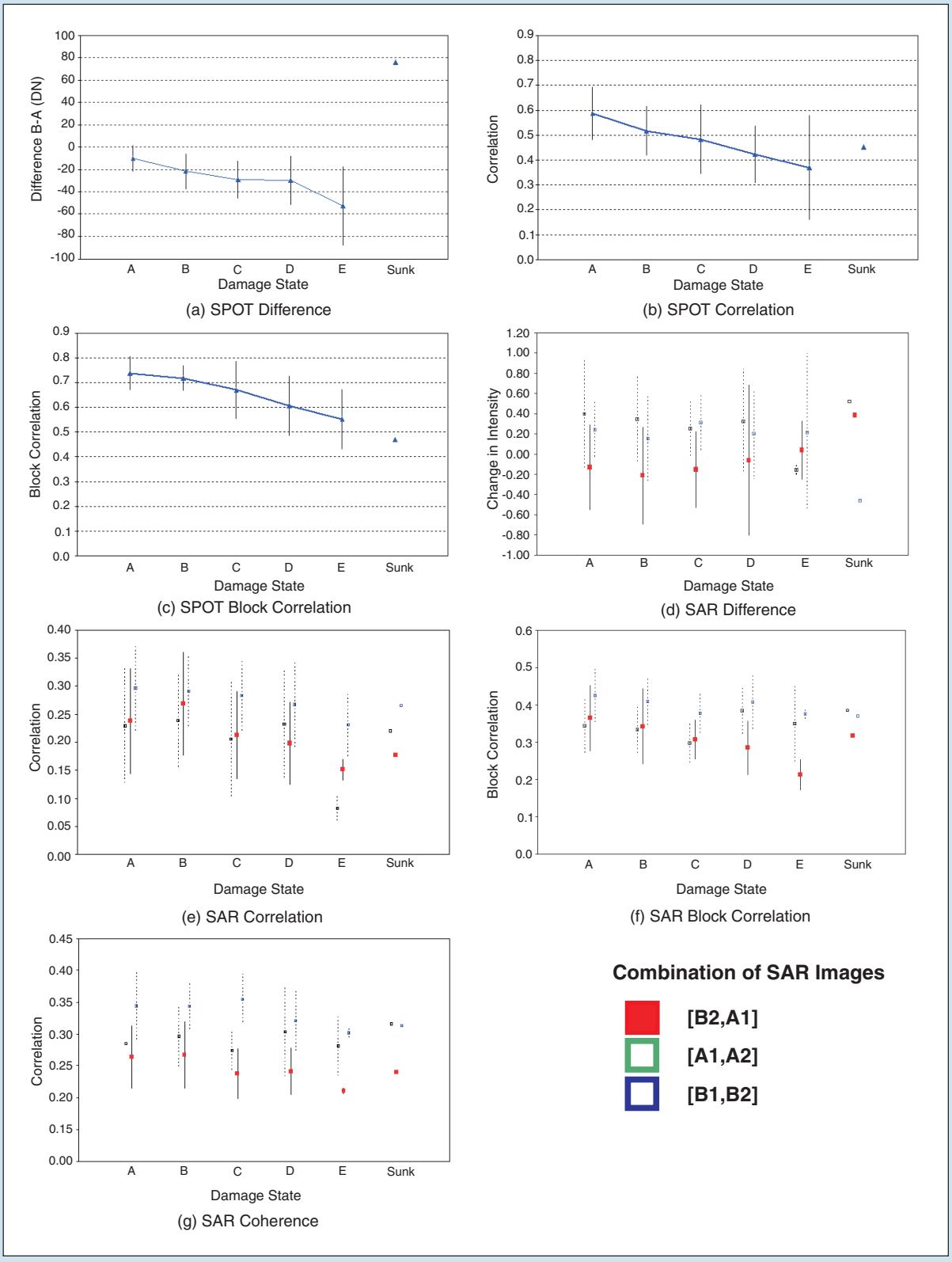

■ Figure 6. Damage Profiles for Golcuk, Showing How Values Recorded in the 70 Sample Zones for Each Index of Change Varies with the Extent of Collapsed Buildings (A-E); Error Bars Represent 1 Standard Deviation about the Mean

the change in intensity is negative for zones experiencing minor damage, and tends towards zero as the percentage of collapsed structures reaches a maximum for class E. These values are somewhat contrary to expectation. In theory, reduced backscatter accompanying building collapse should yield a positive difference, as the 'after' scene is darker than 'before'. However, visual inspection of the constituent intensity images (Figure 4a-b) suggests that the negative values for A-D arise because backscatter is higher throughout the 'after' scene. This baseline offset is independent of earthquake damage, and is instead attributable to varied conditions at the times of imaging, due to weather effects and possibly look angle. Values for class E tend towards zero because the offset due to building collapse is largely mitigated by a universal reduction in backscatter. Overall, these results indicate that intensity difference has limited predictive capability for building damage.

The sliding window and block statistical approaches (Figure 6e-f) reveal a tendency for mean correlation to decrease as building damage escalates. In contrast, the baseline scenarios cor [B1,B2] and cor[A1,A2] lack any obvious trend with the classes A-E. The coherence profiles in Figure 6g exhibit a similar pattern of response. These results suggest that correlation and coherence measures provide a useful association between temporal changes on remote sensing imagery and urban building damage.

Conclusion and Further Research

The visual comparison of optical and SAR remote sensing coverage obtained 'before' and 'after' the 1999 Marmara earthquake, reveals distinct changes in return. Following the earthquake event, surface reflectance on the SPOT coverage increases within the urban center, where numerous buildings collapsed. This suggests that debris piles associated with collapsed structures exhibit a higher return than the original standing structure. Trends are more difficult to discern from simple inspection of the SAR coverage, with temporal changes dominated by scene-wide variations in return. However, from examining derived correlation images, low correlation, indicative of change due to building collapse, is evident throughout central areas of Golcuk.

The preliminary SPOT and ERS change detection algorithms successfully distinguish between spatial variations in the extent of catastrophic building damage observed in Golcuk. For the SPOT panchromatic data, simple subtraction and correlation profiles vary with observed damage. While SAR correlation indices also distinguished trends in the density of collapsed buildings, the subtraction profile was instead dominated by a large radiometric offset between the 'before' and 'after' scenes.

The change detection techniques presented here successfully employ remote sensing technologies to detect and determine the extent of urban building damage. The 24/7, all weather imaging capabilities of SAR sensors offer resilience in the

event of an earthquake occurring at night or in cloudy conditions. Together with the easily interpreted visual representation provided by optical coverage, these advanced technologies promise rapid and accurate post-earthquake damage detection assessment.

Acknowledgements

The authors gratefully acknowledge the financial support of the National Science Foundation (CMS-0085273) and the Multidisciplinary Center for Earthquake Engineering Research (NSF Award Number EEC-9701471) for this study. The help and support of Professor Fumio Yamazaki, from the University of Tokyo and Dr. Masashi Matsuoka of the Earthquake Disaster Mitigation Research Center (EDM) is acknowledged. Appreciation is also extended to: the Architectural Institute of Japan (AIJ), in joint effort with the Japanese Geotechnical Institute (JGS), and the Japan Society of Civil Engineers (JSCE), for use of building damage observations from Golcuk, Turkey; the European Space Agency, for providing ERS SAR data; and NIK Insaat Ticaret Ltd. Istanbul, Turkey, for providing SPOT coverage of Golcuk.

References

Architectural Institute of Japan, (1999), *Report on the Damage Investigation of the 1999 Kocaeli Earthquake in Turkey*, AIJ,Tokyo, Japan.

Aoki, H., Matsuoka, M. and Yamazaki, F., (1998), "Characteristics of satellite SAR images in the damaged areas due to the Hyogoken-Nanbu earthquake," *Proceedings of the 1998 Asian Conference on Remote Sensing*, *http://www.gisdevelopment.net/aars/acrs/1998/ts3/ts3007.shtml.*

Chiroiu, L., Andre, G., Guillande, R. and Bahoken, F., (2002), "Earthquake damage assessment using high resolution satellite imagery," *Proceedings of the 7th National Conference on Earthquake Engineering*, Boston, MA.

Coburn, A., Halling, M.W. and Johnson, L., (1999), Personal Communication.

Earthquake Disaster Mitigation Research Center, (2000), *Report on the Kocaeli, Turkey Earthquake of August 17, 1999*, EDM Technical Report 6.

Eguchi, R.T., Houshmand, B., Huyck, C.K., Shinozuka, M. and Tralli, D.M., (1999), "A New Application for Remotely Sensed Data: Construction of Building Inventories Using Synthetic Aperture Radar Technology," *Research Progress and Accomplishments, 1997-1999,* MCEER-99-SP01, Multidisciplinary Center for Earthquake Engineering Research, University at Buffalo.

Eguchi, R., Huyck, C., Houshmand, B., Mansouri, B., Shinozuka, M., Yamazaki, F. and Matsuoka, M., (2000a), "The Marmara Earthquake: A View from Space," *Section 10: The Marmara, Turkey Earthquake of August 17, 1999: Reconnaissance Report,* Technical Report MCEER-00-0001, Multidisciplinary Center for Earthquake Engineering Research, University at Buffalo.

Eguchi, R.T., Huyck, C.K., Houshmand, B., Shinozuka, M., Yamazaki, F., Matsuoka, M. and Ulgen, S., (2000b), "The Marmara Turkey Earthquake: Using Advanced Technology to Conduct Earthquake Reconnaissance," *Research Progress and Accomplishments, 1999-2000,* MCEER-00-SP01, Multidisciplinary Center for Earthquake Engineering Research, University at Buffalo.

References (Cont'd)

Eguchi, R.T., Huyck, C.K., Houshmand, B., Mansouri, B., Shinozuka, M., Yamazaki, F. and Matsuoka, M., (2000c), "The Marmara Earthquake: A View from Space," *Proceedings of the First MCEER Workshop on Mitigation of Earthquake Disaster by Advanced Technologies, Los Angeles, CA*. MCEER-00-0009, Multidisciplinary Center for Earthquake Engineering Research, University at Buffalo, pp. 181-200.

Huyck, C.K. and Adams, B.J., (2002), *Emergency Response in the Wake of World Trade Center Attack: The Remote Sensing Perspective*, MCEER-02-SP05, Multidisciplinary Center for Earthquake Engineering Research, University at Buffalo.

Huyck, C.K., Eguchi R.T. and Houshmand, B., (2002), *Advanced Technologies for Loss Estimation: Bare-Earth Algorithms for Use with SAR and LIDAR Digital Elevation Models*, MCEER-02-0004, Multidisciplinary Center for Earthquake Engineering Research, University at Buffalo.

Huyck, C.K., Mansouri B., Eguchi R.T., Houshmand, B., Castner L.L. and Shinozuka, M., (2002), "Earthquake Damage Detection Algorithms Using Optical and ERS-SAR Satellite Data - Application to the August 17, 1999 Marmara, Turkey Earthquake," *Proceedings of the 7th National Conference on Earthquake Engineering*, Boston, MA.

Lettis, W., Bachhuber, J. and Witter, R., (2000), "Surface fault rupture," Youd, T.l., Bardet., J and Bray, J.D. (eds.) *Earthquake Spectra Supplement A to Volume 16: Kocaeli, Turkey, Earthquake of August 17, 1999 Reconnaissance Report*, pp.11-53.

Mansouri, B., Huyck, C.K., Houshmand, B., Castner, L., Shinozuka, M. and Eguchi, R.T., (2002), "Remote sensing post-earthquake damage detection in urban areas," *Proceedings of the Joint Workshop on US-Japan Cooperative Research in Urban Earthquake Disaster Mitigation*, Los Angeles, CA.

Matsuoka, M. and Yamazaki, F., (1998), "Identification of damaged areas due to the 1995 Hyogoken-Nanbu earthquake using satellite optical images," *Proceedings of the 1998 Asian Conference on Remote Sensing*, *http://www.gisdevelopment.net/aars/acrs/1998/ps2/ps2009.shtml.*

Matsuoka, M. and Yamazaki, F., (2000), "Satellite remote sensing of damage areas due to the 1995 Kobe earthquake," Toki, K. (ed.), *Confronting Urban Earthquakes, Report of Fundamental Research on the Mitigation of Urban Disasters Caused by Near-field Earthquakes*, pp. 259-262.

Mitomi, H., Matsuoka, M. and Yamazaki, F., (2002), "Application of automated damage detection of buildings by panchromatic television images," *Proceedings of the 7th National Conference on Earthquake Engineering*, Boston, MA.

Rathje, E., (2000), "Strong Ground Motions and Site Effects," in Youd, T.L., Bardet, J.P. and Bray, J.D. (eds.), *Earthquake Spectra Supplement A to Volume 16: Kocaeli, Turkey Earthquake of August 17, 1999 Reconnaissance Report,* pp. 65-96.

Saito, K and Spence, R., (2003), "Using high-resolution satellite images for post earthquake building damage assessment: A study following the 26.1.01 Gujurat earthquake," *Earthquake Spectra*, (in press).

Tralli, D.M., (2001), *Assessment of Advanced Technologies for Loss Estimation*, MCEER-00-SP02, Multidisciplinary Center for Earthquake Engineering Research, University at Buffalo, on CD-ROM.

Wesnousky, S. G., Seeber, L., Rockwell, T. K., Thakur, V., Briggs, R., Kumar, S. and Ragona, D., (2001), "Eight Days in Bhuj: Field report bearing on surface rupture and genesis of the January 26, 2001 Republic Day earthquake of India," *Seismological Research Letters*, Vol. 72, pp. 514-524.

Yusuf, Y., Matsuoka, M. and Yamazaki, F., (2002), "Detection of building damage due to the 2001 Gujurat, India earthquake, using satellite remote sensing," *Proceedings of the 7th National Conference on Earthquake Engineering*, Boston, MA.

Resilient Community Recovery: Improving Recovery Through Comprehensive Modeling

by Stephanie E. Chang and Scott B. Miles

Research Objectives

The objective of this research is to develop an innovative, comprehensive model of urban recovery from earthquake disasters. The study aims to develop a robust conceptual model to frame future research and data reconnaissance, and to build user-friendly geographic information system tools for assisting community planning and preparation.

Understanding urban disaster recovery remains a significant challenge. No comprehensive framework or model of disaster recovery currently exists in the literature. Many studies touch upon facets of recovery, but none take it as their analytical focus. For example, in recent years, researchers have been paying increasing attention to modeling the direct and indirect economic impacts that earthquakes cause to communities (West and Lenze, 1994; Brookshire et al., 1997; Rose et al., 1997; Gordon et al., 1998; Okuyama et al., 2000; Cho et al., 2001; Chang et al., 2002). However, very little research has been conducted on how recovery proceeds over time, on the spatial dimensions of recovery, and on the interdependencies between sectors in the disaster recovery process. Moreover, a comprehensive model of recovery is needed in order to evaluate the potential consequences of decisions that affect disaster losses and recovery timepaths.

By addressing these issues, this study represents an initial attempt at developing a new generation of disaster loss models. This paper describes work completed to date on conceptual framework for disaster recovery, a prototype recovery model, and a test application for the 1995 Kobe earthquake, and associated sensitivity analysis. Further details on the study can be found in Chang and Miles (forthcoming).

This study is guided by numerous theoretical and empirical studies of how cities and their inhabitants recover from disasters. This literature suggests, for example, that marginal groups may not only be especially vulnerable to suffering losses as a result of earthquakes, but they are likely to have more difficulty in recovering from urban disasters (Hewitt, 1997; Blaikie et al., 1994). They may have lesser access to insurance, loans, relief aid, or government bureaucracies and decision-making, or face shortages

Sponsors

National Science Foundation, Earthquake Engineering Research Centers Program

Research Team

***Stephanie E. Chang**, Research Assistant Professor and **Scott B. Miles**, Graduate Student, Department of Geography, University of Washington*

Previous Summaries

***1999-2000**: Chang et al., http://mceer.buffalo.edu/publications/resaccom/9900/chapter1.pdf.*

***1997-1999**: Tierney, et al., http://mceer.buffalo.edu/publications/resaccom/9799/ch2tiern.pdf.*

Links to Current Research

This project builds on MCEER's research on loss estimation methodologies (M. Shinozuka, S. Chang, A. Rose) by extending them in the direction of modeling recovery processes. The project contributes to MCEER's goal of building user-friendly decision-support systems for improving community resilience to earthquake disasters.

in low-income housing (e.g., Bolin and Bolton, 1986; Bolin and Stanford, 1991; Bolin, 1993; Hirayama, 2000). Spatial effects have also been found to be important in disaster recovery. Decentralization of population and economic activity may be accelerated (Chang, 2001). Business losses are correlated with disaster severity in the neighborhood (Tierney and Dahlhamer, 1998). Retail and other locally-oriented businesses generally lag in recovery (Alesch and Holly, 1998; Kroll et al., 1991; Chang and Falit-Baiamonte, forthcoming).

Conceptual Model

The first step in addressing the need for a comprehensive community recovery model is the development of a rigorous and robust conceptual model. The conceptual model was built up by characterizing the attributes and behaviors of economic agents within a community, such as households and businesses, and describing relationships between agents themselves and relationships with their environment, such as buildings of residence and transportation networks (Figure 1). While the recovery model is designed to *measure* recovery at the community and neighborhood levels, it *models* recovery at the scale of the individual business and household.

The conceptual model focuses on the influence of agents' environments on their recovery processes. Specifically, it describes five principal types of recovery influences and processes that are useful in organizing and explaining the relationships expressed by the conceptual model. The five types are: (1) dynamic processes; (2) agent-attribute influences; (3) interaction effects; (4) spatial feedbacks; and (5) policy effects.

Dynamic processes refer here to changes over time. In true dynamic processes, a variable's current level depends upon its level in a previous period. What can be called pseudo-dynamic processes – changes over time that can proceed independently of variable levels in previous periods – also play an important role. Agent-attribute effects describe how the characteristics of a particular business or household may influence their respective recovery trajectory. For example, the demand for a business's product depends on attributes, such as whether it is in a locally-oriented or export-oriented sector and whether it is a large or small business. In particular, if locally-oriented, then the recovery of nearby households in the neighborhood and community matters, as these

Potential users of this research include lifeline organizations, emergency managers, urban planners, and local and federal government agencies concerned with facilitating disaster recovery. End users can use the tools developed as part of this research to explore and analyze strategies for reducing recovery time and any consequences related to failure of critical infrastructure within their community or organization.

are its customers. Interaction effects describe how the relationship between different agents or elements in the system influences their recovery timepath. For example, water availability is influenced by the survival of the electric power and transportation systems. Electric power may be needed to drive pumps that enable the water system to function; transportation disruption can impede the ability of the water utility to make repairs in a timely manner. Considering spatial feedbacks, households and businesses do not exist aspatially, but are affected by conditions in their specific neighborhoods, whether in terms of water availability, transportation conditions, or local consumer demand. Thus, the same type of household or business may recover differently depending upon which neighborhood it is located. Policy or decision effects are community-level decisions made either before the event, such as emergency planning and mitigation measures, or afterwards, such as recovery policy decisions.

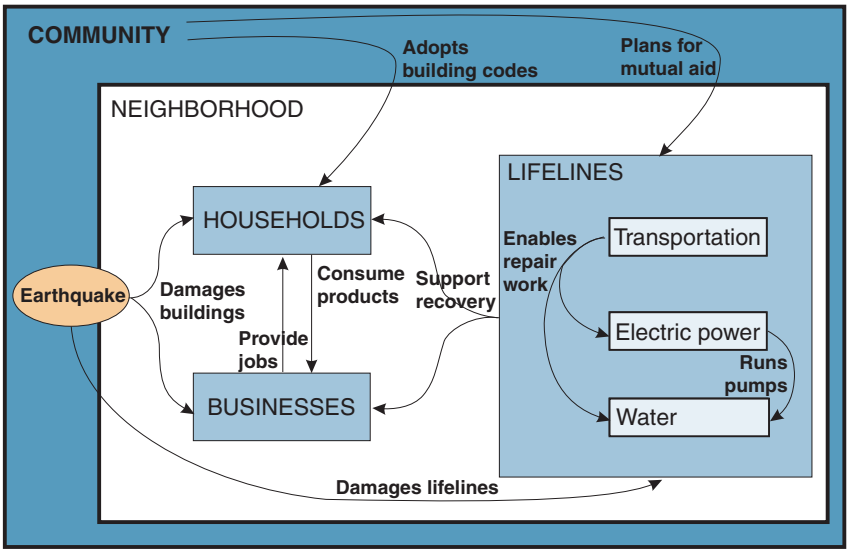

Figure 1. Overview of Disaster Recovery Conceptual Model

Computer Model

For the purposes of proof of concept and prototype development, a simple numerical framework was used in implementing the many relationships of the conceptual model. The prototype recovery model was implemented in the Matlab/Simulink software environment. The model framework takes the form of a series of simultaneous equations. Operationalizing the diverse relationships of the conceptual model was done by specifying each model variable as a relative index that varies between 0 and 1, rather than real world metrics, such as dollars. The approach taken is useful for integrating many metrics that would otherwise be difficult to mathematically combine. With each variable varying between 0 and 1, it was relatively simple to create basic first-order algebraic equations based on the relationships described by the conceptual model.

The subset of model variables referred to in this paper is listed in Table 1. Model variables can be of five different types: (1) driving variables, (2) agent attributes, (3) decision/policy variables, (4) intermediate variables, and (5) recovery indicators (output). Driving variables combine to serve as the temporal engine of a simulation by relating a particular variable (e.g., health recovery) to time with some restoration curve. For simplicity all restoration curves were assumed to be linear curves having some assumed or, potentially, calibrated slope. These slope values are modified within the model equa-

tions based on input variable values (e.g., for *MUT*, *CAP*, and *PRTY*). Driving variables are required as part of the implementation because none of the model inputs are explicit time series data.

To illustrate the algorithmic framework, which is comprised of 32 unique equations, the relationships used to calculate the recovery level (0, 0.25, 0.50, 0.75, or 1) of a particular household and the likelihood of the household moving to the next recovery level are expressed by Equations 1 and 2, respectively.

$$REC_b(t) = \begin{cases} 0.25((PT_b(t) \geq x) + RECH_b(t-1)), & REC_b(t-1) < 1 \\ 1, & REC_b(t-1) = 1 \end{cases} \quad (1)$$

$$PT_b(t) = \begin{cases} 0 & , if\ LEAV_b(t) = 1, \\ & REC_b(t-1) > 0 \\ 0.333\,(CRIT_c + HLTH_b + SHEL_c) & , if\ REC_b(t-1) = 0 \\ 0.2\sqrt{EMPL_c}\,(\sqrt{BL_b} + LL_c + CRIT_c + HLTH_b + SHEL_c) & , if\ REC_b(t-1) = 0.25 \\ 0.25\,EMPL_c\,(BL_b + LL_c + HLTH_b + (1 - DEBT_b)) & , if\ REC_b(t-1) = 0.5 \\ 0.333\,EMPL_b{}^2\,(BL_b{}^2 + LL_c{}^2 + (1 - DEBT_b)^2 & , if\ REC_b(t-1) = 0.75 \\ 1 & , if\ REC_b(t-1) = 1.0 \end{cases} \quad (2)$$

Prototype Simulation of Kobe Recovery

In order to begin to evaluate the usability, effectiveness, and behavior of the community recovery model, we chose to simulate the recovery of the city of Kobe after the catastrophic 1995 M = 6.9 earthquake disaster. For purposes of this analysis, Kobe was divided into four simulation zones (Figure 2): downtown (zone A1), the older urban core (A), the newer urban core (B), and suburban areas (C). These zones aggregated from census blocks and are defined on the

Table1. Selected Variable Definitions for Community Recovery Model

BLh	= availability of building for use, households
BMIT	= pre-earthquake structural mitigation
CAP	= recovery capacity of community (proxy for integration, consensus)
CMIT	= pre-earthquake mitigation to critical facilities
CRIT	= availability of critical facilities
DAID	= driving variable: aid availability status
DBLb	= driving variable: building repair status, businesses
DBLh	= driving variable: building repair status, households
DCRIT	= driving variable: critical facility availability
DEBT	= extent of indebtedness
DEL	= driving variable: electricity availability
DHLTH	= driving variable: health restoration curve
DINS	= driving variable: availability of insurance
DTRNS	= default transportation accessibility
DWAT	= default water availability
EMIT	= pre-earthquake mitigation to electric power system
EMPL	= availability of employment/income
INC	= income group of household
LEAV	= status of household leaving region
LL	= overall lifeline availability status
MUT	= provision for mutual aid in restoration plan
PLAN	= availability of restoration and recovery plan
PRTY	= restoration priority accorded to neighborhood
PT	= probability of transition to next higher recovery level
RECh	= household economic recovery level
SECT	= type of business sector
SHEL	= availability of temporary shelter
SIZE	= business size
STH	= reliance on short-term housing provision in recovery plan
TMIT	= pre-earthquake mitigation to transportation system
WALT	= provision for alternate water sources (water trucks) in plan
WMIT	= pre-earthquake mitigation to water system

Notes: Agent attributes in **bold**. Decision variables in **bold underline**. Driving variables in ***bold italics***. Recovery indicators in *italic underline*.

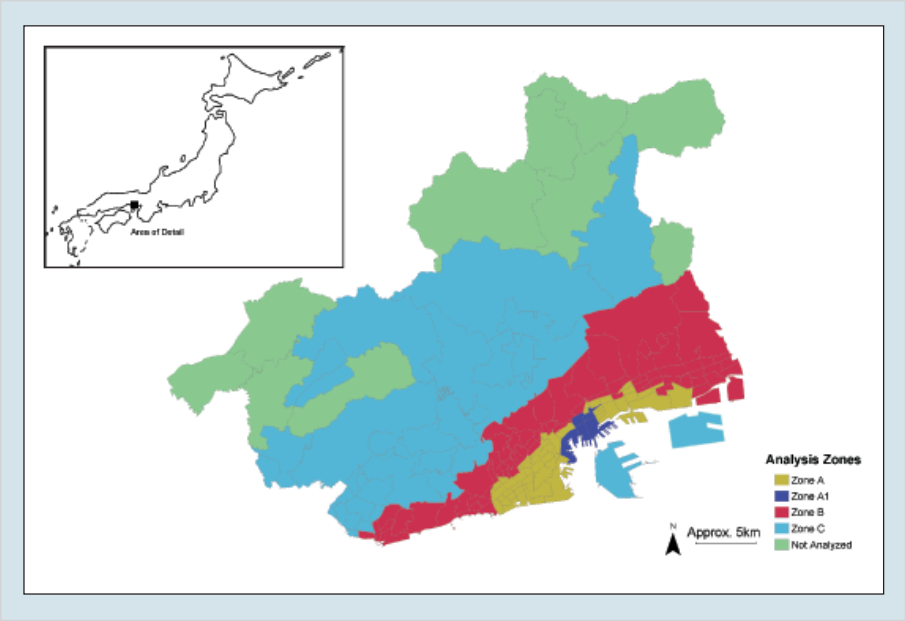

Figure 2. Analysis Zones Comprising Kobe, Japan, Study Area

"The holistic approach described in this paper demonstrates the complex impacts of mitigation, response, and recovery decisions."

basis of demographic, housing, and economic data (see Chang, 2001). In each zone, 100 households and 100 businesses are simulated, each of which can be interpreted as representing a group of similar individual agents.

To the extent possible, empirical data from the Kobe earthquake were used for simulation and calibration. The application required specifying three different groups of input variables: decision/policy variables, demographics (i.e., agent attributes), and the intensity of the earthquake's effects. The decision variables, such as pre-earthquake mitigation to the water supply system, are binary (yes/no) and apply to the entire city of Kobe. This constraint is an obvious simplification of reality. For example, some sections of a water pipeline may have been retrofitted, while other sections have not. The values determined for each of the nine decision variables are listed in Table 2.

Demographic variables are the attributes of each modeled household and business. For households, the demographic variables are relative income level (i.e., high, medium or low) and whether mitigation measures have been taken to improve the resiliency of their residence. For business agents, the demographic variables are relative business size (i.e., small or large), business sector (i.e., export-oriented or local business), and whether mitigation measures have been taken. Data for each of the 4 zones on the distribution of population and businesses according to these demographic groups were derived from census and other statistical publications by the

Table 2. Decision Variable Values for Kobe Application

MUT	CAP	PLAN	STH	
Yes	No	No	Yes	
WALT	**WMIT**	**TMIT**	**EMIT**	**CMIT**
Yes	No	No	No	No

City of Kobe. For both businesses and residences, buildings were classified into "mitigated" / "unmitigated" (better or worse performance) according to their construction vintage. The demographic data for households are shown in Table 3.

Ground motion input for each analysis zone was based on data on Japan Meteorological Association (JMA) intensity level and peak ground acceleration (PGA) (Bardet et al., 1995; EQE, 1995). In the prototype model, seismic intensity is represented by a single normalized value for each zone. This requires spatial aggregation over a wide range of earthquake intensities.

The Kobe earthquake simulation using the prototype model was intended as a first-order validation exercise. Simulation of the Kobe earthquake was performed for a time series of 260 weeks (5 years). Results, while less satisfactory than an earlier test application of the model that used a hypothetical input scenario (Chang and Miles, forthcoming), are instructive for future research directions. For example, one unexpected result was the prediction that no households would leave the region and no businesses would fail. This indicates the need to reexamine these elements of the model.

Figure 3 shows the overall simulated recovery of Kobe including city-wide recovery of households, businesses, buildings, and lifeline network. This figure was constructed by averaging the recovery value for each individual agent (i.e., household or business) across the entire simulation population for each time step. The figure shows that not all households and businesses reached a recovery level of one (i.e., complete recovery), even though no agents failed or left Kobe. The business and household recovery levels reached a plateau after a timeframe of about 55 and 140 weeks, respectively. Overall, lifeline recovery did reach a final value of one after 50 weeks. The general prediction that business and household recovery lags significantly behind lifeline recovery is reasonable. Building restoration was less realistic, only reaching a recovery level of 0.5 after 5 years.

Figure 4 summarizes household recovery across the four analysis zones. Generally speaking, the model is able to replicate the spatial disparities in recovery that were observed after the Kobe earthquake, wherein older neighborhoods lagged newer areas. This derives from both earthquake intensity and household and business demographics. The zones that recovered the slowest and to the lowest final levels of recovery are Zones A and A1, which both had a JMA intensity of 7. The zone that recovered most quickly and to the highest level of recovery was Zone C, which experienced the lowest earthquake intensity. The difference between Zones

■ Table 3. Household Demographic Data by Kobe Zone

Zone A1		Buildings	
		Unmitigated	Mitigated
Income	Low	57%	0%
	Middle	8%	32%
	High	0%	3%

Zone B		Buildings	
		Unmitigated	Mitigated
Income	Low	17%	0%
	Middle	40%	3%
	High	8%	32%

Zone A		Buildings	
		Unmitigated	Mitigated
Income	Low	72%	0%
	Middle	13%	10%
	High	0%	5%

Zone C		Buildings	
		Unmitigated	Mitigated
Income	Low	14%	0%
	Middle	36%	17%
	High	0%	33%

A1 and A can be partly explained by demographics. Zone A has 15% more low income households and 20% more households in old or unretrofitted buildings. Note, however, that these results also demonstrate a "plateau" effect. This derives from a shortcoming of the model, in which the driving variables themselves saturate after some amount of time and have no further influence on the simulation.

Sensitivity Analysis

Because of the large number of model variables and their interrelationships, the behavior of the model is complex. To explore this behavior, sensitivity analysis was conducted with reference to the Kobe simulation. The influence of decision and demographic variables was analyzed separately. In all cases, the basic approach consisted of analyzing each variable independently while holding the other variables constant. For example, to analyze the demographic variable *INC* (income) for households, the simulation was run once with all households assigned a relative income of "low" (a value of zero), with all other input variables retaining the baseline values, and again with all households being assigned a relative income of "high" (a value of 1). Similarly, to analyze the decision variables, the Kobe simulation (demographics) was first run once with all of the decision variables set to zero or "no" (i.e., zero capacity, no mutual aid agreement, no plan, etc.). The simulation was then run nine more times to look at the effect of changing each decision variable to one or "yes", with the other decision variables being set to zero (no). The opposite approach was also taken, where all variables were set to one and then the simulation run for each variable set to zero.

The numerous outputs from the sensitivity analysis do not facilitate concise presentation. To summa-

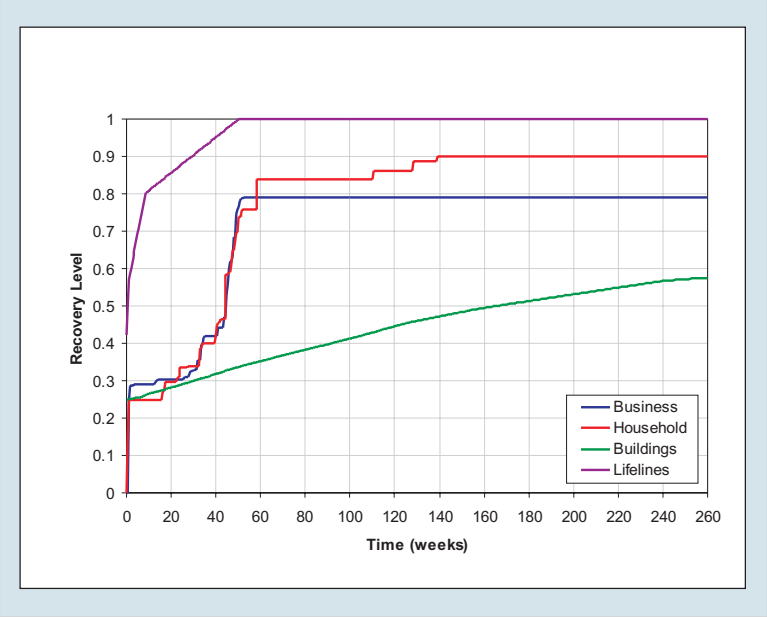

Figure 3. Overall Simulated Recovery of Kobe Using Prototype Model

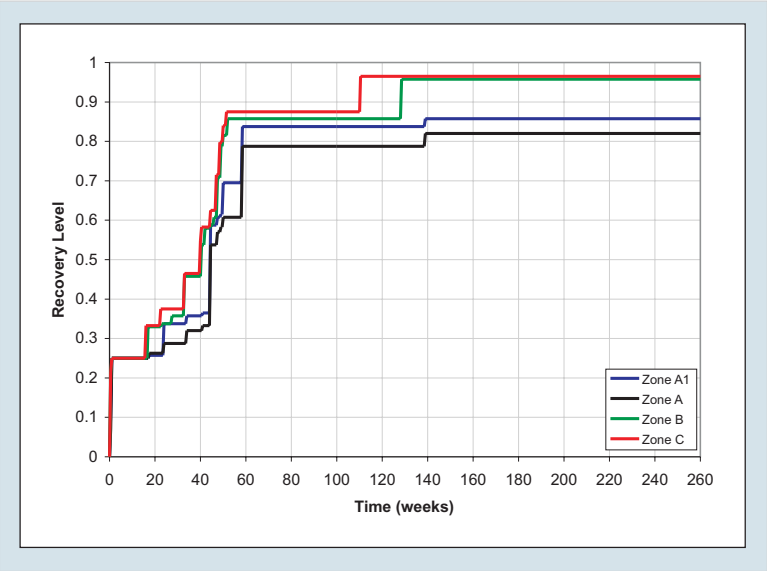

Figure 4. Simulated Recovery of Households by Zone for Kobe using Prototype Model

Table 4. Expectations of Simulation Behavior and Evaluation of Sensitivity Analysis

Business	Household	Expectations
X	✔	*A community with all new or retrofitted buildings (i.e., earthquake resistant) should recover more quickly than a community with all old buildings.
✔	✔	*A community with all high income households should recover more quickly than a community will all low income households.
✔	✔	*A community with all large businesses should recover more quickly than a community with all small businesses.
X	X	*A community with all export-oriented businesses should recover more quickly than a community with all local-oriented businesses.
X	X	All lifeline mitigations should hasten recovery times.
✔	✔	Mitigating transportation should hasten recovery more than mitigating other lifelines.
✔	✔	All planning and response measures should hasten recovery times.
✔	✔	Agents should be less likely to fail or leave as more mitigation and planning measures are taken.

* all else being equal; Note: ✔ = expectation met; X = expectation not met.

rize the results of the sensitivity analysis, Table 4 lists eight *a priori* expectations (i.e., design requirements) for the community recovery model. Listed with each is a general assessment of whether the particular expectation was met, with respect to simulated household and business recovery. For the most part, the sensitivity analysis demonstrated that the recovery model performs as expected, while highlighting several issues for refinement or modification.

Conclusions and Future Research

The work reported here represents the initial stages towards building a community recovery model and spatial decision support system. This effort is distinguished by its attempt to capture the complex interdependencies between sectors (households, businesses, and lifeline infrastructure), the relationships between geographic scales (agent, neighborhood, community), and recovery processes over time. This holistic approach demonstrates the complex impacts of mitigation, response, and recovery decisions. For example, it allows visualization of the disparities that may evolve across an urban area in the disaster recovery process. It illustrates how speeding up the restoration of lifeline systems has substantial recovery benefits across all sectors. It allows comparisons as to the relative effectiveness of various mitigation and preparedness activities for improving community resiliency.

As demonstrated in the prototype application and sensitivity analysis, further research is needed to improve the model itself and its usability for response and recovery decision-support. More detailed validation of the model in the Kobe context is needed. Refinements are needed to resolve data gaps between the types of data required by the model and the types that are available following an actual disaster. The input of stakeholders and

potential end users, such as city planners and emergency managers, will be solicited. This will help to further evaluate the usability of the recovery model, identify additional decision variables, and determine requirements for a decision support system.

Model algorithms will also be refined. This effort is greatly facilitated by the implementation-independent conceptual model and modular computer model design, which permits modification of specific algorithms without requiring changes to the entire model. Specific changes to the algorithms will include rethinking the implementation of the driving variables to simplify their calibration and prevent the model from effectively stalling after a certain time. In addition, work will be continued to incorporate randomness within the model and make it more explicitly probabilistic. The recovery model will be improved to model household migration within the community (i.e., from neighborhood to neighborhood). The decision to migrate can be based on variables such as relative recovery levels of neighborhoods, location, access to financial resources, building damage, and reconstruction status. To facilitate incorporating migration, the community recovery model will be integrated within commercial geographic information systems (GIS) software. GIS integration will address the goal of building a spatial decision support system for improving community resilience to earthquakes.

Acknowledgments

This research was primarily supported by the Earthquake Engineering Research Centers Program of the National Science Foundation, under award number EEC-9701471 to the Multidisciplinary Center for Earthquake Engineering Research. This support is gratefully acknowledged.

References

Alesch, D.J. and Holly, J.N., (1998), "Small Business Failure, Survival, and Recovery: Lessons from the January 1994 Northridge Earthquake," *NEHRP Conference and Workshop on Research on the Northridge, California Earthquake of January 17, 1994*, CUREe, Richmond, California.

Bardet, J.P., Oka, F., Sugito, M. and Yashima, A, (1995), "The Great Hanshin Earthquake Disaster, " *The1995 South Hyogo Prefecture Earthquake, Preliminary Investigation Report*, Civil Engineering Department, University of Southern California, Los Angeles, California, and Civil Engineering Department, Gifu University, Gifu, Japan.

Blaikie, P., Cannon,T., Davis, I. and Wisner, B., (1994), *At Risk: Natural Hazards, People's Vulnerability, and Disasters*, Rutledge, New York.

Bolin, R., (1993), *Household and Community Recovery After Earthquakes*, Institute of Behavioral Science, University of Colorado, Boulder.

Bolin, R. and Bolton, P., (1986), *Race, Religion, and Ethnicity in Disaster Recovery*, Institute of Behavioral Science, University of Colorado, Boulder.

References (Cont'd)

Bolin, R. and Stanford, L., (1991), "Shelter, Housing and Recovery: A Comparison of U.S. Disasters," *Disasters*, Vol. 15, No. 1, pp. 24-34.

Brookshire, D.S., Chang, S.E., Cochrane, H., Olson, R.A., Rose, A. and Steenson, J., (1997), "Direct and Indirect Economic Losses from Earthquake Damage," *Earthquake Spectra*, Vol. 13, No. 4, pp. 683-701.

Chang, S.E., (2001), "Structural Change in Urban Economies: Recovery and Long-Term Impacts in the 1995 Kobe Earthquake," *The Kokumin Keizai Zasshi (Journal of Economics & Business Administration)*, Vol. 183, No. 1, pp. 47-66.

Chang, S.E. and Falit-Baiamonte, A., (forthcoming), "Disaster Vulnerability of Businesses in the 2001 Nisqually Earthquake," *Environmental Hazards*.

Chang, S.E. and Miles, S.B, (forthcoming), "The Dynamics of Recovery: A Framework." Y. Okuyama and Chang, S.E., (eds.), *Modeling the Spatial Economic Impact of Disasters*, Springer-Verlag, in press.

Chang, S.E., Svekla, W.D. and Shinozuka, M., (2002), "Linking Infrastructure and Urban Economy: Simulation of Water Disruption Impacts in Earthquakes," *Environment and Planning B*, Vol. 29, No. 2, pp. 281-301.

Cho, S., Gordon, P., Moore II, J.E., Richardson, H.W., Shinozuka, M. and Chang, S.E., (2001), "Integrating Transportation Network and Regional Economic Models to Estimate the Costs of a Large Urban Earthquake," *Journal of Regional Science,* Vol. 41, No. 1, pp. 39-65.

EQE (1995), *The January 17, 1995 Kobe Earthquake,* EQE Disaster Report, *http://www.eqe.com/publications/kobe/kobe.htm.*

Gordon, P., Richardson, H.W. and Davis, B., (1998), "Transport-Related Impacts of the Northridge Earthquake," *Journal of Transportation and Statistics*, Vol. 1, No. 2, pp. 21-36.

Hewitt, K., (1997), *Regions of Risk: A Geographical Introduction to Disasters*, Addison Wesley Longman Limited, Essex, England.

Hirayama, Y., (2000), "Collapse and Reconstruction: Housing Recovery Policy in Kobe after the Hanshin Great Earthquake," *Housing Studies*, Vol. 15, No. 1, pp.111-128.

Kroll, C. A., Landis, J. D., Shen, Q. and Stryker, S., (1991), *Economic Impacts of the Loma Prieta Earthquake: A Focus on Small Businesses*, Working Paper, University of California at Berkeley, U.C. Transportation Center and the Center for Real Estate and Urban Economics, Berkeley, CA, pp. 91-187.

Okuyama, Y., Hewings, G.J.D. and Sonis, M., (2000), "Sequential Interindustry Model (SIM) and Impact Analysis: Application for Measuring Economic Impact of Unscheduled Events," paper presented at the *47th North American Meetings of the Regional Science Association International*, Chicago, IL.

Rose, A., Benavides, J., Chang, S.E., Szczesniak, P. and Lim, D. (1997), "The Regional Economic Impact of an Earthquake: Direct and Indirect Effects of Electricity Lifeline Disruptions," *Journal of Regional Science*, Vol. 37, No. 3, pp. 437-458.

Tierney, K.J. and Dahlhamer, J.M. (1998), "Business Disruption, Preparedness and Recovery: Lessons from the Northridge Earthquake," *NEHRP Conference and Workshop on Research on the Northridge, California Earthquake of January 17, 1994*, CUREe, Richmond, California.

West, C.T. and Lenze, D.G., (1994), "Modeling the Regional Impact of Natural Disaster and Recovery: A General Framework and an Application to Hurricane Andrew," *International Regional Science Review*, Vol. 17, No. 2, pp. 121-150.

Understanding Sources of Economic Resiliency to Hazards: Modeling the Behavior of Lifeline Service Customers

by Adam Rose and Shu-Yi Liao

Research Objectives

This research refines computable general equilibrium (CGE) modeling for estimating business interruption losses from utilities lifeline disruptions and for estimating the reduction of losses (benefits) from mitigation. The behavioral content of CGE production functions is shown to be able to embody the adaptive behavior of lifeline utility service demand in particular and business operations in general. The individual response types (e.g., conservation, input substitution, import substitution) are linked to specific parameters of these functions. The research also develops algorithms for modifying the parameters on the basis of engineering simulations and empirical data. Also, economic resiliency is defined at the levels of the individual business and of the regional economy as a whole.

Sponsors

National Science Foundation, Earthquake Engineering Research Centers Program

Research Team

***Adam Rose**, Professor, Department of Geography, **Gauri Guha**, **Shu-Yi Liao**, (now an Economist, Demand Analysis Office, California Energy Commission) and **Bo Yang**, Graduate Students, Program in Energy, Environmental and Mineral Economics, Pennsylvania State University*

***Debo Oladosu**, Assistant Professor, School of Environmental Science, Engineering and Policy, Drexel University*

Recent studies indicate that utility lifeline supply disruptions can have significant impacts on regional economic activity in the aftermath of an earthquake, other natural disaster, or terrorist attack (see, e.g., Chang et al., 2000a; Bram et al., 2002). Even businesses that incur no physical damage are likely to have to curtail their production if they are cut off from their electricity, natural gas, water, or communication links. Moreover, such disruptions often set off a chain reaction of further production cutbacks among successive rounds of customers and suppliers that spread through the entire regional economy. Surveys following the Loma Prieta and Northridge earthquakes, Hurricane Andrew, and the 1993 Midwest floods indicated that business interruption losses stemming directly or indirectly from lifeline failures rivaled property damage in dollar terms (see Webb et al., 2000).

For many years, input-output (I-O) analysis was the most widely used modeling approach to the subject. Unfortunately, I-O is characterized by a linear and rigid response, almost devoid of behavioral content. In this approach, it is extremely difficult to incorporate input and import substitution or productivity changes (e.g., conservation). In essence, basic I-O analysis provides only an upper-bound estimate of the direct and indirect responses to a supply shortage (see, e.g., Rose et al., 1997). It is applicable to cases where markets are not working properly or where there are

Previous Summaries

1999-2000:
Chang et al., http://mceer.buffalo.edu/publications/resaccom/9900/Chapter1.pdf

1997-1999:
Tierney et al., http://mceer.buffalo.edu/publications/resaccom/9799/ch2tiern.pdf

serious constraints to responding to price signals. This approach is not capable of modeling most aspects of the adaptive response, or "resiliency" (e.g., Bruneau et al., 2002) to hazards at either the level of the individual firm or overall regional economy.

A promising alternative is computable general equilibrium (CGE) analysis, which is a behavioral model of producer and consumer responses to price signals in a multimarket context (Rose and Guha, 2003). CGE models are nonlinear and readily incorporate behavioral responses, such as input substitution and conservation, under explicit constraints (Shoven and Whalley, 1992). The problem in this context is that most CGE models are intended for long-run equilibrium analysis (e.g., they are based on generous input and import substitution elasticities, and assume the orderly functioning of markets and a costless adjustment to equilibrium). As such, CGE models without extensive refinements reflect only business as usual considerations and generally lead to over-resilient responses. Their results in effect represent a lower-bound estimate of economic impacts.

Work is progressing on improving the CGE methodology for application to supply disruptions of critical inputs in several ways (see also Rose and Liao, 2002). Advances include linking production function parameters to various types of producer adaptations in emergencies, developing algorithms for recalibrating production functions to empirical or simulation data, incorporating realistic supply elasticities to reflect short-run conditions, specifying operational definitions of individual business and regional macroeconomic resiliency, and decomposing partial and general equilibrium responses. We illustrate some of these contributions in a case study of the sectoral and regional adaptive responses and economic impacts of a disruption to the Portland Metropolitan Water System in the aftermath of a major earthquake. As such, our analysis provides a way of further utilizing the extensive empirical and simulation results on business interruption in the aftermath of earthquakes developed by other MCEER researchers (see, e.g., Tierney, 1997; Chang, 2001b).

Responses to Hazards in a CGE Context

The production side of the CGE model used in this paper is composed of a multi-layered, or multi-

The methods and applications from this research should be of broad usefulness. Utility managers can better identify their customers' needs. They can also better evaluate the benefits of mitigation efforts. Businesses can better evaluate their adaptive responses to lifeline disruptions. Emergency planners and high level government officials can evaluate alternative strategies for minimizing regional economic losses due to lifeline service disruptions.

tiered, constant elasticity of substitution (CES) production function for each sector. The CES has several advantages over more basic forms such as the Leontief (linear) or Cobb-Douglas (simple multiplicative) functions. It can incorporate a range of input substitution possibilities (not just the extreme zero and unitary values of the aforementioned functions). The multiple tiers allow for the use of different substitution elasticities for different pairs of inputs. The CES production function is normally applied to aggregate categories of major inputs of capital, labor, energy, and materials, with sub-aggregates possible for each (e.g., the energy aggregate is often decomposed by fuel type—electricity, oil, gas, and coal). Water is usually omitted or incorporated as one of the materials (intermediate goods producing) sectors. We explicitly separate water as a major aggregate in the top tier of the production function so that we can analyze the impacts of a water service disruption. For an application of this approach to electricity lifeline disruptions, the reader is referred to Rose et al., 2003.

CES Production Function

Our constant elasticity of substitution (CES) production function has the following nested form for five aggregate inputs capital, labor, energy, materials, and water:

$$Y = A_1\left(\alpha_1 A_{1W}\ W^{-\rho_1} + \beta_1 KLEM^{-\rho_1}\right)^{-1/\rho_1}$$

1st Tier (1a)

$$KLEM = A_2\left(\alpha_2 M^{-\rho_2} + \beta_2 KEL^{-\rho_2}\right)^{-1/\rho_2}$$

2nd Tier (1b)

$$KEL = A_3\left(\alpha_3 L^{-\rho_3} + \beta_3 KE^{-\rho_3}\right)^{-1/\rho_3}$$

3rd Tier (1c)

$$KE = A_4\left(\alpha_4 K^{-\rho_4} + \beta_4 E^{-\rho_4}\right)^{-1/\rho_4}$$

4th Tier (1d)

where A_i is the factor-neutral technology parameter, $A_i > 0$; A_{1W} is the water-specific technology parameter; α_i, β_i are the factor shares, $0 \le \alpha_i\ \beta_i \le 1$; σ_i is the constant elasticity of substitution, $\sigma_i = \frac{1}{1+\rho_i}$; Y is output; K, L, E, M, W are individual capital, labor, energy, material and water aggregates; $KLEM$ is the capital, labor, energy, and material combination; KEL is the capital, energy and labor combination; and KE is the capital and energy combination.

The fixed coefficient production function of an I-O model would yield an upper-bound estimate of direct output losses from water input disruption, where the percentage loss of the former would be equal to the percentage loss for the latter. All other types of production functions would yield percentage output losses lower than the percentage decrease in water availability because of substitution possibilities. We define *individual business (or sectoral) resiliency* as the difference between the fixed coefficient (proportional) result and the flexible input (disproportional) result, and which is attributable both to the various response mechanisms related directly to water services (1st Tier) and inherent in the overall production function with respect to other inputs (Tiers 2-4).

MCEER Team

***Stephanie E. Chang**, Research Assistant Professor, Department of Geography, University of Washington*

***Ronald Eguchi**, President, ImageCat, Inc.*

***Adam Rose**, Professor, Department of Geography, Pennsylvania State University*

***Masanobu Shinozuka**, Distinguished Professor and Chair, Department of Civil and Environmental Engineering, University of California, Irvine*

***Thomas O'Rourke**, Thomas R. Briggs Professor, Department of Civil Engineering, Cornell University*

***Kathleen J. Tierney**, Co-director, Disaster Research Center, and Professor, Department of Sociology, University of Delaware*

Collaborative Partners

Los Angeles Department of Water and Power

Portland Bureau of Water Works

CGE models used for hazard analysis are likely to yield estimates of business disruptions for some if not all sectors of an economy that differ significantly from the direct loss estimates provided by empirical studies. This is because production function parameters are not typically based on solid data, or, even where they are, the data stem from ordinary operating experience rather than from emergency situations. Hence, it is necessary to explicitly incorporate the resiliency responses below into the analysis. This is accomplished here by altering the parameters in the sectoral production functions of the CGE model.

Production Responses to Natural Hazards

1. Conservation of Water. This response can be implemented immediately and continued through the long-run, i.e., be incorporated into the production process on a permanent basis. One of the silver linings of disasters is that they force businesses to reconsider their use of resources, and often not just at the margin for a single input but also holistically (as noted in item 7 below). The parameter changes for this response in the case of water pertain to the technology trend variable in the first tier of the production function specified above. More generally, in each tier of the production function, the productivity term, A_i, is specified as covering all inputs, i.e., factor neutral. Adjustment of the productivity term for an individual factor, such as the A_{1W} term in equation (1a), orients the productivity improvement in the direction of that factor.

2. Conservation of Other Inputs. This is analogous to water conservation and can be applied to any of the tiers. However, it can often take on more permanence than water conservation, which is a dire necessity in many cases, and is constant over the applicable period rather than decreasing. Examples would include a reduction in number of trucks or maintenance personnel. One other adjustment option can be thought of as a sub-case—an increase in the use of non-water inventories, though only through the very short run.

3. Increased Substitutability of Other Inputs for Water System Deliveries. This response would be exemplified primarily by purchasing water from other sources (by the bottle or truckload), or by moving to another location where less water is needed.

4. Back-up Supplies. This response is often implemented in the immediate aftermath of an earthquake in the short-run. It includes adjustments that incur costs, such as the digging of wells, and rather costless measures, such as collecting rainfall or using riverine water. The costless alternatives can be modeled in a manner similar to conservation and the cost-incurring ones similar to substitution. The use of water inventories (stored water) is best addressed as discussed above. As with the inventory item discussed above, there is some flexibility in how costs are considered temporally.

5. Water Importance. This response requires more explanation because of the widespread use of the term "importance" in its broadest sense in the earthquake research literature. Sometimes, it has been used to encompass all other

responses. In ATC-25 (1991), utility lifeline importance was quantified as the percentage change in a sector's output that would result from a one percent change in input availability. If water were used everywhere in the production process and no resiliency measures were possible, a one percent decrease in water would lead to a one percent decrease in output, or an importance factor of 1.0 (the same as the I-O fixed coefficient production function). The existence of various responses lowers the importance factor, which had a value as low as .30 for the Transportation and Warehouse sector in ATC-25. Here we go to the opposite extreme in the use of the term as the percentage of production activities in a given sector that do not require water to operate. Thus, it refers to the inherent resiliency of a production process in the absence of any explicit adjustment.

6. Time-of-Day Usage. This is a passive response that pertains to hours during which the business is closed, and hence where loss of water has no effect on output (see, e.g., Rose and Lim, 2002, for an example of how this adjustment greatly reduced loss estimates from electricity disruptions in the aftermath of the Northridge earthquake). It is listed here for the sake of comprehensiveness.

7. Change in Technology. This refers to long run (permanent) changes in the overall process, such as replacing open systems, which do not recycle water, with closed systems. It may require the reformulation of the entire production function.

Portland Water System and Economy

The Portland Bureau of Water Works (PBWW) is a rate-financed, City-owned utility that serves 840,000 people in portions of the Portland Metro Area (including businesses responsible for 98% and 72% of sales in Multnomah County and Washington County, respectively). In 1999, PBWW water sales amounted to 39 billion gallons. The largest customers are major manufacturing companies, the Portland City Bureau of Parks and Recreation, and several hospitals.

The PBWW transmission and distribution is comprised of nearly 2000 kilometers of pipelines, 29 pump stations, and 69 major storage tanks. Construction of the PBWW dates back to 1894. About 70% of the system still consists of cast iron pipes, even though the agency began installing ductile iron in the 1960s. Additional information on the PBWW, its maintenance and earthquake mitigation costs, and its earthquake vulnerability can be found in Chang (2001b).

We constructed a CGE model of the portion of Portland Metropolitan Area economy that overlaps with the Portland Bureau of Water Works (PBWW) Service Area. The main data upon which the empirical model is based are the 1998 IMPLAN Social Accounting Matrix (SAM) and Input-Output Table for Multnomah County and Washington County (MIG, 2000). It is divided into several partitions that reveal the structure of the regional economy, including the industry, commodity, factor income, household, government, capital, and trade accounts.

Links to Current Research

Los Angeles Lifeline Demonstration Report

NSF Project on Infrastructure User Costs on Seismic Risk Management

"Our analysis provides a way of further utilizing the extensive empirical and simulation results on business interruption in the aftermath of earthquakes developed by other MCEER researchers"

The SAM industry accounts contain 20 sectors, with the Water & Sanitary Services separated from other utility services in order to pinpoint economic impacts of water supply disruptions in the aftermath of an earthquake. The Total Gross Output of the Portland Metro economy in 1998 is $71.2 billion, including $42.1 billion in interindustry transactions and $29.1 billion of total value-added. The total domestic commodity supply and exports of the Portland Metro Area in 1998 are $43.3 billion and $27.9 billion, respectively, implying the region is moderately self-sufficient. This is further evidenced by the trade accounts. The net domestic trading surplus is about $3.4 billion and the net foreign trading deficit is about $5.2 billion.

Simulating the Response to Natural Hazards

The Portland Area is characterized by moderate seismic activity stemming from the ocean floor Cascadian Subduction Zone and a series of shallow crustal faults. Two damaging earthquakes have taken place in the past 40 years measuring M5.5 and M5.6. However, large subduction earthquakes as great as M9.0 have taken place as recently as 1700 (see Wong et al., 2000).

Chang (2001b) simulated the effects of three alternative mitigation measures (no action, cast-iron pipe replacement, and tank/pump upgrade). The analysis was undertaken in the context of a life-cycle cost model that factored in not only the cost of mitigation over time and its ability to reduce system vulnerability through the year 2050, but also the savings of ordinary maintenance costs.

Chang (2001b) performed simulations for alternative combinations of earthquake types, calendar years, and mitigation options, using several sophisticated geological and engineering models. Each case was subject to 100 Monte Carlo simulations. These simulations were used to estimate direct losses in sectoral output, factoring in an amorphous amount of resiliency. Based on the work by ATC (1991) and Tierney (1997), resiliency is defined by Chang as "the remaining percentage of output that an industry can still produce in the event of total water outage." Sectoral resiliency measures range from a low of 21 percent for Health Services to a high of 49 percent for Transportation and for Communications and Utilities. Note that the definition of resiliency we provided above is a generalization of Chang's definition to cases where the water outage is not a total one. Note also that the ATC definition assumes a linear relationship, but that non-linear relationships are likely to be more realistic. Our methodology can be used to estimate non-linear relationships between water service disruptions and output reduction and hence represents a non-linear measure of resiliency.

The recalibration of the water productivity parameter (A_W) was solved analytically. However, the recalibration of the elasticity of substitution (σ_1) between water (W) and the capital, energy, labor, and material aggregate ($KELM$) could only be undertaken with a numerical solution, in this case uses the numerical bisection method, which is a converging root search routine. In our analysis, we simulate water

conservation and water substitutability with equal 50-50 weights based on survey results for the Northridge earthquake by Tierney (1997).

Water Disruption Simulation Results

Simulations were conducted of the regional economic impact of an earthquake-induced water supply disruption in the Portland Metro Area. Although Chang's engineering vulnerability and direct loss simulations involve many scenarios relating to alternative earthquake magnitudes, outage durations, and resiliency responses, our analysis focuses on a subset of scenarios characterized by:

1. One earthquake type (Bolton crustal fault) of magnitude 6.1.
2. Impacts in the Year 2000.
3. Scenarios for Business as Usual (No Mitigation) and Cast-Iron Pipe Replacement.
4. Outages of varying lengths from 3 to 9 weeks.
5. Four resiliency responses grouped into water conservation and increased substitutability.

We focused on the first characteristic because it represented the "most likely" case, and on characteristics 2-4 to keep the number of simulations manageable.

Note, one other important dimension of our simulations, which relates to pricing of water delivery. Ordinarily, CGE simulations allow prices to fluctuate freely in response to changing supply and demand conditions. However, two features of this situation warrant simulations with fixed water prices. The first is the fact that businesses often resist raising their prices in the aftermath of a natural disaster for reasons of altruistic community concern and to avoid the image of price gouging. Second, the PBWW is not a typical enterprise with fluctuating prices, but rather one in which rates are adjusted only periodically in the context of open public hearings.

No Pre-Event Mitigation; Post-Event Water Conservation and Increased Substitution

We used our recalibration algorithms to explicitly incorporate resiliency adjustments into our model accordingly for water conservation and increased substitutability. In our first simulation, unmitigated sectoral water disruptions sum to a 50.5 %. Our initial reference point of total direct (partial equilibrium) output losses equaling 49.1 % are estimated by our model before any resiliency adjustment. Chang's estimates of direct output losses, amounting to only 33.7 % because they reflect direct sectoral resiliency to water service outages. One measure of direct regional resiliency would be the extent to which the actual direct output reduction deviated from the likely (fixed-coefficient) maximum, which is equivalent to the %age water input disruption. The measure would be 33.3 % in this scenario [(50.5-33.7) ÷ 50.5].

Our estimates of the indirect (net general equilibrium) effects are 7.3 % reduction in regional gross output and a 41.0 % total (gross general equilibrium) reduction in regional gross output for the week. The former represents $99.9 million ($5,197 x 1/52 million) and the

latter $561 million. Chang (2001b) assumes that restoration takes place within four weeks in a straight-line manner, so the total loss in economic output for the Region is estimated to be $1,122 million.

Indirect losses for the first case are only about 22 % the size of direct losses. In the context of I-O, this would be a multiplier of only about 1.22. The Portland Metro economy-wide output multiplier is significantly larger than this, but the CGE model incorporates many other factors that mute the uni-directional and linear nature of the pure interdependence effect of the I-O model. For example, it is able to capture price changes for intermediate goods from cost and demand pressures, various substitutions aside from those relating to water, and various income, substitution and spending considerations on the consumer side. A measure of overall regional economic resiliency to earthquake disruptions of Water Service would be the difference between the total fixed coefficient I-O multiplier and the CGE impacts. The weighted average Type II output multiplier for the Portland Economy is 1.9, or a 90 % increase over direct effects. Thus the regional economic resiliency measure in this case would be 54.4 % [(90-41) ÷ 90].

Pre-Event Pipe Replacement and Post-Event Water Substitution

The results of the scenario of an M6.1 crustal fault earthquake but with cast-iron pipe replacement are based on a reduction of the direct water outage from 50.5 % to 31.0 %. Our initial estimates of direct output losses are 30.7 %, compared to Chang's empirical estimates of 21.3 %. The parameter adjustments needed for the model to replicate the Chang direct loss estimates are lower than the corresponding parameter changes in each sector of the previous case because the direct output losses are projected to be lower in each. Our estimate of indirect losses in Scenario 2 is 9.2 %, which is a 43.2 % the size of direct losses.

Overall, Scenario 2 is estimated to incur a 30.5 % loss in gross output in the Portland Metro economy in the Year 2000 during the first week of water service disruption. In dollar terms, this translates into $418 million. However, Chang (2001b) estimates the system can be restored to full service within three weeks in this case, so, again assuming a linear restoration path, total output loss is $627 million. This is lower than the total economic loss associated with the "No Mitigation" simulation because it reflects both the reduction in loss for the initial disruption period (first week) but also a reduction in the time during which losses take place (from 4 to 3 weeks).

Table 1 decomposes the effects of the cast-iron pipe replacement strategy in the context of water conservation and increased substitutability responses. It indicates that the greatest contribution is from this strategy's reduction in direct losses (30.4 % of the 43.6 % overall reduction in losses for the total outage period). The reduction in loss due to decreased outage time is 13.1 %. The pure mitigation strategy actually increases the indirect losses by 4.8 %, but this is more than offset by the reduced outage time during which these effects

■ Table 1. Decomposition of Gains from Mitigation in Reducing Total Regional Losses from Portland Water Service Disruptions

	Level (10^6)	Percent Reduction
Total Business as Usual Scenario Loss	$1,112	--
Pipe Replacement Loss Reduction Decomposition	-485	-43.6
Change in direct loss (pure mitigation)[a]	-338	-30.4
Change in direct loss (reduced outage time)[b]	-146	-13.1
Change in indirect loss (pure mitigation)[a]	52	4.8
Change in indirect loss (reduced outage time)[b]	-63	-5.7
Index number error term	30	2.7

[a]Loss for a 4-week restoration period.

[b]Loss for a 3-week restoration period

take place. Note, however, that indirect losses are beyond the control of policymakers, and that this may pose a problem in dealing with the effects of various strategies. Fortunately, although it undercuts the cost-effectiveness of the mitigation alternative in this case, the unwanted increase in indirect effects is relatively small. Moreover the qualitative results in this case should not be generalized, because it is possible that, in other cases, indirect effects will be reduced, thereby reinforcing the mitigation effort.

Conclusion

We emphasize that, although we contribute significant advances to CGE modeling of the economic impacts of natural and other types of disasters, we have not remedied all of the problems. We assume that the economy adjusts to a new equilibrium, but we do not incorporate disequilibrium phenomena, except for holding utility lifeline service prices constant. We incorporate mitigation and adaptation costs but not other transition costs (e.g., labor relocation). Still, we believe the use of CGE modeling is legitimate in this case and significantly improves the accuracy of economic loss estimates. With respect to equilibrium adjustment considerations, earthquake ground-shaking may last only thirty seconds, but the time horizon we model includes the extended period of pre-event preparation, as well as the weeks to full recovery of lifeline services and rescheduling of production directly or indirectly interrupted. We compress the period of further general equilibrium adjustments to this time period without loss of generality. The analysis assumes that suppliers without customers and customers without suppliers can be matched during this short period. In fact, emergency management officials are investigating prospects for establishing an information clearinghouse to help expedite such adjustments. Essentially, we utilize a stylized period of analysis that strikes a balance between realism, manageability, and approximations of CGE modeling.

Acknowledgements

The research in this paper was supported by several grants from the NSF-sponsored Multidisciplinary Center for Earthquake Engineering Research (Grant No. EEC-9701471) and by a grant from the National Science Foundation (Grant No. 9802151). The authors acknowledge the contribution of Debo Oladosu, Chunsheng Shang, Gauri Guha, and Ram Ranjan for research related to the paper. We are also grateful to Stephanie Chang for providing us with background information on the Portland Bureau of Water Works network and sharing results of her analysis of network vulnerability, direct economic impacts of earthquake disruptions, and maintenance and mitigation costs. Helpful comments on an earlier draft were provided by Ann Fisher. The authors are solely responsible for any errors and omissions.

References

Applied Technology Council, (ATC), (1991), *Seismic Vulnerability and Impact of Disruption of Lifelines in the Conterminous United States,* Report ATC-25, Redwood City, CA.

Bram, J., Orr, J. and Rappaport, C., (2002), *The Impact of the World Trade Center Attack on New York City: Where Do We Stand?,* Federal Reserve Bank of New York, New York City, NY.

Bruneau, M., Chang, S., O'Rourke, T., Shinozuka, M., Tierney, K. and vonWinterfeldt, D., (2002), "A Framework to Quantitatively Assess and Enhance Seismic Resilience of Communities," Multidisciplinary Center for Earthquake Engineering Research, University at Buffalo.

Chang, S., (2001), *Evaluating Social Benefits of Disaster Mitigation*, Department of Geography, University of Washington, Seattle, WA.

Chang, S., (2001), "Structural Change in Urban Economies: Recovery and Long-Term Impacts in the 1995 Kobe Earthquake," *The Kokumin Keizai Zasshi (Journal of Economics & Business Administration),* Vol. 183, No. 1, pp. 47-66, Special Issue on the Great Hanshin Earthquake: Economic Analysis of the Disaster and the Recovery.

(MIG) Minnesota IMPLAN Group, (2000), *Impact Analysis for Planning System* (*IMPLAN*), Stillwater, MN.

Rose, A. and Guha, G., (2003), "Computable General Equilibrium Modeling of Electric Utility Lifeline Losses from Earthquakes," in S. Chang and Y. Okuyama (eds.), *Modeling the Spatial Economic Impacts of Natural Hazards*, Heidelberg: Springer, forthcoming.

Rose, A. and Liao, S.-Y., (2002), "Modeling Regional Economic Resiliency to Disasters: A Computable General Equilibrium Analysis of Water Service Disruption," *Proceedings of the Seventh National Conference on Earthquake Engineering*, Oakland, CA.

Rose, A. and Lim, D., (2002), "Business Interruption Losses from Natural Hazards: Conceptual and Methodological Issues in the Case of the Northridge Earthquake," *Environmental Hazards: Human and Policy Dimensions,* 4, pp. 1-14.

Rose, A., Oladosu, G. and Salvino, D., (2003), *Regional Economic Impacts of Electricity Outages in California: A Computable General Equilibrium Analysis*, Working Paper, Pennsylvania State University, University Park, PA.

Rose, A., Benavides, J., Chang, S., Szczesniak, P. and Lim, D., (1997), "The Regional Economic Impact of an Earthquake: Direct and Indirect Effects of Electricity Lifeline Disruptions," *Journal of Regional Science*, Vol. 37, pp. 437-58.

References (Cont'd)

Shoven, J. and Whalley, J., (1992), *Applying General Equilibrium*, New York: Cambridge.

Tierney, K., (1997), "Impacts of Recent Disasters on Businesses: The 1993 Midwest Floods and the 1994 Northridge Earthquake," in B. Jones (ed.), *Economic Consequences of Earthquakes: Preparing for the Unexpected*, NCEER-SP-0001, National Center for Earthquake Engineering Research, University at Buffalo.

Webb, G., Tierney, K. and Dahlhamer, J., (2000), "Business and Disasters: Empirical Patterns and Unanswered Questions," *Natural Hazards Review,* Vol. 1, pp. 83-90.

Wong, I. et al., (2000), "Earthquake Scenarios and Probabilistic Ground Shaking Maps for the Portland, Oregon, Metropolitan Area," *Interpretative Maps Series IMS-16,* State of Oregon, Department of Geology and Mineral Industries, Portland, OR.

The MCEER Interface Between Research and Education

by Andrea S. Dargush (Coordinating Author), Makola M. Abdullah, Anil K. Agrawal, Rupa Purasinghe and Billie F. Spencer, Jr.

Educational Objectives

MCEER conducts a program of education and educational outreach to encourage transfer of ideas and knowledge that emerge from its research. The effectiveness of these activities depends heavily on the Center's ability to recognize the needs, expectations and capabilities of the learner/user. With this as a foundation, MCEER education and outreach activities work to build awareness of the earthquake hazard - particularly in those areas of lesser known exposure, to help others to understand and acknowledge the implications of seismic risk, and to encourage implementation of earthquake loss-reducing programs and engineering technologies. In parallel, and using earthquakes as a thematic concept, MCEER works with precollege students and educators to increase their understanding and appreciation of the role that science, technology, engineering and mathematics play in our society. This paper reviews MCEER's ongoing activities and approaches for knowledge transfer, summarizes some obstacles which can inhibit the process, and assesses the potential influence of education and outreach on enhancement of earthquake resiliency.

In order for earthquake research to be effective, those who will put engineering strategies and knowledge into practice must utilize it. This knowledge may be implemented in the form of improved codes and standards, enhanced abilities to prepare, respond and recover from earthquakes, new design methodologies or advanced technological applications, even new educational curricula. How do research outcomes become useable and are there ways that the process of transfer can be improved? It is essential that there be a recognized interface between research and education that must be addressed to further knowledge transfer. This educational process is part of the strategic vision of MCEER. The program has several goals to help advance the Center's mission to enhance community resiliency. Because end-users are derived from a broad variety of educational backgrounds, these goals are necessarily diverse. They include improving science and engineering education in the precollege environment, nurturing new generations of engineering doctorates, providing practicing professionals with substantive opportunities to enhance their techni-

Sponsors

National Science Foundation, Earthquake Engineering Research Centers Program

Research Team

***Andrea S. Dargush**, Assistant Director for Education and Research Administration, **George C. Lee**, Director, and **Nishadi Karunarathne**, **Daniel Fenz** and **Robert Payne**, Research Experience for Undergraduate Students, Multidisciplinary Center for Earthquake Engineering Research,*

***Jeffrey Berman**, Ph.D. Candidate, Department of Civil, Structural and Environmental Engineering, University at Buffalo*

***Makola Abdullah**, Assistant Professor, and **Terri Norton**, Ph.D. Candidate, Department of Civil Engineering, Florida A&M University*

Research Team continued on page 2

Research Team (cont.)

***Anil Agrawal**, Associate Professor, **George Mylonakis**, Assistant Professor, **Susan Romero** and **Miriam Vargas**, Undergraduate Students, Department of Civil Engineering, City College of the City University of New York*

***Rupa Purasinghe**, Professor, **Belan Valencia**, **Art Chianello** and **Marion Calderon**, M.S. Students, Department of Civil Engineering, California State University at Los Angeles*

***Billie F. Spencer**, Nathan Newmark Professor of Civil Engineering, and **Yong Gao**, Ph.D. candidate, Department of Civil Engineering, University of Illinois at Urbana-Champaign*

Previous Summaries

1999-2000:
Dargush and Lee
http://mceer.buffalo.edu/publications/resaccom/9900/Chapter10.pdf

cal proficiencies in earthquake engineering, and encouraging researchers to better incorporate end-user needs in their studies. It is also necessary to reach out to audiences who can benefit from the knowledge conveyed in a condensed and slightly less technical language, such as public officials, facility owners, the popular media and the public-at-large. To do so, we must acknowledge and appreciate the diversity of pedagogical environments within which we operate. Just as mitigative interventions remain singular accomplishments without an integrated systemic approach, so must education efforts address complex user needs in achieving their final mitigation objectives. MCEER builds its education and outreach activities as natural extensions of its research programs and tries to integrate the outcomes with end-user needs. By so doing, practicing engineers are better able to improve the effectiveness of their designs and communicate various risk scenarios with clients. Emergency managers are provided with better tools to develop pre- and post-event strategies; in both cases making more well-informed decisions about resource allocation.

This paper will highlight education work done by several MCEER faculty and professionals at their universities and at MCEER headquarters. The synthesis of these outcomes is intended to make the interface between research and education seamless.

Practice-Oriented Projects and Outreach to High School Students

The California State University at Los Angeles (CSLA) component was aimed at student development through a practice-oriented project. The project is to model and analyze a campus concrete multi-story building for seismic vulnerability with performance-based design concepts. In a parallel application, passive energy dissipation devices were studied as a seismic response modification methodology.

A group of five students, including three underrepresented minority students, worked on the project. The faculty mentor, two industrial representatives, and MCEER researchers guided them. This combination was very helpful in bringing a practice-oriented project

The end users of MCEER education and educational outreach activities span a wide range of audiences, beginning with K-12 students, teachers and parents, university students, and extending to government officials, public and private business executives, practicing professionals, and researchers advancing the state of existing knowledge. In summary, the public-at-large can be considered to be MCEER's end user community.

with advanced technology applications to our urban commuting campus.

The project centered around modeling the campus building with a computer model with ETABS software. The lateral load resisting system for the building is a concrete shear wall system, shown in the computer model (Figure 1). The model was subjected to static, response spectra, and time history loading. A nonlinear static pushover analysis of the building is currently being performed.

In the high school outreach component of our activities, the faculty mentor helped the Alhambra High School MESA students prepare for the national Junior Engineering Teams (JETS) competition in Natural Hazard Mitigation related topics in 2002 and 2003. Through the Campus Structural Engineering Student Chapter, the MCEER students participated in field trips, seminars and the Los Angeles Tall Building Council Annual Conference (May 2002), where they presented a poster on the collapse of the World Trade Center. The MCEER group received several awards recognizing their contributions. The Los Angeles Tall Building Council honored a MCEER student with their student award (2001), and the Southern California Structural Engineers Association honored MCEER students in 2001 and 2003 with their student awards. A MCEER student was honored as the CSLA outstanding civil engineering student in 2003. The faculty mentor was honored with the CSLA Civil Engineering Professor of the Year Award (2003) given by the Engineering Computer Science and Technology Student Council.

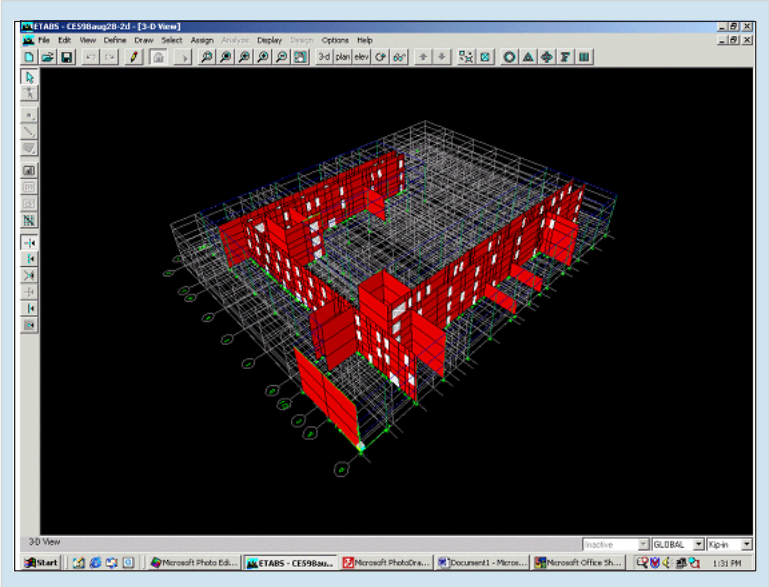

Figure 1. Three Dimensional Computer Model of the Campus Building

Individual Study Programs for Underrepresented Students

The focus of the integrated research and educational initiative at the City College of New York (CUNY) is to involve undergraduate students, including minority and women, in research on smart structural control systems.

During spring 2002, four undergraduate minority students, including two women, were offered Individual Study in Earthquake Engineering. The students were taught basic concepts in structural dynamics and structural control through weekly study assignments, and interactive discussions and assignments with graduate students. The Quansar Instructional Shaking Table was purchased to introduce students to the experimental components of structural dynamics. One of the students, Ms. Susan

Collaborative Partners

MCEER works with various organizations to enhance the impact of its educational activities. Some of these partners include:

- *Earthquake Information Providers Group*
- *Federal Emergency Management Agency*
- *Institutions in Research in Seismology*
- *Mid-America Earthquake Center*
- *Pacific Earthquake Engineering Center*

Romero, was selected to participate in the Research Experiences for Undergraduates program in Japan during the summer of 2002. Following her visit to Japan, Ms. Romero worked with graduate students to carry out some numerical analysis on semi-active control using friction dampers. As a result of this research activity, Ms. Romero has been motivated to join the Ph.D. track program in structural control in the fall of 2003.

During spring 2003, the team at CUNY is offering the individual study course to three undergraduate students, including one minority female student. The students learn basic concepts in structural dynamics and do shaking table experiments with the instructional Quansar Shaking Table. One of the students, Ms. Miriam Vargas, is applying for the Research Experience for Undergraduates program in Japan this year for research in structural control. Figure 2 shows the students using the instructional shake table.

A 5-ton, 5 ft x 5 ft shaking table system for research and education has been developed as part of this effort. The students involved are developing a 5-story building model for experimental research. The laboratory will be fully operational in the summer of 2003. At that time, both graduate and undergraduate students will be involved regularly in experimental research in structural dynamics and control.

As a further part of this effort, several practical issues in structural control are being investigated, such as the modeling of near-field ground pulses, effectiveness of passive damping systems for near-field ground motions, and development of hybrid control systems using passive and semi-active MR or friction dampers. With the development of the 5-ton shaking table, students have better opportunity to get involved in theoretical as well as experimental research.

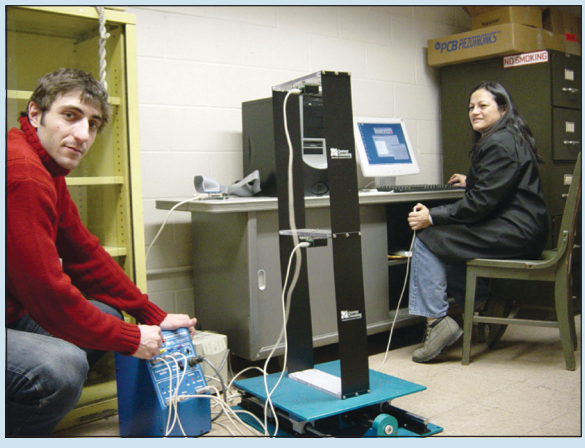

■ Figure 2. Undergraduate Students Using Shaking Table System at CCNY.

WHEEL, the Instructional Shake Table and KiddieEngineer

At Florida A&M University, the Wind Hazard and Earthquake Engineering Laboratory (WHEEL) is structured around three interrelated components: research, education and outreach. The research goal of the lab is to improve structural performance of civil structures to natural hazards. The latest research project involved producing a detailed earthquake analysis of an existing high-rise structure in the southeast region of the United States. The structure was modeled using finite element methods and exposed to moderate and large-scale earthquakes. The probability

of structural and non-structural damage, caused by the building's displacement, was approximated through the use of fragility curves. Repair costs were estimated based on the probability of exceeding each damage state. Passive control devices were used to improve the response of the building and reduce the extent of damage. The findings of this study have been published in the *MCEER Student Research Accomplishments: 2001-2002*. In addition, the results of the study have been presented at conferences in Orlando, Florida and Tokyo, Japan by the faculty and additional participation by graduate students involved in the program.

Florida A&M University/WHEEL has also contributed to the education of earthquake engineering students through the development of lab experiments and demonstrations using an instructional shake table (see Figure 3). The information was published as a part of the University Consortium for Instructional Shaking Tables (UCIST). In addition, these developments assist with the integration of structural dynamics into the Civil Engineering Mechanics course and the undergraduate curricula.

The final component, outreach, is a way of encouraging and involving K-12 students in the field of engineering. ***KiddieEngineer*** was a summer outreach program that engaged two elementary school teachers and a small group of 3rd and 4th grade students (see Figure 4). The teachers developed curricular elements that included teaching the students about natural hazards and their affects on buildings. The students also learned how engineers design structures to resist hazards. At the conclusion of the program, the students formed groups/companies where they constructed LEGO buildings, wrote reports on natural hazards, and tested their buildings on the instructional shake table. The summer program was a trial program to test the new curricular elements and to determine if they agreed with the interest of the students. The future goal of the program is to introduce the information to the local school system.

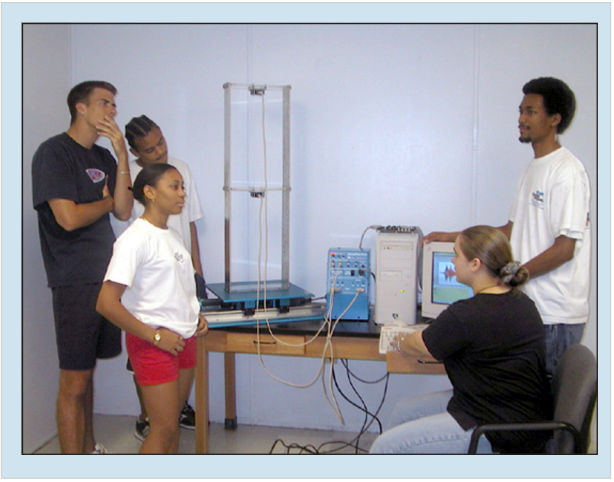

Figure 3. Students at WHEEL Test a Model on the Instructional Shake Table

Figure 4. Elementary School Children Test Lego Buildings on the Instructional Shake Table

"Three of the universities participating in MCEER's Education program, California State University at Los Angeles, the City University of New York and Florida A&M University, are considered minority serving institutions."

MCEER-Coordinated Education and Outreach Activities

The conventional university environment educates students through the completion of course work and theses. Since its earliest days as NCEER, MCEER researchers have also traditionally graduated several Ph.D. candidates each year. However, the system-integrated research environment created by MCEER helps to enhance the conventional university process. As MCEER researchers develop new knowledge, it is integrated into new and exsiting courses at the undergraduate and graduate level. Several new courses and programs, such as the minor in Natural Hazards at Penn State University and the Master's of Earthquake Engineering at the University at Buffalo serve as examples of educational programs which will expand the traditional university learning experience. Undergraduate and graduate students also actively participate in MCEER research as part of formal programs such as the Research Experiences for Undergraduates (see Figures 5 and 6) and the Student Leadership Council (SLC). Both programs are designed to provide a more enriched exposure to the team-based integrated research of the Center.

Figure 5. The 2002 REU Students Participated in a Student Symposium in Keystone, Colorado

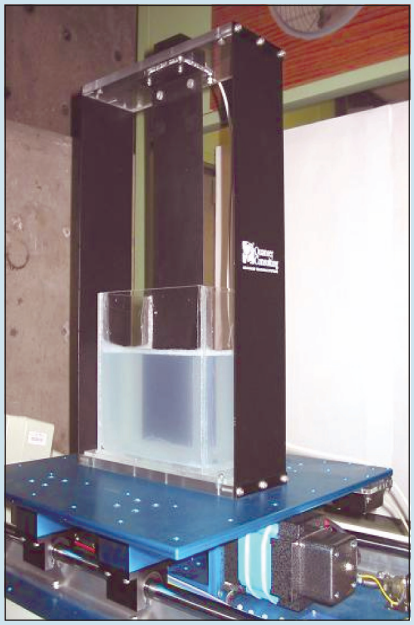

Figure 6. Test Set-up of a Simplified Model of a Viscous Wall by an REU Participant

Opportunities to participate in multi-institutional seminars and earthquake related curricula increase the students' appreciation of the systems approach to earthquake research and the relevance of research participation to emerging advances within the disciplines. Support through individual MCEER research projects and special fellowships help encourage gifted students to pursue careers in academia. This is especially important to increase the number of U.S. students pursuing advanced degrees in engineering. The students regularly publish their results in a special MCEER publication, *Student Research Accomplishments.*

An important new initiative is the Student Field mission, which is a collaborative effort of the three national earthquake centers. The

mission offers advanced graduate students an opportunity to visit centers of excellence in other countries, observe and be mentored, complimented by field excursions to sites of earthquake damage and rebuilding. It provides the students with a more global perspective on research, earthquake impact and recovery. The first mission was held in 2002 in Taiwan, and the participants are shown in Figure 7. The 2003 mission is scheduled to be held in Italy.

Interactions between SLC students and members of MCEER's Industry partnership provide students and practitioners with opportunities to get better acquainted (see Figure 8). Increased involvement of industry partners in MCEER research activities further enhance the graduate experience. Lifeline studies at Cornell University involving Tokyo Gas and utilizing the experimental testing facilities of an MCEER industry partner, Taylor Devices, Inc., illustrate the value of graduate student participation. Current MCEER geotechnical work being carried out at Mactec, Inc. actively involves undergraduate engineers in the research effort. Experiences are especially designed to expose students to different career opportunities, whether in practice or academia, and to expand their professional capabilities.

However, each thrust area has its own unique contribution to advancing education of students, practicing professionals and other members of the community. Utility engineers at the Los Angeles Department of Water and Power (LADWP) are using the GIS-based tools developed as part of the Los Angeles lifeline project. The ability to spatially relate lifeline performance to potential seismic risk would not be available to them without the MCEER research effort. This will offer substantial improvement to LADWP's ability to prepare and respond to the next Los Angeles area earthquake and to restore any loss of function more efficiently. Utility managers have seen an improved way to deal with the consequences of earthquake damages to the utility system. (see MCEER's *Research Progress and Accomplishments: 1999-2000*).

Figure 7. The 2002 Tri-Center Field Mission Participants Visited the Chi-Chi, Taiwan Earthquake Region

Figure 8. Students Display Posters and Discuss Their Research with Industry Partners, MCEER Investigators, and Others at a Variety of Meetings Throughout the Year

Web Sites

Earthquake Information Network:
http://www.eqnet.org

Multidisciplinary Center for Earthquake Engineering Research:
http://mceer.buffalo.edu

MCEER Student Leadership Council:
http://mceer.buffalo.edu/slc/

University Consortium on Instructional Shake Tables:
http://ucist.cive.wustl.edu/

Smart Structures Technology Laboratory:
http://cee.uiuc.edu/sstl/

As the MCEER hospital project progresses and seismic resistant strategies and technologies emerge which can address vulnerabilities in the systems and components of health care facilities, decision support tools are being developed in parallel, which will become educational methods to assist hospital administrators and engineers in making cost-effective decisions to strengthen the facility. Similarly, a database of information developed through the study will be a long-standing, valued educational resource to the hospital community, researchers, and engineering discipline.

An educational tangent from the MCEER program in Response and Recovery, the use of remote sensing and satellite imagery to develop damage recognition algorithms is helping to advance and broaden the use and application of the technology to other spatial phenomena. Several MCEER technical publications have been produced which can educate professionals in other hazard fields about the potential applications of the technology, such as MCEER monographs which are written as a concise guide on advanced technologies for a practicing professional. One publication on the use and application of remote sensing data, in particular, has been produced on CD-ROM so that greater amounts of data can be provided for the user (Tralli, 2000).

The MCEER networking effort is aimed at linking experimental facilities, improving the computational capabilities of Center researchers and increasing the availability and exchange of information and data. Several useful databases and software platforms, in particular, those developed by MCEER for inelastic analysis and design of structures, may be found at *http://mceer.buffalo.edu/research/default.asp*. In collaboration with the MCEER Education program, a series of monthly webcast seminars on topics of timely interest to the earthquake community has been offered for real-time or asynchronous viewing. Seminar topics have been multidisciplinary in nature, focusing on earthquake-related topics and are archived for permanent viewing. Viewers have been drawn in from around the world.

In addition to these educational outcomes, research in each of the Center's thrust areas generates numerous publications in these study areas. MCEER publications and special reports have wide global readership. MCEER participates in and organizes several state-of-the-field conferences each year, with conference proceedings made broadly available. An important recent workshop brought together engineers, scientists, and emergency professionals to examine the potential interactions between earthquake and blast science as they might apply to engineering design, in the aftermath of the World Trade Center disaster. Abstracts of publications from similar events and other technical reports may be viewed online at *http://mceer.buffalo.edu*. In the future, online full document procurement is planned.

MCEER is also coordinating with earthquake engineers in the People's Republic of China at the Institute of Engineering Mechanics and the China State Seismological Bureau on the co-production of a new journal on advances in earthquake engineering, *Earthquake*

Engineering and Engineering Vibration.

The Information Service, headquartered at MCEER, assists thousands of information seekers throughout the world and maintains information exchange agreements with serveral organizations and universities. They acquire and maintain a collection of pertinent literature in related fields, provide extensive reference assistance, and maintain an MCEER-developed bibliographic database, Quakeline©, which includes earthquake references to materials in nontraditional, or fugitive, literature. The Information Service also produces a periodic newsletter with news of the profession and information on new publications. They also pioneered efforts to establish a national web-centric portal to acquire earthquake information from several nationally prominent, credible sources of earthquake information, such as USGS, FEMA, Red Cross and many others. EQNet can be accessed at: *http:/www.eqnet.org*.

The Information Service has also assisted with MCEER's K-12 activities, adding teaching materials and student reference materials to the MCEER web, and participating in teacher training and public outreach events.

Many of these materials have been useful to media, as well. Information has been used as background to popular science articles, news features, documentaries - even articles on New York City real estate - with a focus on the low hazard, high consequence Eastern North American event.

Java-Powered Simulation for Nonlinear Structures

One of the tangible outcomes of this educational project at University of Illinois at Urbana-Champaign (UIUC) is the development of virtual laboratory (VL) experiments to support earthquake engineering research and education. Educators must always strive to better prepare the next generation of structural engineers who can understand and effectively deal with the design of earthquake resistant structures to reduce the associated human and financial losses. One of the challenges of teaching students about the fundamentals of earthquake engineering is giving them an intuitive understanding of the dynamics of structures. Demonstrating the concepts of dynamics using static chalk boards or books is difficult. The best approach is through hands-on laboratories. Unfortunately, few instructors have the necessary facilities readily available to demonstrate structural dynamic concepts through experiments.The main goal of the VL experiments is to provide students and practitioners with a means to interactively develop a fundamental understanding and intuition regarding a wide range of topics in earthquake engineering via the World Wide Web.To allow for universal access, the VL experiments must be built using Sun's Java Programming Language. Note that the Java platform provides for minimization of administrative overhead associated with maintenance of the VL.All of the VL experiments developed to date are accessible at *http://cee.uiuc.edu/sstl/*.

"The Field Mission experience provides students with a more global perspective on research, the impact of earthquakes and recovery."

The focus of the most recently developed module is investigation of the nonlinear response of multi-degree-of-freedom (MDOF) structures subjected to earthquake loading. The VL module, "Java-Powered Simulation for Nonlinear Structures," has been developed at UIUC and is available at *http://cee.uiuc.edu/sstl/java/twostory/animation.html*. In this VL module, the user is allowed to select different nonlinear models to represent the behavior of the structure, to change the parameters of the structure, and to choose different earthquake ground motions to do analysis. This module is intended to be used to increase understanding and provide a conceptual "feel" for various parameter changes on the performance of nonlinear structures under different excitations.

The structure is modeled as a two story building, and can include four types of nonlinearity: (i) linear stiffness and linear viscous damping; (ii) linear stiffness and nonlinear power-law damping; (iii) hysteretic stiffness using the Bouc Wen model and linear viscous damping; (iv) hysteretic bilinear stiffness and linear viscous damping. The same nonlinear behavior is assumed for both storys, while different parameters are allowed for each story. Figure 9 shows example nonlinear structural responses.

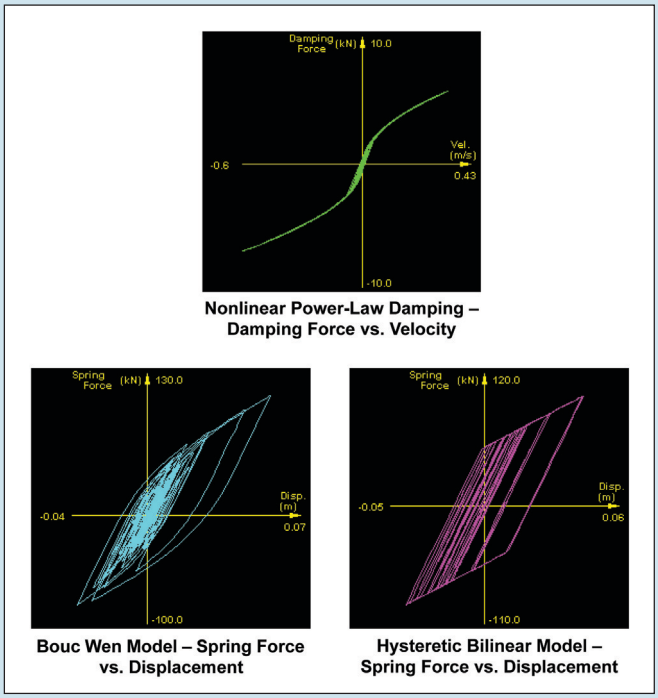

■ Figure 9. Top Floor Responses of a Two Story Structure with Various Nonlinear Models

As shown in Figure 10, this simulator consists of one *animation frame*, one *excitation frame*, two *response frames* and the *control panel*. The animation frame shows the animation of the structure during the earthquake excitation. It is able to show absolute motion or relative motion of the structure with different designs. The excitation frame allows the user to select different excitations for the analysis and can display the excitation in terms of acceleration or displacement. Located at the lower part of this Java simulator are the two response frames. These two frames provide the user with the ability to look at the responses of the same story, e.g., one frame for displacement and the other for force, or to compare the same responses for different storys at the same time. This simulator also includes a control panel, which allows the user to define the structure's characteristics. The help button links to the detailed help page for this VL experiment.

With approximately 500 visitors per month, the Java VL experiments provide an interactive means for students to gain a fundamental understanding and intuition regarding topics in earthquake engineering via the World Wide Web. The VL

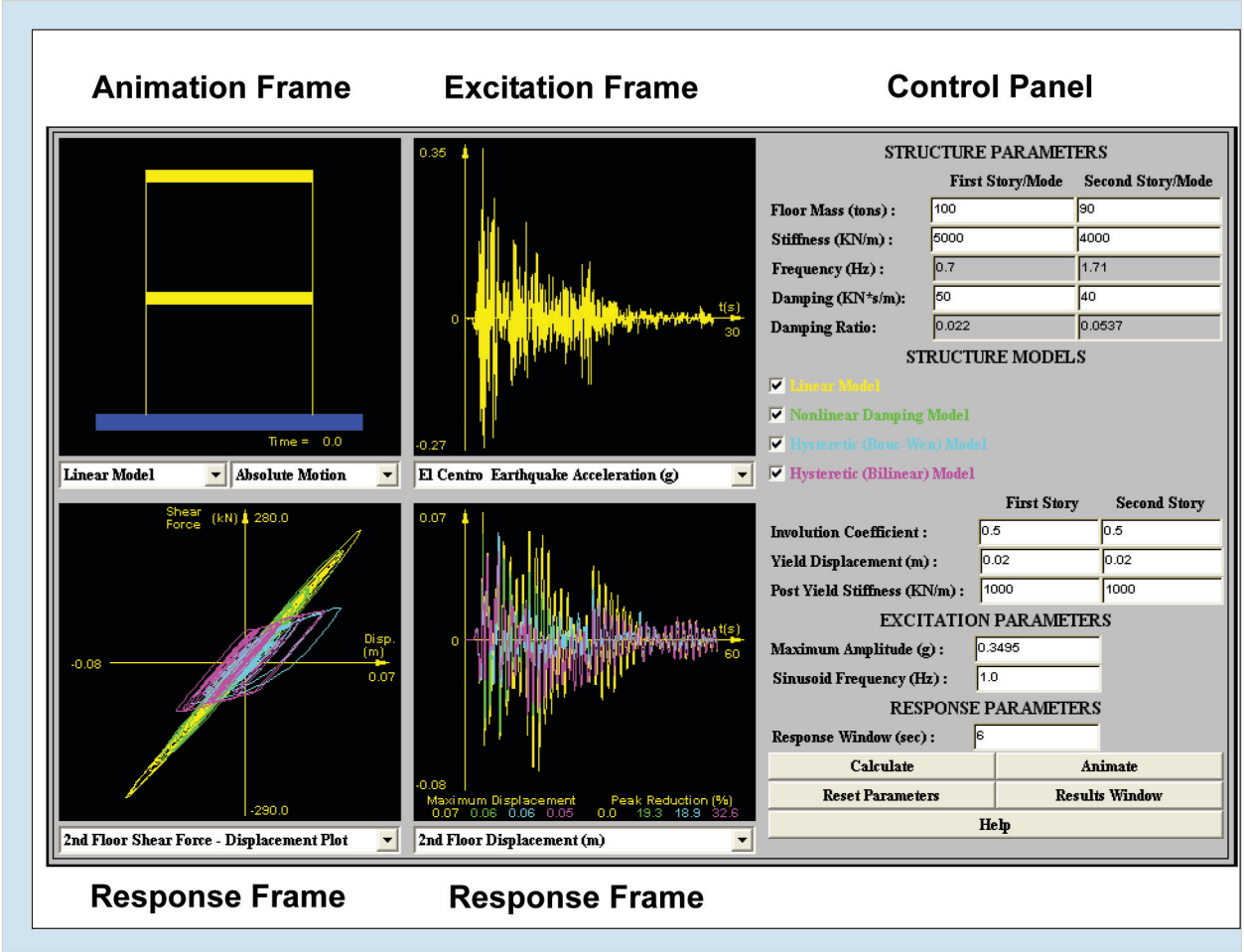

Figure 10. Java-Powered Simulation Applet

modules are accessible to earthquake engineering students, researchers and practitioners throughout the world and have been fully documented with extensive online help pages. Efforts are ongoing to further expand the available modules.

Conclusion

The most advanced and sophisticated techniques to reduce seismic impact can remain unused if end-users are unable to understand or unwilling to acknowledge seismic risk or seismic mitigation; do not understand the relevance of a potential application; are reluctant to risk its use without imperatives or incentives; or are unwilling to assign earthquake improvements higher priority than other concerns.

These factors impact ability to take research results and implement them in the form of better educational tools, seismic rehabilitation methodologies, improved policies for preparedness, response and recovery. All must be better understood and incorporated into the education and technology transfer process. Educational products developed, as a consequence of research, will not independently achieve earthquake mitigation. Although many advances have been

made as a consequence of seismic standards and legislative action, such as the National Earthquake Hazards Reduction Program, regulations dictating seismic improvements cannot realize all goals (Adler and Pittle, 1984). In the event of a disaster, a window of opportunity is presented to advance, yet still all mitigation goals can be accomplished. This underscores the need for a well-coordinated, repetitive, interdisciplinary approach to most effectively deliver earthquake knowledge and technology (National Research Council, 2001). MCEER continues to work with its researchers and other partners throughout the world to use education and outreach to improve educational programs, assist the practice and advance the state of earthquake readiness throughout the world.

Acknowledgment

This research was primarily supported by the Earthquake Engineering Research Centers Program of the National Science Foundation, under award number EEC-9701471 to the Multidisciplinary Center for Earthquake Engineering Research. This support is gratefully acknowledged.

References

Adler, Robert S. and Pittle, R. David, (1984), Cajolery or Command? Are Education Campaigns an Adequate Substitute for Regulation, *Yale Journal on Regulation*, Spring, 1984, pp 159-192.

National Research Council, (2001), *Protecting People and Buildings from Terrorism*, National Academy Press, Washington, DC, USA.

Research Progress and Accomplishments: 1999-2000, MCEER-00-SP01, Multidisciplinary Center for Earthquake Engineering Research, University at Buffalo, May 2000.

Student Research Progress and Accomplishments: 2001-2002; MCEER-02-SP09, Multidisciplinary Center for Earthquake Engineering Research, University at Buffalo, October 2002.

Tralli, D.M., (2000), *Assessment of Advanced Technologies for Loss Estimation*, MCEER-00-SP02, Multidisciplinary Center for Earthquake Engineering Research, University at Buffalo, December, on CD-ROM.

Production Staff

Jane E. Stoyle, Editor
Michelle A. Zuppa, Layout and Design
Hector A. Velasco, Illustration

Acknowledgements

This report was prepared by the Multidisciplinary Center for Earthquake Engineering Research through grants from the Earthquake Engineering Research Centers Program of the National Science Foundation (under NSF award number EEC-9701471), a contract from the Federal Highway Administration and funding from New York State and other sponsors.

Opinions, findings, conclusions or recommendations expressed in this material are those of the author(s) and do not necessarily reflect the views of the National Science Foundation, Federal Highway Administration, Research Foundation of the State University of New York or other sponsors.

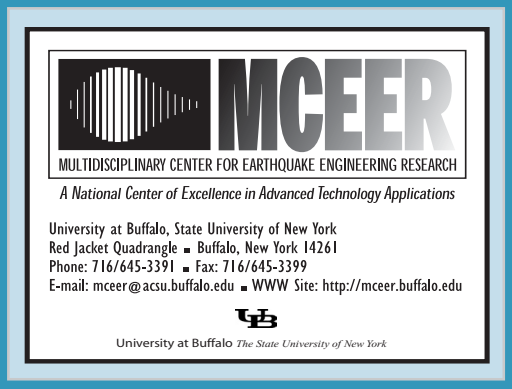
MCEER
MULTIDISCIPLINARY CENTER FOR EARTHQUAKE ENGINEERING RESEARCH
A National Center of Excellence in Advanced Technology Applications
University at Buffalo, State University of New York
Red Jacket Quadrangle ▪ Buffalo, New York 14261
Phone: 716/645-3391 ▪ Fax: 716/645-3399
E-mail: mceer@acsu.buffalo.edu ▪ WWW Site: http://mceer.buffalo.edu
University at Buffalo The State University of New York